PhD Thesis

María Lázaro Berenguer

May 2025

From Structure to Function: Understanding Vip3Aa's Mode of Action

Doctoral Programme in Biomedicine and Biotechnology

Supervisors:

Dr. Juan Ferré Manzanero

Catedrático
Departamento de Genética
Instituto de Biotecnología y Biomedicina
(BIOTECMED) Universitat de València

Dr. Patricia Hernández Martínez

Profesora ayudante doctora
Departamento de Genética
Instituto de Biotecnología y Biomedicina
(BIOTECMED) Universitat de València

El **Dr. Juan Ferré Manzanero**, Catedrático del Departamento de Genética de la Facultad de Ciencias Biológicas de la Universitat de València, y la **Dra. Patricia Hernández Martínez**, Profesora Ayudante Doctora del Departamento de Genética de la Facultad de Ciencias Biológicas de la Universitat de València,

Informan:

Que la **Sra. Maria Lázaro Berenguer**, Graduada en Biotecnología, ha realizado bajo su dirección el trabajo de investigación recogido en esta tesis doctoral que lleva por título "From Structure to Function: Understanding Vip3Aa's Mode of Action", para optar al Grado de Doctor por la Universitat de València.

Y para hacer constancia, de acuerdo con la legislación vigente, firman la presente en Burjassot, a 11 de marzo de 2025.

Directores:

Dr. Juan Ferré Manzanero **Dra. Patricia Hernández Martínez**

Instituto BIOTECMED
Dpto. Genética, Universitat de València
Dr. Moliner 50, 46100 Burjassot, España.

El **Dr. Francisco Estruch Ros**, Catedrático del Departamento de Bioquímica y Biología Molecular de la Facultad de Ciencias Biológicas de la Universitat de València,

Informa:

Que la **Sra. Maria Lázaro Berenguer**, Graduada en Biotecnología, ha realizado bajo su tutorización el trabajo de investigación recogido en esta tesis doctoral que lleva por título "From Structure to Function: Understanding Vip3Aa's Mode of Action", para optar al Grado de Doctor por la Universitat de València.

Y para hacer constancia, de acuerdo con la legislación vigente, firma la presente en Burjassot, a 11 de marzo de 2025.

Tutor:

FRANCISCO BORJA| ESTRUCH|ROS

Firmado digitalmente por FRANCISCO BORJA| ESTRUCH|ROS
Fecha: 2025.03.11 08:55:06 +01'00'

Dr. Francisco Estruch Ros
Dpto. Bioquímica y Biología Molecular, Universitat de València
Dr. Moliner 50, 46100 Burjassot, España.

Acknowledgements/Agradecimientos/Agraïments

En primer lugar, quiero dar las gracias a mis directores de tesis, por haberme guiado en este camino; no podría haber elegido mejor compañía para este viaje.

Joan, gràcies per haver-me acollit al teu grup i per donar-me l'oportunitat de fer una tesi doctoral. Encara recorde la primera trucada de telèfon que vaig rebre aquell estiu de 2014, quan m'oferires ser alumna col·laboradora al teu grup. Qui m'hauria dit aleshores que allò era l'inici d'un camí que avui em porta a llegir la meua tesi. Gràcies per confiar en mi, pel teu suport constant i per la llibertat que m'has donat sempre, tant en el treball experimental com en l'escriptura. Gràcies per haver vist en mi la passió per la investigació i per ajudar-me a aconseguir els meus objectius.

Patri, todo lo que pueda escribirte aquí se queda corto. Gracias por ser mi estrella polar. Me reafirmo en decirte que quisiera parecerme a ti en todos los sentidos. Eres una científica brillante, inteligente, divertida, incansable, luchadora y generosa. Gracias por tus ideas de coche y de ducha, que nunca caen en saco roto, por tu confianza en mí. Pero, sobre todo, gracias por demostrar que ser una buena persona está por encima de todo. Contigo, me iría hasta el fin del mundo.

A los dos, gracias por haberme llevado de la mano y a la vez haberme dejado crecer en libertad. Estoy convencida de que he evolucionado

muchísimo como científica y como persona durante todos estos años, y es en gran parte gracias a vosotros, que me habéis enseñado no solo a volar con mis propias alas, sino también a disfrutar del vuelo.

También quiero agradecer a **todos mis compañeros presentes y pasados de LabCBP**. Ha sido un placer compartir este camino con vosotros. Gracias de corazón por vuestro compañerismo, generosidad y disposición. Siempre he sentido vuestro apoyo, tanto en los momentos de duda como en los de entusiasmo, y he podido contar con vuestro consejo y ayuda cada vez que los he necesitado. Gracias por estar siempre dispuestos a conversar, colaborar, compartir ideas y conocimientos y crear un ambiente de trabajo en el que ha sido un verdadero placer crecer profesional y personalmente. Por esos momentos de café al sol en las escaleras de emergencia, jueves de ATG, WoDs en el Taronja Box, los Canta Baila y Perrea, fiestas de Navidad, congresos y noches de karaoke que han supuesto la parte más divertida de todos estos años. De esta etapa de mi vida no solo me llevo una tesis doctoral, sino también grandes amistades. Vosotros me inspiráis y me hacéis ser mejor cada día, gracias.

También me gustaría agradecer a **Patricia Casino** por su inestimable ayuda en el diseño de mi tesis doctoral y su participación en el proceso de evaluación del manuscrito. Patricia: ha sido un verdadero placer trabajar contigo; he aprendido muchísimo de ti. Gracias por despertar en mí el interés por la biología estructural.

Quiero agradecer en particular a algunas personas su colaboración y ayuda durante el transcurso de mi tesis. **Quan**, thank you for teaching me everything you knew about Vip when I started out, my thesis wouldn't have been the same without your help. **Júlia**, gracias por tu ayuda con los experimentos durante estos últimos años. La pasión que sientes por la ciencia se percibe a distancia y es un lujo poder acompañarte en este camino. **Yolanda**, gracias por tu participación activa en las discusiones sobre Vip, que han sido de mucha ayuda en el desarrollo de mi tesis. Y **Dafne**, gracias infinitas por el precioso diseño de la portada de mi tesis, entre otras muchas cosas.

I would like to thank **Colin Berry** for welcoming me into his lab during my thesis stay. The months I spent in Cardiff were incredibly enriching both professionally and personally. But above all, I take with me friendships of immeasurable value. **Hannah**, thank you for being there when I needed it most, for opening your home to me, for your support and kindness. **Lainey**, thank you for your warmth and for always being so thoughtful and supportive. It's amazing how such strong bonds can form in such a short time.

I also want to express my gratitude to **Neil Crickmore, Kristina Sepčić, Salvador Herrero, Juan Luis Jurat-Fuentes** and **Sara García-Linares** for their invaluable contribution as members of the evaluation committee for my doctoral thesis. I deeply appreciate the time, effort, and dedication you devoted to reviewing my work.

No puedo cerrar esta etapa sin dar las gracias a mi familia, cuyo apoyo ha sido fundamental durante todo este tiempo. **Mamá y Papá**, a vosotros os lo debo todo. Gracias por ser mi puntal, por haberme ayudado a conseguir todas las metas que me ha propuesto la vida. He sentido vuestro respaldo constante y soy tremendamente afortunada de teneros conmigo. Yo también estoy orgullosa de vosotros, pues nada de esto habría sido posible sin vuestra ayuda e inspiración. A mi hermana **Marta**, muchas gracias a ti también por ser apoyo incondicional, mi compañera de travesuras y de vida. Os quiero mucho a los tres. Gracias también a la **familia Sánchez-Sabater** y a la **familia Pastor-Alonso**, a quienes quiero como si fueran mis padres y hermanos. A **mi padrino** y a **mis abuelitos,** que ya no están, ojalá hubierais podido verme leer la tesis, os llevo siempre conmigo en cada paso que doy.

Y **Alberto**, gracias a ti por ser mi alma gemela, pero en versión hater. No sé qué haría sin ti. Gracias por ser mi fan número uno, por cuidarme y quererme como lo haces. Y sobre todo por conseguir que no me muriera de hambre mientras escribía la tesis. En ti encuentro a la mejor pareja, amigo, chef personal y spotter que podría tener. Te quiero muchísimo.

Esta tesis ha sido financiada por la Generalitat Valencia y el Fondo social Europeo, bajo el marco de las Ayudas para la Contratación de personal Investigador en Formación (ACIF/2019/150).

Index of contents

Pg. no.

List of abbreviations, acronyms and symbols

aa – amino acid/s

Ac. No. – accession number

AEBSF – 4-(2-Aminoethyl) benzenesulfonyl fluoride

AH – amphipathic helix

ALP – alkaline phosphatase

Amp – ampicillin

ANOVA – analysis of variance

APN – aminopeptidase N

BBMV – brush border membrane vesicles

BCIP – 5-bromo-4-chloro-3-indolyl phosphate

BPPRC – bacterial pesticidal protein resource centre

BSA – bovine serum albumin

Bt – *Bacillus thuringiensis*

Cas9 – CRISPR-associated protein 9

CBM – carbohydrate binding module

CF – carboxyfluorescein dye

cm – centimetre/s

cm^2 – square centimetre/s

CPE – ceramide phosphoethanolamine

cpm – counts per minute

Cry – crystal proteins

Cryo-EM – cryo electron microscopy

Cryo-ET – cryo electron tomography

CRISPR – clustered regularly interspaced short palindromic repeats

C-t – C-terminal

DAPI – 4′,6-diamidino-2-phenylindole

DF – degrees of freedom

dH_2O – distilled water

DIP – disabled insecticidal protein

DNA – deoxyribonucleic acid

DOPC – 1,2-dioleoyl-sn-glycero-3-phosphocholine

DOPE– 1,2-dioleoyl-sn-glycero-3-phosphoethanolamine

EGTA – ethyleneglycol-bis (β-aminoethyl ether)-N,N,N',N'-tetraacetic acid

EM – electron microscopy

F – forward (primer for PCR)

FGFR – fibroblast growth factor receptor

FL – fiducial limits

GalNAc – N-acetylgalactosamine

GlcNAc – N-acetylglucosamine

GM – genetically modified

GM1 – monosialotetrahexosylganglioside

GPI – glycosylphosphatidylinositol

GST – glutathione S-transferase

G2/M – second growth phase of the cell cycle followed by the mitosis

h – hour/s

HCl – hydrochloric acid

HPTLC – high performance thin layer chromatography

IPP – isoelectric point precipitation

IPM – integrated pest management

IPTG – β-D-1-thiogalactopyranoside

ISAAA – International Service for the Acquisition of Agribiotech Applications

K_d – dissociation constant

kDa – kilodalton/s

kV – kilovolt/s

LB – Luria-Bertani broth

LC_{50} – lethal concentration 50% of mortality

LC_{90} – lethal concentration 90% of mortality

LUVs – large unilamellar vesicles

L3 – larval stage 3

M – molar

MALDI-TOF – matrix-assisted laser desorption/ionization time of flight

mCi – millicurie/s

MET – buffer containing mannitol, Tris and EGTA

mg – milligram/s

$MgCl_2$ – magnesium chloride

min – minute/s

mL – millilitre/s

mM – millimolar

$MnCl_2$ – manganese chloride

MPCA – microbial pest control agent

NaCl – sodium chloride

NaI – sodium iodide

NBT – nitro blue tetrazolium

NCBI – National Centre for Biotechnology Information

ng – nanogram/s

nm – nanometre/s

NS-EM – negative staining-electron microscopy

N-t – N-terminal

N_2 – nitrogen gas

N/A – not applicable

OD_{600} – optical density at 600 nm wavelength

PBS – phosphate-buffered saline

PBST – phosphate-buffered saline with Tween 20

PCR – polymerase chain reaction

PDB – Protein Data Bank

Pg. no. – page number

pH – potential of hydrogen

PIBM – polyisobutyl methacrylate

PM – peritrophic matrix

pmol – picomole/s

PMSF – phenylmethylsulfonyl fluoride

PVDF – polyvinylidene fluoride

R – reverse (primer for PCR)

RH – relative humidity

rpm – revolutions per minute

R_t – binding sites concentration

RT – room temperature

SD – standard deviation

SDM – site-directed mutagenesis

SDS – sodium dodecyl sulfate

SDS-PAGE – sodium dodecyl sulfate - polyacrylamide gel electrophoresis

Se – *Spodoptera exigua*

SE – standard error

SEM – standard error of the mean

*Se*MJ – *Spodoptera exigua* midgut juice

Sf9 – *Spodoptera frugiperda* ovary-derived cell line 9

Sf21 – *Spodoptera frugiperda* ovary-derived cell line 21

SfCHS2 – *Spodoptera frugiperda* chitin synthase 2 gene

SfMyb – Myb transcription factor from *Spodoptera frugiperda*

Sl – *Spodoptera littoralis*

*Sl*MJ – *Spodoptera littoralis* midgut juice

spp. – species

SRCC – scavenger receptor class C

S-S – disulfide bond

TBS – tris-buffered saline

TLC – thin layer chromatography

Tm – melting temperature

Tris – tris(hydroxymethyl)aminomethane

Tween 20 – polyoxyethylene (20) sorbitan monolaurate

UCSF – University of California San Francisco

US or USA – United States of America

Vip – vegetative insecticidal protein

v/v – volume/volume

v/v/v – volume/volume/volume

w/w – weight/weight

w/v – weight/volume

WT or Wt – wild type

x*g* – times gravity (relative centrifugal force, RCF)

XIC – extracted ion chromatograms

X-ray – X-ray radiation

α – alpha

β – beta

β-ME – β-mercaptoethanol

γ – gamma

μg – microgram/s

μm – micrometre/s

μM – micromolar

Å – ångström

~ – approximately

° – degrees (angle)

°C – degrees Celsius

% – percentage

$ – USA dollars

< – less than

> – greater than

χ^2 – chi-square

I – one in roman numbers

II – two in roman numbers

III – three in roman numbers

IV – four in roman numbers

V – five in roman numbers

^{125}I – iodine-125 radioisotope

1D – one-dimensional

2D – two-dimensional

3D – three-dimensional

Index of tables and figures

Pg. no.

TABLES

FIGURES

CHAPTER 2

CHAPTER 3

CHAPTER 4

CHAPTER 5

GENERAL DISCUSSION

SUPPLEMENTARY INFORMATION

Summaries

Resumen extendido

A nivel global, la superficie agrícola abarca aproximadamente 5 mil millones de hectáreas, lo que representa el 37% de la superficie terrestre del planeta. De este total, alrededor del 11% se destina a la producción de cultivos, mientras que el 26% restante se emplea como pastizales para el ganado. La presión sobre las tierras de cultivo a nivel mundial va en aumento, debido a la necesidad de satisfacer la demanda alimentaria de una población en constante crecimiento, que se estima alcanzará los 10 mil millones de personas para el año 2050. Este incremento poblacional impulsa una mayor exigencia de alimentos y acentúa la presión sobre los recursos terrestres, que son limitados.

En consecuencia, los sistemas agrícolas deben optimizar su eficiencia, principalmente a través de la intensificación (aumento del rendimiento de los cultivos) y, en menor medida, mediante la extensificación (expansión de las tierras de cultivo). En este contexto, las plagas agrícolas representan un desafío crucial, provocando pérdidas anuales de entre el 20% y el 40% de la producción global de cultivos. Las enfermedades de las plantas generan costes económicos mundiales de aproximadamente 220 mil millones de dólares cada año, representando las plagas de insectos una pérdida de 70 mil millones de dólares. El desarrollo de estrategias eficaces de control de plagas es, por tanto, una prioridad urgente para garantizar la seguridad alimentaria y demanda agrícola actual y futura.

Ejemplos de plagas de insectos que afectan a cultivos agrícolas de gran importancia son las especies de lepidópteros del género *Spodoptera*. Popularmente conocidos como gusanos cogolleros, dicho género de insectos incluye varias especies de lepidópteros que son plagas agrícolas de gran relevancia global debido a su comportamiento invasivo y amplia distribución. Sus larvas son altamente polífagas, alimentándose de una gran variedad de cultivos, pastos y hortalizas, lo que provoca considerables pérdidas económicas en la agricultura. En la presente tesis doctoral, dos especies del género *Spodoptera* han sido empleadas para caracterizar el modo de acción de la proteína insecticida Vip3Aa. La especie *Spodoptera exigua*, o gusano cogollero de la remolacha, es originaria del sur de Asia y actualmente está ampliamente distribuida en África, Asia, Australia, Norteamérica y el sur de Europa, y afecta diversos cultivos hortícolas y ornamentales, como algodón, maíz, frijoles, tabaco, alfalfa y árboles frutales. La especie *Spodoptera littoralis*, conocida como gusano cogollero del algodón, es nativa del África subsahariana y es una de las plagas más destructivas en áreas tropicales y subtropicales. Está distribuida en África, Europa mediterránea y Oriente Medio, alimentándose de una amplia gama de cultivos, entre ellos maíz, algodón, tomate, pimiento, patata, alcachofa, coles, plátanos, apio, alfalfa, menta y berros.

El control de plagas agrícolas ha dependido históricamente de pesticidas químicos, pero el uso excesivo de estos, ha provocado problemas ambientales y el desarrollo de resistencias en insectos. Como alternativa sostenible, se ha recurrido al uso de la bacteria *Bacillus thuringiensis* (Bt), que produce una variedad de proteínas tóxicas para

distintos invertebrados con alta especificidad, razón por la cual se ha utilizado ampliamente como agente microbiano de control de plagas (MPCA) en la agricultura, siendo los productos a base de Bt los MPCAs más usados a nivel mundial. Su amplio espectro insecticida, los mínimos efectos que provoca sobre organismos no diana, la seguridad para los consumidores y el bajo impacto ambiental que implica su uso en la agricultura, hacen de los productos de Bt una herramienta ideal para la protección de cultivos dentro de los sistemas de manejo integrado de plagas (MIP), especialmente por su compatibilidad con otras estrategias de manejo agrícola tales como el control biológico mediante el uso de enemigos naturales.

La ingeniería genética de plantas ha dado un gran impulso al control de plagas con la introducción en plantas de los genes *cry* de Bt (codificantes para proteínas insecticidas Cry) otorgándoles protección contra el ataque de insectos plaga, dando origen a los llamados cultivos Bt que han sido empleados en agricultura desde la década de 1990. En la actualidad, los cultivos Bt constituyen un componente clave en la agricultura y se cultivan en más de 20 países alrededor del mundo, principalmente en todo el continente americano, el sureste asiático y Australia. Estos cultivos se desarrollan y plantan comercialmente en aproximadamente 101 millones de hectáreas a nivel global, representando más del 50% del área total de cultivos genéticamente modificados en el mundo.

Entre las proteínas insecticidas producidas por Bt, las más conocidas y ampliamente utilizadas en cultivos Bt, son las proteínas Cry, que

forman inclusiones cristalinas parasporales durante la fase estacionaria de crecimiento de la bacteria y presentan toxicidad frente a un amplio espectro de órdenes de insectos como Lepidoptera, Diptera, Coleoptera, Hymenoptera y Hemiptera, además de ciertas especies de nematodos. Otras clases de proteínas producidas por Bt son las proteínas Vip, Xpp, Mpp, Vpa, Vpb, Cyt, Tpp, Sip, Gpp y App. De entre estas proteínas, las proteínas Vip (de sus siglas en inglés *Vegetative insecticidal proteins*) se secretan durante la fase vegetativa de crecimiento de la bacteria y son tóxicas exclusivamente para insectos lepidópteros, la presente tesis doctoral se enfoca en el estudio de la proteína Vip3Aa perteneciente a esta clase de proteínas insecticidas.

Según la base de datos de aprobaciones de organismos modificados genéticamente (GMO) del Servicio Internacional para la Adquisición de Aplicaciones biotecnológicas Agropecuarias (ISAAA), se han aprobado para su comercialización en varios países 67 eventos de maíz, 15 eventos de algodón y 2 eventos de soja que contienen genes *vip3Aa* para la expresión de proteínas Vip3Aa y la protección frente a insectos lepidópteros que son importantes plagas agrícolas. Aunque algunos eventos contienen solo el gen *vip3Aa*, la mayoría de ellos combinan este gen con uno o más genes *cry* para ampliar el espectro insecticida y evitar la aparición de resistencias en insectos. La introducción de varios genes que codifican para proteínas insecticidas con diferentes especificidades en el mismo cultivo transgénico se conoce como "piramidación génica". Esta estrategia permite ampliar el espectro de acción de los cultivos Bt y prevenir la aparición de resistencia en los insectos. Además del maíz, algodón y soja, los genes *vip* también han sido introducidos en otros

cultivos como el arroz y la caña de azúcar y se espera que el número de cultivos que contienen genes *vip* aumente en el futuro próximo.

Para optimizar el uso de las proteínas insecticidas en el control de plagas agrícolas, es fundamental contar con un conocimiento profundo de su espectro de acción y su mecanismo de funcionamiento. Los recientes avances en las técnicas de resolución de estructuras proteicas han sido clave en este campo, ya que han permitido formular hipótesis sobre el modo de acción de estas proteínas, basándose en la homología estructural con otras proteínas previamente estudiadas. Esto, a su vez, facilita el diseño de variantes modificadas e incluso mejoradas, potenciando su efectividad.

La estructura tridimensional de la proteína Vip3Aa ha sido recientemente resuelta mediante criomicroscopía electrónica revelando que consiste en una molécula tetramérica estable con estructura piramidal, y estando cada monómero compuesto por cinco dominios estructurales diferentes. En el extremo N-terminal (N-t) de la proteína se localizan los Dominios I y II con estructura secundaria de plegamiento en α-hélice. Dichos dominios conforman el núcleo central de la proteína y son claves para la oligomerización de la misma. El Dominio I contiene cuatro hélices α, siendo la primera altamente anfipática. Las segunda y tercera hélices α forman un haz antiparalelo que adopta una configuración diferente en los monómeros externos e internos del tetrámero debido a la longitud variable del bucle que conecta las hélices α1 y α2 y que resulta en la rotación de las hélices α2 y α3, formándose un haz de ocho hélices que sobresale del núcleo

tetramérico de la molécula. Tras el Dominio I, en el bucle que conecta el Dominio I con el II, se localiza un sitio de corte proteolítico por tripsina (sitio primario de corte proteolítico). El Dominio II comienza después del sitio de corte primario y está compuesto por cinco hélices α que estabilizan el tetrámero mediante bucles extendidos que proyectan hacia subunidades adyacentes. En el extremo C-terminal (C-t) de la proteína, se localizan tres dominios con estructura globular y plegamiento en hoja-β que permanecen expuestos al solvente (Dominios III, IV y V). Dichos dominios presentan homología estructural con proteínas de unión a carbohidratos. El Dominio III contiene tres hojas β antiparalelas que forman un plegamiento tipo prisma β, comúnmente presente en lectinas. Por otra parte, los Dominios IV y V tienen homología estructural con motivos de unión a carbohidratos (CBM) presentes en hidrolasas de glicósidos, sugiriendo una posible función en la unión a glicanos para estos dominios. De esta forma, la región C-t de la proteína podría desempeñar un papel en la unión de Vip3Aa a sus receptores.

Además, estos estudios estructurales llevados a cabo con la proteína Vip3Aa también revelaron la existencia de un importante cambio conformacional de la proteína tras el procesamiento proteolítico en el sitio de corte primario, ocurriendo a consecuencia del corte proteolítico una reorganización estructural en la parte N-t de la proteína (Dominio I) y distinguiéndose por tanto dos conformaciones estructurales diferentes: la conformación de protoxina, con forma piramidal y donde el Dominio I de los distintos monómeros forma un haz de ocho hélices que sobresale del tetrámero; y la de proteína activada tras el remodelado

estructural, en el que las hélices del Dominio I de los cuatro monómeros forman un *coiled-coil* tetramérico que sobresale del cuerpo de la proteína formando una estructura elongada tipo "aguja" cuyo extremo no presenta estructura organizada, (la hélice α1 de naturaleza anfipática) y que es capaz de insertarse en membranas lipídicas y actuar como canal para el transporte de iones. Estando por tanto el Dominio I implicado en la toxicidad de la proteína en su conformación de proteína activada.

La mayoría de los estudios sobre el modo de acción de las proteínas Vip se han realizado utilizando principalmente proteínas Vip3Aa. Actualmente, se acepta generalmente que las proteínas Vip ejercen su acción tóxica en la siguiente secuencia de eventos: en primer lugar, las proteínas son secretadas en el medio en forma de protoxinas solubles que auto-oligomerizan en tetámeros. Tras la ingestión por las larvas, las proteínas son procesadas por las proteasas intestinales en el lumen, facilitando así la transición de la forma de protoxina a la de proteína activada. Una vez procesadas, atraviesan la matriz peritrófica y alcanzan la membrana del borde en cepillo (membrana apical) de las células epiteliales del intestino, donde se unen a sus receptores específicos. Dicha unión desencadena la inserción en la membrana y la formación de poros que causan la muerte celular por rotura del equilibrio osmótico como mecanismo principal de toxicidad, aunque otros mecanismos de muerte celular además de la formación de poro podrían estar ocurriendo de forma adicional. Sin embargo, muchos aspectos del modo de acción de estas proteínas, tales como la identidad de sus receptores específicos o los detalles de su mecanismo de toxicidad permanecen todavía desconocidos.

En este contexto la investigación de esta tesis doctoral se centra en caracterizar el modo de acción de la proteína Vip3Aa, especialmente centrándose en el estudio de su capacidad de unión a receptores específicos del epitelio intestinal de larvas del género *Spodoptera* y su relevancia para la toxicidad. Se ha llevado a cabo un estudio de varios aspectos estructurales de la proteína que podrían influir en la unión de la misma a sus receptores en el intestino. Los objetivos específicos de la tesis consisten en: (1) evaluar la existencia de sitios de unión compartidos entre las proteínas Vip en el epitelio intestinal de *Spodoptera littoralis* y la funcionalidad de dichos sitios compartidos; (2) evaluar el papel estructural y funcional del Dominio I de la proteína Vip3Aa y el cambio conformacional que ocurre tras la activación proteolítica para la actividad insecticida contra *Spodoptera exigua*; (3) determinar si la unión de Vip3Aa a receptores específicos y funcionales de *S. exigua* está restringida a la conformación de proteína activada; (4) estudiar el papel de los diferentes dominios estructurales de la proteína Vip3Aa en la estabilidad y en la unión específica y funcional en *S. exigua*; y (5) explorar la capacidad de la proteína Vip3Aa para unirse a moléculas lipídicas extraídas de tejido intestinal de larvas de *Spodoptera spp*. así como a lípidos estándares comúnmente encontrados en membranas celulares.

Para la consecución de los distintos objetivos de la tesis se han utilizado diversas técnicas experimentales tales como: la expresión heteróloga de proteínas en *Escherichia coli* y su purificación por diversas técnicas cromatográficas (cromatografía de afinidad, cromatografía de exclusión molecular y cromatografía de intercambio aniónico); la generación de

versiones modificadas de la proteína Vip3Aa mediante mutagénesis dirigida y amplificación de secuencias por PCR y clonaje en vectores de expresión; la realización de bioensayos de toxicidad por contaminación superficial en dieta artificial para evaluar la toxicidad de las proteínas frente a larvas de *Spodoptera spp.*; la realización de ensayos de unión *in vitro* a vesículas de membrana del borde en cepillo (BBMV) con proteínas Vip3Aa marcadas radioactivamente con I^{125}; la extracción de lípidos de tejido intestinal de larvas de *Spodoptera spp.* y realización de ensayos de unión a los mismos mediante dot-blot y cromatografía en capa fina; y la visualización de la estructura de distintas versiones modificadas de la proteína Vip3Aa mediante microscopía electrónica de contraste negativo.

Los resultados de la tesis doctoral se muestran en cinco capítulos diferentes, cada uno de ellos enfocado al abordaje de cada uno de los objetivos específicos planteados en la tesis:

En el **Capítulo 1**, mediante la realización de ensayos de unión *in vitro* a BBMV de *S. littoralis*, se demostró que las proteínas Vip3Aa, Vip3Af y Vip3Ca comparten sitios de unión específicos en el epitelio intestinal de dicha especie. Sin embargo, mientras que Vip3Aa y Vip3Af comparten todos los sitios de unión, Vip3Ca solo es capaz de unirse a una parte de los receptores de las proteínas Vip3A. Dichos resultados implican la existencia de distintas poblaciones de sitios de unión para la proteína Vip3Aa. Además, la realización de ensayos de competencia *in vivo* en larvas de *S. littoralis* permitió distinguir la existencia de sitios funcionales y sitios no relevantes para la toxicidad, siendo los sitios

compartidos entre Vip3Aa y Vip3Af funcionales mientras que los compartidos con Vip3Ca no. Dichos ensayos de competencia *in vivo* consisten en administrar a las larvas combinaciones a ratio creciente de una proteína tóxica (versión silvestre de la proteína) y una versión modificada de la misma (o de otra proteína heteróloga) que no es tóxica, pero sí conserva la capacidad de unión a los receptores intestinales (DIP, *disabled insecticidal proteins*). Si ambas proteínas compartes receptores funcionales, se observa un bloqueo de la toxicidad de la proteína silvestre con el aumento de proteína competidora no tóxica. En este trabajo, también se pudieron observar diferencias en la afinidad de unión a receptores entre las distintas proteínas, Vip3Aa es capaz de unirse con mayor afinidad que Vip3Af a los sitios de unión, aunque Vip3Ca es la más eficiente en unirse a los receptores compartidos con Vip3Aa (a pesar de que estos no son funcionales para la toxicidad de las proteínas Vip3A). Estos hallazgos son relevantes para el diseño de estrategias de control de la aparición de resistencias basadas en la combinación de distintas proteínas en cultivos Bt o "piramidación génica".

En el **Capítulo 2**, se generaron mutantes de Vip3Aa con alteraciones en el Dominio I para evaluar su efecto en la estructura de la proteína y en la toxicidad de la misma. Diversos aspectos estructurales se abordaron, entre ellos la eliminación de la hélice α1 hipotéticamente implicada en la inserción de la proteína en membrana; la alteración del cambio conformacional mediante la formación de puentes disulfuro entre las hélices α del Dominio I impidiendo su remodelado a la conformación activada; la inserción de mutaciones puntuales dentro de la hélice α1

(buscando una mejoría en la toxicidad); en el bucle localizado entre la hélice α1 y α2 para introducir un sitio de corte proteolítico adicional y entre los Dominios I y II para eliminar el sitio proteolítico primario; en la región más estrecha del *coiled-coil* para reducir el diámetro interno del mismo y la eliminación de los dominios C-t IV y V para evaluar su efecto en el cambio conformacional y la toxicidad. Los resultados indicaron que el corte proteolítico en el sitio primario es esencial para el cambio conformacional que a su vez es necesario para la toxicidad, al igual que la integridad de la hélice α1, ya que su eliminación causa la pérdida de toxicidad, y la inserción de la mutación puntual M34L dentro de la misma resulta un aumento de la toxicidad. La ausencia de la hélice α1 también resultó en una conformación constitutiva de proteína activada, demostrando el papel de dicha región de la proteína en el mantenimiento de la conformación de protoxina. De forma similar, la modificación del bucle localizado entre las hélices α1 y α2 (sustitución de residuos de Gly por Lys) afectó la capacidad de remodelado de la proteína a su conformación activada, revelando la importancia de la existencia de flexibilidad en dicha región para la mecánica apropiada del cambio conformacional. Además, se observó que los Dominios IV y V juegan un papel en dicho cambio conformacional, ya que su deleción resulta en la ausencia de remodelado estructural, pudiendo ser esta la causa de la pérdida de toxicidad en el constructo truncado que solo contiene los Dominios I-III. Por otra parte, la reducción del diámetro interno de la estructura de *coiled-coil* no mostró efectos drásticos en la toxicidad, sugiriendo que el flujo de iones a través de la completa

longitud de la molécula no debe ser determinante para la toxicidad y que posiblemente, el flujo ocurra en la parte N-t de la estructura.

En el **Capítulo 3**, mediante el uso de mutantes estructurales que bloquean la conformación de la proteína en su estructura de protoxina o de proteína activada, se abordó el estudio de la capacidad de unión de las diferentes conformaciones de la proteína al epitelio intestinal del insecto *S. exigua*. Mediante ensayos de unión *in vitro* a vesículas del borde en cepillo, se observó que la protoxina presenta una unión fundamentalmente inespecífica, mientras que la proteína activada muestra una unión específica y de mayor afinidad. No obstante, ambas conformaciones comparten receptores específicos, y además, ambas son capaces de unir a receptores funcionales *in vivo*, dado que se observó bloqueo de la toxicidad de la proteína silvestre (*wild type*, WT) por parte de ambos mutantes estructurales en *S. exigua*. Estos resultados indican que la conformación en la que la proteína se encuentra no es relevante para la unión a receptores funcionales.

En el **Capítulo 4**, se emplearon diferentes constructos truncados de la proteína Vip3Aa conteniendo solo algunos de sus dominios estructurales. Dichos mutantes fueron analizados en ensayos de unión *in vitro* a vesículas del epitelio intestinal de *S. exigua* para evaluar el papel de los distintos dominios estructurales en la unión específica. Los resultados confirman el importante papel del Domino III en la unión específica y revelan la contribución parcial de los Dominios IV y V en dicha unión. Además, mediante ensayos de estabilidad frente a proteasas por digestión *in vitro*, se observó que la ausencia de la parte

N-t de la proteína (Dominios I y II) resulta en una baja estabilidad frente a proteasas, lo que puede estar relacionado con la falta de formación de tetrámeros y a su vez con la ausencia de competencia total observada en los ensayos de unión *in vitro*. Finalmente, mediante el empleo del constructo truncado conteniendo los Dominios I-III (el único que conserva la estructura tetramérica, es estable frente a proteasas y es capaz de desplazar toda la unión específica de la proteína WT a las vesículas de *S. exigua*) en ensayos de competencia *in vivo* en larvas de *S. exigua* y *S. littoralis*, se observó que la ausencia de los Dominios IV y V impide la unión a receptores funcionales para la toxicidad, poniendo de manifiesto el relevante papel que estos dominios juegan *in vivo*.

Finalmente, para explorar el papel de los Dominios C-t (III-V) con homología estructural a lectinas y motivos de unión a carbohidratos (CBM), en el **Capítulo 5** se abordó un estudio preliminar de la capacidad de unión de la proteína Vip3Aa a lípidos extraídos del epitelio intestinal de larvas de *Spodoptera spp.* y de lípidos estándares comúnmente presentes en membranas celulares. Los resultados muestran que la proteína Vip3Aa es capaz de unir a lípidos de la membrana intestinal de *Spodoptera spp.*, aunque aún es necesario investigar la especificidad de esta unión y su implicación en la toxicidad. Especialmente considerando que Vip3Aa también es capaz de interaccionar con extractos lipídicos de insectos no susceptibles. Además, derivado de los ensayos de unión a lípidos estándares, varios lípidos de membrana fueron identificados como interactores de Vip3Aa, siendo estos fosfoesfingolípidos (esfingomielina y lisoesfingomielina), glicoesfingolípidos (glucosilceramida) y fosfolípidos más simples (fosfatidilcolina), todos

ellos moléculas lipídicas comunes en las membranas celulares. Estos resultados proporcionan información preliminar sobre los posibles residuos que podrían actuar como epítopos de unión a los lípidos que componen las membranas celulares del epitelio intestinal (fosfocolina y glucosa como principales grupos polares de los lípidos con los que Vip3Aa interacciona). Asimismo, nuestros resultados también sugieren que los tres dominios C-t de la proteína podrían estar involucrados en dichas interacciones.

En resumen, esta tesis se centra en el estudio de las características estructurales de la proteína insecticida Vip3Aa y la relevancia de las mismas para su función, mediante el uso de mutantes de posiciones puntuales y constructos truncados en ensayos de estabilidad frente a proteasas, ensayos de unión al tejido diana *in vitro*, y bioensayos con larvas para evaluar su toxicidad frente a especies del género *Spodoptera.* Los resultados de esta tesis enfatizan varios aspectos estructurales que resultan esenciales para la función de la proteína.

Una de las características estructurales más importantes para garantizar la estabilidad de la proteína frente a proteasas intestinales, la capacidad de unión a receptores específicos y la toxicidad, es la formación de tetrámeros. El Dominio I de la proteína es esencial para la oligomerización, siendo a su vez crucial para la estabilidad de la proteína.

Además de su importante papel en la formación de tetrámeros, el Dominio I presenta un rol central en la toxicidad, siendo su cambio

conformacional que sufre tras la activación proteolítica, otro aspecto estructural clave y de vital importancia para la actividad insecticida de la proteína. Además del rol del Dominio I en este cambio conformacional, nuestros resultados también ponen de manifiesto que los Dominios C-t IV y V son necesarios para el adecuado remodelado conformacional de la proteína a la conformación activada. La hélice α1 (ubicada en el extremo N-t del Dominio I) también es otro aspecto estructural esencial para la toxicidad de la proteína en su forma activada, conteniendo la región putativa transmembrana y consistiendo en una hélice de naturaleza anfipática. No obstante, esta hélice también juega un papel estructural clave en el mantenimiento de la conformación de protoxina al interactuar con las hélices del Dominio II, manteniendo la formación del haz de ocho hélices que le otorga su aspecto piramidal.

En cuanto a la capacidad de la proteína para unirse a sus receptores específicos en la membrana del borde en cepillo del epitelio intestinal, se ha reportado que la conformación de la proteína no es un factor crítico, ya que tanto la protoxina como la proteína activada muestran unión al epitelio intestinal de *S. exigua*. El Dominio III de la proteína ha mostrado ser el dominio más relevante para la unión específica. Sin embargo, no se puede descartar una posible contribución de los Dominios C-t IV y V en la unión específica de Vip3Aa. La formación de tetrámeros tampoco es crítica para la unión específica. Hasta la fecha, se han propuesto varios receptores para las proteínas Vip, aunque ninguno se ha validado completamente *in vivo*, por lo que la identidad de sus receptores funcionales sigue siendo desconocida. Los datos de

unión *in vitro* obtenidos en ensayos con proteínas Vip3A marcadas radiactivamente y vesículas de membrana en cepillo de *Spodoptera spp.* sugieren una gran población de sitios de unión de baja afinidad en comparación con las proteínas Cry. Además, la población de sitios de unión de Vip3Aa revelada en los ensayos *in vitro* no refleja completamente los receptores involucrados en la toxicidad de la proteína, ya que algunos sitios de unión detectados *in vitro* no son funcionales, como hemos demostrado mediante ensayos de competencia *in vivo* entre diferentes proteínas Vip. Adicionalmente, el uso de mutantes conformacionales (con conformación constitutiva de protoxina o de proteína activada) en estos ensayos de competencia *in vivo*, reveló que la conformación de la proteína no es una característica crítica para la unión a receptores funcionales, lo que sugiere que el cambio conformacional de la proteína procesada proteolíticamente podría ocurrir tanto antes como después de la unión a los receptores intestinales. Sin embargo, el contexto y momento en el que ocurre dicho cambio de conformación podría tener un importante efecto en la capacidad de la proteína de insertarse en la membrana y consecuentemente en la toxicidad.

Aunque la presencia de los Dominios I-III es suficiente para la unión específica *in vitro*, nuestros resultados muestran que la presencia de los Dominios IV y V es necesaria para la toxicidad de Vip3Aa *in vivo*, el remodelado estructural de la proteína activada y la unión a receptores funcionales. Dado que ambas conformaciones de la proteína se unen a receptores funcionales, podemos asumir que la falta de toxicidad en el constructo Vip3Aa_I-III no se debe a la ausencia de cambio

conformacional, sino que está relacionada con la ausencia de unión a sitios de unión funcionales. Dado el reciente descubrimiento de la interacción de la proteína Vip3Aa con la matriz peritrófica de larvas de *Spodoptera frugiperda* a través del Dominio V y su relevancia para la toxicidad, podemos hipotetizar que una alteración en este paso del modo de acción previo a la unión en el epitelio intestinal, podría ser causante de la ausencia de unión a sitios funcionales y consecuente pérdida de toxicidad del constructo truncado que carece de los Dominios IV y V, junto con su incapacidad de adoptar la conformación de proteína activada. Más estudios son necesarios para validar esta hipótesis y comprender el papel funcional de estos dominios de la proteína.

Dado que los dominios C-t III-V de Vip3A muestran homología estructural con lectinas (el Dominio III presenta un plegamiento tipo prisma β) e hidrolasas de la familia CBM16 (Dominios IV y V), junto con el hecho de que estas proteínas parecen presentar una amplia población de sitios de unión de baja afinidad, de los cuales algunos no son funcionales para la toxicidad, hemos hipotetizado que las proteínas Vip podrían unirse a diferentes tipos de moléculas glicosiladas en la membrana apical de las células del epitelio intestinal. Para probar esta hipótesis, hemos explorado la capacidad de la proteína Vip3Aa para unirse a moléculas lipídicas, que están presentes en gran cantidad en las membranas celulares y se han descrito como receptores para otras proteínas formadoras de poros. Nuestros hallazgos sugieren que Vip3Aa podría estar interactuando con lípidos de membrana tanto en su forma de protoxina como en la procesada por tripsina,

probablemente mediante la unión a sus grupos hidrofílicos. Sin embargo, la especificidad de esta unión y su posible papel en la facilitación de la toxicidad aún deben ser determinados, especialmente dado que Vip3Aa también se une a extractos lipídicos de insectos no susceptibles. No obstante, podemos plantear la hipótesis de la existencia de un mecanismo de unión en dos pasos, donde una unión primaria a lípidos y glicoconjugados en la superficie de las células del epitelio intestinal, incluso si dicha unión no es selectiva o específica, podría facilitar el acercamiento de la proteína a la membrana y su interacción posterior con receptores específicos, mediando su toxicidad. Mecanismos de unión de este tipo se han sugerido para otras proteínas de Bt.

En definitiva, la resolución de la estructura tridimensional de las proteínas Vip ha avanzado significativamente nuestra comprensión de su modo de acción. Se han realizado descubrimientos clave, como la identificación de dos conformaciones estructurales distintas: la protoxina y la proteína activada, así como la capacidad de la proteína activada para insertarse en las membranas lipídicas a través de su región N-t, facilitando el flujo de iones. Además, se ha identificado homología estructural entre los dominios C-t y las proteínas de unión a glicanos. Estos avances han permitido una investigación más dirigida sobre el modo de acción de las proteínas Vip. Nuestra investigación se ha centrado en evaluar la capacidad de unión a receptores de ambas conformaciones estructurales, explorando el papel crucial de la región N-t (Dominio I) y su remodelado para la toxicidad, e hipotetizando interacciones potenciales con moléculas de diferente naturaleza

bioquímica a través de los dominios C-t. Sin embargo, muchos aspectos del modo de acción de las proteínas Vip aún no se comprenden completamente. Se requieren estudios adicionales para desentrañar completamente estos procesos y comprender sus implicaciones para el uso de proteínas Vip en el control biotecnológico de plagas.

Las **conclusiones** de la presente tesis doctoral son las siguientes:

(1) las proteínas Vip comparten sitios de unión en la membrana del borde en cepillo de *Spodoptera littoralis*. Vip3Aa tiene múltiples poblaciones de sitios de unión, pero las que comparte con Vip3Ca no contribuyen a su toxicidad. En contraste, Vip3Aa y Vip3Af comparten sitios de unión funcionales *in vivo*, siendo Vip3Aa la que muestra una mayor afinidad por ellos;

(2) varias características estructurales de la proteína Vip3Aa son esenciales para su toxicidad contra *Spodoptera exigua*: la formación de tetrámeros, el remodelado estructural del Dominio I en su conformación activada tras el procesamiento proteolítico en el sitio primario (entre los Dominios I y II) y la integridad de la hélice α1 en el extremo N-t;

(3) tanto la conformación estructural de protoxina como la de proteína activada de Vip3Aa se unen a sitios de unión funcionales en *S. exigua.* Aunque la unión de la protoxina es principalmente no específica. La proteína activada muestra una unión específica y de mayor afinidad;

(4) Los Dominios IV y V, localizados en el extremo C-t, no son necesarios para la formación del tetrámero ni para la estabilidad de la proteína

frente a las proteasas intestinales; sin embargo, su ausencia afecta al cambio de conformación a la de proteína activada. Además, estos dominios no son esenciales para la unión de Vip3Aa a sitios específicos en la membrana del borde en cepillo de *S. exigua in vitro*, aunque su presencia es crucial para la unión *in vivo* a sitios funcionales en *S. exigua* y *S. littoralis*;

(5) Vip3Aa puede unirse a los lípidos extraídos del tejido intestinal de larvas de *S. exigua* y *S. littoralis*, aunque la especificidad de su unión y el papel en la toxicidad siguen sin estar claros. Su capacidad para unirse a los lípidos de insectos no susceptibles sugiere un posible mecanismo de unión en dos etapas, donde interacciones iniciales no específicas podrían ayudar a la proteína a alcanzar receptores específicos en la membrana. Además, los residuos de glicanos podrían servir como epítopos de unión para estas interacciones a través de los Dominios C-t III-V de la proteína.

Summary

This doctoral thesis focuses on characterizing the mode of action of the insecticidal protein Vip3Aa from *Bacillus thuringiensis*. This protein specifically targets lepidopteran insects, which are significant agricultural pests, making it a valuable tool for genetically modified crops that express insecticidal protein genes to confer resistance against insect attacks.

Vip3Aa adopts a pyramidal tetrameric structure, with each monomer composed of five distinct structural domains. At the N-terminus (N-t), Domains I and II form the protein core, facilitating oligomerization. Domain I is crucial for insecticidal activity, as it undergoes a conformational change upon proteolytic activation. This transformation converts the eight-helix bundle seen in the protoxin structure into an elongated coiled-coil structure in the activated protein conformation, allowing membrane insertion and ion channel formation, which are responsible for its toxicity. Domains III, IV, and V, located at the C-terminal (C-t) end, exhibit structural homology with carbohydrate-binding proteins (lectins and hydrolases), suggesting that these domains may play a role in receptor binding. Upon ingestion by larvae, Vip3Aa is processed by intestinal proteases, crosses the peritrophic matrix, and binds to receptors in the midgut epithelium, forming pores that disrupt osmotic balance and trigger cell death. While this toxicity mechanism is widely accepted as the primary mode of action, many details remain unknown.

This thesis investigates the protein's ability to bind to specific receptors in the midgut epithelium of *Spodoptera spp.* larvae and the relevance of this binding for toxicity. The research adopts a structure-function relationship approach, addressing several structural aspects of the protein that might influence receptor binding and insecticidal activity across five objectives: (1) evaluation of shared binding sites among different Vip proteins and their functionality in *Spodoptera littoralis*; (2) analysis of the structural and functional role of Domain I and the conformational change occurring after proteolytic activation in the toxicity against *Spodoptera exigua*; (3) determination of whether Vip3Aa binding to specific receptors in *S. exigua* is restricted to its activated conformation; (4) investigation of the structural domains' role in protein stability and functional binding to *S. exigua*; and (5) exploration of Vip3Aa's ability to bind to lipid molecules from the midgut epithelium of *Spodoptera spp*. and standard lipids.

A variety of experimental techniques were employed: heterologous protein expression in *Escherichia coli*, chromatographic purification, site-directed mutagenesis, larval toxicity bioassays, binding assays to brush border membrane vesicles (BBMV) with radiolabelled proteins, lipid extraction from insect midgut tissue, binding to lipids via dot-blot assays and TLC-overlays, and negative-stain electron microscopy to characterize structural aspects of the protein.

The results are presented across five chapters, each addressing one of the stated objectives:

In **Chapter 1,** through *in vitro* binding assays to BBMV with radiolabelled Vip3Aa**,** we have demonstrated that Vip3Aa, Vip3Af, and Vip3Ca proteins share binding sites in the midgut epithelium of *S. littoralis*, although Vip3Ca binds to only a subset of Vip3Aa's receptors. *In vivo* competition assays revealed that the shared sites between Vip3Aa and Vip3Af are functional for Vip3A's toxicity, whereas those shared with Vip3Ca are not. These findings suggest distinct populations of binding sites for Vip3A proteins, with varying relevance for toxicity.

In **Chapter 2**, Vip3Aa mutants with alterations in Domain I were generated to assess its role in structure and toxicity. Proteolytic cleavage at the primary site was found essential for the required conformational change, which is also necessary for toxicity, as is the integrity of helix α1. The M34L point mutation increased the protein's toxicity against *S. exigua*. Additionally, Domains IV and V were shown to influence the conformational change, as their removal resulted in loss of toxicity and absence of structural remodelling into the activated conformation.

In **Chapter 3**, we investigated the binding capacity of Vip3Aa in its different conformations to *S. exigua* midgut epithelium. The protoxin binds non-specifically, whereas the activated protein exhibits specific binding with higher affinity. Nevertheless, both conformations share specific and functional receptors, suggesting that the conformational change might occur either before or after receptor binding.

In **Chapter 4**, we assessed the role of the different structural domains in the specific binding and stability. Domain III was found crucial for specific receptor binding, while the contribution of Domains IV and V

could not be ruled out, as their absence prevented binding to functional receptors. Furthermore, the absence of Domain I resulted in a lack of stability against proteases.

Finally, in **Chapter 5** we explored Vip3Aa's ability to bind lipids extracted from the midguts of *Spodoptera spp*. larvae and standard lipids commonly found in cellular membranes. Vip3Aa showed affinity for phosphosphingolipids and glycosphingolipids, suggesting a potential two-step binding mechanism in which an initial interaction with membrane lipids would facilitate proximity and binding to specific receptors mediating toxicity.

In summary, this thesis identifies several structural aspects essential for Vip3Aa's function: tetramerization is crucial for stability, receptor binding, and toxicity; Domain I is central to the conformational change required for the insecticidal activity, while Domains IV and V influence binding to functional receptors; the protein's activated conformation is not determinant for receptor binding but is essential for membrane insertion and toxicity; additionally, Vip3Aa's interaction with membrane lipids may facilitate its approach to specific receptors, suggesting a complex mode of action that warrants further study to enhance its agricultural applications.

Contributions

Chapter	Concept	Experiments	Writing	Review	Funding
Introduction	JF	-	YB JF PHM MLB	PHM	JF
Chapter 1	JF PHM	MLB YQ	JF MLB	JF PHM	JF
Chapter 2	YB PC JF MLB	YB MLB RNR FPM	PC MLB	EAP PC JF	EAP PC JF
Chapter 3	JF PHM MLB	MLB	MLB	JF PHM	JF
Chapter 4	PC JF PHM MLB	JGA MLB	MLB	JF PHM	JF
Chapter 5	CB HLB PHM MLB	MLB	MLB	JF PHM HLB	CB JF

Contributors: Ernesto Arias-Palomo (EAP), Yolanda Bel (YB), Colin Berry (CB), Hannah L. Best (HLB), Patricia Casino (PC), Juan Ferré (JF), Júlia G. Ases (JGA), Patricia Hernández-Martínez (PHM), Maria Lázaro-Berenguer (MLB), Rafael Núñez-Ramírez (RNR), Francisco Paredes-Martínez (FPM), Yudong Quan (YQ).

Introduction

Adapted from:
Ferré J, Bel Y, Lázaro-Berenguer M, Hernández-Martínez P. 2023. Vip3 insecticidal proteins: structure and mode of action. Adv Insect Phys 65, 93–122. https://doi.org/10.1016/bs.aiip.2023.09.006

I. Agricultural pests

Globally, agricultural land encompasses approximately 5 billion hectares, accounting for 37% of the Earth's land surface. Of this, about 11% is dedicated to crop production and the remaining 26% is used as pasture for livestock (FAO, 2024). The global cropland base faces mounting pressure to meet the food demands of a growing population, projected to reach 10 billion by 2050 (United Nations, 2024). This increasing population drives higher food demand and intensifies the strain on finite land resources. Consequently, agricultural systems must become more efficient, primarily through intensification (increased crop yields) and, to a lesser extent, extensification (expansion of cropland) (Sands *et al.*, 2023). In this context, agricultural pests present a critical challenge, causing annual losses of 20% to 40% of global crop production (FAO, 2024). Plant diseases incur global economic costs of approximately $220 billion each year, while invasive insects account for $70 billion, as reported by the Food and Agriculture Organization of the United Nations. Addressing these issues with effective pest control strategies is therefore an urgent priority to sustain current and future food consumption needs.

I.1 The *Spodoptera* genus

The *Spodoptera* genus, commonly known as armyworms owing to the gregarious behavior of their larvae (Fitzgerald and Costa, 1999), comprises several lepidopteran species widely recognized as major global pests. These insects have become major invaders, colonizing multiple continents outside their native range (Allen, 2022; Kergoat *et*

al., 2021). Their larvae are extremely polyphagous, causing extensive damage by feeding on a wide range of crops, grasses and vegetables, resulting in significant financial losses for agriculture globally (Allen, 2022; Pogue *et al.*, 2002; Sharma *et al.*, 2017). In this thesis, two different species of the genus have been used as a model to study the mode of action of the Vip3Aa insecticidal protein.

Spodoptera exigua

S. exigua (Lepidoptera: Noctuidae) (Hübner, 1808), is commonly known as the beet armyworm. This pest originated in South Asia and is nowadays widely distributed, affecting crop production in Africa, Asia, Australia, America and the south of Europe. It affects many horticultural and ornamental crops including vegetables, cotton, corn, beans, tobacco, alfalfa, flowers, and fruit trees (Azidah *et al.*, 2006; Kranz *et al.*, 1978; Mehrkhou *et al.*, 2012; Saeed *et al.*, 2010; Showler *et al.*, 2001). The life cycle of this lepidopteran is divided in four different stages: (1) egg, (2) larvae (with five different larval instars), (3) pupa, and (4) the adult moth (imago) (**Figure I1**).

Spodoptera littoralis

S. littoralis (Lepidoptera: Noctuidae) (Boisduval, 1833), is commonly known as the Egyptian cotton leafworm. It is native to Sub-Saharan Africa, and is one of the most destructive agricultural pests in subtropical and tropical areas, being widely distributed throughout Africa, Mediterranean Europe and the Middle East. It feeds on a wide range of commercial and ornamental crops such as: corn, cotton, tomato, pepper, potatoes, artichoke, cabbages, banana, celery, lucerne,

mint and watercress (Allen, 2022; EFSA, 2015; Hosny *et al.*, 1986; Sallama *et al.*, 1971). The life cycle of this lepidopteran is divided in four different stages: (1) egg, (2) larvae (with six different larval instars), (3) pupa, and (4) the imago (**Figure I1**).

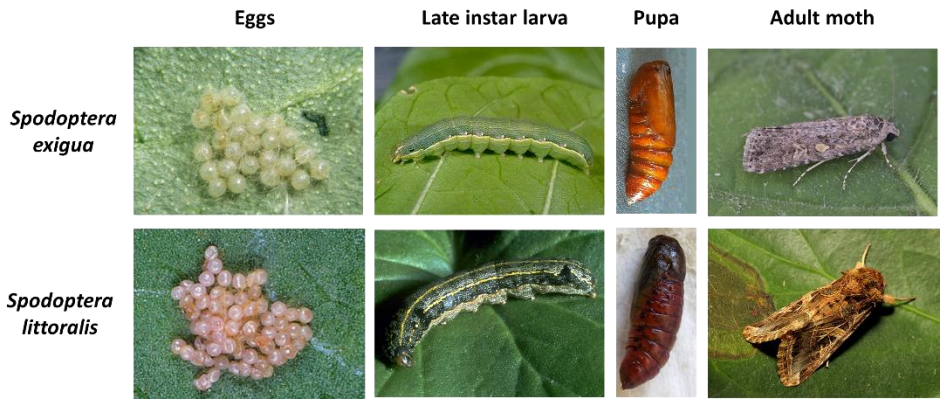

Figure I1. Life stages of *Spodoptera spp*. *S. exigua* eggs and adult moth photos by Kansas State University, Department of Entomology (entomology.k-state.edu) larva photo by Jeff Gore, pupa photo by Oregon State University (uspest.org). *S. littoralis* eggs photo by Nigel Cattlin, larva photo by Biologische Bundesanstalt für Land-und Forstwirtschaft (bugwood.org), pupa photo by Manuel Ramírez Mogrera, adult moth photo by Koppert España (koppert.es).

II. *Bacillus thuringiensis* general aspects and applications

Bacillus thuringiensis (Bt) (Firmicutes: Bacillaceae) (Berliner, 1915), was first identified in 1902 by Japanese biologist Shigetane Ishiwata, who discovered it in dead silkworms (*Bombyx mori*) (Lepidoptera: Bombycidae) (Linnaeus, 1758) suffering from a previously unknown disease affecting the silk industry. Ishiwata initially named it "Sottokin-Bacillus" which translates into English as "Sudden-death Bacillus" (Ishiwata, 1901, 1905). Shortly after, in 1911, German biologist Ernst Berliner isolated Bt from infected chrysalids of the Mediterranean flour moth (*Ephestia kuehniella*) (Lepidoptera: Pyralidae) (Zeller, 1879) from

the province of Thuringe, describing the bacterium and naming it after the German region as "*Bacillus thuringiensis*" (Berliner, 1911, 1915).

Bt is a gram-positive and endospore-forming bacterium that belongs to the *Bacillus cereus* group (**Figure I2**). It is a ubiquitous microorganism, its spores can be found in a wide variety of environments including soil, dead and living insects, stored grains and stagnant water surfaces. While the persistence of Bt in soil and on leaf surfaces is debated, the bacterium does not require insects to multiply, therefore being considered as an opportunistic pathogen (de Maagd *et al.*, 2001; Dubois *et al.*, 2012; Martin, 1994).

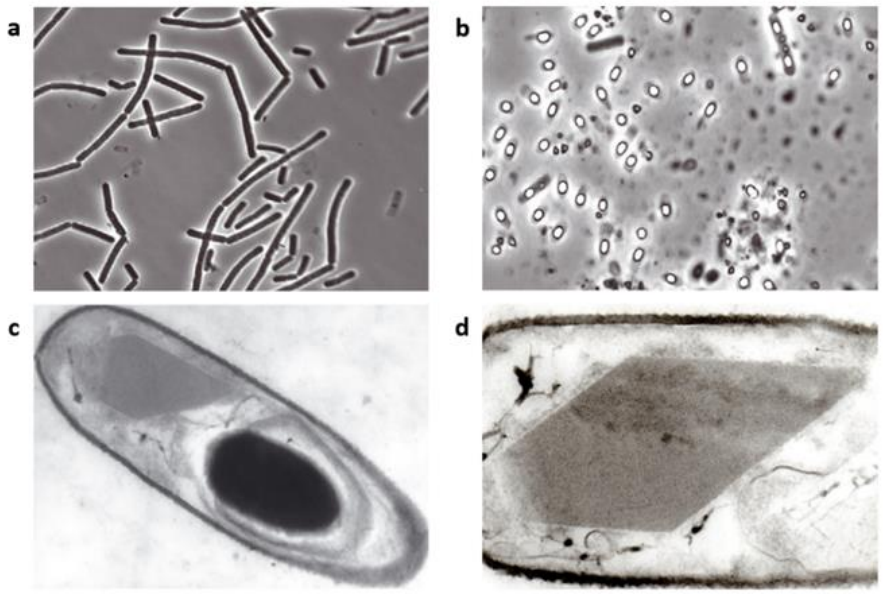

Figure I2. ***Bacillus thuringiensis* phase photomicrographs** of vegetative cells (a) and spores (b) at 1000X. Transmission electron micrographs of longitudinal sections of *B.thuringiensis* towards the end of sporulation, showing the spore (black ovoid structure) and the toxins with insecticidal properties (c), that accumulate to form a large bipyramidal crystal inclusion (d). Figure modified from Sanchis *et al.* (2011).

Bt produces a variety of proteins which are toxic to different invertebrates with high specificity, reason why it has been widely utilized as a microbial pest control agent (MPCA) for controlling agricultural pests, being Bt products the most widely used MPCAs globally (Deshayes *et al.*, 2017; Lacey *et al.*, 2015; Trajković and Žikić, 2023). Bt's broad insecticidal spectrum, minimal effects on non-target organisms, safety for consumers, and low environmental impact make Bt products an ideal tool for crop protection within Integrated Pest Management (IPM) systems (Belousova *et al.*, 2021; Betz *et al.*, 2000; Deshayes *et al.*, 2017). Especially given their compatibility with other crop management strategies, such as biological control using natural enemies (Koller *et al.*, 2023; Trajković and Žikić, 2023). The first commercial Bt biopesticides were developed between the 1930s and 1960s. However, after World War II, the widespread use of synthetic pesticides began as agricultural systems intensified (Alexandratos and Bruinsma, 2012; Sanchis, 2011). The overuse of chemical pesticides led to environmental contamination, health issues, and the appearance of resistance in insect populations, prompting the search for more sustainable agricultural solutions. In this context, efforts to develop new MPCAs or expand their applications have grown in recent decades to support more sustainable agriculture.

Plant genetic engineering has given a tremendous boost to pest control with the introduction of *cry* genes from Bt coding for Cry insecticidal proteins into plants (so called Bt-crops) since the 1990s, conferring them protection against the attack of insects (James, 1997; Estruch *et al.*, 1997; Gassmann and Reisig, 2023; Shelton, 2012). Nowadays, Bt-crops

constitute a key component in agriculture and are found in over 20 countries distributed across the globe, mainly in North and South America, South and East Asia and Australia (ISAAA, 2024). They are commercially developed and planted in approximately 101 million hectares worldwide and represent more than 50% of the global genetically modified (GM) crops cultivated area (ISAAA, 2024; James, 2015, 2017; Moar *et al.*, 2017).

Beyond its role as an insect pathogen, additional applications have been attributed to Bt (Jouzani *et al.*, 2017; Kumar *et al.*, 2021). For instance, Bt has been shown to promote plant growth as a rhizobacterium (Azizoglu, 2019) and has gained interest in medicine for its parasporins, which exhibit strong activity against human cancer cell lines (Santos *et al.*, 2022). In addition to these, other Bt industrial applications include bioremediation of heavy metals (Wróbel *et al.*, 2023), biosynthesis of silver nanoparticles (Banu *et al.*, 2014), and production of polyhydroxyalkanoate biopolymers (Singh *et al.*, 2013).

III. Bt insecticidal proteins

Among the insecticidal proteins produced by *B. thuringiensis*, the most well-known and widely utilized are the Cry proteins which conform parasporal crystalline inclusions that are formed during the stationary growth phase of the bacterium (**Figure I2**) and target a wide range of insect orders including Lepidoptera, Diptera, Coleoptera, Hymenoptera and Hemiptera, as well as certain species of nematodes (Rhabditida) (Crickmore *et al.*, 2024; Palma *et al.*, 2014) (**Figure I3**).

Other commercially important Bt proteins are Vip proteins, which are toxic against many Lepidopteran pests (Chakroun *et al.*, 2016a; Crickmore *et al.*, 2024; Schnepf *et al.*, 1998) (**Figure I3**). Other types of Bt toxins include Xpp proteins, toxic against Lepidoptera, Hymenoptera, Coleoptera and Rhabditida. Mpp proteins, active against Lepidoptera and Coleoptera. Vpa and Vpb proteins, toxic against Hemiptera and Coleoptera. Cyt and Tpp proteins, toxic against Diptera and Coleoptera. Sip and Gpp proteins with activity against Coleoptera, and App proteins which are toxic against Rhabditida (Crickmore *et al.*, 2024; Palma *et al.*, 2014) (**Figure I3**). Besides these proteins, Bt also produces several broad-spectrum virulence factors, including α- and β-exotoxins, hemolysins, enterotoxins, chitinases, and phospholipases, all contributing to Bt's necrotrophic nature (de Maagd *et al.*, 2001; Malovichko *et al.*, 2019).

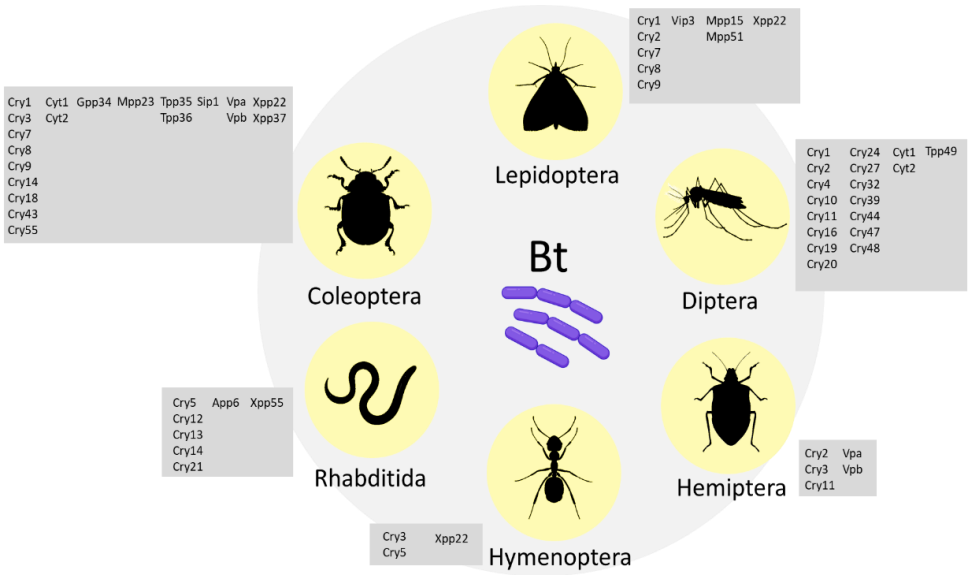

Figure I3. Host spectrum of Bt proteins according to invertebrate order. Information on toxicity adapted from Palma *et al.* (2014). Updated nomenclature of proteins according to Crickmore *et al.* (2021).

III.1. Vegetative insecticidal proteins (Vip)

Despite the success of Bt-crops expressing Cry proteins, some important insect pests have shown to be recalcitrant and the evolution of resistance to these proteins prompted the search for alternative insecticidal proteins (Bravo *et al.*, 2023; Downes and Mahon, 2012; Storer *et al.*, 2012; Tabashnik and Carrière, 2019). In this context, screening programs were started with the aim to find novel insecticidal proteins. Vip proteins were described in the late 90s in a screening focused on the search for insecticidal proteins produced before sporulation (Estruch *et al.*, 1996). In contrast to Cry proteins that accumulate in the parasporal crystal, Vip proteins are secreted to the culture media during the vegetative growth phase, and their name "Vip" is an acronym from "Vegetative Insecticidal Protein". However, the notion that Vip proteins are entirely secreted to the media has recently been challenged by a study suggesting the potential retention of Vip3Aa molecules within the mother cell (Wang *et al.*, 2021).

In Estruch *et al.* (1996), three different protein families were described, Vip1 and Vip2 were isolated from a *Bacillus cereus* strain and were active against *Diabrotica spp.* (Coleoptera: Chrysomelidae) (Estruch *et al.*, 1996). Whereas the third family, Vip3 proteins, were isolated from culture supernatants of *B. thuringiensis* strains highly toxic to *Agrotis ipsilon* (Lepidoptera: Noctuidae) (Hufnagel, 1766) and other lepidopterans (Estruch *et al.*, 1996). These new insecticidal proteins, Vip1, Vip2 and Vip3, were given names according to the Bt Toxin Nomenclature Committee, which classified insecticidal proteins mainly based on amino acid sequence similarity (Crickmore *et al.*, 1998). However, more

recently, a new nomenclature has been proposed based not only on the previous criteria but also based on structural features (Crickmore *et al.*, 2021). In this new nomenclature system, Vip1 and Vip2 are now named Vpa and Vpb respectively, whereas the use of the name "Vip" is restricted just to the previously named Vip3 proteins (Crickmore *et al.*, 2021). Vip proteins are classified into three different subfamilies based on their sequence homology: Vip3A, Vip3B and Vip3C. Among them, Vip3A is the most studied and widely used in pest control. In turn, Vip3A subfamily comprises several subtypes, such as Vip3Aa, Vip3Ab and Vip3Ac, with up to 95% sequence identity.

III.1.1. Vip insecticidal spectrum

Among Vip proteins, Vip3A show strong insecticidal activity against many lepidopterans (Chakroun *et al.*, 2016a). **Figure I4** shows a qualitative classification of some important agricultural pests according to their susceptibility to Vip proteins. In general, Vip3Aa, Vip3Ac, Vip3Ae, Vip3Af and Vip3Ag are active against most species tested, whereas Vip3Ab, Vip3B and Vip3C have activity against a limited number of them and Vip3Ad has no activity to any of the species tested.

Figure I4. Toxicity of Vip proteins. Only insect pests tested against at least 3 different Vip proteins are included. Data was extracted from BPPRC (https://www.bpprc.org). Toxicity is indicated as strong when LC_{50} is < 500 ng/cm², mL or mg (green circles), moderate (yellow circles, with LC_{50} > 500 ng/cm², mL or mg), and non-active (red).

III.1.2. Vip structure

Several conclusions can be drawn after alignment of Vip3A, Vip3B and Vip3C sequences (**Figure I5**). First of all, the N-terminal (N-t) part of the protein is highly conserved and contains a signal peptide responsible for the secretion of the protein, similar to other signal peptides described for *Bacillus* genus (a number of positively charged amino acids followed by a hydrophobic region) that ranges from 11 to ~30 amino acids in Vip3Aa (Doss *et al.*, 2002; Estruch *et al.*, 1996; Palma *et al.*, 2012; Rang *et al.*, 2005; Sauka *et al.*, 2013; Sellami *et al.*, 2018; Zhang *et al.*, 2022). Unlike most secreted proteins, the signal peptide region is not processed during Vip export (Chen *et al.*, 2003; Doss *et al.*, 2002; Estruch *et al.*, 1996) and it has been recently reported that it is crucial for Vip3Aa secretion via membrane vesicles (Zhang *et al.*, 2022). On the contrary, the C-terminal (C-t) part of the protein is the most variable part among Vip proteins. In the majority of the Vip members the sequence of the C-t half reveals a predicted carbohydrate binding module (CBM), generally present between amino acid positions ~535 to ~670 (Boonyos *et al.*, 2021; Chakroun *et al.*, 2016a; Chi *et al.*, 2019; Sellami *et al.*, 2018). It is also worth noting that there is a highly conserved trypsin processing site around amino acid residue 200, which splits the protein in two main fragments of 19 kDa and 65 kDa that remain attached after cleavage (Banyuls *et al.*, 2018; Bel *et al.*, 2017; Chakroun and Ferré, 2014; Quan and Ferré, 2019; Zack *et al.*, 2017). At the N-t of Vip proteins, there is also a conserved cleavage site (R∗ALPSF) which is responsible for the removal of the first 10–20 amino acids during the proteolytic processing of the protein (Zack *et al.*, 2017).

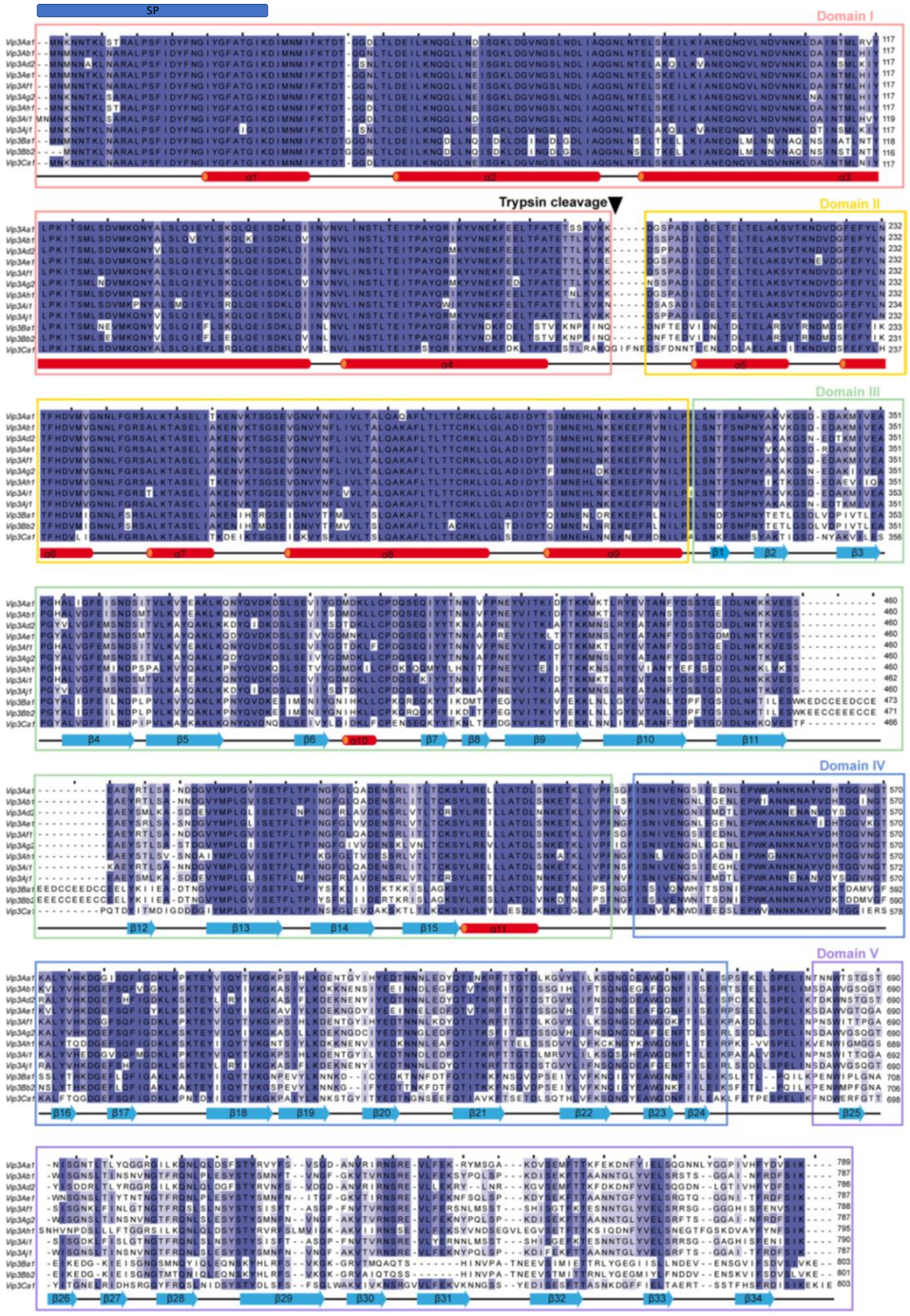

Figure I5. Multiple sequence alignment of the Vip family. Sequence identity is indicated using colours, where dark blue is 100–80% sequence identity, cobalt blue is 80–70%, light blue is 70–40% and white is < 40%. Structural domains are highlighted in coloured boxes. Secondary structure assignments refer to the Vip3Aa protoxin structure. SP, signal peptide. Figure modified from Núñez-Ramírez *et al.* (2020), published as supplementary information.

The Vip3Aa protein structure was recently solved at the near-atomic level by cryo-electron microscopy (cryo-EM) (Núñez-Ramírez *et al.*, 2020), confirming that it assembles into highly stable tetramers in agreement with previous reports (Zack *et al.*, 2017; Kunthic *et al.*, 2017; Palma *et al.*, 2017; Quan and Ferré, 2019). The 3D reconstruction of the protoxin revealed that the tetramer is in fact a dimer of dimers with a pyramid-shaped structure where the N-t region forms the core and apex of the molecule, and the C-t domains are exposed to the solvent (**Figure I6**) (Núñez-Ramírez *et al.*, 2020).

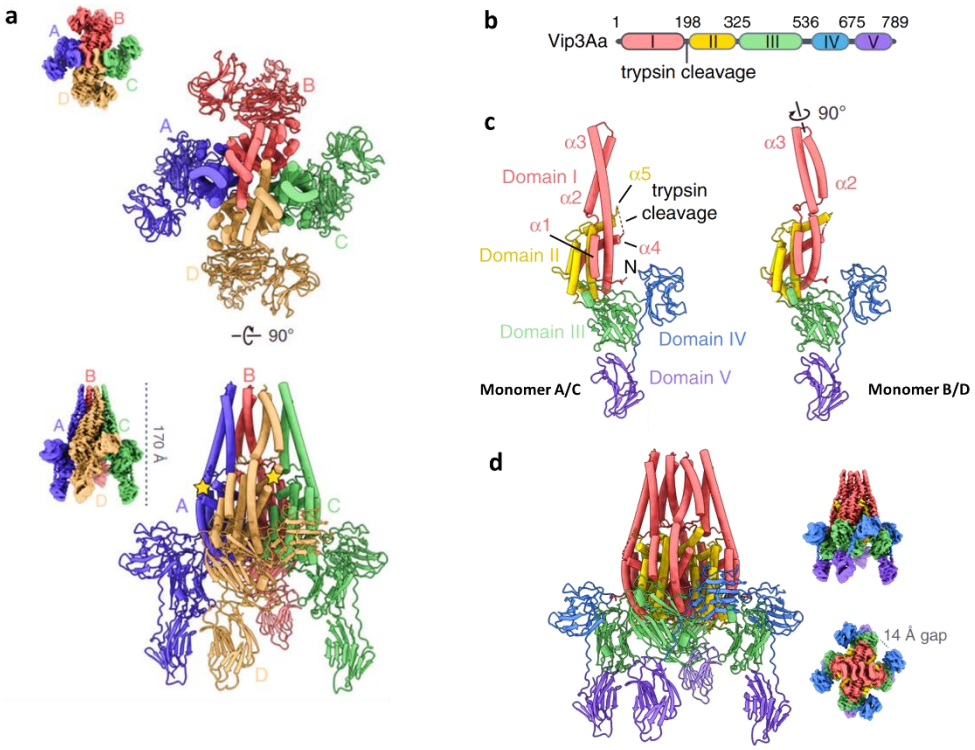

Figure I6. Protoxin structure of Vip3Aa. (a) Two orthogonal views of the protoxin with monomers coloured differently. Yellow stars indicate main trypsin cleavage site. Unsharpened EM maps are shown on the left. (b) Primary structure of Vip3Aa with domains organization. (c) Vip3Aa is formed by two types of monomers, outer (left), and inner (right), that exhibit a ~90° rotation of the α2–α3 helical bundle. (d) Vip3Aa protoxin tetramer coloured according to domain organization. Two orthogonal views of the EM reconstruction are shown on the right. Figure from Núñez-Ramírez *et al.* (2020).

The cryo-EM structure also confirmed that the Vip3Aa protein is composed of five distinct domains (**Figure I6b–d**) in agreement with earlier predictions (Quan and Ferré, 2019). The N-t domains I and II adopt secondary structure with α-helical folding whereas the C-t domains III-V show β-sheet folding (**Figure I6**) (Núñez-Ramírez *et al.*, 2020). Domain I extends up to the primary proteolytic site (K195) (Bel *et al.*, 2017; Zhang *et al.*, 2018) and contains four α-helices (α1–α4). The first helix is highly amphipathic and the second and third helices form an antiparallel bundle that adopts a different configuration in the outer and inner monomers (chains A, C and B, D respectively) (**Figure I6c**). Specifically, the variable length of the α1–α2 loop allows α2 and α3 of the internal monomers to rotate ~90° compared with the external subunits (Núñez-Ramírez *et al.*, 2020). This leads to the formation of an eight-helix bundle that protrudes from the tetrameric core of the protoxin molecule (**Figure I6a, d**). Domain II (residues 200-325) starts immediately after the trypsin cleavage site, which is located in a fully exposed loop that connects helix α4 and α5 (**Figure I6c**). This second domain is composed of five α helices and embodies the core of the tetramer (**Figure I6d**), playing an important structural role stabilizing the tetramer mainly through two extended loops (comprising residues 221–226 and 239–247, respectively) that project towards the adjacent subunit of the oligomer (Núñez-Ramírez *et al.*, 2020). The C-t region of the protein is composed of three globular domains that are mostly solvent exposed and do not show interactions between different monomers (Núñez-Ramírez *et al.*, 2020), existing a minimum separation gap of ~14 Å between neighbouring monomers (**Figure I6d**). Domain III

comprises residues 328–532 and contains three antiparallel β-sheets that form a β-prism fold with high structural similarity to the β-prism domain found in members of the Cry family, which has been associated to the binding function of these other insecticidal proteins (**Figure I7a**) (Bravo *et al.*, 2023; Li *et al.*, 1991; Núñez-Ramírez *et al.*, 2020). This third domain of the Vip3Aa, interacts and clamps the N-t helix α1 of Domain I (residues 14–23), against the core of the tetramer (Núñez-Ramírez *et al.*, 2020) (**Figure I7b**). The last two domains Domain IV (residues 536–668) and Domain V (681-789), bear similar CBM folds and are connected by a long linker (Núñez-Ramírez *et al.*, 2020). The DALI server (Holm and Sander, 1995) revealed that they show structural similarity to CBM16 modules present in glycoside hydrolases (Bae *et al.*, 2008), often found in tandem to increase affinity of these enzymes for polysaccharides (Borastom *et al.*, 2004). Domains IV and V show a high flexible nature maintaining the putative glycan binding sites exposed to the solvent (Núñez-Ramírez *et al.*, 2020) (**Figure I7c**).

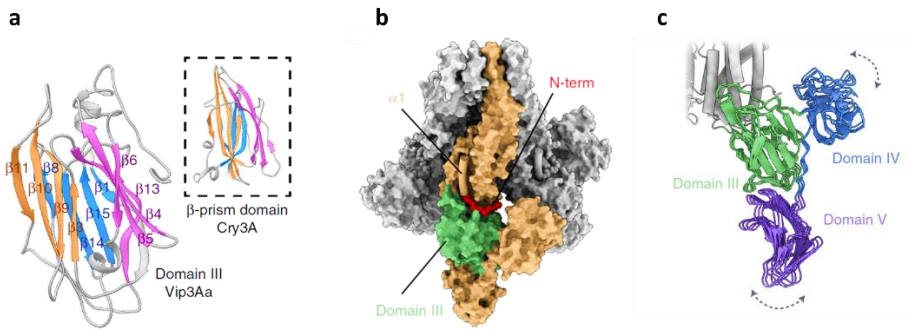

Figure I7. The C-terminal domains contain motifs found in other toxins. (a) Domain III forms a β-prism fold similar to that found in Domain II of the Cry toxins. (b) The N-t helix α1 of the four monomers (red) is inserted into a groove formed between Domain III (green) and the core of the particle. (c) Superposition of domains III, IV and V, docked into the three most distant positions found in the focused 3D classification, showing the flexibility of these domains in the Vip3Aa reconstruction. Figure modified from Núñez-Ramírez *et al.* (2020).

The resolution of the structure of Vip3Aa after trypsin incubation revealed that the proteolytic processing at the primary site triggers a large molecular reorganization of the protein (Núñez-Ramírez *et al.*, 2020) where the four monomers adopt an identical conformation arranged around the fourfold symmetry axis of the particle (**Figure I8a**), and confirmed that the cleaved fragments remain tightly associated. Interestingly, although the efficiency of the tryptic digestion was elevated (>95% according to the SDS-PAGE gel), approximately 30% of the molecules maintained a configuration similar to that of the undigested sample (protoxin conformation from now on). However, the majority of the particles (~70%) adopted a syringe-like structure (activated protein or toxin conformation from now on) (Núñez-Ramírez *et al.*, 2020).

The activated conformation of Vip3Aa shows the same domain organization described for the protoxin, and domains II–V maintain a similar global architecture (**Figure I8b**). However, Domain I suffers a large conformational change that remodels the helix-bundle conforming the apex of the pyramid in the protoxin into a ~200 Å-long extended stalk in the activated protein (Núñez-Ramírez *et al.*, 2020). During this remodelling, the three antiparallel N-t helices α2–α4 undergo a set of rotations, to form a long continuous helix that assembles into a parallel four-helical coiled-coil that extends for 160 Å in the activated Vip3Aa tetramer (**Figure I8c**), with an average internal radius of 1.46 Å (Núñez-Ramírez *et al.*, 2020). This coiled-coil is relatively ordered starting at α2 (~D45) but has a flexible end formed by the most N-t region of the protein, the helix α1 (**Figure I8c**). The length of this helix matches the

width of the membrane (Hildebrand *et al.*, 2004), which together with its highly amphipathic nature, suggest that it could become ordered in contact with the lipid bilayer to form a four-helix bundle which could transport protons and divalent metals through the membrane as has been reported for other structurally similar proteins such as influenza M2 protein (Cady *et al.*, 2010; Hong *et al.*, 2012; Joh *et al.*, 2014; Wang *et al.*, 2009).

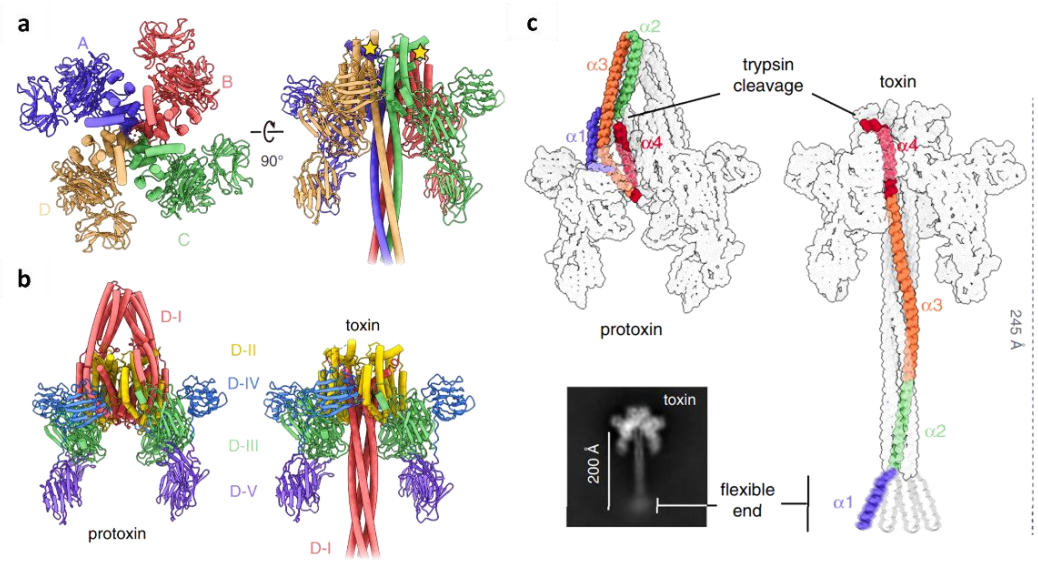

Figure I8. Molecular architecture of the trypsin activated Vip3Aa. (a) Two orthogonal views of the Vip3Aa toxin show that the four monomers are organized around a central pore. The different monomers have been coloured as in Figure I5a. Yellow stars indicate the position of the trypsin cleavage site. (b) Similar views of the Vip3Aa protoxin and activated toxin conformations coloured by domain organization as in Figure I5b. Domains are labelled as D-I-V. (c) The α-helices that comprise Domain I undergo a large reorganization that leads to the formation of an extended coiled-coil. The four helical bundle is ordered starting from residue ~45 and the most N-t region appears to be flexible. Figure modified from Núñez-Ramírez *et al.* (2020).

Classic coiled-coils are structures with repeating patterns where certain positions correspond to hydrophobic residues (Crick, 1952, 1953). In the Vip3Aa protein, while most residues at these positions are hydrophobic (~80%), some are polar, with asparagine being the most common (Núñez-Ramírez *et al.*, 2020). These hydrophilic residues, called N@d layers, can bind ions or water molecules in the central cavity of the tetrameric coiled-coil (Hartmann *et al.*, 2009; Tarbouriech *et al.*, 2000). Interestingly, in the case of Vip3Aa, a cluster of four symmetry related asparagines (N163) likely binds a divalent ion, that was assigned to a magnesium ion based on the buffer composition (Núñez-Ramírez *et al.*, 2020).

In addition to the structure of Vip3Aa, three other structures of Vip proteins have been reported at the atomic level. The structure of a Vip3B protoxin and two truncated constructs of Vip3B and Vip3Aa lacking Domain I were solved by X-ray crystallography (Zheng *et al.*, 2020; Jiang *et al.*, 2020a). The lack of Domain I resulted in dimer formation instead of tetramers, pointing to the necessity of Domain I for the correct oligomerization of these proteins.

The structure of Vip3Bc was also solved by cryo-EM both as protoxin and trypsin-activated toxin (Byrne *et al.*, 2021), revealing a significant structural similarity between Vip3Bc and Vip3Aa in both conformations. In addition, cryo-electron tomography (cryoET) allowed the visualization of how the activated Vip3Bc protein partially inserted into artificial liposomes via the N-t region (**Figure I9a, b**) and suggested that the helical bundle in the coiled-coil structure forms a pore of ~5 Å that could shuttle small ions, altering membrane permeability (Byrne *et*

al., 2021). These results also indicated that receptor binding is not required for membrane insertion and pore formation, since activated Vip3Bc was able to insert into large unilamellar vesicles (LUVs) of artificial composition (DOPC:DOPE, 6:4), allowing for the measurement of membrane permeability and ion transport (**Figure I9c**).

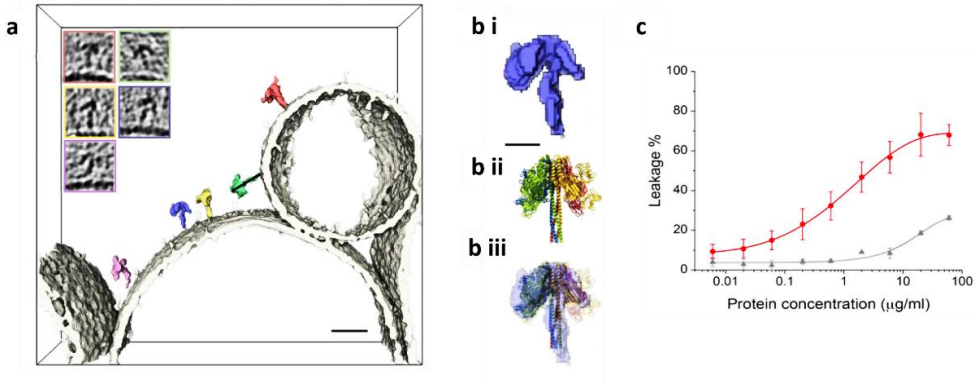

Figure I9. Vip3Bc activated protein insertion and pore formation in artificial liposomes. (a)Cryo-ET shows interaction of activated Vip3Bc1 (coloured) with the unilamellar vesicle (DOPC:DOPE, 6:4) (white). Images inset show section through the tomogram of the matching particle in segmentation. Scale bar 20 nm. (b) scaled comparison between segmented density for a single particle in the tomogram, with 5 nm scale bar (bi) compared to activated Vip3Bc1 model (bii) and with an overlay showing that the stalk density fits the 4-helix bundle well (biii). The helical stalk modelled in activated Vip3Bc1 does not account for all of the stalk density observed in the sub-volume, suggesting membrane insertion. (c) CF dye release from LUVs upon addition of ActVip3Bc1 (red) and ProVip3Bc1 (grey). Plotted data represents the mean and the error bars the standard deviation of the measurements from three independent replicates. Figure modified from Byrne *et al.* (2021).

Altogether, the obtaining of high-resolution structures of Vip proteins has confirmed previous hypotheses suggesting that the N-t region is involved in toxicity via membrane interaction, while the C-t region might play a role in receptor-binding functions (Banyuls *et al.*, 2018; Quan and Ferré, 2019; Chakroun *et al.*, 2016a).

III.1.3. Vip proteins mode of action

Most studies on the mode of action have been performed using mainly Vip3Aa proteins, whereas there is limited information on other Vip proteins. It is generally accepted that Vip exert their toxic action in the following sequence of events: they are secreted into the medium as soluble protoxin forms which self-oligomerize into tetramers. After ingestion by the larvae, the proteins are processed by midgut proteases in the lumen, thereby facilitating the transition from the inactive to the active form. Once processed, they cross the peritrophic matrix (PM) and reach the brush border membrane (apical membrane) of midgut epithelial cells where they bind to specific receptors. This leads to membrane insertion and pore formation and/or other mechanisms causing cell death (**Figure I10**).

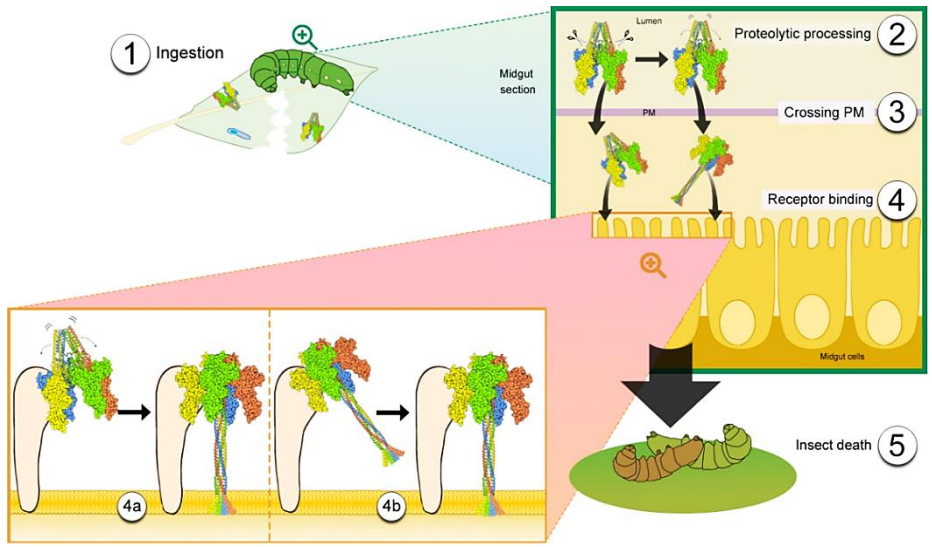

Figure I10. Proposed mode of action of Vip proteins. After ingestion (1), the full-length protoxin is proteolytically processed (2) and crosses the peritrophic matrix either in protoxin or activated conformation (3). Both scenarios are represented as it is not clear when the conformational change of the proteolytically-processed protein takes place. Then, the protein binds to receptors on the apical membrane of gut cells, followed by membrane insertion (4) and eventually the insect death (5).

III.1.3.1. Proteolytic processing

For other Bt proteins such as Cry proteins, it has been reported that different susceptibilities among insect species can be correlated with proteolytic processing capability (Abdelgaffar *et al.*, 2019). Similar studies have been carried out with Vip3A proteins, showing that the rate of protoxin processing into the active form accounts for differences in toxicity to several insect species (Abdelkefi-Mesrati *et al.*, 2011; Caccia *et al.*, 2014; Chakroun *et al.*, 2012; Gomis-Cebolla *et al.*, 2017; Jiang *et al.*, 2023a; Sun *et al.*, 2025). Vip proteins can be processed *in vitro* by the gut fluids of different non susceptible insects, rendering the expected activated form (Chakroun *et al.*, 2012; Gomis-Cebolla *et al.*, 2017; Lee *et al.*, 2003) which is toxic when fed to susceptible insects (Yu *et al.*, 1997). Therefore, as for Cry proteins, proteolytic activation of Vip proteins is a necessary step in the mode of action but not sufficient to cause toxicity *in vivo*.

Nowadays, there is agreement regarding the essential role of the five domains of Vip proteins in insect toxicity. However, previously there was a significant debate regarding which was the minimal fragment required for toxicity. Early studies claimed that the Vip3A toxic core was contained within a fragment ranging from 62 to 70 kDa (Abdelkefi-Mesrati *et al.*, 2011; Ben Hamadou-Charfi *et al.*, 2013; Gayen *et al.*, 2012; Lee *et al.*, 2003, 2006; Li *et al.*, 2007; Liu *et al.*, 2011). However, some studies with deletions in the N-t pointed out that the integrity of the 20 kDa fragment beyond residue 39 was needed for toxicity (Li *et al.*, 2007; Selvapandiyan *et al.*, 2001). Later, it was shown that the 20 kDa fragment remains strongly attached to the main fragment (62–70 kDa) after

activation by proteases (Bel *et al.*, 2017; Chakroun and Ferré, 2014; Quan and Ferré, 2019; Zack *et al.*, 2017). Finally, the resolution of the activated protein structure suggested the essential role that the N-t part of the protein (Domain I) might play in Vip toxicity (Byrne *et al.*, 2021; Núñez-Ramírez *et al.*, 2020).

It is important to note that several studies have shown that Vip proteins may have different modes of action depending on whether they are activated or not. It has been proposed that activated Vip proteins are able to insert into the membrane and induce pore formation (Byrne *et al.*, 2021; Lee *et al.*, 2003; Liu *et al.*, 2011), causing the larval death. On the other hand, studies carried out with cultured insect cells (*ex vivo* assays) have shown that Vip3A protoxins are toxic to cells, inducing apoptosis after being internalized (Hou *et al.*, 2020; Jiang *et al.*, 2016; Nimsanor *et al.*, 2020). However, a small fraction of activated Vip3Aa protein was detected after incubation of Vip3Aa protoxin with Sf9 cells (Jiang *et al.*, 2018a). Therefore, the presence of some activated Vip3Aa in other experiments performed with cultured insect cells cannot be excluded.

III.1.3.2. Interaction with the peritrophic matrix

The PM is a semi-permeable acellular structure composed mainly of chitin, proteins and glycoproteins (Terra, 2001). Besides improving digestion, it protects the epithelium from mechanical abrasion, pathogens and/or their virulence factors (Erlandson *et al.*, 2019). For other Bt toxins such as Cry1Ac, it has been reported that the passage through the PM is restricted via protein entrapment by binding to glycosylated proteins and chitin (Hayakawa *et al.*, 2004). However,

retention by the PM does not necessarily correlate with a lack of Cry proteins toxicity (Bravo *et al.*, 1992; Denolf *et al.*, 1993; Aranda *et al.*, 1996). In the case of Vip proteins, early histopathological observations suggested that the PM did not provide an efficient barrier for the Vip3A toxin in susceptible insects (Yu *et al.*, 1997). However, no direct information was available about this step until a recent study showing that Vip3Aa proteins bind to the PM via Domain V (Jiang *et al.*, 2023b). The authors proposed that this interaction contributes to Vip3Aa insecticidal activity, though it is not clear the mechanism by which this interaction can enhance toxicity. In addition, glycan array assays with purified biotin-labelled Vip3Aa indicate that it is able to bind chitin and chitosan, major components of the PM, as well as Lacto-N-tetraose and several monosaccharides including 6-deoxy-hexose, D-Fucose, L-Fucose and and L-Rhamnose (Jiang *et al.*, 2020b). Binding to these glycan molecules could explain the interaction of the protein to the PM, most likely through the CBM modules found in Domains IV and V.

III.1.3.3. Binding to the midgut epithelium

After crossing the PM, Vip proteins bind to their specific midgut receptors. It is generally accepted that this interaction eventually leads to cell death either by forming pores in the midgut cells or through other mechanisms that are discussed in more detail below. Binding of Vip proteins to the midgut epithelial cells has been extensively described by different approaches, including histological sections of the midgut probed with antibodies (Chakroun and Ferré, 2014; Yu *et al.*, 1997), ligand blots of brush border membrane vesicles (BBMV) (Lee *et al.*, 2003,

2006) and *in vitro* quantitative binding analysis using labelled proteins and BBMV (Chakroun and Ferré, 2014; Gomis-Cebolla *et al.*, 2017; Lee *et al.*, 2003, 2006; Quan *et al.*, 2021a; Sena *et al.*, 2009). *In vivo* immunolocalization of Vip proteins in the midgut of intoxicated larvae showed binding to the brush border membrane of midgut cells (**Figure I11**), confirming that midgut is the target site for these proteins (Chakroun and Ferré, 2014; Yu *et al.*, 1997).

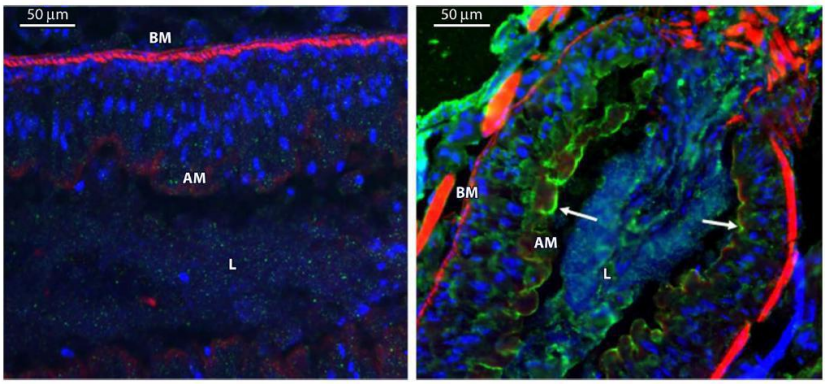

Figure I11. Immunolocalization of Vip3Aa in midgut tissue sections (10 µm) after *in vivo* ingestion by *Spodoptera frugiperda* larvae. Binding of Vip3Aa was revealed by Alexa Fluor-conjugated secondary antibody (green signal) using fluorescence microscopy. Nuclei were stained with DAPI (blue), and the apical and the basal membranes were stained with phalloidin (red). Magnification × 400. (Left) Larvae not exposed to Vip3Aa; (Right) larvae that ingested Vip3Aa. BM, basal membrane; AM, apical membrane; L, gut lumen. White arrows show the Vip3Aa protein bound to the midgut apical membrane. Figure from Chakroun and Ferré, (2014).

Specific binding to BBMV was shown for the first time using biotin-labelled Vip3Aa (Lee *et al.*, 2003). As well as for Cry proteins, binding was proven necessary though not sufficient for toxicity, as Vip3A proteins also bind specifically to BBMV from non-susceptible insects (Gomis Cebolla *et al.*, 2017; Lee *et al.*, 2003). Quantitative binding parameters have been obtained using ^{125}I labelled Vip3Aa, Vip3Af, and

Vip3C proteins with BBMV from several insect species (Chakroun and Ferré, 2014; Chakroun *et al.*, 2016b; Kahn *et al.*, 2018; Pinos *et al.*, 2020; Quan *et al.*, 2021a; Quan *et al.*, 2021b). Interestingly, both equilibrium dissociation constants (K_d) and the concentration of binding sites (R_t) are higher (around 10-fold) than the ones obtained for Cry proteins (Chakroun and Ferré, 2014), suggesting lower binding affinity and a higher number of binding sites.

The lack of shared binding sites among different insecticidal proteins makes them appropriate to be used in combination in transgenic crops and in spray products, even when the molecular identities of their surrogate receptors are not known (Jakka *et al.*, 2015). A large number of independent studies have shown that Vip3A and Cry proteins do not share binding sites (Bergamasco *et al.*, 2013; Chakroun and Ferré, 2014; Gouffon *et al.*, 2011; Hamadou-Charfi *et al.*, 2013; Lee *et al.*, 2006; Liu *et al.*, 2011; Quan *et al.*, 2021a; Sena *et al.*, 2009). Exceptionally, Bergamasco *et al.* (2013) reported partial competition of Cry1Ia for Vip3Aa-binding sites in *Spodoptera eridania* (Lepidoptera: Noctuidae) (Stoll, 1782). Within Vip proteins, all tested Vip3A proteins competed for the same binding sites, with no main differences in their binding affinity (Chakroun and Ferré, 2014; Quan *et al.*, 2021a).

Nowadays some putative Vip3Aa receptors have been proposed, including the ribosomal S2 protein (Singh *et al.*, 2010), the scavenger receptor class C protein (SRCC) (Jiang *et al.*, 2018b), the fibroblast growth factor receptor protein (FGFR) (Jiang *et al.*, 2018a), the prohibitin 2 (An *et al.*, 2022), and a tenascin-like glycoprotein (Estruch and Yu, 2001; Osman *et al.*, 2018, 2019). It is important to note that all the putative

receptors, except the tenascin-like glycoprotein, have been identified from *Spodoptera frugiperda* (Lepidoptera: Noctuidae) (Smith, 1797) ovary derived cultured cell lines (Sf9 and Sf21 cells). The tenascin-like glycoprotein was characterized as a potential receptor for Vip3A proteins from BBMV of *A. ipsilon*, though its role as functional receptor has not been shown (Osman *et al.*, 2018; Osman *et al.*, 2019). The role of the S2, SRCC, FGFR and prohibitin 2 proteins as receptors of Vip3Aa has been validated using cell cultures (Jiang *et al.*, 2018a; Jiang *et al.*, 2018b; An *et al.*, 2022). Nevertheless, since the ribosomal S2 protein is not localized in the plasma membrane, it seems unlikely that this protein is a binding molecule for the membrane interaction of Vip3Aa. The role of SRCC and FGFR as Vip3A receptors has been challenged by a recent study (Shan *et al.*, 2022) in which the authors showed that knocking out the genes encoding these two proteins using the CRISPR/Cas9 system on *S. frugiperda* larvae, did not alter susceptibility to Vip3Aa compared to that of the control strain. It is evident that more studies are necessary to shed light on the interacting membrane partners of Vip3A proteins.

III.1.3.4. Mechanisms of toxicity

The events that lead to toxicity after binding of Vip3A proteins to their specific receptors are not fully understood, though nowadays it is widely accepted that after insertion into the membrane Vip3A proteins produce osmotically-induced cell lysis by forming ion channels. However, additional mechanisms could also account for other aspects of toxicity, including the initiation of apoptosis (Jiang *et al.*, 2016). Early

studies showed extensive damage to midgut cells when susceptible insects were fed with Vip3A proteins (Yu *et al.*, 1997). The symptoms (cell swelling and lysis) matched what would be expected from the insertion of the protein into the cell membrane forming ion channels. Therefore, studies were undertaken to show the ability of Vip3A proteins to form pores on the membrane (Kunthic *et al.*, 2017; Lee *et al.*, 2003; Liu *et al.*, 2011). Using voltage clamping techniques, Lee *et al.* (2003) reported the formation of pores in dissected midguts of susceptible insects when incubated with trypsin-treated Vip3Aa, whereas the protoxin was unable to form pores. These early results showing that proteolytic activation was required for the pore forming activity was already evidencing that proteolytic processing is critical for the Vip3A mode of action. The trypsin-treated protein was unable to form pores in midguts from non-susceptible insects. The study also showed that the activated Vip3Aa made pores in planar lipid bilayers and that these were different from those formed by Cry1Ab based on the conductance stage and cation specificity (Lee *et al.*, 2003). Trypsin-activated Vip3Aa was also shown to form ion channels in BBMV from *Helicoverpa armigera* (Lepidoptera: Noctuidae) (Hübner, 1808) (Liu *et al.*, 2011) and permeabilize artificial liposomes (Kunthic *et al.*, 2017). In dye release assays with unilamellar vesicles, activated Vip3Bc was much more efficient (more than 100-fold) than the unprocessed protein, and its insertion into the membrane of the liposomes was directly observed (Byrne *et al.*, 2021).

Although the pore formation mechanism of Vip3A proteins is well accepted, different data support the idea that the mechanism of toxicity

may not be limited to pore formation, and that other mechanisms may also account for Vip toxicity, such as endocytosis (internalization) and apoptosis. However, it is important to note that most of the research on these other mechanisms used the Vip3Aa protoxin rather than activated Vip3Aa and experiments were performed on cultured *S. frugiperda* ovary derived cells. Singh *et al.* (2010) reported for the first time the internalization of the Vip3Aa protoxin into Sf21 cells and suggested that this process may be involved in toxicity. Internalization of Vip3Aa was suggested after immunolocalization in *S. frugiperda* midgut tissue sections (Chakroun and Ferré, 2014). Finally, another study reported internalization, via receptor mediated endocytosis, of the Vip3Aa protoxin into Sf9 cells (Jiang *et al.*, 2018b). The role of internalization on toxicity was validated using endocytosis inhibitors. Activated Vip3Aa was also shown to be internalized in Sf9 cells (Nimsanor *et al.*, 2020). The authors suggested that after internalization, the activated Vip3Aa protein may interact with cytosolic proteins, leading the disruption of cell division that subsequently could trigger cell death via apoptosis. Apoptosis has been described as a cellular response mechanism after exposure to different pore forming toxins (Cancino-Rodezno *et al.*, 2009; Galindo *et al.*, 2004). Indeed, an early report proposed that Vip3Aa may trigger an apoptotic pathway after binding to its midgut receptors in susceptible insects (Estruch and Yu, 2001). More recently, it has been shown that Vip3Aa proteins promote apoptosis in Sf9 cells by mitochondrial dysfunction after being internalized (Jiang *et al.*, 2016). The same group reported that Vip3Aa protoxin causes cell arrest at G2/M phase and induces apoptosis via disruption of mitochondrial

membrane potential and activation of Sf-caspase-1 (Jiang *et al.*, 2016). Later, Hou *et al.* (2020), showed the importance of lysosomes in the apoptosis process. The Vip3Aa protoxin promotes mitochondrial dysfunction, accumulation of reactive oxygen species, and activation of two caspases (3 and 9). However, adding a caspase inhibitor (Z-VAD-FMK) did not block the toxic effect of Vip3Aa protoxin to Sf9 cells, suggesting that other apoptosis-independent cell death mechanisms might be involved in toxicity (Hou *et al.*, 2020). Interestingly, *in vivo* assays showed that apoptosis occurred in insect midgut epithelial cells from *S. exigua* larvae treated with sublethal concentrations of Vip3Aa and Vip3Ca, but not at lethal concentrations (Hernández-Martínez *et al.*, 2017). Therefore, whether apoptosis is involved in Vip toxicity or it is related to the host defence mechanisms needs further study.

III.1.4. Vip expression in transgenic plants

According to the GM Approval Database from the International Service for the Acquisition of Agri-biotech Applications (ISAAA), 67 events of maize, 15 events of cotton and 2 events of soybean containing *vip3Aa* genes have been approved for commercialization in several countries (ISAAA, 2024). Nowadays, Vip3Aa proteins constitute a valuable component of commercialized Bt-maize and Bt-cotton protected against insects (Gassmann and Reisig 2023; Gupta *et al.*, 2021). Although a few events contain only the *vip3Aa* gene, most of them combine this gene with one or more *cry* genes. The introduction of various genes coding for insecticidal proteins with different specificity in the same transgenic crop is known as "gene pyramiding". This strategy allows to expand the

target spectrum of Bt-crops and prevent the appearance of insect resistance (Carrière *et al.*, 2015; Moar and Anilkumar, 2007; Tabashnik and Carrière, 2017).

Besides maize, cotton and soybean, *vip* genes have been introduced in other crops such as cowpea, rice and sugar cane, conferring them high protection against insect pests (Bett *et al.*, 2017; Riaz *et al.*, 2020; Xu *et al.*, 2018), and it is expected that the number of crops carrying *vip* genes increases in the future.

III.1.5. Evolution of Vip resistance

Few cases of resistance to Vip proteins have been reported, primarily through laboratory selection (Barkhade and Thakare, 2010; Bernardi *et al.*, 2016; Chakroun *et al.*, 2016b; Jin *et al.*, 2023; Liu *et al.*, 2024; Mahon *et al.*, 2012; Pickett *et al.*, 2017; Quan *et al.*, 2021b; Yang *et al.*, 2018, 2020; Wang *et al.*, 2022; Wen *et al.*, 2023) and, consistently with their non-shared binding sites, these Vip3A resistant insects were not cross-resistant to Cry1 and Cry2 proteins or this was extremely low. In agreement, insects resistant to Cry1 or Cry2 proteins were not cross-resistant to Vip3Aa or Vip3C proteins (Gomis Cebolla *et al.*, 2018; Tabashnik *et al.*, 2022; Qi *et al.*, 2021; Niu *et al.*, 2021; Jackson *et al.*, 2007; Anilkumar *et al.*, 2008; Welch *et al.*, 2015; Vélez *et al.*, 2013; Huang *et al.*, 2014; Fang *et al.*, 2007).

Studies estimating Vip3Aa resistance allele frequencies in field populations found that the appearance of major resistance alleles is not negligible (Bernardi *et al.*, 2015; Lin *et al.*, 2022; Mahon *et al.*, 2012; Yang *et al.*, 2013, 2018, 2020). In fact, an increase in Vip3Aa tolerance was

observed in *Helicoverpa zea* (Lepidoptera: Noctuidae) (Boddie, 1850) field populations in the US (Yang *et al.*, 2021). The majority of Vip3A resistance cases have been identified as recessive and likely conferred by a single autosomal gene, however a recent report has identified potential multi-genic Vip3A tolerance (Pezzini *et al.*, 2024). The underlying genetic mechanism of Vip resistance is unclear in most species, with a recent report of a midgut-specific chitin synthase (SfCHS2) gene being involved in Vip3A resistance in *S. frugiperda* (Liu *et al.*, 2024). Besides chitin synthase, other resistance-associated genes have also been reported recently: a previously undescribed gene HaVipR1 was first identified in *H. armigera* (Bachler *et al.*, 2024) and corroborated in *S. frugiperda* (Zhang *et al.*, 2024), and the transcription factor SfMyb was reported in *S. frugiperda* (Jin *et al.*, 2023). How these genes are involved in the resistance mechanism is still a matter of study. The primary mechanism of resistance to Cry proteins is altered midgut binding (Jurat-Fuentes *et al.*, 2021). However, Vip3Aa-resistant strains typically exhibit no binding alterations (Chakroun *et al.*, 2016b; Quan *et al.*, 2021b; Pinos *et al.*, 2020), except in one Vip3Aa resistant *H. zea* strain where reduced binding was observed (Kerns *et al.*, 2023). Therefore, either the current Vip binding assays do not reflect binding to the functional receptors or resistance is generally due to the alteration of post-binding events. Also, two resistance cases reported in *Spodoptera litura* (Lepidoptera: Noctuidae) (Fabricius, 1775) and *H. armigera* were linked to slower protoxin activation kinetics (Barkhade and Thakare, 2010; Chakroun *et al.*, 2016b).

Objectives

The general objective of this thesis is to characterize the mode of action of the *Bacillus thuringiensis* Vip3Aa insecticidal protein, specially focusing in its binding to specific receptors in the midgut epithelium of *Spodoptera spp.*, and the relevance of this binding for the toxicity. We have performed a structure-driven study of several aspects which might influence the binding of the protein to its midgut receptors. The specific objectives of the thesis are:

OBJECTIVE 1. Evaluate the existence of shared binding sites among Vip proteins in the midgut of *Spodoptera littoralis* and the functionality of shared binding sites;

OBJECTIVE 2. Evaluate the structural and functional role of Vip3Aa's Domain I and the conformational change occurring after proteolytic activation for the insecticidal activity against *Spodoptera exigua***;**

OBJECTIVE 3. Determine whether binding of Vip3Aa to *S. exigua* specific and functional receptors is restricted to the activated conformation;

OBJECTIVE 4. Study the role of the different structural domains of the Vip3Aa protein for the stability and the specific and functional binding to *S. exigua*;

OBJECTIVE 5. Explore the ability of the Vip3Aa protein to bind lipid molecules extracted from *Spodoptera spp*. midgut cells, and standard lipids commonly found in cellular membranes.

General materials and methods

I. Vip WT proteins, point mutations and truncated constructs

Table M1 summarizes the information on the various Vip WT proteins, truncations, and mutations used, detailing their purposes and indicating the chapters where the corresponding results are presented.

Table M1. Vip proteins used in the thesis

Protein	Information	Uses	Results
Vip3Aa90 WT	NCBI Ac. No. AAW65132	*In vitro* biding to *S. littoralis* (*Sl*)[a] BBMV[b] *In vivo* competition in *Sl*	Chapter 1
		Toxicity bioassays in *S. exigua* (*Se*) [c] Structure visualization by NS-EM[d]	Chapter 2
		In vitro digestion (Trypsin, *Se* gut juice and *Se* BBMV)	Chapters 2 and 4
		In vivo digestion in *Se*	Chapter 2
		In vitro binding to *Se* BBMV with conformational mutants as competitors *In vivo* competition with conformational mutants in *Se*	Chapter 3
		In vitro binding to *Se* BBMV with truncated constructs competitors *In vivo* competition with truncated constructs in *Se*	Chapter 4
		Binding to *Spodoptera spp.* lipids and standard lipids	Chapter 5
Vip3Af1 WT	NCBI Ac. No. CAI43275	*In vitro* binding in *Sl* BBMV *In vivo* competition in *Sl*	Chapter 1
Vip3Ca2 WT	NCBI Ac. No. AEE98106	*In vitro* binding in *Sl* BBMV *In vivo* competition in *Sl*	Chapter 1
Vip3Aa DIP1	S164C L166C	*In vitro* binding in *Sl* BBMV *In vivo* competition in *Sl*	Chapter 1
Vip3Aa DIP2	E168A	*In vitro* binding in *Sl* BBMV *In vivo* competition in *Sl* *In vivo* competition in *Se*	Chapter 1 Chapter 3
Vip2Af DIP	E168A	*In vitro* binding in *Sl* BBMV *In vivo* competition in *Sl*	Chapter 1
Vip3Ca DIP	S164C L166C	*In vitro* binding in *Sl* BBMV *In vivo* competition in *Sl*	Chapter 1

Protein	Information	Uses	Results
Vip3Aa_M34L	Gain of function, point mutation in helix α1 (Domain I)	Toxicity bioassays in *Se* *In vitro* digestion (Trypsin and *Se* gut juice)	Chapter 2
Vip3Aa_S-S	Constitutive protoxin conformation, point mutations in Domain I helices α2 (D66C N69C) and α3 (Q96C L100C)	Toxicity bioassays in *Se* Structure visualization by NS-EM *In vitro* digestion (Trypsin and *Se* gut juice)	Chapter 2
		I*n vitro* binding to *Se* BBMV *In vivo* competition in *Se*	Chapter 3
Vip3Aa_$\Delta\alpha$1	Constitutive activated conformation, deletion of Domain I helix α1	Toxicity bioassays in *Se* Structure visualization by NS-EM *In vitro* digestion (Trypsin and *Se* gut juice)	Chapter 2
		I*n vitro* binding to *Se* BBMV *In vivo* competition in *Se*	Chapter 3
Vip3Aa_ 41-KVKK_44	Introduction of proteolytic site in loop helices α1-α2 (Domain I), mutation 41-DTGG-44 to 41-KVKK-44	Toxicity bioassays in *Se* Structure visualization by NS-EM *In vitro* digestion (Trypsin and *Se* gut juice)	Chapter 2
Vip3Aa_ 195-AVAA-198	Removed primary trypsin cleavage site (loop Domains I-II), mutation 195-KVKK-198 to 195-AVAA-198	Toxicity bioassays in *Se* Structure visualization by NS-EM *In vitro* digestion (Trypsin and *Se* gut juice)	Chapter 2
Vip3Aa_L146F	Reduced coiled-coil diameter, point mutation in helix α3	Toxicity bioassays in *Se* *In vitro* digestion (Trypsin and *Se* gut juice)	Chapter 2
Vip3Aa_L146M	Reduced coiled-coil diameter, point mutation in helix α3	Toxicity bioassays in *Se* *In vitro* digestion (Trypsin and *Se* gut juice)	Chapter 2
Vip3Aa_I-III	Truncated construct lacking Domains IV-V	Toxicity bioassays in *Se* Structure visualization by NS-EM	Chapter 2
		In vitro digestion (Trypsin and *Se* gut juice)	Chapters 2 and 4
		In vitro binding to *Se* BBMV *In vivo* competition in *Se*	Chapter 4
		Binding to *Se* and standard lipids	Chapter 5

Protein	Information	Uses	Results
Vip3Aa_II-V	Truncated construct lacking Domain I	*In vitro* digestion (Trypsin and *Se* gut juice) *In vitro* binding to *Se* BBMV *In vivo* competition in *Se*	Chapter 4
		Binding to *Se* and standard lipids	Chapter 5
Vip3Aa_III-V	Truncated construct lacking Domains I-II	*In vitro* digestion (Trypsin and *Se* gut juice) *In vitro* binding to *Se* BBMV *In vivo* competition in *Se*	Chapter 4
		Binding to *Se* and standard lipids	Chapter 5
Vip3Aa_IV-V	Truncated construct lacking Domains I-III	*In vitro* digestion (Trypsin and *Se* gut juice) *In vitro* binding to *Se* BBMV *In vivo* competition in *Se*	Chapter 4
		Binding to *Se* and standard lipids	Chapter 5

[a] *Sl, Spodoptera littoralis*

[b] BBMV, brush border membrane vesicles

[c] *Se, Spodoptera exigua*

[d] NS-EM, negative staining electron microscopy

II. Site directed mutagenesis (SDM)

II.1. Generation of disabled insecticidal proteins (DIPs)

Disabled insecticidal proteins (DIPs) are mutant proteins engineered to retain their ability to bind membrane receptors while lacking insecticidal activity. Their use in *in vivo* competition assays enables the identification of shared functional binding sites between different proteins. In this thesis, various Vip DIP variants were generated by introducing point mutations in Domain I, the region of the protein involved in toxicity. The mutants Vip3Aa DIP1 and Vip3Ca DIP (carrying mutations S164C and L166C) were generated based on a previous report (Wang *et al.*, 2019) where a Vip3Aa DIP variant was generated by the introduction of a disulphide bond between Domain I

α-helices impairing its remodelling into the activated conformation. The mutant Vip3Aa DIP2 (carrying E168A mutation) was generated based on previous studies showing that this point mutation in Vip3Af results in a lack of toxicity but retains tetrameric structure and we hypothesized that could also behave as a DIP mutant (Quan and Ferré., 2019; Banyuls *et al.*, 2018). Site directed mutagenesis (SDM) was performed by the technique of the whole plasmid amplification, following the protocol described previously (Banyuls *et al.*, 2021). Briefly, plasmid amplification reaction was performed with the high-fidelity KAPA HiFi™ DNA polymerase kit (KK2101, Kapa Biosystems) using the WT clones as templates (Vip3Aa cloned in pET14b and Vip3Ca cloned in pMAAB10 vector, both carrying a 6x-His N-t tag) following the instructions provided by the manufacturer. Primers pairs used for SDM of the different Vip DIPs are collected in **Supplementary Table S1.1**. The remaining parental plasmids were digested with Fast Digest DpnI (Thermo Scientific) and mutant plasmids were transformed into *Escherichia coli* DH10β heat-shock competent cells (EC0113, Thermo Fisher) following the instructions provided by the manufacturer. Plasmid purification was performed for each mutant with NucleoSpin® Plasmid Kit (Macherey-Nagel) and mutations were confirmed by DNA Sanger sequencing using the primers described in **Supplementary Table S1.1** prior to their transformation into *E. coli* BL21 (DE3) heat shock competent cells (EC0114, Thermo Fisher) for protein expression.

II.2. Generation of Domain I mutants

The mutant proteins Vip3Aa_S-S (D66C, N69C, Q96C, L100C), Vip3Aa_41-KVKK_44, Vip3Aa_195-AVAA-198, Vip3Aa_L146F and Vip3Aa_L146M were obtained using the Q5 Site-Directed Mutagenesis Kit (E0554S, New England Biolabs) following the instructions provided by the manufacturer and using the WT vector (Vip3Aa 10-789 cloned in LIC 1.5, pETNKI-StrepII-3C-LIC-AmpillinR vector containing an N-t StrepII-tag followed by a 3C PreScission protease cleavage site) as a template to generate the mutant proteins. Mutant plasmids were checked by DNA sequencing and finally transformed into *E. coli* C43 (DE3) for protein expression. The mutant protein Vip3Aa_M34L was generated by the technique of the whole plasmid amplification from Vip3Aa WT clone in pET14b, following the protocol described above and was finally transformed into *E. coli* BL21 (DE3) competent cells. See **Supplementary Table S2.1** for description of the primers used to generate each Domain I mutant protein and plasmid sequencing.

II.3. Generation of truncated constructs

The truncated proteins Vip3Aa_Δα1 (residues 40-789), Vip3Aa_I-III (residues 10-532), Vip3Aa_II-V (residues 203-789), Vip3Aa_III-V (residues 325-789) and Vip3Aa_IV-V (residues 532-789) were generated by amplification of the corresponding sequences from the Vip3Aa WT template and subcloning into the same vector LIC 1.5. Primers used for amplification of the corresponding sequences are compiled in **Supplementary Tables S2.1** and **S4.1**. Mutant plasmids were transformed into *E. coli* BL21 (DE3) for protein expression.

III. Protein expression and purification techniques

III.1. Heterologous expression in *Escherichia coli*

Vectors containing Vip3Aa, Vip3Af and Vip3Ca WT proteins and their different mutant versions were expressed in *E. coli* cells (BL21, C43 or WK6 depending on the clone). Briefly, cells were grown overnight at 37°C in Luria-Bertani (LB)-agar plates supplemented with 100 μg/mL Ampicillin (Amp). A loop of a single colony was grown overnight in 20 mL of LB Amp overnight at 37°C with 180 rpm shaking. A final culture was inoculated with 7 mL of preculture in 700 mL of LB medium supplemented with Amp (100 μg/mL) and grown to exponential phase (OD_{600} ~ 0.6-1.2) by incubating at 37°C with 180 rpm shaking. Then, protein expression was induced with 0.5-1 mM isopropyl β-d-1-thiogalactopyranoside (IPTG) and cultures were incubated at 37°C for 3-6 h (full length proteins) or 25°C overnight (truncated constructs). Induced cultures were centrifuged and cells were collected and stored at −20°C until lysis and protein purification.

III.2. Cell lysis and protein purification

For purification, thawed cells were resuspended in lysis buffer (20 mM Tris–HCl, 150 mM NaCl pH 8.6 buffer or 50 mM Tris–HCl, 150-500 mM NaCl, 50 mM $MgCl_2$ pH 8.0 buffer) supplemented with 3 mg/mL lysozyme, 10 μg/mL DNase and 100 μM PMSF for chemical lysis. Lysates were incubated for 30 min at 37°C with 180 rpm shaking. After chemical lysis, the lysate was sonicated for 5 min and centrifuged at 25,000 ×*g* for 30 min to recover the supernatant containing soluble Vip proteins for further protein purification.

III.2.1. His Trap affinity chromatography

His-tagged Vip proteins (Vip3Aa, Vip3Af, Vip3Ca WT proteins, their DIP variants and Vip3Aa_M34L point mutation) were purified by metal-chelate affinity chromatography using His-trap FF crude 1 mL columns (GE Healthcare). Clarified lysate supernatants were loaded onto the column previously equilibrated with 50 mM phosphate buffer containing 300 mM NaCl and 10 mM imidazole. Then, the column was washed with the same buffer and an increased imidazole concentration (45 mM), and the proteins were eluted rising imidazole concentration to 250 mM in the same buffer. Purified proteins were dialyzed overnight against 20 mM Tris–HCl, 150 mM NaCl pH 8.6 buffer and clarified by centrifugation (16,100 ×*g*, 4°C, 10 min), quantified by Bradford (Bradford, 1976) using bovine serum albumin (BSA) as standard and stored at −20°C until use.

III.2.2. Strep Trap affinity chromatography

StrepII-tagged Vip proteins (Vip3Aa_10-789 WT, all the rest of Domain I point mutations and truncated constructs) were purified by affinity chromatography using a 5 mL StrepTrap column (Cytiva) previously equilibrated in 50 mM Tris–HCl, 150 mM NaCl, 5 mM $MgCl_2$ pH 8.0 buffer. The proteins were eluted with 5 mM d-desthiobiotin (Sigma-Aldrich) dissolved in the same buffer. The StrepII tag was removed by treating with 3C PreScission Protease (Cytiva) followed by dialysis in the same buffer to eliminate d-desthiobiotin. The sample was then subjected to another step of affinity chromatography with the StrepTrap column to separate the nontagged protein from any remaining tagged

molecules, and pure proteins were eluted in 50 mM Tris–HCl, 150 mM NaCl, 5 mM $MgCl_2$ pH 8.0 buffer, quantified by Bradford and stored at −20°C until use.

III.2.3. Isoelectric point precipitation (IPP)

Isoelectric point precipitation (IPP) was performed as described previously (Chakroun *et al.*, 2012). Briefly, the clarified lysate was lowered at pH 5.6 for Vip3Aa and Vip3Af (WT and mutant proteins) and at pH 5.9 for Vip3Ca (WT and mutant proteins) with 0.1 M acetic acid. Then, the lysate with the adjusted pH was aliquoted and the precipitation pellet was recovered by centrifugation (16,100 ×*g*, 4°C, 10 min) and stored at –20°C. Before being used in bioassays, pellet aliquots were dissolved in 20 mM Tris–HCl, 150 mM NaCl pH 8.6 buffer, and clarified by centrifugation (16,100 ×*g*, 4°C, 10 min). Protein purity was checked by SDS-PAGE and protein concentration was calculated by densitometry using BSA as standard and TotalLab 1D software.

IV. Proteolytic profiles characterization

IV.1. *In vitro* digestion

Purified proteins were quantified by Bradford and a fixed amount of protein (10 µg) was incubated with 10% (w/w; 1 µg) commercial trypsin, α-chymotrypsin (both from bovine pancreas, Sigma-Aldrich), 10% (w/w) *Spodoptera spp.* midgut juice or 10% (w/w) *S. exigua* BBMV. The digestion was carried out in a final volume of 20 µL, in Tris-HCl buffer (50 mM Tris–HCl, 150-500 mM NaCl, 5 mM $MgCl_2$ pH 8.0), or in 20 mM

carbonate buffer at pH 10, depending on the pH conditions required. All samples were incubated for 1.5 h at 37°C for trypsin and α-chymotrypsin digestions and at 30°C for midgut juice and BBMV digestions. Then, samples were clarified by centrifugation (16,100 ×*g* for 10 min at 4°C) and the supernatant containing the processed proteins was incubated for 10 min at room temperature (RT) with 10 mM AEBSF [4-(2-aminoethyl) benzenesulfonyl fluoride HCl] serine protease inhibitor to avoid further processing of the proteins. Proteolytic fragments were separated on 12% acrylamide SDS-PAGE gels.

Midgut juice of *S. exigua* and *S. littoralis* was prepared following the protocol described elsewhere (Chakroun *et al.*, 2012). Briefly, last instar larvae were dissected and whole guts were extracted and collected in pools in 1.5 mL microtubes placed on ice. Midgut samples were centrifuged at 16,100 ×*g* for 10 min at 4°C and supernatant containing the gut juice was collected, aliquoted, flash-frozen in liquid nitrogen and stored at −80°C until use. BBMV from *S. exigua* were prepared by the differential magnesium precipitation method (Wolfersberger, 1993) and stored at −80°C as well (see section VI.1 for protocol description). Total protein concentration in the gut juice and BBMV was determined by Bradford just before their use in *in vitro* proteolytic assays.

IV.2. *In vivo* digestion and western blot

Purified proteins diluted in 50 mM Tris–HCl, 150 mM NaCl, 5 mM $MgCl_2$ pH 7.5 buffer, were mixed with phenol red and sucrose (18 µl of 2 mg/mL protein, 2 µL of phenol red and 2.5 µL of 1.6 M sucrose). Then, *S. exigua* L3 larvae were starved for at least 4 h and fed by drop-feeding

with the protein mixtures. Larvae that ingested the protein mixtures were separated and dissected at time intervals (15 min and 16 h post-ingestion). Control larvae were just fed with the buffer-dye mixture. Individual midguts of treated larvae were homogenized in 10 μL of 10 mM AEBSF and incubated at RT for 10 min to stop any further proteolytic processing of the proteins. Samples were subjected to 12% SDS-PAGE along with a Dual Color Molecular Marker (Bio-Rad). After SDS-PAGE, the proteins were transferred into a nitrocellulose membrane (GE Healthcare Armershan™ Hybond™—ECL) by humid transference in blotting buffer (39 mM glycine, 48 mM Tris-base, 0.037% SDS, 20% methanol) using the Bio-Rad system. The lane of the molecular marker was separated from the rest using a clean razor. The two pieces of the membrane were blocked overnight with 5% skimmed milk dissolved in PBST buffer (PBS 1X, 0.1% Tween 20). The part of the membrane containing the proteins was incubated for 1 h at RT (with shaking) with a primary antibody anti-Vip3Aa raised in rabbit at 1/5,000 antibody dilution in PBST containing 0.5% skimmed milk. After 3 washing steps with PBST (5 min each), the membrane was incubated for 1 h at RT with the secondary antibody anti-rabbit conjugated with HRP peroxidase (Sigma-Aldrich) at 1/20,000 antibody dilution in PBST containing 0.5% skimmed milk. The part of the membrane containing the molecular marker was incubated for 1 h at RT with Precision Protein StrepTactin-HRP (Bio-Rad) at 1/20,000 dilution in PBST. After three washing steps (5 min each) with PBST, the bands were visualized with the Amersham TM ECL Prime Western Blotting Detection Reagent (GE Healthcare) using an Image Quant LAS 4000 (GE Healthcare).

V. Insect rearing and bioassays with *Spodoptera spp.*

V.1. LC_{50} bioassays

Surface contamination bioassays were performed with laboratory populations of *S. exigua* and *S. littoralis* maintained on semi-synthetic diet (Bell and Joachim, 1976) in a rearing chamber at 25 ± 2°C, 70% ± 5% RH, and 16:8 h light:dark photoperiod. Increasing concentrations of purified proteins dissolved in Tris-HCl buffer (20 mM Tris–HCl, 150 mM NaCl pH 8.6 buffer or 50 mM Tris–HCl, 150-500 mM NaCl, 5 mM $MgCl_2$ pH 8.0 buffer) were prepared and dispensed (50 µL) over the surface of 2 cm^2 wells filled with semi-synthetic diet. At least 16 wells were used for each protein concentration. After the diet surface was dry, one neonate was gently placed into each well and plates were sealed. Trays were maintained in a climatic chamber under rearing conditions and the mortality was recorded after 10 days. At least three biological replicates of the assay were performed for each protein. The toxicity of the proteins was quantified by Probit analysis using PoloPlus software and graphical representations were performed with GraphPad Prism software.

V.2. *In vivo* competition assays

In vivo competition bioassays were conducted as described for surface contamination bioassays (see section V1) by using different toxic protein:non-toxic competitor molar ratios (1:0, 1:10, 1:100, 1:1,000, 1:2,500 and 1:10,000) in Tris-HCl buffer (20 mM Tris–HCl, 150 mM NaCl pH 8.6 buffer or 50 mM Tris–HCl, 150 mM, NaCl 5 mM $MgCl_2$ pH 8.0

buffer). Different Vip DIPs, Vip3Aa structural mutants (Vip3Aa_Δα1 and Vip3Aa_S-S) and Vip3Aa_I-III truncated construct were used as competitors for the Vip3Aa and Vip3Af WT proteins. Negative controls included buffer (labelled as 0) and an excess of non-toxic competitor (labelled as 0:1,000, 0:2,500 or 0:10,000 representing the highest competitor concentration used). The Cry1Ab R99E mutant protein, described previously as nontoxic but able to block the toxicity of its WT counterpart, was used as a negative control of competition (Chen et al, 2021; Hernández-Martínez *et al.*, 2022; Jerga *et al.*, 2019). Vip3Aa and Vip3Af proteins at a constant concentration resulting in 60–80% of mortality (determined from LC_{50} bioassays performed in *S. exigua* and *S. littoralis* neonates), were mixed with corresponding amounts of competitor proteins to create the desired ratios. Each *in vivo* competition protein combination was replicated at least three times. Statistical analysis of mortality differences between 1:0 and other protein:competitor ratios was performed using One-Way ANOVA with post hoc Bonferroni tests in Prism (GraphPad), ensuring rigorous assessment of significance with P-values higher than an α-value of 0.05.

VI. *In vitro* binding to BBMV with radiolabelled proteins

VI.1. Preparation of *Spodoptera spp.* BBMV

Brush border membrane vesicles (BBMV) from *S. exigua* and *S. littoralis* were prepared by the differential magnesium precipitation method (Wolfersberger, 1993). This method isolates BBMV through selective precipitation based on differences in membrane-$MgCl_2$ aggregates charge to separate apical from lateral and basal membranes and enrich

the sample in brush border membrane fragments. Last instar larvae were previously dissected and midguts were extracted, snap-frozen in liquid nitrogen and stored at −80°C. Frozen midguts were used as starting material for BBMV preparation. Briefly, midgut tissue was homogenised in cold MET buffer (300 mM D-mannitol, 5 mM EGTA, 17 mM Tris-HCl pH 7.5) with an electric potter homogenizer, 9 mL of buffer per gram of tissue were used and 6-9 homogenisation strokes were performed. After homogenisation, the suspension was filtered with cotton gauze to remove larger debris and the suspension was mixed with an equal volume of a 24 mM $MgCl_2$ solution and incubated on ice for 15 min to allow aggregates formation. Two sets of low-speed (2,500 ×*g*, 15 min, 4°C) and high-speed (31,000 ×*g*, 30 min, 4°C) centrifugations were performed in a Beckman Avanti JXN-26 refrigerated centrifuge to enrich the sample in small aggregates containing BBMV. Between both centrifuge sets, the sample was homogenised in half the original volume of MET buffer by performing 6-7 strokes with the electric potter homogeniser and the incubation with $MgCl_2$ was repeated (15 min on ice). The final BBMV pellet was resuspended in 1-2 mL of half-strength MET (1/2 dilution of MET solution), aliquots were prepared, flash-frozen in liquid nitrogen and stored at -80°C until use. BBMV were quantified by Bradford, measuring the amount of total protein present in the samples.

VI.2. Protein radiolabelling with ^{125}I

Radiolabelling of Vip protoxins was performed by the Chloramine T method (Van Rie *et al.*, 1989) following the protocol described

previously (Chakroun and Ferré, 2014) with minor modifications. Pure Vip protoxins (25 μg) were mixed with 0.3 mCi of [^{125}I]-NaI and 1/3 (v/v) of 18 mM Chloramine T and the labelling reaction was carried out for 45 seconds. The reaction was then stopped by adding 1/4 (v/v) of 23 mM sodium metabisulfite and 1/4 (v/v) of 1M NaI solutions. The excess of free ^{125}I was separated from the labelled protein using a PD10 desalting column (GE Healthcare). The purity of the ^{125}I radiolabelled protein was checked by analysing the eluted fractions by SDS-PAGE with further exposure of the dry gel to an X-ray film. Labelled proteins were stored at 4°C and used up to 1 month after the labelling reaction.

VI.3. Binding assays to BBMV

All *in vitro* binding assays with radiolabelled Vip proteins were performed by incubation with BBMV for 1 h in 100 μL final volume of binding buffer (20 mM Tris–HCl, 1 mM $MnCl_2$, 0.1% BSA pH 7.4). After incubation, the reaction was halted by centrifugation at 16,000 ×*g* for 10 min at 4°C, and the pellet was washed with 500 μL of binding buffer. Radioactivity retained in the pellet was quantified using a model 2480 WIZARD2 γ-counter (Perkin Elmer) to assess bound labelled protein. Bindability assays were performed with a fixed amount of labelled protein (0.2 nM), increasing concentrations of BBMV and an excess of unlabelled competitor (1,000-fold molar ratio). Competition assays were performed by mixing a fixed amount of labelled protein (0.2 nM) with increasing concentrations of unlabelled homologous or heterologous competitor proteins and a fixed amount of BBMV (0.05-0.1 mg/mL) established according to the shape of their respective total binding

curves in bindability assays. For measuring binding reversibility, chase-time experiments were performed by incubating a fixed amount of trypsin-processed labelled proteins (0.2 nM) with a fixed amount of BBMV (0.05-0.1 mg/mL) for 1 h and afterwards adding a 1,000-fold molar excess of unlabelled competitor. Samples were collected after 5 min, 30 min and 1 h of incubation with the competitor (chase-time). The samples were centrifuged and washed as for the rest of binding assays, the radioactivity retained in the pellet corresponding to the remaining labelled protein bound after the chase time was quantified for the different time points. At least two technical replicates were performed for each binding assay, competition assay or chase-time experiment. Graphical representations were obtained with Prism (GraphPad). The binding parameters equilibrium dissociation constant (K_d) and binding site concentration (R_t), were estimated using LIGAND (Munson and Rodbard, 1980). Trypsin-treatment of labelled proteins and competitor samples used in binding assays was performed with commercial trypsin from bovine pancreas (Sigma Aldrich) at 1% (w/w), incubating at 37°C for 1 h in all cases.

VII. *In vitro* binding assays to insect midgut lipids

VII.1. Preparation of insect lipids

Lipids were purified from midgut tissue of last instar larvae of *S. exigua* and *S. littoralis* into two chemical phases by the Svennerholm partitioning method (Svennerholm and Fredman, 1980). Larvae were dissected and midguts were flash frozen in liquid nitrogen and stored

at -80°C until use. Before extraction, midguts were rinsed in dH_2O and flash frozen in liquid nitrogen and thawed at RT three times. Pellets were sonicated and lipid extraction was performed at 37°C for 2 h with agitation in a mixture of chloroform:methanol:water with a final ratio of 4:8:3 v/v/v. Samples were centrifuged at 1,400 ×*g* for 5 min to split into upper phase (hydrophilic, attracts more polar lipids and glycolipids) and lower phase (hydrophobic, attracts simpler and nonpolar lipids). Silica-based hydrophobic cartridges (WAT036810, Sep-Pak tC18) were used to purify and concentrate upper phase lipids. All samples were dried under N_2 at 40°C and resuspended in 50 μL methanol (upper phase) and 200 μL 1:1 chloroform to methanol (lower phase). Lipid samples from other insect species representative of all insect orders were also extracted from whole insects following the same extraction protocol.

VII.2. Thin-Layer Chromatography (TLC)

Thin-layer chromatography (TLC) was performed using HPTLC plates (M5631-5, Fisher-Scientific) equilibrated in a mobile phase of chloroform:methanol:water (65:25:4, v/v/v). TLC chambers were prepared by adding the mobile phase to cover the middle edge of the chamber, and the system was equilibrated for 30 min at RT. TLC plates were marked 2.5 cm from the bottom with lanes spaced 1.5 cm apart and equilibrated in the chamber for 1 h before drying at 100°C for 10 min. Lipid samples were dissolved by incubation in a humid bath at 42°C with sonication for 15 min. Samples were applied to the plates in 1-cm bands with volumes of 5–30 μL depending on the analysis, and plates

were dried at 50–70°C for 10 min. Plates were developed in the equilibrated chamber until the mobile phase reached the upper edge (approximately 1 h) and dried again at 50–75°C for 10 min. Visualization was performed by spraying the plates with a solution of 50 mL acetic acid, 1 mL sulfuric acid, and 0.5 mL p-anisaldehyde in a fume hood, followed by heating at 75–120°C until bands were clearly visible.

VII.3. Lipid dot-blot assays

Dot-blots were performed as described previously (Best *et al.*, 2022) with some modifications. PVDF membranes with 0.2 μm pores (ISEQ00010 Immobilon-PSQ PVDF) were used for blotting. Lipid standards were added at 2 μg in a volume no larger than 4 μL, while larvae-extracted lipids were applied as 5 μL (upper phase) or 2 μL (lower phase) of the final suspension. Blots were dried for 30 min at RT, blocked with TBS containing 5% BSA for 4 h at 4°C with agitation, and washed three times with TBS (5 min each wash). Protoxin, trypsin-processed Vip3Aa_Wt, or truncated constructs (4 μg/mL or equimolar concentrations for truncated constructs) were incubated overnight at 4°C in TBS with 1% BSA and shaking. After washing three times with TBS, membranes were probed for 1h at RT with a primary anti-Vip3Aa antibody raised in rabbit (1/5,000 dilution in TBS-0.1% BSA), followed by three more washing steps with TBS and incubation with an anti-rabbit HRP-conjugated secondary antibody (Sigma-Aldrich; 1/20,000 dilution) for 1 h at RT. All steps were performed with shaking. After three final washes with TBS, visualization was performed using a LI-COR C-Digit

chemiluminescence western blot scanner and the WESTAR ECL-Sun HRP detection kit (K1-0052, GENEFLOW LIMITED).

Lipid standards were also used in dot-blot assays, the following species were sourced from Avanti Polar Lipids: sphingomyelin (ref: 860062, at 10 mg/mL dissolved in chloroform), lyso-sphingomyelin (ref: 860600, at 10 mg/mL dissolved in chloroform), glucosylceramide (ref: 131304, at 2 mg/mL dissolved in ethanol), phosphatidylcholine (ref: 131601, at 10 mg/mL dissolved in chloroform), ceramide phosphoethanolamine (CPE, ref: 860066, at 10 mg/mL dissolved in chloroform), porcine brain total ganglioside extract (ref: 860053P, at 2 mg/mL dissolved in a chloroform:ethanol 2:1 mixture) and C20 ceramide (ref: 860520P, at 10 mg/mL dissolved in ethanol). Mixed bovine gangliosides (ref:1065, at 10 mg/mL dissolved in a chloroform:ethanol 2:1 mixture) was sourced from Matreya LLC.

VII.4. TLC-overlay assays

TLC for overlay assays was performed by using glass-backed silica-60 HPTLC plates (Merck). Plates equilibration, sample application, running, drying and visualization of the stained plates was performed as described above (see section VII.2). For overlay assays with protein, Vip3Aa was trypsin-activated (10% w/w for 1.5 h at 37°C with T8002 bovine pancreas trypsin from Sigma Aldrich) and Biotin-labelled with a Biotinylation Kit (ab201795, abcam) following the instructions provided by the manufacturer. Plates were fixed with 50 mL hexane for 2 min and 50 mL of 0.1% polyisobutyl methacrylate (PIBM) in hexane for 2 min. Plates were dried at 50°C for 10 min and blocked with 0.5% BSA in PBS

containing 0.01% Tween-20 for 30 min at RT. Plates were probed with biotin-labelled trypsin-activated Vip3Aa (4 μg/mL in blocking buffer) for 2 h at RT with shaking. Then, plates were washed twice with 10 mL of blocking solution and incubated with streptavidin-linked alkaline phosphatase (ALP, AK-5000 Vectastain Kit, Vector Labs) in blocking buffer for 1 h at RT without shaking. After three 1-min washes, plates were incubated with a solution of 5-Bromo-4-Chloro-Indolyl-Phosphatase (BCIP) and Nitro blue Tetrazolium (NBT) solution (BCIP/NBT-Blue, B3679 Sigma-Aldrich) for 10–15 minutes until bands were visible and air-dried overnight.

VIII. Negative-Staining Electron Microscopy (NS-EM)

Purified protein samples were analysed by electron microscopy after being adsorbed to glow-discharged carbon-coated grids and stained with 2% (w/v) uranyl acetate as described previously (Núñez-Ramírez *et al.*, 2020). Grids were observed using a JEOL JEM-1230 transmission electron microscope, operated at 100 kV, at a nominal magnification of 40,000. EM images were taken under low dose conditions with a CMOS TvipsTemCam-F416 camera at 2.84 Å per pixel. Image processing was performed using the SCIPION package (de la Rosa-Trevín *et al.*, 2016). The contrast transfer function of the microscope for each micrograph was estimated using CTFFIND4 (Rohou and Grigorieff, 2015). Particles were then automatically picked using the Xmipp routine inside SCIPION (Abrishami *et al.*, 2013) and subjected to 2D classification using RELION (Scheres, 2012).

Chapter 1

In vivo competition assays between Vip proteins confirm the occurrence of shared binding sites in *Spodoptera littoralis*

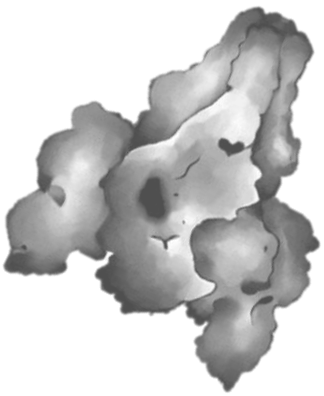

Adapted from:
Lázaro-Berenguer M, Quan Y, Hernández-Martínez P, Ferré J. 2022. *In vivo* competition assays between Vip3 proteins confirm the occurrence of shared binding sites in *Spodoptera littoralis*. Sci Rep 12, 4578.
https://doi.org/10.1038/s41598-022-08633-y

I. Introduction

Genetically modified crops expressing *cry* insecticidal genes from *Bacillus thuringiensis* (Bt-crops), have been used since the mid-90s to control insect pests. However, their extensive use has led to the phenomenon of field-evolved resistance to Cry proteins, for some lepidopteran and coleopteran pests (Downes and Mahon, 2012; Storer *et al.*, 2012; Tabashnik and Carrière, 2019). Pyramided Bt-crops (which combine different insecticidal proteins with different specificity and mode of action) have been proposed as an interesting tool to delay or avoid the appearance of insect resistance (Carrière *et al.*, 2015; Moar and Anilkumar, 2007). In this context, Vegetative Insecticidal Proteins (Vip), known as a second generation of Bt proteins, are gaining importance in crop protection strategies. Most studies have dealt with Vip3Aa proteins, which are already expressed in commercial Bt-crops, are active against lepidopteran species that have already developed resistance against Cry proteins, and do not share binding sites with them (Chakroun and Ferré, 2014; Gouffon *et al.*, 2011; Lee *et al.*, 2006; Quan *et al.*, 2021a; Sena *et al.*, 2009).

Vip proteins have a tetrameric structure, with each monomer containing five structural domains (Byrne *et al.*, 2021; Núñez-Ramírez *et al.*, 2020; Zheng *et al.*, 2020). The N-terminal (N-t) domains I–II are highly conserved and play a crucial role in maintaining the tetramer (Núñez-Ramírez *et al.*, 2020; Quan and Ferré, 2019). Domain I has been shown to form, upon activation, a coiled-coil structure that inserts into the epithelial membrane (Byrne *et al.*, 2021; Núñez-Ramírez *et al.*, 2020). Domain III has recently been proposed as responsible of binding to the

midgut specific receptors (Jiang *et al.*, 2020a; Quan *et al.*, 2021a), whereas the C-terminal (C-t) domains IV–V have a highly variable sequence and are not essential for maintaining the tetrameric structure, though they are critical for the insecticidal activity *in vivo* (Banyuls *et al.*, 2018; Quan and Ferré, 2019). These domains show structural homology to carbohydrate binding motifs (CBM) and their function remains still unknown (Byrne *et al.*, 2021; Núñez-Ramírez *et al.*, 2020; Zheng *et al.*, 2020).

In vitro binding assays to midgut binding sites have been used to establish binding site models which are useful to predict the appearance of cross-resistance and select the best protein combinations for pyramided Bt-crops (Gouffon *et al.*, 2011; Höfte and Whiteley, 1989; Lee *et al.*, 2006). More recently, *in vivo* competition assays have been proposed as a novel tool to complement the *in vitro* binding models and obtain information about protein interactions *in vivo* (Chen *et al.*, 2021; Hernández-Martínez *et al.*, 2022; Jerga *et al.*, 2019; Wang *et al.*, 2019). Studies based on *in vitro* binding of ^{125}I-Vip3A to brush border membrane vesicles (BBMV) using heterologous Vip proteins as competitors led to propose a binding site model in which Vip proteins share binding sites in *Spodoptera frugiperda* and *Spodoptera exigua* (Quan *et al.*, 2021a; Chakroun and Ferré 2014). In the present study, using a ^{125}I-Vip3Aa labelled protein, we have extended the *in vitro* binding site model of Vip proteins to another *Spodoptera* species, *Spodoptera littoralis*, with the aim to understand the relevance of binding to the midgut binding sites observed *in vitro* on the insecticidal activity of these proteins. For this purpose, we have performed *in vivo* competition

assays with *S. littoralis* larvae, using Vip Disabled Insecticidal Proteins (DIP) carrying mutations in Domain I as competitors for blocking the toxicity of Vip3Aa and Vip3Af wild type (WT) proteins. DIP mutants are engineered in such a way that they lack insecticidal activity without losing the capacity of binding to membrane receptors with the aim to see if they compete with WT proteins *in vivo* for functional binding sites, as detected in toxicity assays (Hernández-Martínez *et al.*, 2022; Jerga *et al.*,2019). The results of our *in vivo* competition assays confirm the occurrence of functional shared binding sites for Vip proteins and confirm the binding site model proposed by *in vitro* binding using ^{125}I-Vip3A proteins.

II. Materials and methods

II.1. Expression of Vip proteins and engineering of DIP mutants

All Vip proteins contained an N-t 6x-His tag. Vip3Aa90 (ac. no. AAW65132) was expressed in recombinant *Escherichia coli* BL21 cells following the protocol described elsewhere (Chakroun *et al.*, 2012). Vip3Ca2 (ac. no. AEE98106) (Palma *et al.*, 2012), Vip3Af1 (ac. no. CAI43275) and mutant Vip3Af E168A (kindly provided by BASF Belgium Coordination Center – Innovation Center Ghent) were expressed in recombinant *E. coli* WK6 cells following the protocol described previously (Ruiz de Escudero *et al.*, 2014). Briefly, *E. coli* cells were grown in 700 mL of Luria-Bertani (LB) with 100 μg/mL Ampicillin to exponential phase (OD_{600} ~ 0.6-1.2) and protein expression was induced with 1 mM isopropyl β-d-1-thiogalactopyranoside (IPTG), incubating at 37°C with 180 rpm shaking overnight. Then cultures were

centrifuged and cells were stored at −20°C until lysis and protein purification was carried out.

For constructing the Vip DIPs, the mutation S164C L166C was selected based on a previous report (Wang *et al.*, 2019) where a Vip3Aa DIP variant was generated by the introduction of two cysteines in enough proximity to make a S–S bond and prevent Domain I to unfold, a critical step in the activation of the Vip proteins (Byrne *et al.*, 2021; Núñez-Ramírez *et al.*, 2020). The mutation E168A was selected based on previous studies showing that Vip3Af E168A loses toxicity but retains the tetrameric structure and we hypothesized that could also behave as a DIP mutant (Quan and Ferré., 2019; Banyuls *et al.*, 2018). The DIP proteins Vip3Aa S164C L166C (DIP1), Vip3Aa E168A (DIP2) and Vip3Ca S164C L166C were generated for this work by SDM following the protocol described elsewhere (Banyuls *et al.*, 2021), using the WT clones as templates. Primers and annealing temperatures used for SDM Polymerase Chain Reaction (PCR) and sequencing are collected in **Supplementary Table S1.1**. Mutant clones were expressed and lysed following the same conditions used for their WT homologues.

II.2. Purification of Vip proteins

For the *in vitro* binding assays, proteins were purified by metal-chelate affinity chromatography using His-trap FF crude (GE Healthcare) 1 mL columns (Chakroun *et al.*, 2012). Briefly, cells were lysed by resuspending them in 20 mM Tris-HCl, 150 mM NaCl pH 8.6 buffer supplemented with 3 mg/mL lysozyme, 10 μg/mL DNase and 100 μM PMSF and incubated for 30 min at 37°C with shaking. The lysate was

then sonicated for 5 min and centrifuged at 25,000 ×*g* for 30 min. Clarified lysates were loaded onto the column previously equilibrated with 50 mM phosphate buffer containing 300 mM NaCl and 10 mM imidazole. Then, the column was washed with the same buffer and an increased imidazole concentration (45 mM), and the His-tagged Vip protein was eluted rising imidazole concentration to 250 mM in the same buffer. Purified proteins were dialyzed overnight against 20 mM Tris–HCl, 150 mM NaCl pH 8.6 buffer and clarified by centrifugation (16,100 ×*g*, 4°C, 10 min), quantified by Bradford (Bradford, 1976) using bovine serum albumin (BSA) as standard, aliquoted and stored at −20°C. The purity of the protein preparations was checked by SDS-PAGE (**Supplementary Figure S1.1**). Just before use, Vip proteins used as competitors were trypsin-treated (1% w/w) with trypsin from bovine pancreas (SIGMA T8003, Sigma-Aldrich) at 37°C for 1 h, clarified by centrifugation (16,100 ×*g* for 10 min at 4°C), and quantified by Bradford. In the *in vivo* competition assays, we observed that His-trap purified proteins rendered less reproducible results compared to the isoelectric point precipitation (IPP) purified proteins, most probably due to a higher stability of the latter on the surface of the diet for 10 days at 25°C. For this reason, proteins meant to be used for *in vivo* competition assays were purified by IPP (Chakroun *et al.*, 2012). Briefly, the clarified lysate was lowered at pH 5.6 for Vip3Aa and Vip3Af (WT and mutant proteins) and at pH 5.9 for Vip3Ca (WT and mutant protein) with 0.1 M acetic acid. Then, the lysate with the adjusted pH was aliquoted and the precipitation pellet was recovered by centrifugation (16,100 ×*g*, 4°C, 10 min) and stored at –20°C. Before being used in bioassays, the pellet

aliquots were dissolved in 20 mM Tris–HCl, 150 mM NaCl pH 8.6 buffer, and clarified by centrifugation (16,100 ×*g*, 4°C, 10 min). Protein purity was checked by SDS-PAGE (**Supplementary Figure S1.2**) and protein concentration was calculated by densitometry using BSA as standard and the TotalLab 1D v 13.01 software.

II.3. *S. littoralis* brush border membrane vesicles (BBMV) preparation

Last instar larvae of *S. littoralis* were dissected and midguts were kept at −80°C. BBMV were prepared from the midguts by the differential magnesium precipitation method (Wolfersberger *et al.*, 1987), flash frozen in liquid nitrogen, and stored at −80°C until use. The protein concentration in the BBMV preparations was determined by Bradford.

II.4. Vip3Aa ^{125}I radiolabelling

Radiolabelling of Vip3Aa protoxin was performed by the Chloramine T method (Van Rie *et al.*, 1989) following the protocol described previously (Chakroun and Ferré, 2014) with some modifications. His-trap purified Vip3Aa (25 µg) was mixed with 0.3 mCi of [^{125}I]-NaI and 1/3 (vol/vol) of 18 mM Chloramine T. The excess of free ^{125}I was separated from the labelled protein using a PD10 desalting column (GE Healthcare). The purity of the ^{125}I labelled protein was checked by analysing the eluted fractions by SDS-PAGE with further exposure of the dry gel to an X-ray film (**Supplementary Figure S1.3**). The specific activity of the labelled ^{125}I-Vip3Aa was 5.7 µCi/µg.

II.5. *In vitro* binding assays with ^{125}I -Vip3Aa and *S. littoralis* BBMV

Before use, labelled ^{125}I-Vip3Aa protein was trypsin treated (1% w/w with bovine pancreas trypsin, 37°C, 1 h) and stored at 4°C. BBMV were thawed on ice, centrifuged (10 min at 16,000 ×*g* and 4°C) and resuspended in binding buffer (20 mM Tris–HCl, 1 mM MnCl2, 0.1% BSA pH 7.4). For all the assays, trypsin-treated ^{125}I-Vip3Aa was incubated with BBMV for 1 h at room temperature (RT) in a 0.1 mL final volume of binding buffer. The reaction was stopped by centrifuging the tubes at 16,000 ×*g* for 10 min at 4°C, and the pellet was washed once with 500 µL of cold binding buffer (Chakroun and Ferré, 2014). The radioactivity retained in the pellet was measured in a model 2480 WIZARD2 gamma counter (Perkin Elmer). A binding assay with a fixed amount of ^{125}I-Vip3Aa (0.2 nM), increasing concentrations of BBMV and an excess of unlabelled competitor (1,000-fold His-trap purified, trypsin-treated, Vip3Aa) was performed to determine the appropriate amount of BBMV to use in the binding competition assays and estimate nonspecific binding (**Supplementary Figure S1.4**). Competition assays were performed by mixing a fixed amount of ^{125}I-Vip3Aa (0.2 nM) with increasing concentrations of unlabelled competitor (His-trap purified, trypsin-treated, Vip proteins) and a fixed amount of BBMV (0.05 mg/mL). At least three replicates were performed for each binding or competition assay. Graphical representations were performed with GraphPad Prism. Equilibrium dissociation constants (K_d) and the concentration of binding sites (R_t) were estimated using the LIGAND software (Munson and Rodbard, 1980).

II.6. Insect rearing and bioassays

Surface contamination bioassays were performed with a laboratory population of *S. littoralis* maintained on semi-synthetic diet (Bell and Joachim, 1976) in a rearing chamber at 25 ± 2°C, 70 ± 5% RH and 16:8 h L:D photoperiod. To calculate the LC_{50} values of WT proteins, increasing doses of proteins purified by IPP and dissolved in Tris buffer (20 mM, 150 mM NaCl pH 8.6) were prepared. Protein preparations were dispensed (50 µL) over the surface of the assay wells (2 cm^2 diameter) filled with semi-synthetic diet, 16 wells were used for each protein dose. After the diet surface was dry, one neonate was gently placed into each well and the plates were sealed. Trays were maintained in a climatic chamber at the same conditions used for colony rearing and mortality was recorded after 7 and 10 days of incubation. At least three replicates were performed for each protein, and the LC_{50} values and FL95% were calculated using PoloPlus software.

For *in vivo* competition assays, protein:competitor ratios of 1:0, 1:10, 1:100 and 1:1,000 were prepared in Tris buffer (20 mM, 150 mM NaCl pH 8.6). Controls consisted of just buffer (labelled as 0) and just competitor (labelled as 0:1,000 corresponding to the maximum amount of competitor used in the assay). Constant concentrations of IPP-purified Vip3Aa (13 ng/cm^2) and Vip3Af (30 ng/cm^2), which resulted in 60–80% of mortality, were mixed with the corresponding amount of IPP-purified competitor to prepare the different ratios. Bioassays were performed following the same protocol described previously, and at least three biological replicates were performed for each *in vivo* competition protein combination. Graphical representations were

performed with GraphPad Prism, and for assessing the statistical significance of mortality differences between 1:0 and the rest of protein:competitor ratios, a One-Way ANOVA with post-hoc Bonferroni test was performed using the same software.

III. Results

III.1. Toxicity of Vip WT and Domain I mutant proteins

Surface contamination bioassays were performed to determine the toxicity of Vip WT and disabled proteins against *S. littoralis* (**Table 1.1**). LC_{50} values (concentration resulting in 50% of mortality) of the WT proteins served to establish the doses to perform *in vivo* competitions. Vip3Aa and Vip3Af proteins are both highly toxic to *S. littoralis*, whereas for Vip3Ca, limited mortality though a strong growth inhibition was observed as already reported by Palma *et al.*, 2012. The Vip DIP mutants lacked of detectable insecticidal activity (**Table 1.1**).

Table 1.1. Toxicity of Vip proteins against *S. littoralis* neonate larvae.

Protein	LC_{50} (FL 95%) (ng/cm²) [a]	Slope ± SEM	χ^2
Vip3Aa WT	13.9 (5.8 - 41.7)	2.4 ± 0.6	5.1
Vip3Aa DIP1 (S164C L166C)	>13000	-	-
Vip3Aa DIP2 (E168A)	>30000	-	-
Vip3Af WT	28.8 (22.7 - 39.3)	2.3 ± 0.2	3.0
Vip3Af DIP (E168A)	>30000	-	-
Vip3Ca WT	>1000	-	-
Vip3Ca DIP (S164C L166C)	>30000	-	-

[a] The LC_{50} and the 95% fiducial limits (FL 95%) after 10 days. At least three biological replicates were performed for each protein except Vip3Ca WT which was estimated from a single assay.

III.2. ^{125}I-Vip3Aa *in vitro* binding assays

Specific binding of ^{125}I-Vip3Aa to *S. littoralis* BBMV was shown by the competition with unlabelled Vip3Aa (**Figure 1.1**, black line; **Supplementary Figure S1.4**). The unlabelled protein displaced at least 70% of the labelled protein's initial binding, indicating that in our experimental conditions around 30% was non-specific binding. The analysis of the competition curve provided an equilibrium dissociation constant (K_d) of 51.0 ± 8.3 nM, with a concentration of binding sites (R_t) of 170 ± 32 pmol/mg of BBMV protein (**Supplementary Table S1.2**).

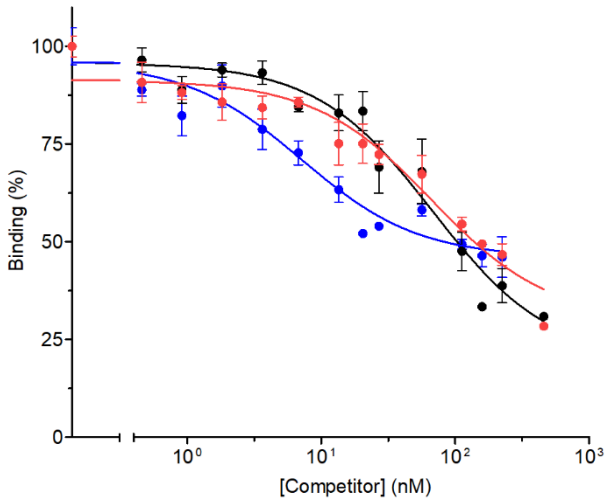

Figure 1.1. *In vitro* binding competition assays among Vip WT proteins. Labelled ^{125}I-Vip3Aa was used with a fixed concentration of BBMV (0.05 mg/ml) and increasing concentrations of unlabelled Vip3Aa (black) and the heterologous proteins Vip3Af (red) and Vip3Ca (blue) as competitors. Each data point represents the mean of at least three replicates (± SEM).

Heterologous competitors (Vip3Af and Vip3Ca) were used to evaluate the existence of shared binding sites with ^{125}I-Vip3Aa. The results showed that Vip3Af was able to displace all ^{125}I-Vip3Aa specific binding

(**Figure 1.1**, red line) in a similar way as homologous Vip3Aa does. The analysis of the heterologous curve using Vip3Af WT as competitor yielded an estimated K_d of 130 ± 39 nM and an R_t of 492 ± 202 pmol/mg of BBMV protein (**Supplementary Table S1.2**). However, though Vip3Ca could compete for ^{125}I-Vip3Aa binding, it could not do it completely (**Figure 1.1**, blue line); the competition curve reaches a plateau at 50% of the binding which indicates that Vip3Aa had more than one population of binding sites and that not all are shared with Vip3Ca. Accordingly, the analysis of the heterologous curve using Vip3Ca WT as competitor yielded an estimated K_d of 6.6 ± 1.3 nM and an R_t of 18.3 ± 3.4 pmol/mg of BBMV protein (**Supplementary Table S1.2**), indicating a high affinity for the receptors shared with Vip3A proteins. However, according to the low R_t value, Vip3Ca protein only shares with Vip3A proteins a small number of its binding sites.

III.3. Effect of Domain I mutations on *in vitro* binding

The ability of Domain I mutant proteins to bind to BBMV has been shown by using ^{125}I-Vip3Aa and the unlabelled mutant proteins as competitors. The results showed that all mutants were able to compete with the labelled protein similarly to the unlabelled Vip3Aa WT homologous competitor (**Figure 1.2**), indicating that they maintained the ability to bind despite having lost their insecticidal activity. The estimation of the binding parameters (K_d and R_t) from the heterologous competitions with ^{125}I-Vip3Aa and DIP competitors indicated that the mutations did not significantly affect the binding properties compared to their respective WT proteins (**Supplementary Table S1.2**).

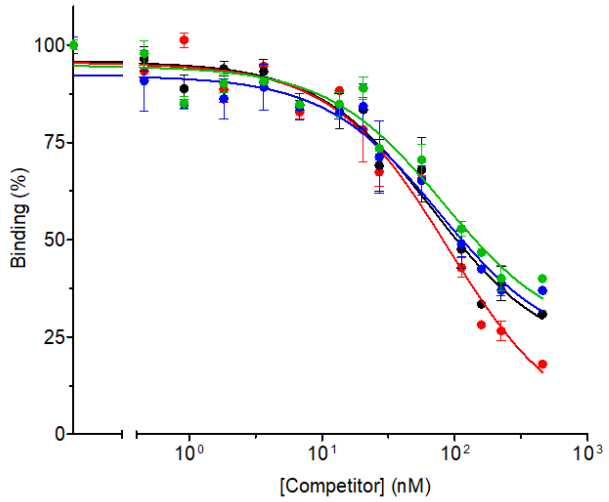

Figure 1.2. *In vitro* binding competition assays of Domain I Vip mutants. Labelled ^{125}I-Vip3Aa was used with a fixed concentration of BBMV (0.05 mg/ml) and increasing concentrations of unlabelled Vip3A Domain I mutants: Vip3Aa DIP1 (red), Vip3Aa DIP2 (blue), and Vip3Af DIP (green). The homologous competition with unlabelled Vip3Aa WT (black, overlapped with that of Vip3Aa DIP2 in blue) is included as a control. Each data point represents the mean of at least three replicates (±SEM).

III.4. Vip3Aa *in vivo* competition assays.

In vivo competition assays were performed to test whether the *in vitro* binding model drawn using Vip heterologous competitors actually reflected competition for functional binding sites. At ratios 1:100 or higher of WT:mutant protein, both Vip3Aa Domain I mutants (Vip3Aa DIP1 and DIP2) were able to block the toxicity of Vip3Aa WT (**Figure 1.3A, B**). Therefore, both disabled Vip3Aa mutants presumably bind to the same sites as the Vip3Aa WT protein, preventing it to exert its toxic action. The same type of approach was used with heterologous Vip competitors (Vip3Af DIP and Vip3Ca DIP). The Vip3Af mutant protein was able to block Vip3Aa WT's toxicity *in vivo* at the highest ratio tested

(1:1,000), whereas the Vip3Ca mutant was not able to block the toxicity of Vip3Aa WT event at the highest competitor ratio (**Figure 1.3C, D**).

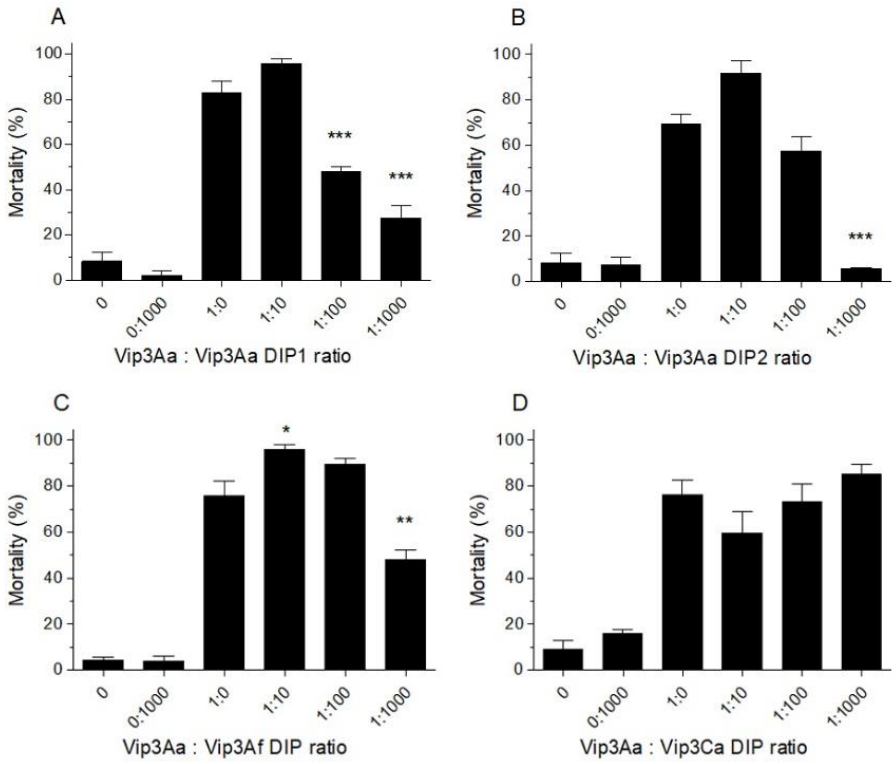

Figure 1.3. Vip3Aa *in vivo* competition assays against Domain I mutants. Vip3Aa WT protein was used at a constant concentration (13 ng/cm^2) with increasing ratios of homologous Vip3Aa mutant competitors **(A)** Vip3Aa DIP1 and **(B)** Vip3Aa DIP2, and heterologous competitors **(C)** Vip3Af DIP and **(D)** Vip3Ca DIP. The mean percent mortality (±SEM) of at least three replicates is represented for each protein ratio. The two first columns of each graph correspond to the negative controls 0 (just buffer) and 0:1,000 (no WT but highest amount of competitor used in the assay, 13 μg/cm^2). The rest of the columns represent the different protein:competitor ratios used in the assays. The asterisks over the bars indicate level of significance (* $P < 0.05$, ** $P < 0.01$ and *** P value < 0.001) compared to the ratio 1:0 in a One-Way ANOVA with Bonferroni post hoc test.

III.5. Vip3Af *in vivo* competition assays

In vivo competition assays were also performed using the Vip3Af WT protein. In the homologous *in vivo* competition assay using the Vip3Af DIP mutant, the competitor blocked the toxicity of Vip3Af WT at a 1:1,000 ratio (**Figure 1.4A**). In agreement with the results obtained in the *in vivo* competition assays with Vip3Aa WT, Vip3Aa DIP2 blocked the toxicity of Vip3Af WT (**Figure 1.4B**), whereas Vip3Ca DIP did not block it even at the highest ratio tested (**Figure 1.4C**). Interestingly, Vip3Aa DIP2 was very efficient, significantly blocking the toxicity of the Vip3Af WT protein at a ratio as low as 1:10.

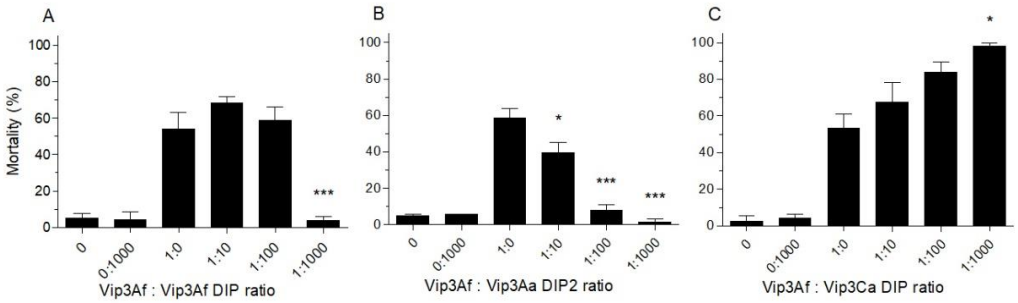

Figure 1.4. Vip3Af *in vivo* competition assays against Domain I mutants. Vip3Af WT protein was used at a constant concentration (30 ng/cm^2) with increasing ratios of homologous mutant competitor **(A)** Vip3Af DIP, heterologous mutant competitors **(B)** Vip3Aa DIP2 and **(C)** Vip3Ca DIP. The mean percent mortality (± SEM) of at least three replicates is represented for each protein ratio. The two first columns correspond to the negative controls 0 (just buffer) and 0:1,000 (no WT but highest amount of competitor used in the assay, 30 μg/cm^2). The rest of the columns represent the different protein:competitor ratios used in the assay. The asterisks over the bars indicate level of significance (*P < 0.05, and *** P < 0.001) compared to the ratio 1:0 in a One-Way ANOVA with Bonferroni post hoc test.

IV. Discussion

Understanding Vip proteins mode of action is essential for guiding a better application of these insecticidal proteins in pest management and crop protection strategies. Special emphasis must be placed on their binding properties, which drive their insect specificity and help designing the best protein combinations for pyramided Bt-crops. *In vitro* binding assays with radiolabelled proteins has proven to be a useful method for studying protein binding to insect midgut receptors (Gouffon *et al.*, 2011; Höfte and Whiteley, 1989; Lee *et al.*, 2006). Here, by using ^{125}I-Vip3Aa and *S. littoralis* BBMV in *in vitro* binding assays we have shown that Vip3Aa and Vip3Af proteins share all the binding sites whereas Vip3Ca only competes partially for Vip3A binding sites. This binding model is in agreement with the one proposed for *S. exigua* and *S. frugiperda* using ^{125}I-Vip3Af (Quan *et al.*, 2021a). The partial competition of Vip3Ca for Vip3A binding sites was not detected in a previous study with *S. frugiperda* BBMV (Kahn *et al.*, 2018). In that study the binding conditions were different from ours, such as the lower purity of the proteins used as competitors and the presence of NaCl in the binding buffer, which has been shown to interfere with Vip3Af binding, potentially by blocking electrostatic interactions (Quan *et al.*, 2021a).

Disabled insecticidal proteins have been proposed as a novel tool for studying the occurrence of shared receptors between different proteins *in vivo*. These proteins are engineered with mutations that eliminate their insecticidal activity without affecting their binding to membrane receptors (Hernández-Martínez *et al.*, 2022; Jerga *et al.*, 2019). We have

now applied this approach to Vip proteins in *S. littoralis* with the aim to test the relevance of *in vitro* derived binding site models to predict the interaction of these proteins *in vivo*. Vip disabled proteins were generated by the introduction of mutations in Domain I and they were used as competitors in *in vivo* competition assays, which consist on giving a constant dose of a toxic protein and increasing concentrations of the disabled competitor. If the toxicity is blocked by an excess of competitor, it can be assumed that the proteins share functional receptors, and thus, the binding of the non-toxic protein prevents the binding and the subsequent toxicity of the WT protein (Chen *et al.*, 2021; Hernández-Martínez *et al.*, 2022; Jerga *et al.*, 2019; Wang *et al.*, 2019). However, in this type of approach, a dominant-negative phenotype can happen if, at very low concentrations of nontoxic competitor, an important inhibition of toxicity is observed, indicating that the competitor is sequestering the WT protein by forming hetero-oligomers (Carmona *et al.*, 2011; Jiménez-Juárez *et al.*, 2007; Rodríguez-Almazán *et al.*, 2009). This is not happening in this case, since Vip proteins spontaneously form very stable tetramers (Núñez-Ramírez *et al.*, 2020; Byrne *et al.*, 2021) and because the inhibition of toxicity at very low concentrations of competitors is not observed. Our results from *in vitro* binding assays show that, as expected, the Vip disabled proteins carrying point mutations in Domain I were all able to bind specifically to *S. littoralis* BBMV, but none of them was toxic against *S. littoralis* larvae, confirming the essential role that Domain I plays on the toxicity (Banyuls *et al.*, 2018; Jerga *et al.*, 2019). In addition, from the *in vivo* competition assays we can also draw some conclusions that allow us to

better understand the behaviour of Vip proteins *in vivo*. Disabled Vip3Aa and Vip3Af proteins blocked the toxicity of their respective homologous WT proteins, though they did it at different ratios. While disabled Vip3Aa proteins blocked Vip3Aa WT at a 1:100 ratio, a 1:1,000 ratio was needed for disabled Vip3Af to block Vip3Af toxicity. In the heterologous competition assays, disabled Vip3Aa DIP2 blocked Vip3Af WT at a ratio 1:10, whereas disabled Vip3Af DIP blocked Vip3Aa WT only at a ratio as high as 1:1,000. The fact that Vip3Aa and Vip3Af disabled proteins blocked each other's WT proteins confirms the occurrence of shared binding sites *in vivo*, in agreement with the *in vitro* binding assays. Furthermore, the different ratios WT:disabled required to block toxicity reveal differences in the efficiency between Vip3Aa and Vip3Af proteins, being disabled Vip3Af less efficient than disabled Vip3Aa in competing for the WT proteins. These results are in agreement with the differences in affinity of these two proteins for the binding sites observed *in vitro*. Vip3Af has a higher K_d than Vip3Aa, indicating lower affinity for the binding sites, in agreement with the lower efficiency in blocking the toxicity in the *in vivo* competition assays. Despite Vip3Ca being able to compete *in vitro* for part of the binding sites of Vip3Aa, the disabled Vip3Ca did not block the toxicity of either of these two proteins even at the highest ratio tested in *in vivo* competition (**Figures 1.3D** and **1.4C**). The partial competition of Vip3Ca *in vitro* for Vip3A binding sites implies that Vip3Aa has distinct types of binding sites, in agreement with recent reports proposing different receptors for this protein (Jiang *et al.*, 2018a; Jiang *et al.*, 2018b; Osman *et al.*, 2019; Singh *et al.*, 2010). Therefore, one explanation for the result

obtained *in vivo* is that Vip3Ca cannot block all functional binding sites of Vip3A proteins and, thus, the non-shared binding sites are sufficient for Vip3A proteins to exert their toxic effect. Alternatively, the Vip3A binding sites shared with Vip3Ca may be those of less relevance for Vip3A toxicity or those occurring in less abundance compared to other Vip3A sites. Since Vip3Ca was not labelled (for the *in vitro* binding assays) or used as the WT protein in the *in vivo* competition assays, we cannot discard that it could have additional binding sites not shared with Vip3A proteins. The existence of redundant binding sites for Vip3A proteins could also help explain the fact that resistance to Vip3Aa has not so far been associated with a lack of *in vitro* binding to BBMV in any of the lepidopteran Vip3Aa-resistant populations studied (Chakroun et al 2016b; Pinos *et al.*, 2020; Quan *et al.*, 2021b).

An unexpected result observed in our *in vivo* competition assays using disabled Vip3A proteins as competitors is the increase of toxicity of the WT protein when mixed with the disabled protein at low ratios (**Figures 1.3C** and **1.4C**). One possible explanation for this effect is that the excess of disabled protein would block non-specific binding sites that otherwise would trap some of the WT molecules. Also, the excess of disabled proteins could have a protective effect to the WT protein in the lumen by reducing the ratio proteases:Vip3A molecules. This slight enhancement of the mortality disappears when the ratio of disabled protein increases due to the greater contribution of the binding-sites blocking effect, except when using Vip3Ca DIP as competitor since this protein is unable to block Vip3A WT binding sites.

V. Conclusions

In summary, the *in vivo* competition assays are a good complement to the *in vitro* competition binding assays. In this study, in addition to proposing a binding site model for *S. littoralis* based on *in vitro* binding competition using radiolabelled proteins, the *in vivo* competition assays confirm the occurrence of functional shared binding sites for Vip proteins. The results point out to the existence of multiple binding sites for Vip proteins, which might have different relevance in the toxicity or different abundance in the midgut membrane. The occurrence of redundant receptors may have the effect of masking the importance of the ones most involved in the toxicity by providing an average picture of the overall binding to the membrane sites.

Here, we propose the model shown in **Figure 1.5** as the most likely binding site model for Vip proteins in *Spodoptera spp.* based both on *in vitro* binding and *in vivo* competition assays among Vip proteins.

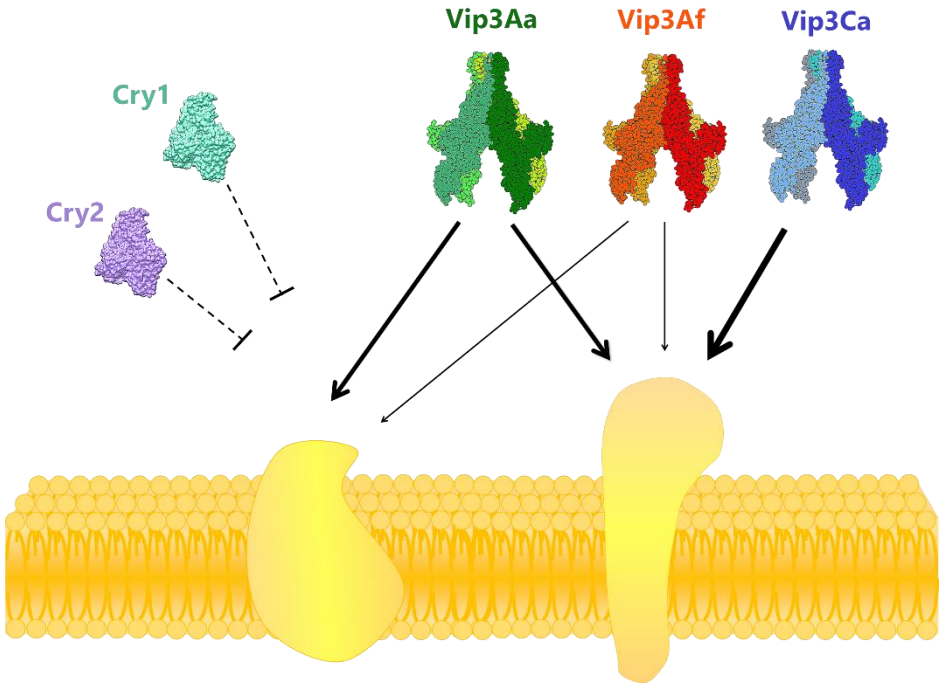

Figure 1.5. Proposed binding site model for Vip proteins in *Spodoptera spp.* Based on *in vitro* binding of ^{125}I-Vip3Aa and ^{125}I-Vip3Af (Quan *et al.*, 2021b) and *in vivo* competition assays, Vip3Aa and Vip3Af share all the binding sites including functional binding sites as shown *in vivo* for *S. littoralis*. Vip3Ca competes only partially for Vip3A binding sites and does not block Vip3A functional receptors in *S. littoralis*. Cry proteins do not share receptors with Vip proteins. Thickness of the arrows represents differences in the binding affinity (thicker arrows indicate higher affinity according to K_d parameters). Dashed lines indicate lack of shared binding sites. Figure modified from Ferré *et al.*, 2023 and Lázaro-Berenguer *et al.*, 2022b.

Chapter 2

Structural and functional role of Domain I for the insecticidal activity of the Vip3Aa protein against *Spodoptera exigua*

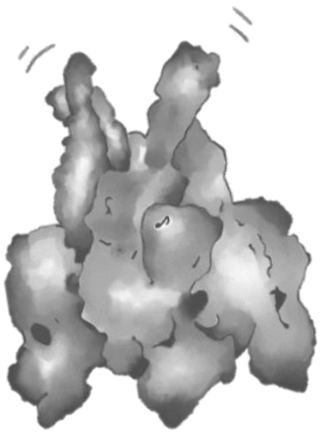

Adapted from:

Lázaro-Berenguer M, Paredes-Martínez F, Bel Y, Núñez-Ramírez R, Arias-Palomo E, Casino P, Ferré J. 2022. Structural and functional role of Domain I for the insecticidal activity of the Vip3Aa protein from *Bacillus thuringiensis*. Microb Biotechnol 15(10), 2607–2618. https://doi.org/10.1111/1751-7915.14110

I. Introduction

Vegetative insecticidal proteins (Vip) are produced during the vegetative growth phase of the bacterium *Bacillus thuringiensis*, and are toxic against a wide range of lepidopteran pests (Chakroun *et al.*, 2016a; Estruch *et al.*, 1996; Palma *et al.*, 2014; Ruiz de Escudero *et al.*, 2014). Notably, members of the Vip3A family have been used in Bt-crops (expressing one or more *B. thuringiensis* genes) in combination with the Cry insecticidal proteins to prevent the evolution of insect-resistant populations (Carrière *et al.*, 2015; Tabashnik and Carrière, 2017), since they are toxic for insect species that have already developed resistance against Cry proteins and do not share binding sites with them (Chakroun and Ferré, 2014; Gouffon *et al.*, 2011; Lee *et al.*, 2006; Quan *et al.*, 2021a; Sena *et al.*, 2009).

Vip proteins are secreted as protoxins of ~89 kDa which, once ingested by the larvae, are processed by midgut proteases into two different fragments of ~20 and ~65 kDa that remain attached and conform the activated protein (Bel *et al.*, 2017; Chakroun and Ferré, 2014; Quan and Ferré, 2019; Zack *et al.*, 2017). Once processed, Vip proteins are able to bind to specific receptors located on the brush border membrane of the midgut epithelium cells (Chakroun and Ferré, 2014; Quan *et al.*, 2021a) where they exert their toxic effect. Regarding their mode of action, it has been shown that Vip proteins get inserted into the membrane and induce pore formation, leading to the death of the larvae (Lee *et al.*, 2003; Liu *et al.*, 2011). In addition, and mainly in studies with cultured cells, it has been reported that Vip3A proteins can induce apoptosis through the

mitochondrial apoptotic pathway after being internalized into the cells (Hou *et al.*, 2020; Jiang *et al.*, 2016; Nimsanor *et al.*, 2020).

Recently, the structure of Vip proteins has been determined by cryo-electron microscopy (cryo-EM), revealing that they consist of a tetramer in which each subunit is composed of five structural domains (Byrne *et al.*, 2021; Núñez-Ramírez *et al.*, 2020; Zheng *et al.*, 2020) (**Figure 2.1**). Comparison between Vip protoxin and trypsin-activated protein structures has demonstrated a major conformational change at the N-terminal (N-t) Domain I (**Figure 2.1A, B**). In the protoxin conformation, the N-t forms a helix bundle that is remodelled into a tetrameric coiled-coil as observed in the activated protein conformation, with a flexible end that most probably is formed by helix α1 (Byrne *et al.*, 2021; Núñez-Ramírez *et al.*, 2020). The tip of this coiled-coil structure has been shown to get inserted into the membrane of liposomes (Byrne *et al.*, 2021). At the C-terminus (C-t), Domains IV and V (**Figure 2.1C**) are carbohydrate-binding motifs that do not contact the N-t part of the protein or directly interact with other subunits, and are dispensable for oligomer formation (Byrne *et al.*, 2021; Núñez-Ramírez *et al.*, 2020; Quan and Ferré, 2019; Zheng *et al.*, 2020). Also, it has recently been shown that they are not necessary for the specific binding of Vip3Af to *Spodoptera spp.* brush border membrane vesicles (BBMV) and *Spodoptera frugiperda* Sf21 cultured cells, or for exerting cell toxicity (Jiang *et al.*, 2020a; Quan *et al.*, 2021a). Nevertheless, many reports have shown that they are necessary for the toxicity of Vip3A proteins *in vivo* (Banyuls *et al.*, 2018, 2021; Gayen *et al.*, 2012, 2015; Li *et al.*, 2007; Quan and Ferré, 2019; Selvapandiyan *et al.*, 2001).

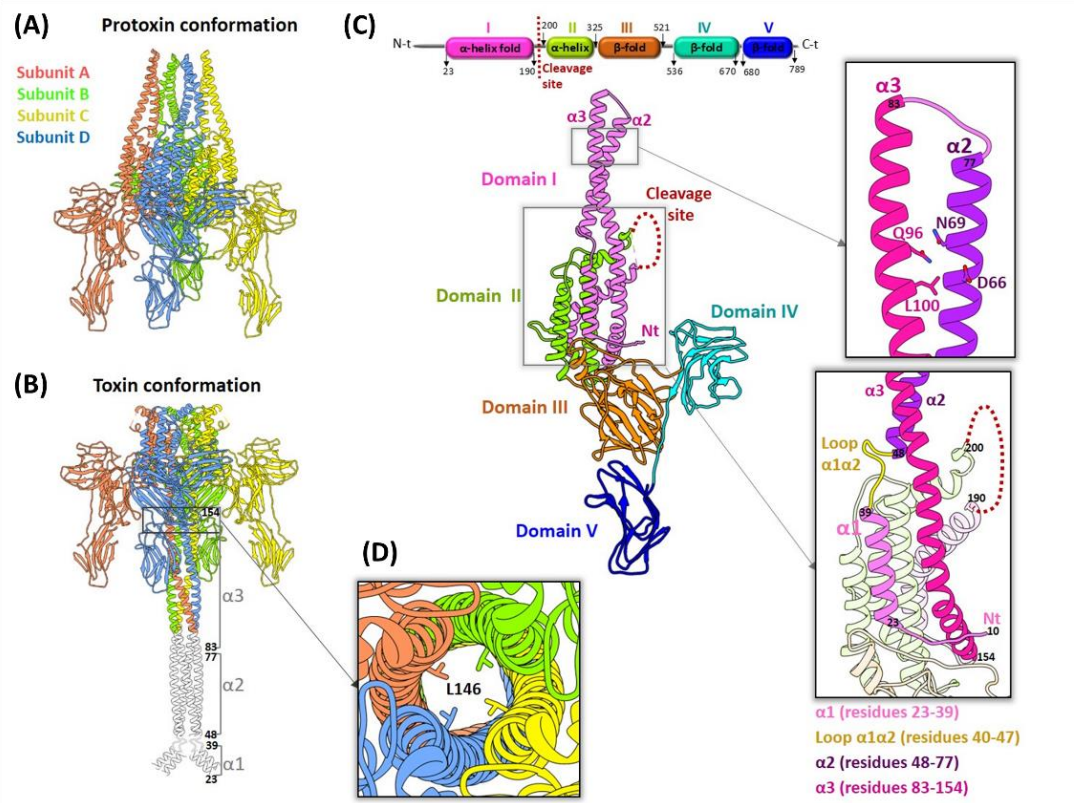

Figure 2.1. Structural features of Vip3Aa. (A) Protoxin conformation of Vip3Aa (PDB: 6TFJ; subunits in the tetramer are coloured coded). (B) Activated toxin conformation of Vip3Aa (PDB: 6TFK) composed by a tetrameric coiled-coil traced till residue 95. Modelled coiled-coil in white till residue 23. Helices forming the coiled-coil are labelled and numbered. (C) Domain composition of a subunit from the protoxin conformation highlighting each domain coloured coded and the loop containing the cleavage site. Boxes are extracted to zoom the helices α2 and α3 with the residues mutated to Cys for disulphide bond cross-linking and to zoom helix α1 connected to helix α2 by loop α1α2. (D) Zoom of a box shown in B showing the internal tetrameric coiled-coil with L146 coming from each subunit.

To better understand the relevance of Domain I for Vip3Aa's toxicity and the role of the C-t Domains IV and V *in vivo*, we have engineered a deletion mutant of these domains in addition to mutations aimed to restrict remodelling of Domain I as well as to modify it. Since activation of Vip3A proteins by the insect midgut proteases is a key step for the insecticidal activity (Chakroun *et al.*, 2016a; Hernández-Martínez *et al.*, 2013; Lee *et al.*, 2003), the behaviour of these mutants upon proteolytic processing has been characterized. Also, we have performed negative staining electron microscopy (NS-EM) and toxicity bioassays against the lepidopteran species *Spodoptera exigua*, to determine the effect of these mutations on the protein structure and how this affects the insecticidal activity. The results demonstrate that the integrity and the remodelling of Domain I (coiled-coil formation) are essential for the insecticidal activity of Vip3Aa *in vivo*.

II. Materials and methods

II.1. Mutagenesis of Vip3Aa

Vip3Aa90 (NCBI accession No. AAW65132) (residues 10–789) was cloned in LIC 1.5, as previously described (Núñez-Ramírez *et al.*, 2020), and then was used as a template vector to prepare the mutant vectors used in this study. Specifically, the sequences of Vip3Aa_Δα1 and Vip3Aa_ΔIV-V were prepared by amplification of the vector template from residue 40 to 789 and residue 10 to 535, respectively, then cloned in LIC 1.5. The rest of the mutants were obtained using the Q5 Site-Directed Mutagenesis Kit (New England Biolabs) with the vector

template to obtain the corresponding mutant vectors containing the mutant proteins. See **Supplementary Table S2.1** for description of the primers used to prepare each mutant protein.

II.2. Protein expression and purification

Vip3Aa WT and mutants were produced as described previously (Núñez-Ramírez *et al.*, 2020). Briefly, protein expression was conducted in *Escherichia coli* C43 (DE3) cells grown in Luria-Bertani (LB) broth supplemented with 100 μg/mL Ampicillin to exponential phase (OD_{600} ~ 0.6) and induced with 0.5 mM isopropyl β-d-1-thiogalactopyranoside (IPTG), incubated at 37°C for 3 h and then centrifuged and stored at −20°C. For purification, thawed cells were resuspended in buffer A (50 mM Tris–HCl, 0.5 M NaCl, 50 mM $MgCl_2$) at pH 8.0, with 1 mM phenylmethanesulfonyl fluoride and 1 mM Tris (2-carboxyethyl) phosphine hydrochloride, and sonicated for 5 min. The cell lysate was centrifuged at 25,000 x*g* for 30 min and the clarified supernatant was loaded into a 5 mL StrepTrap column (GE, Healthcare). The protein was eluted with 5 mM d-desthiobiotin dissolved in buffer A. The StrepII-tag was removed with 3C PreScission protease (GST-tagged) at a 1:1/25 (protein:protease) molar ratio followed by dialysis in buffer A. The sample was then subjected to two other steps of affinity chromatography with StrepTrap and GST-Trap columns to separate the non-tagged protein from any remaining tagged protein and protease. The non-tagged protein was further purified by gel filtration chromatography using a ProteoSEC 16/60 6–600 HR (Generon). Pure proteins were stored at −80°C for further use.

II.3. *In vitro* proteolytic assays

Purified proteins diluted in buffer A at pH 7.5 were quantified by the Bradford method (Bradford, 1976). A fixed amount of protein (10 μg) was incubated with 10% (w/w; 1 μg) commercial trypsin or α-chymotrypsin (both from bovine pancreas, Sigma-Aldrich), or 10% (w/w) midgut juice or 10% (w/w) BBMV from *S. exigua*. Midgut juice of *S. exigua* was prepared following the protocol described elsewhere (Chakroun *et al.*, 2012), flash-frozen in liquid nitrogen and stored at −80°C. BBMV from *S. exigua* were prepared by the differential magnesium precipitation method (Wolfersberger, 1993) and stored at −80°C as well. Total protein concentration in the midgut juice and BBMV was determined by the Bradford method just before use. The reaction was carried out in a final volume of 20 μL, in buffer A at pH 7.5 or in 20 mM carbonate buffer at pH 10, depending on the pH conditions required. All samples were incubated for 1.5 h at 37°C for trypsin and α-chymotrypsin digestions and at 30°C for midgut juice and BBMV digestions. Then, samples were clarified by centrifugation (16,100 x*g* for 10 min at 4°C) and the supernatant containing the processed proteins was incubated for 10 min at room temperature (RT) with 10 mM AEBSF [4-(2-aminoethyl) benzenesulfonyl fluoride HCl] serine protease inhibitor to avoid further processing of the proteins. Proteolytic fragments were separated on 12% acrylamide SDS-PAGE gels.

II.4. Protein structure visualization by NS-EM

Purified samples were analysed by electron microscopy after being adsorbed to glow-discharged carbon-coated grids and stained with 2% (w/v) uranyl acetate as described previously (Núñez-Ramírez *et al.*, 2020). Grids were observed using a JEOL JEM-1230 transmission electron microscope, operated at 100 kV, at a nominal magnification of 40,000. EM images were taken under low dose conditions with a CMOS TvipsTemCam-F416 camera at 2.84 Å per pixel. Image processing was performed using the SCIPION package (de la Rosa-Trevín *et al.*, 2016). The contrast transfer function of the microscope for each micrograph was estimated using CTFFIND4 (Rohou and Grigorieff, 2015). Particles were then automatically picked using the Xmipp routine inside SCIPION (Abrishami *et al.*, 2013) and subjected to 2D classification using RELION (Scheres, 2012).

II.5. Insect rearing and toxicity bioassays

Surface contamination bioassays were performed with a laboratory population of *S. exigua* maintained on semi-synthetic diet (Bell and Joachim, 1976) in a rearing chamber at 25 ± 2°C, 70% ± 5% RH, and 16:8 h light:dark photoperiod. Increasing concentrations of purified proteins dissolved in buffer A at pH 7.5, were prepared and dispensed (50 µL) over the surface of 2 cm^2 wells filled with semi-synthetic diet; at least 16 wells were used for each protein concentration. After the diet surface was dry, one neonate larva was gently placed into each well and plates were sealed. Trays were maintained in a climatic chamber under rearing conditions and the mortality was recorded after 10 days. At least three biological replicates of the assay were performed for each protein. The

toxicity of the proteins was quantified by Probit analysis using PoloPlus software. Graphical representations (**Supplementary Figure S2.1**) were performed with GraphPad Prism.

II.6. *In vivo* digestion with *S. exigua* larvae and western blot

Purified WT and Vip3Aa_195-AVAA-198 proteins, diluted in buffer A at pH 7.5, were mixed with phenol red and sucrose (18 µl of 2 mg/ml protein + 2 µL of phenol red + 2.5 µL of 1.6 M Sucrose). Then, *S. exigua* L3 larvae were starved for at least 4 h and fed by drop-feeding with the protein mixtures. Larvae that ingested the protein mixtures were separated and dissected at time intervals (15 min and 16 h post-ingestion). Control larvae were just fed with the buffer-dye mixture. Individual midguts of treated larvae were homogenized in 10 µL of 10 mM AEBSF and incubated at RT for at least 10 min to stop any further proteolytic processing of the proteins. Samples were subjected to 12% SDS-PAGE along with a Dual Color Molecular Marker (Bio-Rad). After SDS-PAGE, the proteins were transferred to a nitrocellulose membrane (Ge healthcare Armershan™ Hybond™—ECL) by humid transference in blotting buffer (39 mM glycine, 48 mM Tris-base, 0.037% SDS, 20% methanol) using the Bio-Rad system. The lane of the molecular marker was separated from the rest using a clean razor. The two pieces of the membrane were blocked overnight with 5% skimmed milk dissolved in PBST buffer (PBS + 0.1% Tween 20). The part of the membrane containing the proteins was incubated for 1 h at RT (with shaking) with a primary antibody anti-Vip3Aa raised in rabbit at 1/5,000 antibody dilution in PBST containing 0.5% skimmed milk. After 3 washing steps with PBST (5 min each), the membrane was incubated for 1 h at RT with

the secondary antibody anti-rabbit conjugated with HRP peroxidase (Sigma-Aldrich) at 1/20,000 antibody dilution in PBST containing 0.5% skimmed milk. The part of the membrane containing the molecular marker was incubated for 1 h at RT with Precision Protein StrepTactin-HRP (Bio-Rad) at 1/20,000 dilution in PBST. After three washing steps (5 min each) with PBST, the bands were visualized with the Amersham ECL Prime Western Blotting Detection Reagent using an Image Quant LAS 4000.

III. Results

III.1. Engineering of Vip3Aa mutant proteins

To better understand the role of the structural features of Domain I in the toxicity, we have engineered several mutants targeting different regions or processes which can be grouped into four categories: (i) mutants directed to affect the N-t part of the protein, named as Vip3Aa_Δα1, Vip3Aa_41-KVKK-44 and Vip3Aa_M34L, (ii) mutants directed to affect the proteolytic processing and conformational change of the activated protein, named as Vip3Aa_195-AVAA-198 and Vip3Aa_S-S, (iii) mutants directed to reduce the internal diameter of the tetrameric coiled-coil observed in the activated conformation, named as Vip3Aa_L146F and Vip3Aa_L146M, and (iv) a mutant lacking the C-t Domains IV and V (Vip3Aa_ΔIV-V). Details of the mutations and their expected effect on the structure and/or properties of the protein, according to the structural data, are summarized in **Table 2.1**.

Table 2.1. Nomenclature and description of the Vip3Aa mutants

Category	Mutation name	Mutation description [a]	Expected consequence of the mutation
Mutants directed to affect the N-t part of the protein and helix α1	Vip3Aa_Δα1	Deletion from N-t to residue 39 which removes helix α1	To remove helix α1
	Vip3Aa_41-KVKK-44	Mutation of residues 41-DTGG-44 for 41-KVKK-44 that incorporates a new trypsin proteolytic cleavage site after helix α1	To insert a new trypsin cleavage site to remove helix α1
	Vip3Aa_M34L	Point mutation M34L in helix α1	To increase the insecticidal activity of the protein (Banyuls *et al.*, 2021)
Mutants directed to affect the proteolytic processing and the conformational change of the activated protein	Vip3Aa_195-AVAA-198	Mutation of residues 195-KVKK-198 to 195-AVAA-198.	The trypsin proteolytic cleavage site is changed in order to avoid trypsinization (Zhang *et al.*, 2018)
	Vip3Aa_S-S	Mutation to Cys of four residues located in domain I: D66C and N69C in helix α2 and Q96C and L100C in helix α3	To block the protoxin conformation by disulphide bridges formation through the introduced Cys residues
Mutants directed to reduce the inner diameter of the coiled-coil structure	Vip3Aa_L146F	Mutation L146F in helix α3	To change the inside diameter of the coiled-coil
	Vip3Aa_L146M	Mutation L146M in helix α3	To change the inside diameter of the coiled-coil
Mutant directed to affect C-t domains	Vip3Aa_ΔDIV-V	Deletion of C-t domains IV and V	To check the role of C-t domains on maintaining the structure and function

[a] See Figure 2.1

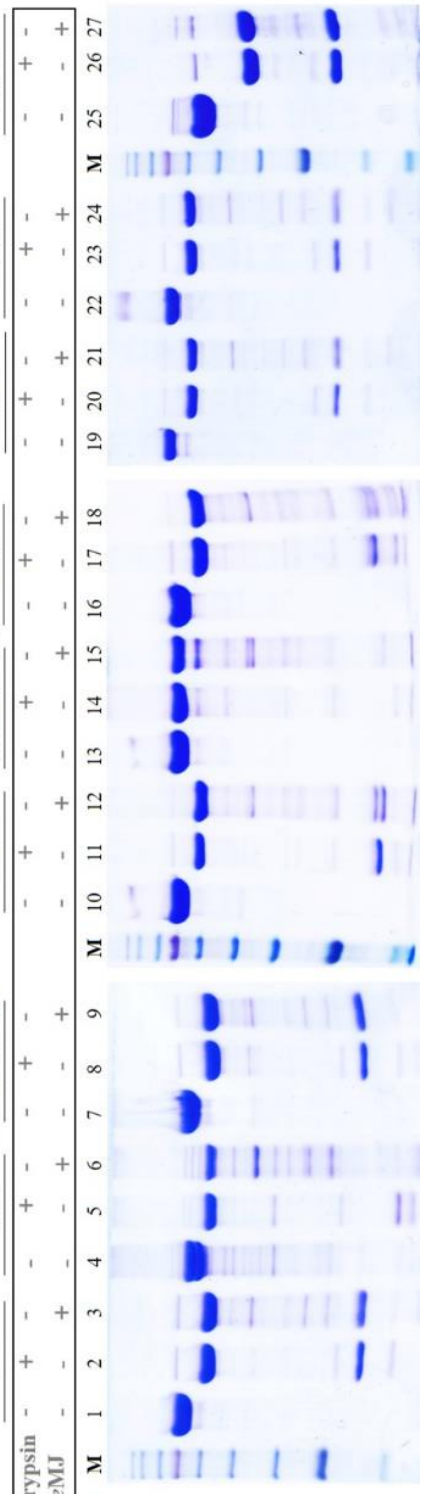

Figure 2.2. *In vitro* proteolytic processing of the Vip3Aa WT and mutant proteins. Proteins were incubated with either commercial trypsin (10% w/w at pH 7.5) or *S. exigua* midgut juice (10% w/w at pH 7.5) and the resulting fragments were separated in SDS-PAGE. Band sizes were estimated according to the Blue Star molecular marker (M) (NIPPON Genetics).

III.2. *In vitro* proteolytic processing of the Vip3Aa WT and mutants

The Vip3Aa WT and mutant proteins were subjected to proteolytic processing *in vitro* under two conditions: using commercial trypsin and using midgut juice of *S. exigua* larvae (*Se*MJ). As can be observed in **Figure 2.2**, the WT protein (~85 kDa), rendered two fragments of 20 and 65 kDa (corresponding to N-t Domain I and C-t Domains II–V, respectively) in both proteolytic conditions. The mutant Vip3Aa_Δα1, which lacks helix α1 (**Figure 2.1C**), showed a doubled band pattern before proteolysis (bands of ~80 and ~75 kDa) (**Figure 2.2**), probably due to different unfolding stages of the dissociated subunits under denaturing conditions affecting the electrophoretic mobility of protein-SDS interaction. MALDI-TOF analysis of the two bands indicated that they were the same protein with 99.5% of confidence. Indeed, upon processing by trypsin, both bands disappeared rendering the 65 kDa band shown in the WT and an N-t band that runs as ~16 kDa, instead of 20 kDa, due to the absence of helix α1. Using *Se*MJ, only the 65 kDa band was observed (**Figure 2.2**), presumably by the degradation of the ~16 kDa fragment by midgut proteases. The mutant Vip3Aa_41-KVKK-44, which includes a proteolytic site in the loop α1α2 aimed to remove helix α1 (**Figure 2.1C**), unexpectedly showed the same proteolytic pattern as the WT in both digestion conditions (**Figure 2.2**), indicating that this site was not sufficiently exposed to be cleaved by proteases. The mutant Vip3Aa_195-AVAA-198, designed to eliminate the trypsin proteolytic site KVKK located in the loop α4α5 between Domains I and II (**Figure 2.1C**), was not digested by the commercial trypsin, as previously described (Zhang *et al.*, 2018). However, a slight

band corresponding to the 65 kDa fragment was observed upon incubation with *Se*MJ, pointing to slight processing by the mixture of proteases in the midgut juice (**Figure 2.2**). The mutant Vip3Aa_S-S, which contained mutations D66C and N69C located in helix α2, as well as, mutations Q96C and L100C located in helix α3, (**Figure 2.1C**) was designed to cross-link helices α2-α3 by two disulphide bonds (D66C-L100C and N69C-Q96C) to avoid remodelling of both helices upon activation. This mutant showed a similar proteolytic pattern to the WT protein under reducing conditions (**Figure 2.2**). However, under non-reducing conditions the 20 kDa band runs faster in SDS-PAGE (**Supplementary Figure S2.2**) indicating a more compact conformation of Domain I probably due to the cross-link between helices α2 and α3. The presence of the disulphide bonds was also confirmed by MALDI-TOF (**Supplementary Figure S2.3**) and LC–MS tandem MS (**Supplementary Figure S2.4**). The three single residue mutants, the mutant Vip3Aa_M34L, having a mutation within helix α1 (**Figure 2.1C**), and the mutants Vip3Aa_L146F and L146M designed to reduce the internal diameter of the tetrameric coiled-coil upon activation (**Figure 2.1D**), as L146 is located in α3 (**Figure 2.1B, C**), all showed a similar pattern to the WT (**Figure 2.2**). Finally, the mutant Vip3Aa_ΔIV-V, lacking the C-t Domains IV and V, showed a proteolytic pattern in both conditions composed of two bands, the 20 kDa for the Domain I and a ~38 kDa comprising Domains II and III (**Figure 2.2**). Overall, all the mutants, except Vip3Aa_195-AVAA-198, showed proteolytic processing upon incubation with *Se*MJ or trypsin, although some of them had changes in the electrophoretic mobility of the protein bands

compared to the WT. The fact that Vip3Aa_195-AVAA-198 could not be processed by trypsin but was slightly processed by *Se*MJ indicates that a different type of proteases may cleave the mutated binding site *in vivo*, or that there is an alternative cleavage site close to the mutated one.

III.3. NS-EM visualization of Vip3Aa WT and mutants

Mutant proteins Vip3Aa_Δα1, Vip3Aa_41-KVKK-44, Vip3Aa_195-AVAA-198, Vip3Aa_S-S and Vip3Aa_ΔIV-V, (all except single point mutations), were analysed by NS-EM before and after trypsin-treatment to explore their effect at the structural level to influence the switch from protoxin to activated protein conformation (**Figure 2.3**).

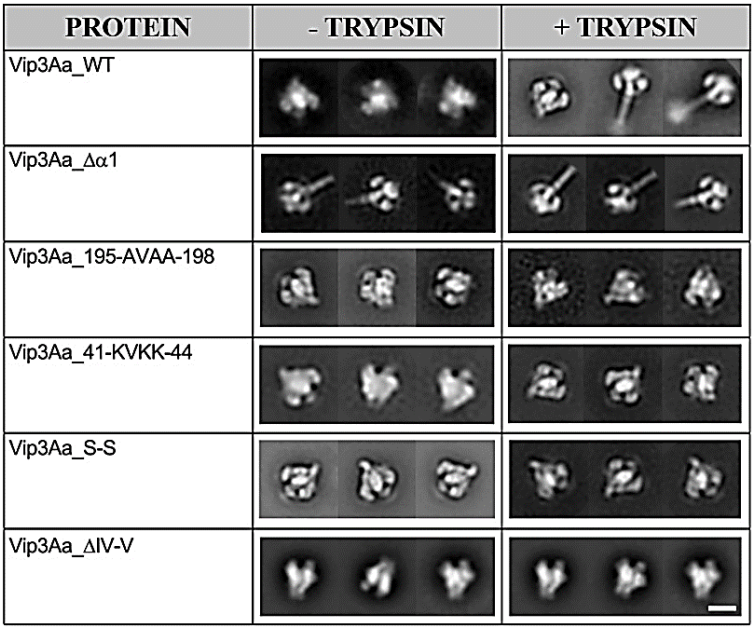

Figure 2.3. Negative staining transmission electron microscopy of Vip3Aa WT and selected mutants. Pictures were taken both before and after trypsin treatment of the samples. The bar at the bottom right represents 10 nm.

As expected, the WT shows the protoxin conformation before incubation with trypsin and the activated conformation after it, in a large fraction of the molecules (**Figure 2.3**). From our previous structural studies, we know that proteolytic processing is necessary to trigger the remodelling into the activated conformation, though the percentage of molecules that undergo the conformational change is variable (50–70%) (Núñez-Ramírez *et al.*, 2020). Interestingly, we observed that the mutant Vip3Aa_Δα1 adopted the activated conformation independently of the incubation with trypsin (**Figure 2.3**). This result indicated that the N-t comprising helix α1 had a relevant role in the stabilization of the helices at Domain I. Indeed, in the protoxin conformation helix α1 interacts with the core of the tetramer formed by Domain II and it is also connected to the loop α1α2 that allows the twist of helix α2 (**Figure 2.1C**). Thus, its absence might release the tension generated by the twist, lowering the energetic barrier required to trigger the remodelling of helices α2 and α3. For the mutants Vip3Aa_41-KVKK-44, Vip3Aa_S-S, and Vip3Aa_ΔIV-V, the majority of the molecules showed the protoxin conformation before and after incubation with trypsin (**Figure 2.3**), which indicates that despite the trypsin cleavage is produced, the shift towards the activated conformation was not favoured. In the case of Vip3Aa_41-KVKK-44, the mutation may have reduced the flexibility of the loop α1α2 in the WT (41-DTGG-44) provided by two Gly residues, slowing down the remodelling of the helices. As originally intended, mutant Vip3Aa_S-S might have cross-linked helices α2 an α3 by disulphide bonds, impairing remodelling. The lack of remodelling of Vip3Aa_ΔIV-V

suggests that the C-t domains IV and V may provide a frame to sustain Vip3Aa during remodelling. In the case of the mutant Vip3Aa_195-AVAA-198, just the protoxin conformation was observed as no cleavage was produced by trypsin (**Figure 2.3**). Thus, our results indicate that remodelling of Domain I is driven by a fine-tuned mechanism where not only proteolytic cleavage is necessary but also an appropriate free energy barrier to favour the conformational change.

III.4. Insecticidal activity of Vip3Aa and its mutants against *S. exigua*

To test the effect of the mutations on the toxicity of the protein, all the mutants were bioassayed against neonate larvae of *S. exigua*. The WT protein showed LC_{50} and LC_{90} values of 19.5 (8.6–28) and 62.9 (47–98) ng/cm^2, respectively (**Table 2.2**). The mutant Vip3Aa_Δα1, lacking helix α1, was non-toxic (**Table 2.2** and **Supplementary Figure S2.1A**); however, the mutant Vip3Aa_41-KVKK-44, designed to eliminate the same helix α1 by trypsin digestion, retained toxicity at the LC_{50} level with a value of 55.1 (26–129) ng/cm^2, whereas it essentially lost all toxicity at the LC_{90} level, indicating a different dose–response compared to the WT (**Table 2.2** and **Supplementary Figure S2.1A**). The mutant Vip3Aa_M34L showed enhanced toxicity compared to the WT (**Table 2.2** and **Supplementary Figure S2.1A**), with LC_{50} and LC_{90} values of 4.5 (1.2–8.6) and 27.7 (17–46) ng/cm^2, respectively. The mutant Vip3Aa_195-AVAA-198, in which the cleavage site was eliminated, showed toxicity values very similar to that of the WT (**Table 2.2** and **Supplementary Figure S2.1B**).

Table 2.2. Toxicity of the WT and mutant proteins against *S. exigua* larvae by Probit analysis

Protein	LC_{50} (95% F.L. [a]) ng/cm²	Relative potency [b] (95% F.L.) at LC_{50}	LC_{90} (95% F.L.) ng/cm2	Relative potency (95% F.L.) at LC_{90}	Slope [c] ± SE [d]	X^2 [e]	DF [f]
Vip3Aa_WT	19.5 (8.6-28)	-	62.9 (47 - 98)	-	2.5 ± 0.4	45	28
Vip3Aa_Δα1	>315	-	>315	-	-	-	-
Vip3Aa_41-KVKK-44	55.1 (26-129)	3.8 (1.9-7.6)	3082 (694-183530)	53.1 (5.7-498)	0.7 ± 0.2	12	12
Vip3Aa_M34L	4.5 (1.2-8.6)	0.23 (0.18-0.31)	27.7 (17-46)	0.42 (0.28-0.64)	1.6 ± 0.3	34	26
Vip3Aa_195-AVAA-198	18.1 (8.8-25)	1.4 (1-2)	56.3 (42-96)	0.9 (0.6-1.3)	2.6 ± 0.6	11	11
Vip3Aa_S-S	>315	-	>315	-	-	-	-
Vip3Aa_L146F	14.9 (7.9-24)	1.7 (1.1-2.6)	376 (155-2439)	6.3 (2.7-15)	0.9 ± 0.1	24	14
Vip3Aa_L146M	54.4 (17-83)	1.8 (1.2-2.6)	202 (128-485)	3.9 (2-7.5)	2.3 ± 0.6	14	15
Vip3Aa_ΔDIV-V	>315	-	>315	-	-	-	-

[a] "95% F.L." indicates the fiducial limits at 95% of confidence. [b] Relative potency values around 1 indicate that mutant proteins have similar toxicity compared to the WT, values higher than 1 indicate a lower toxicity for the mutants, whereas relative potency values smaller than 1 indicate an enhanced toxicity. [c] Similar slope values indicate similar dose-responses. [d] SE indicates the standard error for the calculated slope values. [e] Higher X^2 values indicate higher heterogeneity of the data in the Probit analysis.

In contrast, the mutant Vip3Aa_S-S, in which the conformational change that follows the proteolytic activation is prevented, showed a complete lack of toxicity (**Table 2.2** and **Supplementary Figure S2.1B**). That lack of toxicity could hardly be attributed to the individual mutations, as the single mutant N69C or the double mutant D66C/N69C showed toxicity values similar to the WT protein (LC_{50} values of 7.5 with FL 4.3–10.5 ng/cm^2, and 21.0 with FL 15.3–27.4 ng/cm^2, respectively) and the single mutants Q96C and L100C also showed similar toxicity as the WT (LC_{50} values of 9.6 with FL 6.3–12.8 ng/cm^2, and 18.4 with FL 6.4–33.3 ng/cm^2, respectively). The mutants Vip3Aa_L146F and Vip3Aa_L146M, which according to the amino acid substitutions in the atomic models likely count with a reduced internal diameter in the tetrameric coiled-coil (**Supplementary Figure S2.5**), did not differ from the WT at the LC_{50} level, but had significantly lower toxicity at the LC_{90} level, with a different dose–response compared to the WT protein (**Table 2.2** and **Supplementary Figure S2.1C**). Finally, the mutant Vip3Aa_ΔIV-V, lacking the C-t Domains IV and V, also showed a complete lack of toxicity (**Table 2.2** and **Supplementary Figure S2.1D**).

Overall, these results indicate that helix α1 is essential for Vip3Aa activity, as well as remodelling of helices α2 and α3 and the presence of the C-t domains. The increased activity of Vip3Aa_M34L reinforces the role of helix α1 as a hot spot in the mode of action of this protein. Moreover, Vip3Aa_41-KVKK-44 has a decreased activity, as do Vip3Aa_L146F and Vip3Aa_L146M. The fact that Vip3Aa_195-AVAA-198 showed the same insecticidal activity as the WT suggests an alternative *in vivo* proteolytic cleavage site.

III.5. Proteolytic processing of the Vip3Aa_195-AVAA-198 mutant

The observation that the mutant Vip3Aa_195-AVAA-198, engineered to destroy the cleavage site, showed similar toxicity values compared to the WT despite the fact that it was not activated *in vitro* by commercial trypsin and only barely by *Se*MJ, made us search for other *in vitro* conditions that emulated better the *in vivo* conditions. Thus, we performed the *in vitro* digestion with trypsin at higher pH, incubating with *S. exigua* BBMV, and replacing trypsin with α-chymotrypsin, another relatively common serine peptidase in the lepidopteran larvae midgut (Caccia *et al.*, 2014) (**Figure 2.4A**). The mutant protein could not be processed under any of these new *in vitro* conditions, whereas the WT protein was completely processed by trypsin at both pH conditions and partially processed by *S. exigua* BBMV and α-chymotrypsin.

Since we failed to show the *in vitro* processing of the Vip3Aa_195-AVAA-198 mutant, we set out to demonstrate that this protein was processed at an alternative cleavage site *in vivo*. The *in vivo* digestion assay was performed by drop-feeding *S. exigua* larvae with either the mutant or the WT protein and then dissecting the larvae at different times. The processed proteins were detected by western blot (**Figure 2.4B**). The results showed that both, the WT and mutant Vip3Aa_195-AVAA-198 were completely processed *in vivo* at 16 h after ingestion. However, the kinetics of activation for the mutant protein seemed to be slower, since at 15 min after ingestion the WT protein was completely processed whereas almost half of the mutant proteins still remained undigested. The *in silico* analysis of the proteolytic cleavage

sites in the surroundings of 195-AVAA-198, using the ExPASy Peptide Cutter tool (Bioinformatics Resources, Swiss Institute of Bioinformatics), predicts 14 potential trypsin/chymotrypsin cleavage sites in a range from 8 to 22 amino acids upstream and downstream of the 195-AVAA-198 sequence. Most probably, *in vivo*, some of these sites become available for trypsin or chymotrypsin cleavage.

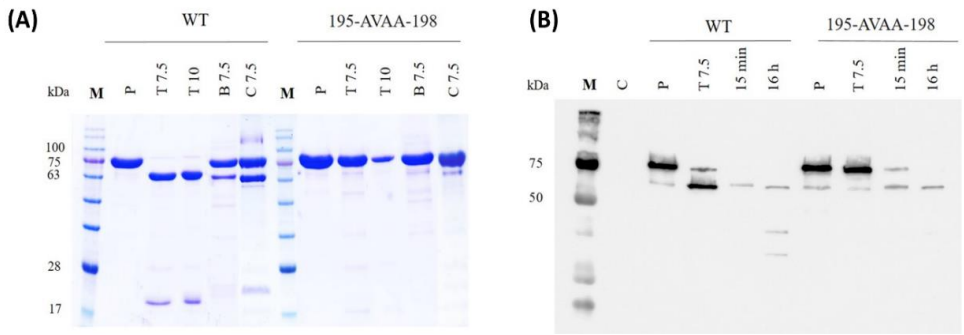

Figure 2.4. Proteolytic processing of the Vip3Aa_195-AVAA-198 mutant under different conditions. (A) The proteins were incubated *in vitro* under different conditions and then subjected to SDS-PAGE. P, protoxin samples; T7.5, samples digested with trypsin (10% w/w) at pH 7.5; T10, samples digested with trypsin (10% w/w) at pH 10; B7.5, samples digested with *S. exigua* BBMV (10% w/w) at pH 7.5; C7.5, samples digested with α-chymotrypsin (10% w/w) at pH 7.5. Band sizes were estimated according to the Blue Star molecular marker (M) (NIPPON Genetics). (B) Larvae fed with either protein were dissected after 15 min or 16 h and the midgut sample was subjected to SDS-PAGE. The Vip3Aa (WT and mutant) digestion fragments were detected by western blot. C, control midgut sample from non-intoxicated larvae; P, controls of protoxin samples (100 ng); T7.5, controls of *in vitro* trypsin-treated proteins at pH 7.5 (100 ng); 15 min, *in vivo* processed proteins after 15 min of ingestion; 16 h, *in vivo* processed proteins after 16 h of ingestion. Band sizes were estimated according to the Dual Color molecular marker (M) (NIPPON Genetics).

IV. Discussion

The recent structures of Vip3Aa and Vip3Bc in the protoxin and activated conformations have revealed that remodelling events at Domain I may impact insecticidal activity. To shed light on this mechanism, we engineered several Vip3Aa mutants, in highly conserved residues of Domain I (**Supplementary Figure S2.6**), and then, characterized their proteolytic profile and insecticidal activity, as well as their conformational flexibility trying to correlate their structural features with their activity *in vivo*.

Our data indicate that remodelling and toxicity are interconnected by a fine-tuned mechanism where the free energy that involves remodelling depends on the appropriate coordination of several structural features. One of these structural features corresponds to helix α1 which has proven to be essential. Its absence leads to a complete loss of toxicity, in agreement with previous reports showing that the lack of the first 33 and 39 residues at the N-t abolished the insecticidal activity of the protein (Bhalla *et al.*, 2005; Selvapandiyan *et al.*, 2001). Our data also reveal that the absence of helix α1 induces the spontaneous conformation of activated protein. Thus, we can envision that helix α1 may be holding Domain I in the protoxin conformation through interactions with Domain II until the protein has been proteolytically processed in the surroundings of the membrane of the midgut cells, to favour remodelling and interaction with the membrane at the appropriate location and timing. The mutant Vip3Aa_M34L, which carries a point modification within helix α1, shows enhanced toxicity

compared to the WT protein, in agreement with previous results obtained with the Vip3Af protein and the related species *Spodoptera littoralis* (Banyuls *et al.*, 2021). The fact that a point mutation inside this region increases the toxicity can be related to the amphipathic nature of helix α1, increasing its hydrophobicity to improve the interaction with the hydrophobic nature of the membrane since the hydrophobic index of Leu (0.943) is higher than Met (0.738) (Black and Mould, 1991). In amphipathic helices (AH), the hydrophobic side of the helix inserts into the interior of the bilayer, while the hydrophilic side interacts with the lipid headgroups (Drin and Antonny, 2010; Roberts *et al.*, 2013), thus, promoting membrane curvature and membrane fission (Campelo *et al.*, 2008; Martyna *et al.*, 2017). AHs of many fission-inducing proteins contain at least two basic residues (Arg and/or Lys) each at the polar-non-polar interface (Zhukovsky *et al.*, 2019). Helix α1 (with aa sequence 23-IYGFATGIKDIMNMIFK-39) contains two Lys, K31 and K39 which may indicate that Vip3Aa could induce membrane fission. Then, that would lead to a better insertion in the membrane to further interact with some transmembrane or intracellular compounds to lead the cell death, possibly through its internalization and activation of the apoptotic pathways as has already been described (Hernández-Martínez *et al.*, 2017; Hou *et al.*, 2020; Jiang *et al.*, 2016; Nimsanor *et al.*, 2020). Vip proteins can get inserted into the membrane of liposomes through the N-t part of Domain I (Byrne *et al.*, 2021) and have been described as pore-forming proteins (Lee *et al.*, 2003; Liu *et al.*, 2011). The tetrameric coiled-coil in the structure of Vip3Aa holds a divalent ion bound in an internal diameter of ~3 Å (Núñez-Ramírez *et al.*, 2020) which size could

impact pore formation, although it is much narrower compared to the pore diameters described for other pore-forming proteins (Dal Peraro and van der Goot, 2016; Meusch *et al.*, 2014; Mueller *et al.*, 2009). Thus, mutations at L146 to Phe and Met were aimed to reduce the diameter and possibly affect ion transportation, as these are more voluminous residues than Leu. However, just a reduction of toxicity at the LC_{90} level was detected, indicating that the inside diameter of the coiled-coil is not a critical feature for Vip3Aa insecticidal activity. Thus, ion binding to the tetrameric coiled-coil might help to maintain the structural stability and dynamics of the coiled-coil (Hartmann, 2017) and not serve for ion transportation, though it cannot be ruled out that the interaction of Domain I with the membrane might facilitate ions crossing the membrane through other mechanisms.

A second structural feature that is essential for the Vip3Aa activity is the remodelling of helices α2 and α3, as the mutant Vip3Aa_S-S which locked the protein in the protoxin conformation impaired the insecticidal activity. These two long helices comprise the total length of the tetrameric coiled-coil (**Figure 2.1B**) and possibly serve as a scaffold for the action of helix α1 in the toxicity exerted by the activated protein.

A third structural feature that has been demonstrated to be relevant is the loop α1α2 (residues 40–47). We mutated the sequence 41-DTGG-44, which contains two Gly, for 41-KVKK-44, resulting in the reduction of the toxicity of this mutant. Although our mutation was intended to introduce a cleavage site for the release of helix α1, the mutation has demonstrated that stiffness in the loop between helices α1 and α2 is

deleterious. Thus, flexibility in this region is important for remodelling and therefore, for the insecticidal activity of the protein.

A fourth structural feature that unexpectedly has resulted to be critical for remodelling is the C-t part of the protein, formed by Domains IV and V which are not interacting with Domain I. Their absence in Vip3Aa favoured the protoxin conformation and abrogated toxicity. This is in agreement with previous reports showing a drastic lack of toxicity of Vip3Aa truncations at the C-t when tested in bioassays with several lepidopteran pests, including *S. exigua* (Banyuls *et al.*, 2018, 2021; Gayen *et al.*, 2012, 2015; Li *et al.*, 2007; Quan and Ferré, 2019; Selvapandiyan *et al.*, 2001). The fact that the protoxin conformation was favoured in the absence of Domains IV and V points out a role for the C-t during remodelling, most likely through the interaction with the epithelial membrane of the cells. Thus, the absence of both domains may impair Vip3A from targeting the membrane, affecting recognition to find an interacting surface. However, we cannot discard that the lack of these domains could affect the proteolytic activation process of the protein *in vivo*, and so, the absence of toxicity could be the result of different factors.

Finally, the 195-AVAA-198 cleavage site is also an essential structural feature for remodelling and toxicity. Surprisingly, we have found that alternative proteolytic processing may also take place *in vivo*, and this explains why the toxicity of this mutant does not differ from that of the WT, at least against *S. exigua*. Our results are in contrast to those obtained by Zhang *et al.* (2018), where the same mutant protein showed

a significant reduction of toxicity to *S. exigua*. It is important to note that the mortality values obtained by these authors for all the Vip3Aa proteins tested were much lower than ours, suggesting important differences in the susceptibility of the *S. exigua* colonies against Vip3Aa proteins.

V. Conclusions

In conclusion, we have demonstrated here the crucial role of helix α1 and the remodelling which takes place in the activated conformation at Domain I for the insecticidal activity of the Vip3Aa protein. We have proposed several structural features that are relevant for the timing in which Vip3Aa remodelling occurs to drive its biological activity: the role of helix α1, essential for toxicity, holding the Domain I in the protoxin conformation and most probably interacting with the membrane in the activated conformation, the flexibility of the loop α1α2, the remodelling of helices α2 and α3, the proteolytic processing that takes place at the loop α4α5 between Domains I and II and the role of the C-t Domains IV and V to sustain the conformational change.

Chapter 3

Receptor interactions of protoxin and activated Vip3Aa structural conformations in *Spodoptera exigua*

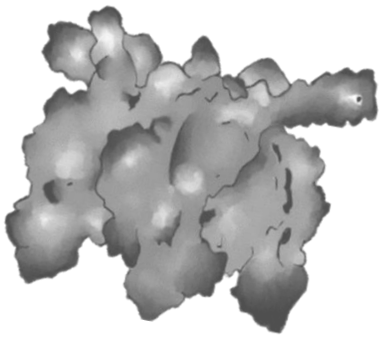

Adapted from:
Lázaro-Berenguer M, Ferré J, Hernández-Martínez P. 2024. Receptor interactions of protoxin and activated Vip3Aa structural conformations in *Spodoptera exigua*. Pest Manag Sci 80(12), 6142–6149. https://doi.org/10.1002/ps.8341

I. Introduction

The *Spodoptera* genus, commonly known as armyworms owing to the well-known gregarious behaviour of their larvae, comprises several lepidopteran species widely recognized as major global pests (Allen and DEFRA, 2024). These insects have become major invaders, colonizing multiple continents outside their native range (Kergoat *et al.*, 2021). Their larvae are extremely polyphagous, causing extensive damage by feeding on a wide range of crops, resulting in significant financial losses for agriculture on a global scale (Sharma *et al.*, 2017).

Entomopathogenic bacteria can help to control these pests by providing us with a variety of insecticidal compounds. Cry proteins produced by *Bacillus thuringiensis* (Bt) are the most widely used and better studied among insecticidal proteins (Bravo *et al.*, 2023; Palma *et al.*, 2014). The genes coding for these proteins have been incorporated into transgenic plants (Bt-crops), offering effective pest control since the mid-90s (Estruch *et al.*, 1997; James, 2015; Shelton, 2012). However, resistance evolution to Cry proteins in some insect pests has prompted the search for alternative insecticidal proteins (Bravo *et al.*, 2023; Downes and Mahon 2012; Storer *et al.*, 2012; Tabashnik and Carrière, 2019). In this context, Vip proteins, also produced by Bt, have emerged as valuable candidates as a consequence of their potency against lepidopteran insects and, most important, the fact that they do not share binding sites with Cry proteins (Chakroun and Ferré, 2014; Gouffon *et al.*, 2011; Hamadou-Charfi *et al.*, 2013; Lee *et al.*, 2003; Liu *et al.*, 2011; Quan *et al.*, 2021a; Sena *et al.*, 2009), and there is no reported case of cross-resistance between them (Tabashnik and Carrière, 2020). Therefore, Vip proteins

have become excellent partners for Cry proteins in pyramided Bt-crops, which combine different insecticidal proteins with different specificity to expand the target spectrum and prevent the appearance of insect resistance (Carrière *et al.*, 2015; Moar and Anilkumar, 2007; Tabashnik and Carrière, 2017). To date, numerous events of maize and cotton containing vip3Aa genes combined with *cry* genes have been approved for commercialization globally, with expectations for their adoption in many more crops in the future (Gupta *et al.*, 2021).

Vip proteins are produced by Bt during its vegetative growth phase and are secreted into the media as tetrameric molecules. Each tetramer comprises four identical monomers, with each monomer composed by five structural domains (Byrne *et al.*, 2021; Núñez-Ramírez *et al.*, 2020; Zheng *et al.*, 2020). The N-terminal (N-t) Domains I and II play roles in tetramer maintenance and toxicity (Ferré *et al.*, 2023; Jiang *et al.*, 2020a; Jiang *et al.*, 2023b; Lázaro-Berenguer *et al.*, 2022a). Domains II–III, have been associated with binding functions (Quan *et al.*, 2021a; Jiang *et al.*, 2023b), whereas the C-terminal (C-t) Domains IV–V are carbohydrate binding motifs, and it has been proposed that they may be involved in peritrophic matrix interactions and glycosylated molecules engagement (Byrne *et al.*, 2021; Jiang *et al.*, 2020a; Jiang *et al.*, 2023b; Núñez-Ramírez *et al.*, 2020).

Cryo Electron Microscopy (cryo-EM) resolution of trypsin processed Vip3Aa and Vip3Bc proteins revealed a structural remodelling occurring at the N-t region. This enabled the distinction between two different structural conformations: the protoxin and the activated protein (Byrne *et al.*, 2021; Núñez-Ramírez *et al.*, 2020). In the protoxin,

the tetramer adopts a pyramidal structure in which the N-t (Domains I and II) forms a helix bundle. That region of the protein gets unfolded and remodelled into a tetrameric coiled-coil in the activated protein, which consists of a central core from which a long stalk protrudes. This coiled-coil structure is formed by Domain I and has a flexible end consisting of helix α1 (residues 23–39) (**Figure 3.1**).

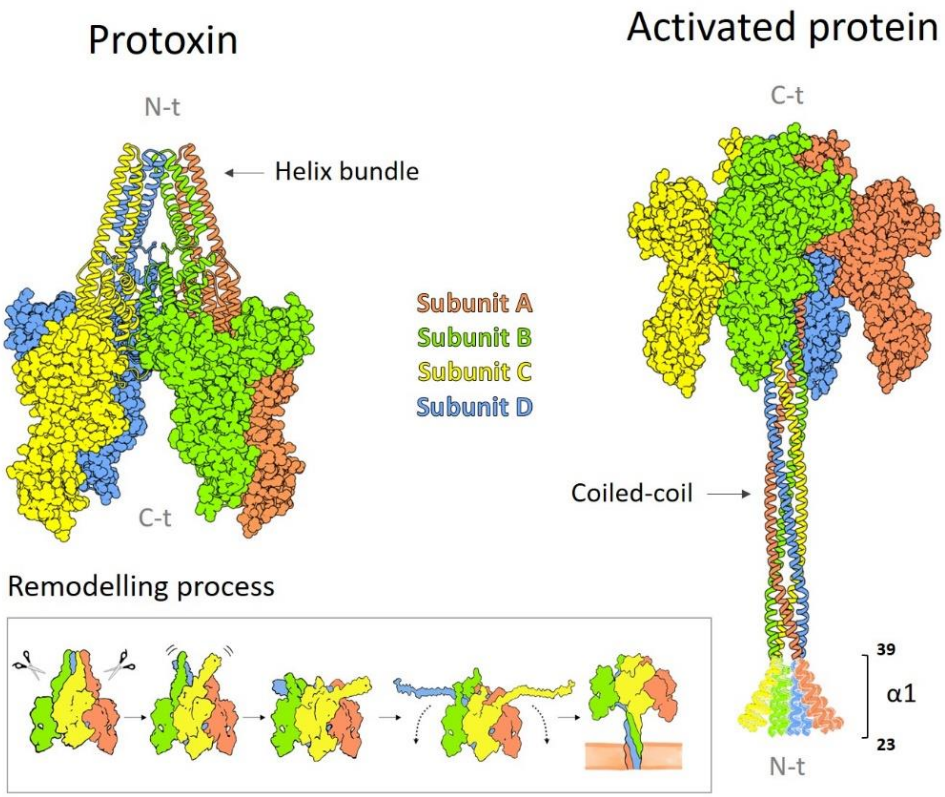

Figure 3.1. Vip3Aa protein structural remodelling. Vip proteins form tetramers composed by four identical subunits. In the protoxin conformation (left), the N-t composed by Domains I and II, forms a helix bundle that, after proteolytic cleavage at the primary site (residues 195–198 in the loop between Domains I and II), is remodelled into a tetrameric coiled-coil (involving Domain I) in the activated conformation (right), with a flexible end consisting of helix α1 (residues 23–39). The bottom panel (modified from Byrne *et al.*, 2021) shows the remodelling process proposed for Vip proteins.

The end of the stalk structure has been observed to insert into the membrane of liposomes (Byrne *et al.*, 2021; Shao *et al.*, 2024), in agreement with the DeepTMHMM transmembrane prediction tool (Hallgren *et al.*, 2022) which indicates a putative transmembrane region in residues 12–30 of Vip3Aa (**Supplementary Figure S3.1**).

Regarding Vip proteins' mode of action, it is generally accepted that upon ingestion by larvae, the proteins are proteolytically cleaved between helices α4 and α5 by midgut proteases, bind specifically to their receptors in the apical membrane of the midgut epithelium (which identity is still under debate) and get inserted into the cell membrane after remodelling into the activated conformation (Byrne *et al.*, 2021; Ferré *et al.*, 2023; Lázaro-Berenguer *et al.*, 2022a). Because it is not clear whether the remodelling to the activated protein conformation requires binding to the membrane receptors or can take place before binding, this study aims to examine if Vip3Aa is able to bind to *Spodoptera exigua* midgut binding sites in both structural conformations. To address this question, we have used protoxin and trypsin-processed Vip3Aa proteins in *in vitro* binding assays to *S. exigua* brush border membrane vesicles (BBMV) and *in vivo* competition assays. In addition, two different structural mutants that lock the protein in either its protoxin or its activated-protein conformation have been used. On the one hand, the mutant Vip3Aa_Δα1, which lacks α-helix 1, has a constitutive activated-protein conformation owing to the loss of contacts between helix α1 and Domain II α-helices that stabilize the protoxin structure (Lázaro-Berenguer *et al.*, 2022a). On the other, the mutant Vip3Aa_S-S displays a constitutive protoxin conformation as a result of the

introduction of disulphide bonds cross-linking Domain I α-helices 2 and 3 which avoids its remodelling to the coiled-coil structure that is formed in the activated conformation (Lázaro-Berenguer *et al.*, 2022a). Both mutants were described as nontoxic against *S. exigua* larvae, indicating the importance of the helix α1 and the conformational change for the toxicity of the protein (Lázaro-Berenguer *et al.*, 2022a). Our results show that both structural conformations of the Vip3Aa protein share binding sites in *S. exigua* midgut epithelium.

II. Materials and methods

II.1. Protein expression and purification

The production of the Vip3Aa wild type (WT) protein (Vip3Aa_Wt) and its structural mutants (Vip3Aa_$\Delta\alpha$1 and Vip3Aa_S-S) was performed as described previously with minor modifications (Lázaro-Berenguer *et al.*, 2022a; Núñez-Ramírez *et al.*, 2020). Briefly, protein expression was conducted in *Escherichia coli* C43 (DE3) cells containing each of the construct vectors. Cells were grown in 700 mL Luria-Bertani broth supplemented with Ampicillin (100 μg/mL) to exponential phase [optical density at 600 nm (OD_{600}) ~ 0.6–0.8], then induced with 1 mM isopropyl b-D-1-thiogalactopyranoside (IPTG) and incubated at 25°C overnight. Cells were collected and stored at −20°C. For purification, thawed cells were resuspended in buffer A (50 mM Tris–HCl, 150 mM NaCl, 5 mM $MgCl_2$ pH 8.0) supplemented with 3 mg/mL lysozyme, 10 μg/mL DNase and 100 μM PMSF and incubated for 30 min at 37°C with shaking. The lysate was then sonicated for 5 min and centrifuged at 25,000 ×*g* for 30 min. The clarified supernatant was loaded onto a 5-mL

StrepTrap column (Cytiva) for protein purification. The protein was eluted with 5 mM d-desthiobiotin dissolved in buffer A at pH 8.0. The Strep II-tag was removed by treating with 3C PreScission Protease (Cytiva) followed by dialysis in buffer A. The sample was then subjected to another step of affinity chromatography with the StrepTrap column to separate the nontagged protein from any remaining tagged molecules, and pure proteins were eluted in buffer A. The mutant protein Vip3Aa DIP (disabled insecticidal protein) E168A was used as positive control for *in vivo* competition assays. The protein was produced as described previously (Banyuls *et al.*, 2018; Lázaro-Berenguer *et al.*, 2022b). The mutant protein Cry1Ab R99E was used as negative control for *in vivo* competition assays. Heterologous expression in *E. coli*, cell lysis, protoxin solubilization, trypsin-activation and purification by anion-exchange were performed as described previously (Martínez-Solís *et al.*, 2018). Pure proteins were checked in 12% acrylamide SDS-PAGE gels (**Supplementary Figure S3.2**), aliquoted, flash-frozen with liquid nitrogen, and stored at −80°C for further use.

II.2. Preparation of *S. exigua* brush border membrane vesicles (BBMV)

The BBMV were obtained using the differential magnesium precipitation method (Wolfersberger, 1993) starting with frozen midgut tissue from last instar larvae of *S. exigua*. After preparation, vesicles were divided into aliquots, rapidly frozen in liquid nitrogen, and stored at −80°C. Before their utilization in *in vitro* binding assays, BBMV were thawed, centrifuged and resuspended in binding buffer. The protein

concentration in the BBMV samples was then quantified using the Bradford assay (Bradford, 1976).

II.3. Protein ^{125}I radiolabelling

Vip3Aa_Wt and Vip3Aa_Δα1 protoxins were radiolabelled by the Chloramine T method (Van Rie *et al.*, 1989) following the protocol described elsewhere (Quan *et al.*, 2021a; Lázaro-Berenguer *et al.*, 2022b). Briefly, 25 μg of pure protein were mixed with 0.3 mCi of [^{125}I]-NaI and 1/3 (v/v) of 18 mM Chloramine T. The excess of free ^{125}I was separated from the labelled protein using a PD10 desalting column (Cytiva). The purity of the labelled proteins was checked by analysing the eluted fractions by SDS-PAGE with 12% acrylamide gels and autoradiography (**Supplementary Figure S3.3**). Vip3Aa_Wt was labelled twice being the specific activity 5.07 and 5.90 μCi/μg, respectively. The specific activity of radiolabelled Vip3Aa_Δα1 was 2.60 μCi/μg. Labelled proteins were stored at 4°C and used up to 1 month.

II.4. *In vitro* binding assays with radiolabelled proteins and BBMV

In vitro binding assays were performed as described previously (Lázaro-Berenguer *et al.*, 2022b). Briefly, for all kind of assays, labelled proteins were incubated with BBMV for 1 h in 100 μL final volume of binding buffer (20 mM Tris–HCl, 1 mM $MnCl_2$, 0.1% BSA pH 7.4). After incubation, the reaction was halted by centrifugation at 16,000 ×*g* for 10 min at 4°C, and the pellet was washed with 500 μL of binding buffer. Radioactivity retained in the pellet was quantified using a model 2480 WIZARD2 γ-counter (Perkin Elmer) to assess bound labelled protein.

Bindability assays with a fixed amount of labelled protein (0.2 nM), increasing concentrations of BBMV and an excess of unlabelled competitor (1,000-fold molar ratio) were performed for both non-processed and trypsin-treated samples of Vip3Aa_Wt and Vip3Aa_Δα1 labelled proteins. Competition assays were performed by mixing a fixed amount of trypsin-processed labelled proteins (0.2 nM) with increasing concentrations of unlabelled homologous and heterologous competitors and a fixed amount of BBMV established according to the shape of their respective total binding curves in bindability assays (0.05 mg/mL for Vip3Aa_Wt and 0.1 mg/mL for Vip3Aa_Δα1 radiolabelled proteins based on BBMV concentration in which total binding is not saturated). For measuring binding reversibility, chase-time experiments were performed by incubating a fixed amount of trypsin-processed labelled proteins (0.2 nM) with a fixed amount of BBMV (0.05 mg/mL for Vip3Aa_Wt and 0.1 mg/mL for Vip3Aa_Δα1). After an incubation time of 1 h, a 1,000-fold molar excess of unlabelled competitor was added to the tubes and samples were collected after 5 min, 30 min and 1 h chase-time. The samples were centrifuged and washed as for the rest of binding assays; radioactivity retained in the pellet corresponding to the remaining labelled protein bound after the chase time was quantified for the different time points. Trypsin-treatment of labelled proteins and competitor samples was performed at 1% w/w with commercial trypsin from bovine pancreas (Sigma Aldrich), incubating at 37°C for 1 h in all cases. The proteolytic profile of Vip3Aa_Wt, Vip3Aa_Δα1 and Vip3Aa_S-S competitor proteins after trypsin-incubation can be observed in **Supplementary**

Figure S3.2. At least two technical replicates were performed for each binding assay, competition assay or chase-time experiment. Graphical representations were obtained with Prism (GraphPad). The binding parameters equilibrium dissociation constant (K_d) and binding site concentration (R_t), were estimated using LIGAND (Munson and Rodbard, 1980) for the homologous competition curves of both Vip3Aa_Wt and Vip3Aa_Δα1 radiolabelled proteins.

II.5. *S. exigua* colony rearing and *in vivo* competition assays

For surface contamination bioassays, a laboratory population of *S. exigua* was reared on semi-synthetic diet (Bell and Joachim, 1976) under controlled conditions: 25 ± 2°C, 70 ± 5% RH and a photoperiod of 16:8 h, light:dark. *In vivo* competition bioassays were conducted using different protein:competitor molar ratios (1:0, 1:10, 1:100 and 1:1,000) in buffer A, the structural mutants Vip3Aa_Δα1 and Vip3Aa_S-S were used as competitors. Negative controls included buffer (labelled as 0) and an excess of competitor (labelled as 0:1,000 representing the highest competitor concentration used). A Vip3Aa DIP mutant carrying the point mutation E168A, which lacks toxicity but maintains its binding capacity, was used as a positive control of *in vivo* competition based on previous results found in *Spodoptera littoralis* (Lázaro-Berenguer *et al.*, 2022b). The Cry1Ab R99E mutant protein, described previously as nontoxic but able to block the toxicity of its WT counterpart, was used as a negative control of competition (Chen et al, 2021; Hernández-Martínez *et al.*, 2022; Jerga *et al.*, 2019). Pure Vip3Aa at a constant concentration of 20 ng/cm^2 determined from previous median lethal

concentration (LC_{50}) values (Lázaro-Berenguer *et al.*, 2022a) was mixed with corresponding amounts of pure competitor proteins to create the desired ratios. Dispensing 50 μL of protein preparations onto the surface of assay wells (2 cm^2 diameter) filled with semi-synthetic diet, we employed 16 wells per protein dose. Following drying of the diet surface, a single neonate larva was gently introduced into each well, and the plates were sealed. Trays were kept in a climatic chamber mimicking rearing conditions, and mortality was recorded after 7 and 10 days of incubation. Each *in vivo* competition protein combination underwent at least three biological replicates. Statistical analysis of mortality differences between 1:0 and other protein: competitor ratios was performed by a One-Way ANOVA with post hoc Bonferroni test in Prism (GraphPad), ensuring rigorous assessment of significance with P-values higher than an α-value of 0.05.

III. Results

III.1. *In vitro* binding assays to *S. exigua* BBMV with radiolabelled Vip3Aa proteins

In order to examine the ability of protoxin conformation and activated toxin conformation to bind to midgut receptors, radiolabelled Vip3Aa non-processed and trypsin-processed samples were used in binding assays to BBMV from *S. exigua*. Our results showed that Vip3Aa was able to bind in both conformations (**Figure 3.2A, B**). However, although the protoxin showed a higher total binding (60%) (**Figure 3.2A**) than the trypsin-processed protein (20% at the highest BBMV dose tested), practically most of the binding of the protoxin was nonspecific, in

contrast to the binding of the trypsin-processed Vip3Aa (**Figure 3.2B**). We also performed *in vitro* binding assays with the Vip3Aa_Δα1 mutant, which shows a constitutive activated-protein conformation without the need of proteolytic cleavage. Both non-processed and trypsin-treated samples showed specific binding (**Figure 3.2C, D**). Interestingly, the nonspecific binding was not dose-dependent. In addition, the trypsin-processed Vip3Aa_Δα1 showed lower nonspecific binding than the non-processed Vip3Aa_Δα1.

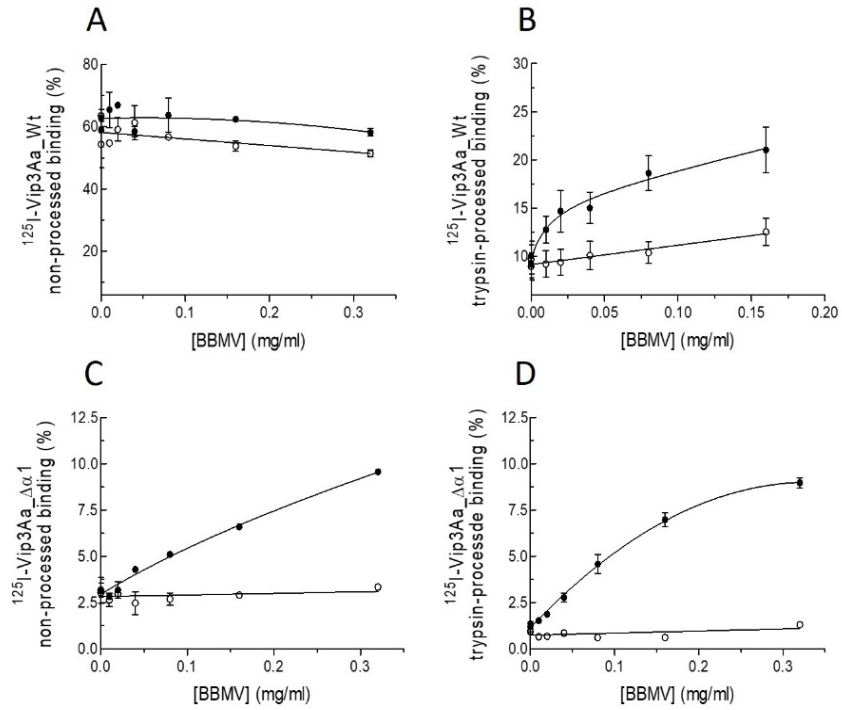

Figure 3.2. ^{125}I-Vip3Aa_Wt and ^{125}I-Vip3Aa_Δα1 binding assays in *S. exigua* BBMV. *In vitro* binding assays were performed using non-processed ^{125}I-Vip3Aa_Wt (A) with only protoxin molecules, trypsin-processed ^{125}I-Vip3Aa_Wt (B) having a mixture of molecules in protoxin and activated conformations, non-processed ^{125}I-Vip3Aa_Δα1 (C) and trypsin-processed ^{125}I-Vip3Aa_Δα1 (D), both samples having only activated structure, in combination with increasing concentrations of *S. exigua* BBMV. Full circles and open circles represent total and nonspecific binding (determined with 1000-fold unlabelled homologous competitors), respectively. Each data point represents the mean of at least two replicates (±SEM). Wt, wild type.

III.2. *In vitro* binding competition assays

Competition assays were performed using trypsin-treated ^{125}I-Vip3Aa_Wt and increasing concentrations of non-labelled homologous competitor. The analysis of the curve provided a dissociation constant (K_d) of 117 ± 43 nM, with a concentration of binding sites (R_t) of 129 ± 52 pmol/mg of BBMV protein. We also used two Vip3Aa structural mutants that lock the protein in its protoxin (Vip3Aa_S-S) or its activated conformation (Vip3Aa_Δα1) as heterologous competitors. Both trypsin-processed mutant proteins were able to compete for the specific binding of trypsin-treated ^{125}I-Vip3Aa_Wt (**Figure 3.3A–C**). Using trypsin-processed Vip3Aa_Δα1, Vip3Aa_S-S and Vip3Aa_Wt as competitors for trypsin-processed ^{125}I-Vip3Aa_Δα1, the three proteins were able to compete for the specific binding of the labelled protein (**Figure 3.3D–F**) confirming that both conformations bind to the same sites. The analysis of the homologous competition curve for trypsin-treated ^{125}I-Vip3Aa_Δα1 provided a K_d of 22.7 ± 5.2 nM and an R_t of 11.8 ± 2.0 pmol/mg of BBMV protein.

III.3. *In vitro* binding reversibility assays

Chase-time experiments were performed to assess the binding reversibility of ^{125}I-Vip3Aa_Wt and ^{125}I-Vip3Aa_Δα1 to the BBMV. Trypsin-processed ^{125}I-Vip3Aa_Wt showed 50% irreversible binding, occurring the binding displacement at the beginning of the chase-time (**Figure 3.4A**), whereas trypsin-processed ^{125}I-Vip3Aa_Δα1 exhibited higher irreversible binding (80%) and the binding displacement took place later (**Figure 3.4B**).

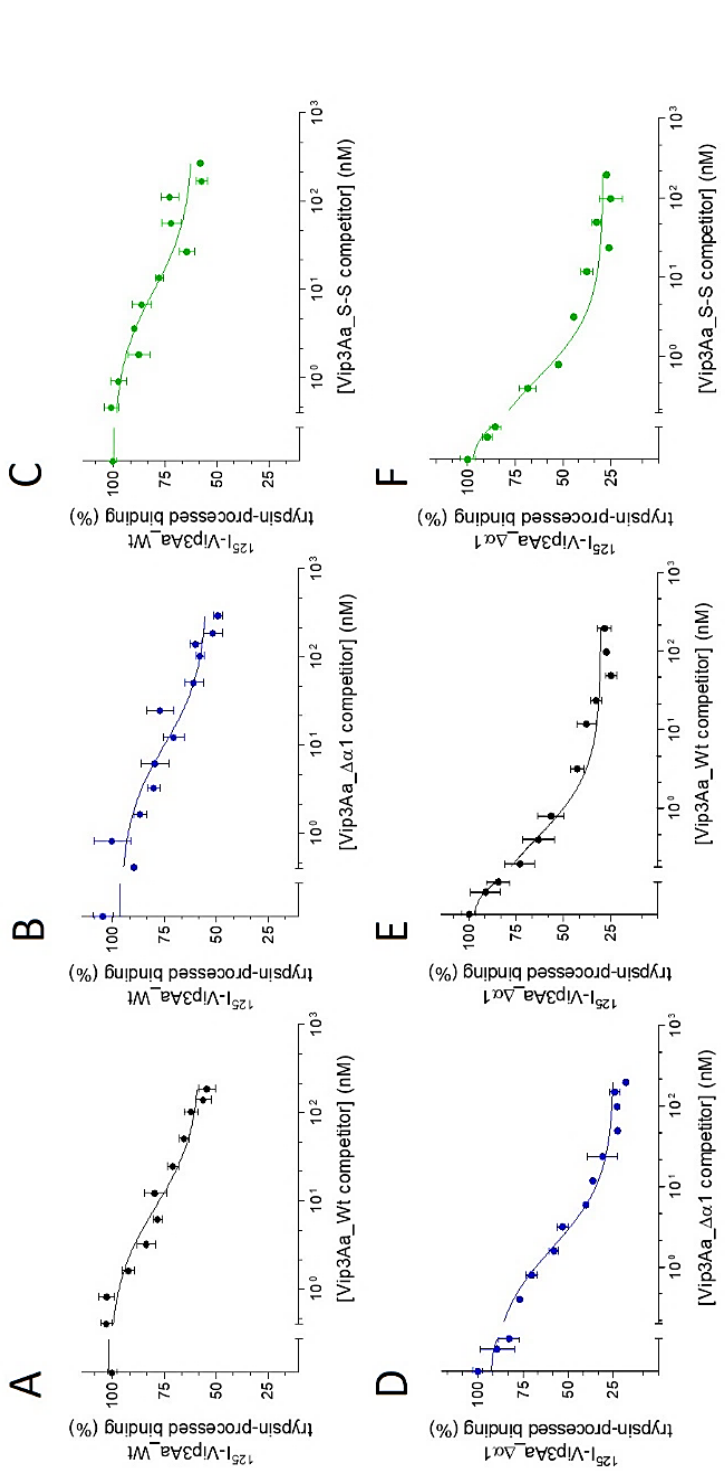

Figure 3.3. ^{125}I-Vip3Aa_Wt and ^{125}I-Vip3Aa_Δα1 competition binding assays in *Spodoptera exigua* brush border membrane vesicles (BBMV). Trypsin-processed labelled proteins ^{125}I-Vip3Aa_Wt (A–C) and ^{125}I-Vip3Aa_Δα1 (D–F) were used with a fixed concentration of BBMV and increasing concentrations of unlabelled competitors. Competitions in black colour refer to the use of trypsin-processed Vip3Aa_Wt as competitor, which contains a mixture of protoxin and activated-protein structural conformations. Competitions in blue refer to the use of trypsin-processed Vip3Aa_Δα1 as competitor, which displays a constitutive activated-protein structure. Competitions in green refer to the use of trypsin-processed Vip3Aa_S-S as competitor, showing a constitutive protoxin conformation. Each data point represents the mean of at least two replicates (± SEM). Wt, wild type.

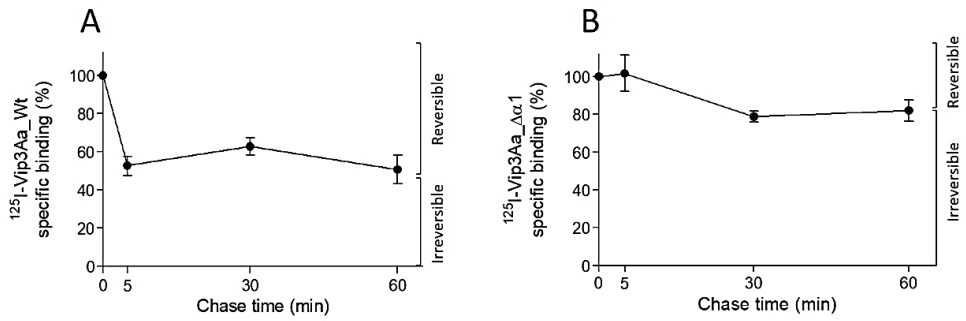

Figure 3.4. ^{125}I-Vip3Aa_Wt and ^{125}I-Vip3Aa_Δα1 binding reversibility assays in *Spodoptera exigua* brush border membrane vesicles (BBMV). Chase-time experiments were performed by pre-incubating trypsin-processed ^{125}I-Vip3Aa_Wt (A) (containing a mixture of both structural conformations), and trypsin-processed ^{125}I-Vip3Aa_Δα1 (B) (containing only molecules in the activated-protein conformation), with a fixed amount of *S. exigua* BBMV before adding an excess (1000x) of homologous nonlabelled competitors. Samples were collected after 5, 30 and 60 min of incubation with competitor proteins to quantify the remaining binding and evaluate binding reversibility. Each data point represents the mean of at least two replicates (± SEM). Wt, wild type.

III.4. Vip3Aa *in vivo* competition against conformational mutants

Finally, to evaluate the functionality of the Vip3Aa binding in its both structural stages, we performed *in vivo* competition assays using the conformational mutants as competitors, since none of them is toxic against *S. exigua* larvae (Lázaro-Berenguer *et al.*, 2022a) and both are able to compete with Vip3Aa *in vitro*. The Vip3Aa E168A and Cry1Ab R99E mutant proteins were used as positive and negative controls of competition, respectively. The bioassays showed that in a similar way to the Vip3Aa DIP mutant used as positive control (**Figure 3.5A**), both structural mutants Vip3Aa_Δα1 and Vip3Aa_S-S, were able to block the Vip3Aa_Wt's toxicity (**Figure 3.5B, C**), indicating that both conformations of the protein bind to functional receptors *in vivo*. However, as expected given the lack of shared receptors among Cry1A

and Vip3A proteins, the mutant Cry1Ab R99E did not block the Vip3Aa_Wt's toxicity (**Figure 3.5D**).

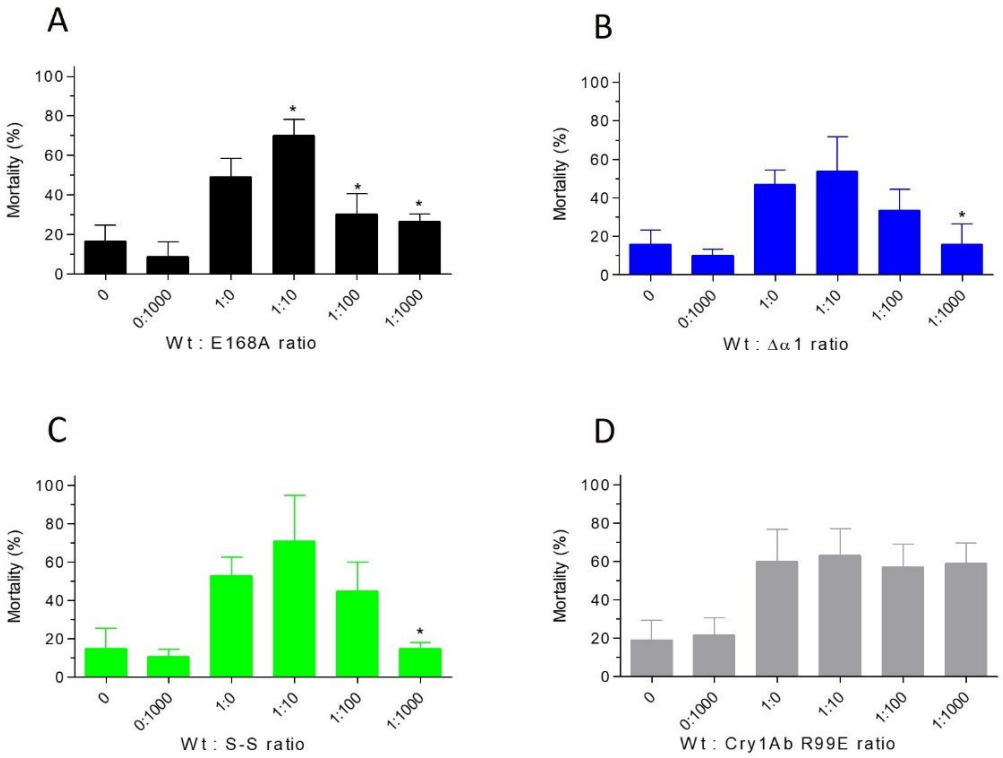

Figure 3.5. Vip3Aa *in vivo* competition assays against conformational mutants in *Spodoptera exigua* larvae. Bars represent the mortality recorded after 10 days for each protein: competitor molar ratio. 0, just buffer; 0:1000, just nontoxic competitor at the highest concentration tested; 1:0 just Vip3Aa_Wt at the LC_{50} dose; 1:10, 1:100 and 1:1000 ratio of Vip3Aa_Wt (at the LC_{50} dose) and nontoxic competitor. Error bars show the standard deviation (SD) among replicates. The asterisks over the bars indicate significance ($P < 0.05$) compared to the ratio 1:0 in a One-Way ANOVA with Bonferroni post hoc test. Wt, wild type.

IV. Discussion

The present study focuses on examining how both the protoxin and activated protein structural conformations of the Vip3Aa insecticidal protein, bind to *S. exigua* midgut receptors. Employing an experimental approach comprising *in vitro* binding assays to BBMV and *in vivo*

competition toxicity assays, our objective was to determine how the structural conformation of the protein affects its binding capacity.

The initial *in vitro* binding assays, employing radiolabelled trypsin-treated Vip3Aa_Wt, yielded results consistent with previous findings on Vip3A proteins in *Spodoptera spp*. BBMV, showing 50% of specific binding and a rapid binding saturation (**Figure 3.2B**) (Chakroun and Ferré, 2014; Lázaro-Berenguer *et al.*, 2022b; Quan *et al.*, 2021a). Based on prior cryo-EM and Negative Staining EM (NS-EM) observations (Núñez-Ramírez *et al.*, 2020; Lázaro-Berenguer *et al.*, 2022a), the trypsin-processed Vip3Aa sample contains a mixture of both protein conformations, with the proportion of molecules in the sample undergoing structural remodelling varying across replicates (50–70%). Considering these previous observations, to characterize the binding of the activated protein conformation alone, we decided to label the mutant protein Vip3Aa_Δα1 which shows a constitutive activated protein structure without the need of proteolytic processing owing to the lack of α-helix 1, which is critical for maintaining the protoxin structure (Lázaro-Berenguer *et al.*, 2022a). Compared with the WT protein, Vip3Aa_Δα1 had a lower nonspecific binding, which could be related with the protein conformation, but also with the lack of helix α1. In addition, comparing the non-processed Vip3Aa_Δα1 with the trypsin-treated Vip3Aa_Δα1, the non-processed protein had a higher nonspecific binding, indicating that not only the structural conformation, but also the proteolytic cleavage as well has an impact on binding specificity (**Figure 3.2C, D**).

Binding competition assays using trypsin-processed Vip3Aa_Δα1 and Vip3Aa_S-S structural mutants as competitors for the WT radiolabelled protein provided further insights into the binding mechanism. Despite differences in their structural conformations, both mutants effectively competed with trypsin-processed Vip3Aa_Wt for its binding sites on *S. exigua* BBMV, indicating that both conformations of Vip3Aa are able to recognize the same binding sites (**Figure 3.3B, C**). If the different conformations of Vip3Aa would bind to different binding sites, the mutant proteins could not compete completely with the Vip3Aa_Wt labelled protein and the competition curves would differ. Competition assays with the trypsin-processed Vip3Aa_Δα1 radiolabelled protein confirmed that Vip3Aa in its two conformations binds to the same binding sites *in vitro* (**Figure 3.3E, F**). Furthermore, *in vivo* competition assays with the structural mutants confirmed the results found *in vitro*, showing that the two Vip3Aa conformations bind to functional receptors in the insect midgut because both effectively blocked the toxicity of Vip3Aa_Wt against *S. exigua* larvae (**Figure 3.5B, C**).

Interestingly, Vip3Aa_Wt protoxin is able to bind to *S. exigua* BBMV and shows higher total binding (60%) compared to the trypsin-processed protein (20%). However, this binding is mainly nonspecific (**Figure 3.2A**). Therefore, despite that almost all of the protoxin's binding is nonspecific, it includes the specific and functional binding sites of the activated protein, explaining the competition observed *in vitro* for the BBMV binding sites, and the ability of the Vip3Aa_S-S mutant to block the WT's toxicity *in vivo*. The observation that both structural conformations are able to bind to the same receptors supports the

proposed role of Domains II–III in receptor binding (Jiang *et al.*, 2023b; Quan *et al.*, 2021a), as this part of the protein does not undergo any dramatic structural remodelling after proteolytic processing (Núñez-Ramírez *et al.*, 2020) (**Figure 3.1**).

Nonetheless, our results of binding reversibility suggest potential differences in membrane interactions possibly attributable to the remodelling into the activated structure, because the trypsin-processed Vip3Aa_Δα1 mutant (constitutive activated conformation), despite lacking of the putative transmembrane region, shows a higher level of irreversible interactions with the BBMV compared to the trypsin-processed WT protein (mixture of both structural conformations) (**Figure 3.4**). Thus, binding irreversibility may not reflect membrane insertion, and although the primary role in receptor binding may reside in Domains II–III, the involvement of the N-t part of the activated protein in membrane engagement cannot be disregarded, as these irreversible interactions could be highly relevant for the protein's function. Differences in the binding properties of both structural stages are further supported by the analysis of binding parameters performed

with the homologous competition curves of Vip3Aa_Wt and Vip3Aa_Δα1 trypsin-processed radiolabelled proteins. For the Vip3Aa_Δα1 protein, a lower K_d value was obtained, indicating a higher affinity for its binding sites in the BBMV compared to the affinity of the WT protein. Also, the higher binding affinity observed for the Vip3Aa_Δα1 mutant protein could be related with the higher percentage of irreversible interactions displayed by this mutant.

V. Conclusions

In this study, we have investigated how the structural conformation of Vip3Aa affects its capacity of binding to midgut receptors in *S. exigua*. Altogether, our findings point to both protoxin and activated protein structural conformations contributing to receptor binding. Therefore, either spontaneous structural shift upon proteolytic cleavage or receptor-mediated remodelling could be occurring *in vivo*. In terms of binding, protein conformation seems not to be a critical feature, because the protoxin structure, despite its high nonspecific binding observed *in vitro*, is nonetheless able to block functional binding sites *in vivo*. However, the timing and context in which the conformational change into the activated protein structure occurs, could profoundly influence membrane insertion and subsequent toxicity. Our results show the complex interplay between proteolytic processing, protein structure and receptor interactions in Vip3Aa's toxicity against *S. exigua.* Nonetheless, the higher binding affinity observed for the Vip3Aa_Δα1 mutant protein suggests that the activated conformation would be favoured *in vivo*.

Chapter 4

Role of the different Vip3Aa structural domains in the specific and functional binding to *Spodoptera spp.* midgut receptors

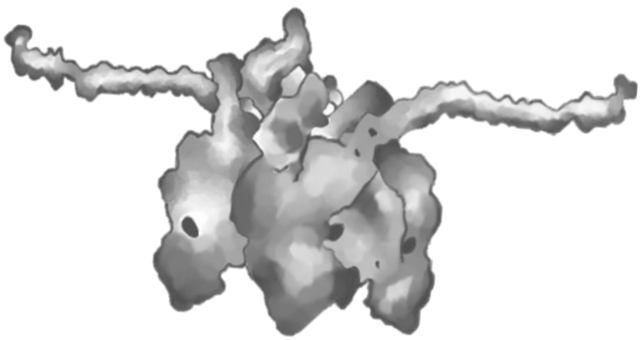

I. Introduction

Vip insecticidal proteins are produced by the bacterium *Bacillus thuringiensis* (Bt) during its vegetative growth phase (Estruch *et al.*, 1996). They are valuable candidates for the use in transgenic Bt-crops due to their insecticidal activity against lepidopteran pests and lack of shared binding sites with Cry proteins (Chakroun and Ferré, 2014; Gouffon *et al.*, 2011; Hamadou-Charfi *et al.*, 2013; Lee *et al.*, 2003; Liu *et al.*, 2011; Quan *et al.*, 2021a; Sena *et al.*, 2009), with no reported cases of cross-resistance between them (Tabashnik and Carrière, 2019). To date, more than 80 events of maize, cotton and soybean containing *vip3Aa* genes in combination with *cry* genes have been approved for commercialization in several countries (ISAAA, 2024; Gupta *et al.*, 2021). There is consensus that upon ingestion by larvae, Vip proteins are processed by midgut proteases in the lumen, cross the peritrophic matrix (PM), bind specifically to their receptors in the apical membrane of the midgut epithelium (which identity is still under debate) and get inserted into the cell membrane after remodelling into the activated conformation, exerting their insecticidal activity mainly through pore formation (Ferré *et al.*, 2023). They are secreted into the media as tetrameric molecules, with each tetramer consisting of four identical monomers, and each monomer comprising five distinct structural domains (Byrne *et al.*, 2021; Núñez-Ramírez *et al.*, 2020; Zheng *et al.*, 2020). Many efforts have been made to understand the role of each of the structural domains of the Vip3A protein on the different steps of its mode of action. It is known that the N-terminal (N-t) Domain I (residues 1–198) is strongly related with toxicity (Banyuls *et al.*, 2018; Byrne *et al.*,

2021; Jiang *et al.*,2023b; Lázaro-Berenguer *et al.*, 2022a; Selvapandiyan *et al.*, 2001; Shao *et al.*, 2024), and plays a key role in structure maintenance. It is composed by 4 α-helices and has proven to be essential for oligomerization (Jiang *et al.*, 2020a; Zheng *et al.*, 2020), the remodelling into the activated protein conformation after proteolytic processing (Byrne *et al.*, 2021; Lázaro-Berenguer *et al.*, 2022a; Núñez-Ramírez *et al.*, 2020) and membrane interaction through pore formation (Byrne *et al.*, 2021; Shao *et al.*, 2024). Domain II (residues 200–325) is composed of five α-helices, it embodies the core of the tetramer and plays an important structural role stabilizing the oligomer (Banyuls *et al.*, 2018; Byrne *et al.*, 2021; Núñez-Ramírez *et al.*, 2020). In addition to its structural role, its participation in receptor binding functions in combination with other domains of the protein has also been suggested (Jiang *et al.*, 2023b). The C-terminal (C-t) part of the protein is composed by three globular domains that are exposed to the solvent. Domain III (residues 328–532) contains three antiparallel β-sheets that form a β-prism fold (Byrne *et al.*, 2021; Núñez-Ramírez *et al.*, 2020; Zheng *et al.*, 2020). It has been related with specific binding to the midgut epithelium of several *Spodoptera spp.* and Sf cultured cells (Jiang *et al.*, 2020a; Jiang *et al.*, 2023b; Quan *et al.*, 2021a). However, Domain III alone has shown low or no ability to bind Sf9 cells or the midgut epithelium (Jiang *et al.*, 2020a; Jiang *et al.*, 2023b), pointing out to the need of additional domains for the binding. Domains IV and V (residues 536–668 and 681-789 respectively), show similar carbohydrate binding module (CBM) folds and are connected to the core of the molecule by a long and flexible loop (Núñez-Ramírez *et al.*, 2020). *In silico* DALI analysis of these domains

(Holm and Sander, 1995) identifies a number of structural homologs with glycan binding capabilities (Byrne *et al.*, 2021; Núñez-Ramírez *et al.*, 2020; Zheng *et al.*, 2020). It has therefore been suggested that they may play a role in receptor engagement through binding to glycosylated molecules. However, these domains were not necessary for Vip3Af specific binding to *Spodoptera spp.* brush border membrane vesicles (BBMV) and Sf21 cells (Quan *et al.*, 2021a), nor Vip3Aa binding to Sf9 cells (Jiang *et al.*, 2023b). Also, point mutations and truncations in Domains IV and V significantly reduce protein toxicity by causing instability, as shown in multiple studies (Banyuls *et al.*, 2018; Gayen *et al.*, 2012, 2015; Li *et al.*, 2007; Quan and Ferré, 2019; Selvapandiyan *et al.*, 2001). Additionally, the absence of these domains completely abolishes the protein's toxicity *in vivo*, which can be due to the possible role of Domains IV and V on driving the structural remodelling into the activated conformation (Lázaro-Berenguer *et al.*, 2022a), but could also be associated to a reduced stability against midgut proteases or an alteration in receptor binding *in vivo*.

This study aims to clarify the role of the different structural domains in the specific and functional binding of Vip3Aa to the midgut epithelium of *Spodoptera spp*. larvae. We have generated several truncated constructs having only some of the structural domains of Vip3Aa, and used them as competitors for the WT protein in *in vitro* binding assays to *Spodoptera exigua* BBMV and *in vivo* competition assays in *S. exigua* and *Spodoptera littoralis* larvae. Our findings reinforce the critical role of Domain III in the binding, while demonstrating the important role of Domains IV and V for Vip binding to functional receptors *in vivo*.

II. Materials and methods

II.1. Vip3Aa truncated constructs generation

Vip3Aa (residues 10–789) was cloned in LIC 1.5 vector, as previously described (Núñez-Ramírez *et al.*, 2020), and served as a template vector to prepare the truncated constructs used in this study by amplifying the sequences coding for the desired domains and cloning them in LIC 1.5. Primers used for amplification of the sequences coding for the corresponding protein fragments and molecular mass of the resulting truncated proteins are compiled in **Supplementary Table S4.1**.

II.2. Protein expression and purification

The production of Vip3Aa WT (full length protein) and truncated constructs Vip3Aa_I-III, Vip3Aa_II-V, Vip3Aa_III-V and Vip3Aa_IV-V containing only the selected domains, was performed as described previously (Lázaro-Berenguer *et al.*, 2024). Briefly, proteins were expressed in *Escherichia coli* C43 (DE3), cells were grown in 700 mL Luria-Bertani broth supplemented with 100 μg/mL Ampicillin to exponential phase (OD_{600} ~ 0.6–0.8), expression was induced with 1 mM isopropyl β-D-1-thiogalactopyranoside (IPTG) by incubating at 25°C overnight with shaking. Cells were collected and stored at −20°C. For purification, thawed cells were resuspended in buffer A (50 mM Tris–HCl, 150 mM NaCl, 5 mM $MgCl_2$ pH 8.0) supplemented with 3 mg/mL lysozyme, 10 μg/mL DNase and 100 μM PMSF and incubated for 30 min at 37°C with shaking. The lysate was then sonicated for 5 min and centrifuged at 25,000 ×*g* for 30 min. The clarified supernatant was loaded onto a 5-mL StrepTrap column (Cytiva) for protein purification and the protein was eluted with 5 mM d-desthiobiotin dissolved in buffer A at

pH 8.0. The Strep II-tag was removed by treating with 3C PreScission Protease (Cytiva) followed by dialysis in buffer A. The sample was subjected to a second step of affinity chromatography with the StrepTrap column to separate nontagged protein from remaining tagged molecules. Pure proteins were eluted in buffer A, checked by 12% SDS-PAGE, aliquoted, flash-frozen with liquid nitrogen and stored at −80°C for further use.

II.3. Preparation of *S. exigua* brush border membrane vesicles (BBMV)

The BBMV were obtained by the differential magnesium precipitation method (Wolfersberger, 1993) starting with frozen midgut tissue from last instar larvae of *S. exigua*. After preparation, vesicles were aliquoted, flash-frozen in liquid nitrogen, and stored at −80°C until use.

II.4. Protein ^{125}I radiolabelling

Vip3Aa protoxin was radiolabelled by the Chloramine T method (Van Rie *et al.*, 1989) following the protocol described elsewhere (Quan *et al.*, 2021a; Lázaro-Berenguer *et al.*, 2022b). Briefly, 25 μg of pure protein were mixed with 0.3 mCi of [^{125}I]-NaI and 1/3 (v/v) of 18 mM Chloramine T. The excess of free iodine was separated from the labelled protein using a PD10 desalting column (Cytiva). The purity of the radiolabelled proteins was checked by 12% SDS-PAGE and autoradiography (**Supplementary Figure S3.3A, B**). Vip3Aa was labelled twice being the specific activity 5.07 and 5.90 μCi/μg, respectively.

II.5. *In vitro* binding assays with ^{125}I-Vip3Aa to *S. exigua* BBMV

Before their used in *in vitro* binding assays, BBMV were thawed, centrifuged and resuspended in binding buffer. Protein concentration in the BBMV samples was quantified by the Bradford assay (Bradford, 1976). *In vitro* binding assays were performed as described previously (Lázaro-Berenguer *et al.*, 2022b; Lázaro-Berenguer *et al.*, 2024). Briefly, ^{125}I-Vip3Aa was trypsin-processed with commercial trypsin from bovine pancreas (Sigma Aldrich) at 10% w/w for 1 h at 37°C, and incubated with BBMV for 1 h in 100 μL final volume of binding buffer (20 mM Tris–HCl, 1 mM MnCl2, 0.1% BSA pH 7.4). After incubation, the reaction was stopped by centrifugation (16,000 ×*g* for 10 min at 4°C) and radioactivity retained in the pellet was quantified using a model 2480 WIZARD2 γ-counter (Perkin Elmer) to assess bound labelled protein. A bindability assay was performed with 0.2 nM trypsin-processed ^{125}I-Vip3Aa, increasing concentrations of BBMV and an excess of unlabelled trypsin-processed Vip3Aa_Wt (1,000-fold molar ratio). Competition assays were performed by mixing 0.2 nM of trypsin-processed ^{125}I-Vip3Aa, 0.05 mg/mL BBMV, and increasing concentrations of unlabelled competitor proteins. Vip3Aa_Wt and truncated construct Vip3Aa I-III were used trypsin-activated; the rest of the constructs lacking Domain I were not trypsin-treated for their use in competition assays. At least two technical replicates were performed for each binding assay. Graphical representations were obtained with Prism (GraphPad).

II.6. *In vitro* proteolytic assays

A fixed amount of protein (10 μg) was incubated with 10% (w/w; 1 μg) commercial trypsin (from bovine pancreas, Sigma-Aldrich), or 10% (w/w) midgut juice. Gut juice of *S. exigua* and *S. littoralis* was prepared following the protocol described elsewhere (Chakroun *et al.*, 2012), flash-frozen in liquid nitrogen and stored at −80°C. Total protein concentration in the midgut juice was determined by Bradford just before use. The reaction was carried out in a final volume of 20 μL in buffer A (50 mM Tris–HCl, 150 mM NaCl, 5 mM $MgCl_2$ pH 8.0). All samples were incubated for 1.5 h at 37°C for trypsin digestions and at 30°C for midgut juice digestions. Then, samples were clarified by centrifugation (16,100 x*g* for 10 min at 4 °C) and the supernatant containing the processed proteins was incubated for 10 min at room temperature with 10 mM AEBSF [4-(2-aminoethyl) benzenesulfonyl fluoride HCl] serine protease inhibitor to avoid further processing of the proteins. Proteolytic fragments were separated by 12% SDS-PAGE.

II.7. *Spodoptera spp.* colonies rearing and *in vivo* competition assays

For surface contamination bioassays, laboratory populations of *S. exigua* and *S. littoralis* were reared on semi-synthetic diet (Bell and Joachim, 1976) under controlled conditions: 25 ± 2°C, 70 ± 5% RH and 16:8 h light:dark photoperiod. *In vivo* competition assays were conducted as described previously (Lázaro-Berenguer *et al.*, 2022b; Lázaro-Berenguer *et al.*, 2024). Vip3Aa at 20 ng/cm^2 for *S. exigua* and 3.7 ng/cm^2 for *S. littoralis*, was mixed with Vip3Aa_I-III at the desired molar ratios in buffer A (1:0, 1:10, 1:100, 1:1,000, 1:2,500 for *S. exigua* and 1:0, 1:10, 1:100,

1:1,000, 1:10,000 for *S. littoralis*). Negative controls included buffer (labelled as 0) and an excess of Vip3Aa_I-III (labelled as 0:2,500/0:10,000). At least three replicates were performed for each species. Statistical analysis was performed by a One-Way ANOVA with post hoc Bonferroni test in Prism (GraphPad) with an α-value of 0.05.

III. Results

III.1. *In vitro* binding of ^{125}I-Vip3Aa to *S. exigua* BBMV

Radiolabelled Vip3Aa showed a 20% of total binding to *S. exigua* BBMV, with half of this binding (50%) being non-specific (**Supplementary Figure S4.1**). Truncated constructs were used as heterologous competitors for the radiolabelled WT protein to evaluate their binding capacity. The results show that all constructs were able to displace totally or partially the specific binding of the radiolabelled full-length (WT) activated protein (**Figure 4.1**), pointing out to the participation of several domains in the specific binding of the protein. The only construct showing complete competition for the WT binding sites was Vip3Aa_I-III (**Figure 4.1A**), with a competition curve identical to the homologous curve (open circles and dashed lines in **Figure 4.1**). The construct containing all C-t domains (**Vip3Aa_III-V**) could displace almost all the specific binding (~35% of the total binding) (**Figure 4.1B**), whereas the construct containing only the CBM domains (Vip3Aa_IV-V) and the construct containing all structural domains except Domain I (Vip3Aa_II-V) could only displace ~20% of the total binding (**Figure 4.1C, D** respectively).

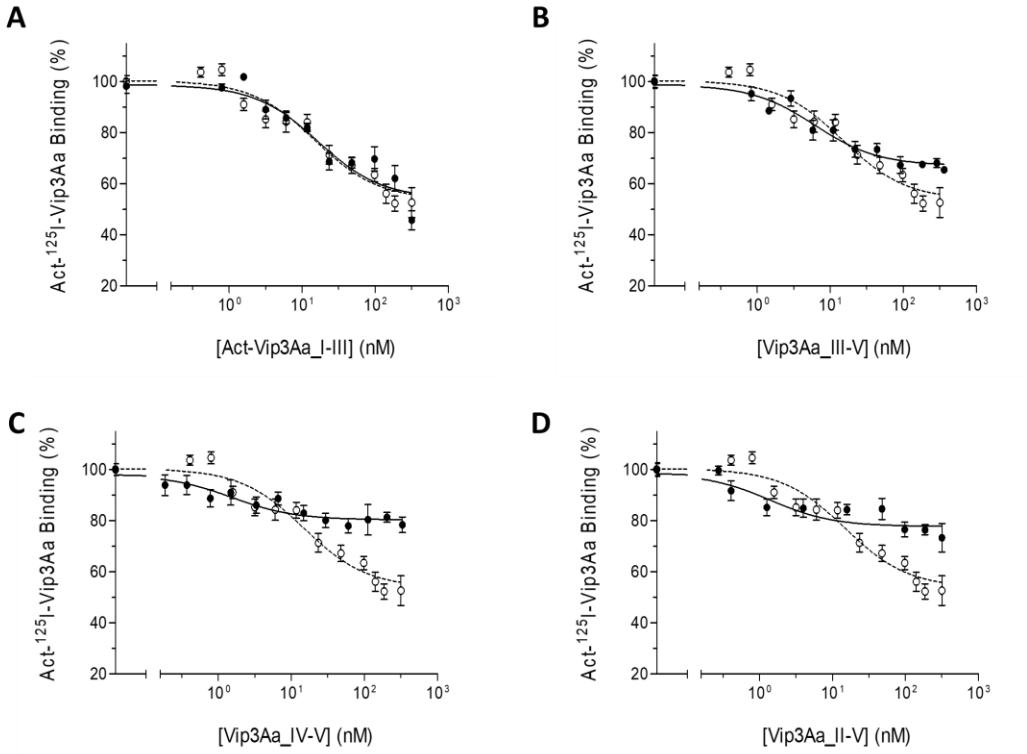

Figure 4.1. ^{125}I-Vip3Aa competition binding assays vs truncated constructs in *Spodoptera exigua* brush border membrane vesicles (BBMV). Trypsin-processed ^{125}I-Vip3Aa was used with a fixed concentration of BBMV and increasing concentrations of unlabelled competitors: Trypsin processed Vip3Aa_I-III (A), Vip3Aa_III-V (B), Vip3Aa_IV-V (C) and Vip3Aa_II-V (D). Full circles and black lines represent the competition observed for each truncated construct. Open circles and dashed lines represent the homologous competition vs the trypsin-processed Vip3Aa WT protein (full-length protein) for comparison. Each data point represents the mean of at least two replicates (± SEM).

III.2. *In vitro* proteolytic assays

To test the stability of the truncated constructs against proteolytic conditions, *in vitro* assays were performed using commercial trypsin and *S. exigua* gut juice. The incubation of the WT protein with proteases renders a proteolytic profile with two main bands of 65 and 19 kDa in SDS-PAGE, corresponding to domains II-V and Domain I respectively (Ferré *et al.*, 2023; **Figure 4.2**, lanes 2 and 3). To test the stability of the

different truncated constructs against midgut proteases, we performed *in vitro* proteolytic assays incubating them with commercial trypsin and gut juice extracted from midgut samples of *S. exigua* larvae (*Se*MJ). Our results show that only the construct Vip3Aa_I-III was stable after proteolysis with trypsin and gut juice, rendering an SDS-PAGE proteolytic profile with two main bands of 35 and 19 kDa (**Figure 4.2**, lanes 5 and 6), corresponding to domains II-III and Domain I respectively (Quan and Ferré, 2019). On the contrary, all truncated constructs lacking the N-t Domain I showed reduced stability against midgut proteases, exhibiting overprocessing in SDS-PAGE (**Figure 4.2**).

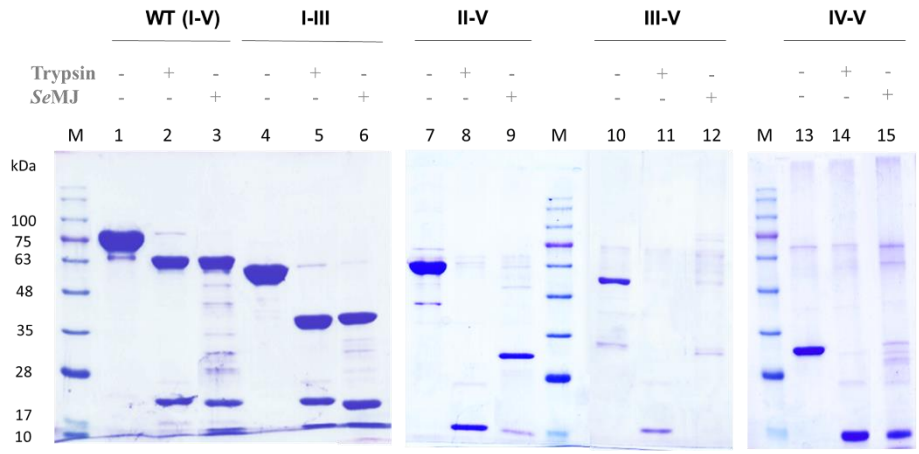

Figure 4.2. *In vitro* proteolytic processing of Vip3Aa Wt and truncated constructs. The proteins were incubated *in vitro* under different conditions and then subjected to SDS-PAGE. Lanes 1, 4, 7, 10 and 13 correspond to protoxin samples; lanes 2, 5, 8, 11 and 14 correspond to samples digested with trypsin (10% w/w); lanes 3, 6, 9, 12 and 15 correspond to samples digested with *S. exigua* gut juice (10% w/w). Band sizes were estimated according to the Blue Star molecular marker (M) (NIPPON Genetics). WT (I-V), full length protein. Truncated constructs: Domains I-III, Vip3Aa_I-III; Domains II-V, Vip3Aa_II-V; Domains III-V, Vip3Aa_III-V; Domains IV-V, Vip3Aa_IV-V.

III.3. *In vivo* competition assays vs Vip3Aa_I-III in *Spodoptera spp.*

The only truncated construct which was stable in proteolytic conditions and able to displace all the specific binding of the full-length protein to the BBMV, was Vip3Aa_I-III. To evaluate its capacity of binding to functional receptors in the gut of *S. exigua* larvae, we performed *in vivo* competition assays using this truncated construct as competitor for the WT protein, since we know that this truncation results in a complete lack of toxicity in *S. exigua* (Lázaro-Berenguer *et al.*, 2022a; **Table 2.2** in chapter 2) while retaining the ability to bind to specific receptors *in vitro*. Our results show that the construct lacking domains IV and V was not able to block the WT's toxicity in *S. exigua*, even at the highest competitor ratio tested (a 2,500-fold higher molar ratio of competitor protein compared to the WT protein) (**Figure 4.3A**).

To evaluate if higher ratios of competitor Vip3Aa_I-III would result in toxicity blocking, we decided to perform this same experiment in the related species *S. littoralis*. The mean lethal concentration (LC_{50}) of Vip3Aa in this insect species was significantly lower compared to that found for *S. exigua*: 3.7 ng/cm^2 (1.1-6,9 95% F.L.) in *S. littoralis* (**Supplementary Figure S4.2**) compared to 19.5 ng/cm^2 (8.6-28 95% F.L.) in *S. exigua* (Lázaro-Berenguer *et al.*, 2022a; **Table 2.2** in chapter 2). The higher toxicity of the protein in *S. littoralis* allowed us to use lower doses of the WT protein to reach 50% of mortality and therefore reduce the amount of competitor Vip3Aa_I-III used, reaching higher WT:competitor molar ratios. Our results show that the construct Vip3Aa_I-III was not able to block the WT's toxicity in *S. littoralis* either, even at the 1:10,000 protein:competitor molar ratio (**Figure 4.3B**) despite

being stable against midgut proteases of this insect species (**Supplementary Figure S4.3**). These results confirm that the lack of domains IV and V someway prevents Vip3Aa to bind to functional receptors *in vivo*.

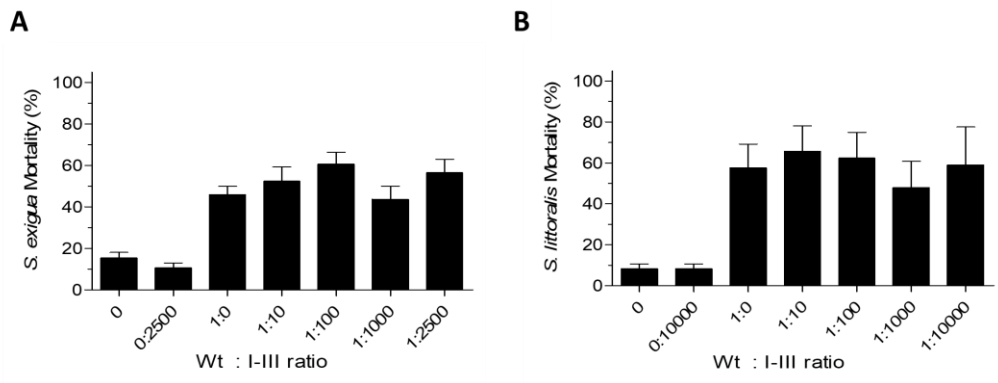

Figure 4.3. Vip3Aa *in vivo* competition assays against Vip3Aa_I-III in *Spodoptera spp*. *S. exigua* larvae (A) and *S. littoralis* larvae (B), were used in *in vivo* competition assays with the truncated construct lacking Domains IV and V (Vip3Aa_I-III). Bars represent the mortality recorded after 10 days for each Vip3Aa:Vip3Aa_I-III molar ratio. 0, just buffer; 0:2500/0:10000, just nontoxic competitor at the highest concentration tested; 1:0 just Vip3Aa_Wt at the LC_{50} dose (20 ng/cm^2 for *S. exigua* and 3.7 ng/cm^2 for *S. littoralis*); 1:10, 1:100, 1:1000, 1:2500 and 1:10000 ratio of Vip3Aa_Wt (at the LC_{50} dose) and nontoxic competitor fold. Error bars show the standard deviation (SD) among replicates. Wt, wild type; I-III, Vip3Aa_I-III.

IV. Discussion

In this study, we have generated several Vip3Aa truncated constructs and used them in *in vitro* binding assays and *in vivo* competition assays to evaluate the role of the different structural domains of the protein in the specific and functional binding to the midgut epithelium of *Spodoptera spp*. Our results confirm previous reports defining Domain III as the most relevant domain for the specific binding to the brush border membrane of the midgut epithelium (Quan *et al.*, 2021a; Jiang *et*

al., 2023b; Infante *et al.*, 2024; Hou *et al.*, 2024), since we could only observe complete competition for the radiolabelled Vip3Aa_Wt (full length) specific binding with the construct containing domains I-III (Vip3Aa_I-III, **Figure 4.1A**). Previous reports have suggested that the presence of Domain II together with Domain III could be relevant for the binding (Jiang *et al.*, 2023b, Quan *et al.*, 2021a). Our results show that the presence of Domain II in combination with the C-t domains (Vip3Aa_II-V construct, **Figure 4.1D**) does not improve the binding compared to the construct containing just the C-t domains (Vip3Aa_III-V construct, **Figure 4.1B**). It has been reported by X-ray crystallography that the C-t fragments of Vip proteins lacking Domain I form dimers (Jiang *et al.*, 2020a, Zheng *et al.*, 2020). The differences in binding observed between the constructs Vip3Aa_II-V and Vip3Aa_III-V in our *in vitro* assays could then be related with the different quaternary structure observed for these two constructs, indicating that dimer formation might have reduced specific binding capacity compared to monomeric form. Most importantly, our results highlight that tetramer formation might be a critical feature for the specific binding of the protein, since none of the truncated constructs lacking the N-t part of the protein would be able to form tetramers (Jiang *et al.*, 2020a; Zheng *et al.*, 2020) and none of them could displace all the specific binding of the full-length protein despite having all the C-t domains (**Figure 4.1B-D**). However, the lack of the N-t part of the protein also results in reduced stability of the truncated constructs against *S. exigua* midgut proteases (**Figure 4.2**). Thus, in addition to the lack of tetrameric structure, the partial competition observed for the

truncated constructs lacking Domains I and II could also be associated with a reduced stability during the incubation with *S. exigua* BBMV in the binding assays, which have shown ability to partially process the Vip3Aa protein when incubated with them due to the effect of membrane-associated proteases (Lázaro-Berenguer *et al.*, 2022a; **Figure 2.4A** in chapter 2). In our *in vitro* proteolysis assays, only the construct I-III was completely stable against *S. exigua* midgut proteases, and only this construct was able to displace all the specific binding of the full-length WT protein to the BBMV. Altogether, these results emphasize the crucial structural role that the N-t part of the protein plays in oligomerization and the importance of tetramer formation for protein stability in the midgut conditions.

While the presence of Domains IV and V was not necessary for protein stability against midgut proteases from *Spodoptera spp*. (**Figure 4.2, Supplementary Figure S4.3**) and specific binding to *S. exigua* BBMV (**Figure 4.1A**), 20% of the WT's specific binding to the BBMV could be displaced by the Vip3Aa_IV-V construct (having only domains IV and V) (**Figure 4.1C**) in our *in vitro* binding assays. These results suggest that Domains IV and V might also be involved in the binding of Vip3Aa to the brush border membrane of midgut cells. In the case of the Vip3Af protein, domains IV-V were not able to compete for the Vip3Af full-length radiolabelled protein in binding assays with *S. exigua* BBMV (Quan *et al.*, 2021b). This discrepancy could be related with protein subtype, as we have already reported differences in the binding of Vip3Aa and Vip3Af to their shared receptors (Lázaro-Berenguer *et al.*, 2022b), showing Vip3Aa a higher binding affinity than Vip3Af

(**Supplementary Table S1.2**; **Figure 1.5** in chapter 1). Furthermore, the contribution of Domains IV and V to Vip3Aa binding capacity *in vivo* seems critical, given that the construct Vip3Aa_I-III lacking domains IV and V could not block the toxicity of the WT protein in *S. exigua* nor *S. littoralis* (**Figure 4.3**) despite being stable against midgut proteases of both insect species. Meaning that the presence of these domains of the protein could be important for the binding to occur *in vivo*. Interestingly, a previous report showed that a construct containing the predicted CBM in Domain IV of Vip3Aa was able to block the toxicity of the WT protein in *in vivo* competition assays performed in *Spodoptera litura* and *S. exigua* (Boonyos *et al.*, 2021). However, given the instability of monomeric constructs containing the C-t domains against midgut proteases, it is surprising that a small fragment of Domain IV could withstand protease action and block Vip3Aa toxicity *in vivo*. Additionally, the lack of *in vivo* competition observed for the construct Vip3Aa_I-III could also be the consequence of an alteration in a different step of the mode of action occurring prior to the binding, such as the interaction with the PM, affecting the capacity of the truncated protein to reach the midgut epithelium and bind to the brush border membrane. In fact, a recent study shed light on the capacity of Vip3Aa's Domain V to bind the PM of *Spodoptera frugiperda* (Jiang *et al.*, 2023b), which is a semi-permeable structure composed mainly of chitin and glycosylated proteins (Terra, 2001; Erlandson *et al.*, 2019). The authors proposed that this interaction contributes to the protein's insecticidal activity although the mechanism by which this interaction can enhance the toxicity is not clear. The ability of other Bt proteins such as Cry1A and Cry1I to bind to the PM has also

been reported (Feng *et al.*, 2015; Hayakawa *et al.*, 2004; Rees *et al.*, 2009; Valaitis and Podgwaite, 2013). However, for Cry proteins this interaction has been described as detrimental for their toxicity, with protein trapping in the PM resulting in reduced activity.

V. Conclusions

In summary, our results confirm previous reports defining Domain III of the Vip3Aa protein as the most relevant domain for specific binding to the brush border membrane of the midgut cells. However, while the presence of Domains IV and V is not necessary for Vip3Aa to specifically bind *in vitro* to all its binding sites in the BBMV of *S. exigua*, the contribution of these domains *in vivo* seems critical, since they are required for the insecticidal activity of the protein and the binding *in vivo* to functional binding sites. This could be related with an alteration of pre-binding events, such as the recently described interaction with the peritrophic matrix or with the need for a correct positioning of the protein while interacting with the membrane. In any case, the details of Domains IV and V binding properties and their role *in vivo* still needs further characterization.

Chapter 5

Preliminary insights into Vip3Aa binding to lipid molecules in the midgut epithelium of *Spodoptera spp.*

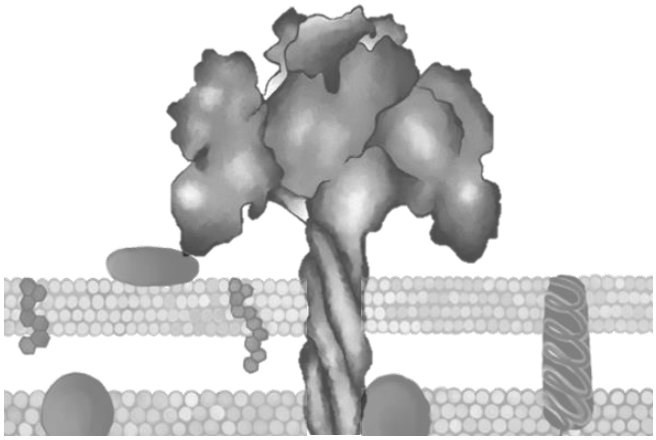

I. Introduction

The cellular plasma membrane is primarily composed of phospholipids which are arranged in a bilayer with hydrophilic heads (headgroups) facing outward and hydrophobic tails facing inward. Embedded within this bilayer are proteins which perform various functions, including transport, enzymatic activity, signal transduction, cell recognition, and structural support (Alberts *et al.*, 2015; Nelson and Cox, 2021a). Sterol molecules, found interspersed within the bilayer, modulate membrane fluidity, stability and permeability (Alberts *et al.*, 2015; Nelson and Cox, 2021a). Some membranes also contain specialized lipids like sphingolipids, which are important for signalling processes and structural roles (Best *et al.*, 2023; Hannun and Obeid, 2008). Additionally, carbohydrates are attached to proteins (forming glycoproteins) or lipids (forming glycolipids) on the extracellular side of the membrane, these glycoconjugates play crucial roles in cell-to-cell recognition, signalling processes, and adhesion (Alberts *et al.*, 2015; Nelson and Cox, 2021b; Varki *et al.*, 2009).

It is well established that glycoconjugates in cell membranes serve as receptors for toxins (Best *et al.*, 2023; Zuverink and Barbieri *et al.*, 2018). For instance, Pertussis toxin and Aerolysin rely on glycoprotein binding (Stein *et al.*, 1994; Diep *et al.*, 1998), whereas Lysenin, Cytolysin or Ostreolysin bind glycolipid molecules (Sepcić *et al.*, 2004; Tweten, 2005; Yamaji *et al.*, 1998). And, others like Ricin bind to specific carbohydrate moieties found on either glycolipids or glycoproteins (Fu *et al.*, 1996). Particularly in the mode of action of the bacterial entomopathogen *Bacillus thuringiensis* (Bt), several proteins located in the apical

membrane of insect midgut cells serve as surrogate receptors for different members of the Cry family (Adang *et al.*, 2014; Bravo *et al.*, 2023; Heckel, 2020). Some of these midgut receptors are known glycoproteins (i.e. cadherins and aminopeptidase N, APN) (Best *et al.*, 2023), and it has been described that Cry proteins mainly bind specifically to them through a lectin-like domain (Domain II), which leads to toxicity (Bravo *et al.*, 2023; Pardo-Lopez *et al.*, 2013; Pigott *et al.*, 2007; Zavala *et al.*, 2011; Zhao *et al.*, 2017). Additionally, for the Cry1Ac protein, a low-affinity binding to N-acetylgalactosamine (GalNAc) mediates its further specific interaction with these receptors in some lepidopteran species (Burton *et al.*, 1999; Derbyshire *et al.*, 2001; Jenkins *et al.*, 2000). Glycosphingolipids are also known toxin receptors (Geny and Popoff, 2006), they are found enriched in lipid rafts (Bieberich, 2018), membrane microdomains involved in signal transduction and transport functions (Simons and Ikonen, 1997; Brown and London, 1998). For instance, Cholera toxin and Shiga toxin bind to lipid rafts (Kabbani *et al.*, 2020; Smith *et al.*, 2006). Also, some Bt nematicidal proteins (i.e., Cry5Ba and Cry14A) specifically bind glycosphingolipids, with this binding being carbohydrate-dependent and relevant for the toxicity against *Caenorhabditis elegans* (Griffitts *et al.*, 2003, 2005). Additionally, other Bt proteins such as the Tpp family with mosquitocidal activity, have also been reported to bind glycan motifs common in glycoconjugates, with this interaction involved in toxicity (Best *et al.*, 2022; Broadwell and Baumann, 1987; Sharma *et al.*, 2018). Therefore, both glycoproteins and glycolipids are of interest when considering potential membrane receptors for insecticidal proteins.

Vip proteins are also produced by Bt and are specifically toxic against Lepidoptera insects (Chakroun *et al.*, 2016a; Estruch *et al.*, 1996; Ferré *et al.*, 2023). They are of special interest given that they do not share binding sites with Cry proteins (Chakroun and Ferré, 2014; Gouffon *et al.*, 2011; Hamadou-Charfi *et al.*, 2013; Lee *et al.*, 2003; Liu *et al.*, 2011; Quan *et al.*, 2021a; Sena *et al.*, 2009) and there is no cross-resistance between them (Tabashnik and Carrière, 2020), suggesting that their receptor molecules are different, therefore being good partners for pyramided Bt-crops (Carrière *et al.*, 2015; Moar and Anilkumar, 2007). Vip proteins contain five different structural domains, the N-terminal (N-t) Domains I-II are involved in toxicity and structure maintenance (Byrne *et al.*, 2021; Jiang *et al.*, 2020a; Jiang *et al.*, 2023b; Lázaro-Berenguer *et al.*, 2022a; Núñez-Ramírez *et al.*, 2020; Shao *et al.*, 2024). The C-terminal (C-t) part of the protein is composed by three globular domains (Domains III-V). Domain III contains three antiparallel β-sheets that form a β-prism fold (Byrne *et al.*, 2021; Jiang *et al.*, 2020a; Núñez-Ramírez *et al.*, 2020) and it has been reported that it is involved in the specific binding to *Spodoptera spp.* midgut cells (Jiang *et al.*, 2023b; Quan *et al.*, 2021a). Similar β-prism folding patterns have been noted in numerous carbohydrate-binding proteins which are referred to as β-prism fold lectins (Sharma *et al.*, 2007). Interestingly, Vip proteins Domain III resembles Domain II of the Cry proteins (Byrne *et al.*, 2021; Núñez-Ramírez *et al.*, 2020). In addition to their lectin-like Domain III, Vip proteins also have additional domains with structural similarity to carbohydrate binding proteins, Domains IV and V strongly resemble to hydrolases of the CBM16 family (Byrne *et al.*, 2021; Jiang *et al.*, 2020a;

Núñez-Ramírez *et al.*, 2020) which bind polysaccharide substrates (Bae *et al.*, 2008). It has therefore been hypothesized that these domains might also contribute to Vip binding by engaging glycosylated molecules. However, only the interaction of Vip3Aa with the peritrophic matrix (PM, a chitin-rich acellular structure that surrounds the midgut) through Domain V has been reported so far (Jiang *et al.*, 2023b).

In this work, we have explored the ability of Vip3Aa to bind lipid molecules, which are present in high numbers in cellular membranes. We have used lipids extracted from midgut tissue of *Spodoptera exigua* and *Spodoptera littoralis* larvae, as well as standard lipids in dot-blot binding assays and thin-layer chromatography (TLC)-overlay assays. Our results provide preliminary insights into lipid molecules which could act as putative receptor moieties for the Vip3Aa protein in the midgut epithelium of lepidopteran pests.

II. Materials and methods

II.1. Protein expression and purification

The production of WT Vip3Aa and truncated constructs (Vip3Aa_I-III, Vip3Aa_III-V, and Vip3Aa_IV-V) was carried out as described previously (Lázaro-Berenguer *et al.*, 2024). Proteins were expressed in *Escherichia coli* C43 (DE3) grown in 700 mL Luria-Bertani broth supplemented with 100 μg/mL Ampicillin to an OD_{600} of 0.6–0.8, with expression induced using 1 mM IPTG at 25°C overnight with shaking. Cells were harvested and stored at −20°C. For purification, thawed cells were resuspended in buffer A (50 mM Tris–HCl, 150 mM NaCl, 5 mM $MgCl_2$, pH 8.0) containing lysozyme (3 mg/mL), DNase (10 μg/mL), and

PMSF (100 μM), incubated at 37°C for 30 min with shaking, sonicated for 5 min, and centrifuged at 25,000 ×*g* for 30 min. The supernatant was purified using a 5-mL StrepTrap column (Cytiva), with proteins eluted using 5 mM d-desthiobiotin in buffer A. The Strep II-tag was removed with 3C PreScission Protease (Cytiva), followed by dialysis in buffer A. A second StrepTrap purification step was performed to isolate nontagged proteins, which were eluted in buffer A, aliquoted, flash-frozen in liquid nitrogen, and stored at −80°C.

II.2. Insect lipids extraction

Lipid samples were extracted from midgut tissue of last instar larvae of *S. exigua* and *S. littoralis* into two chemical phases by the Svennerholm partitioning method (Svennerholm and Fredman, 1980). This protocol allows to separate lipids from the mixture into an upper phase which is more hydrophilic and is enriched in charged lipids and complex glycolipids with bigger polar carbohydrate structures, and a lower phase which is more hydrophobic and collects lipids with lower complexity and nonpolar lipids including sterols. Larvae were dissected and midguts were flash frozen in liquid nitrogen and stored at -80°C until use. Before extraction, midguts were rinsed in dH_2O and flash frozen in liquid nitrogen and thawed at room temperature (RT) three times. Pellets were sonicated and lipid extraction was performed at 37°C for 2 h with agitation in a mixture of chloroform, methanol, and water with a final ratio of 4:8:3 v/v/v. Samples were centrifuged at 1,400 ×*g* for 5 min to split into upper phase and lower phase. Silica-based hydrophobic cartridges (WAT036810, Sep-Pak tC18) were used to purify and concentrate upper phase lipids. All samples were dried

under N_2 at 40°C and resuspended in 50 μL methanol (upper phase) and 200 μL 1:1 chloroform to methanol (lower phase). Lipid samples from other insect species representative of all insect orders were also extracted from whole insects following the same protocol. *Manduca sexta* (Lepidoptera), *Aedes aegypti* (Diptera), *Culex quinquefasciatus* (Diptera), *Drosophila melanogaster* (Diptera), *Acanthoscelides obtectus* (Coleoptera), *Zophobas morio* (Coleoptera), *Pachnoda marginata* (Coleoptera), *Diabrotica virgifera* (Coleoptera) and *Periplaneta americana* (Blattodea) were used.

II.3. Insect lipids analysis by Thin-Layer Chromatography

TLC was performed using HPTLC plates (M5631-5, Fisher-Scientific) equilibrated in a mobile phase of chloroform:methanol:water (65:25:4, v/v/v). TLC chambers were prepared by adding the mobile phase to cover the middle edge of the chamber, and the system was equilibrated for 30 min at RT. TLC plates were marked 2.5 cm from the bottom with lanes spaced 1.5 cm apart and equilibrated in the chamber for 1 h before drying at 100°C for 10 min. Lipid samples were dissolved by incubation in a humid bath at 42°C with sonication for 15 min. Samples were applied to the plates in 1 cm bands with volumes of 5–30 μL depending on the analysis, and dried the plates at 50–70°C for 10 min. Plates were developed in the equilibrated chamber until the mobile phase reached the upper edge (approximately 1 h) and dried again at 50–75°C for 10 min. Visualization was performed by spraying the plates with a solution of 50 mL acetic acid, 1 mL sulfuric acid, and 0.5 mL p-anisaldehyde in a fume hood, followed by heating at 75–120°C until bands were clearly visible. At least two replicates were performed for each TLC assay.

II.4. Dot-blot binding assays

Trypsin-activation of Vip3Aa WT and Vip3Aa_I-III proteins was performed by incubating them with trypsin from bovine pancreas (T8003, Sigma-Aldrich) at 10% (w:w) for 1h at 37°C. Proteins were left overnight at 4°C before using them for dot-blot incubation. Dot-blots were performed as described previously (Best *et al.*, 2022) with some modifications. PVDF membranes with 0.2 μm pores (ISEQ00010 Immobilon-PSQ PVDF) were used for blotting. Lipid standards were added at 2 μg in a volume no larger than 4 μL, while larvae-extracted lipids were applied as 5 μL (upper phase) or 2 μL (lower phase) of the final suspension. Blots were dried for 30 minutes at RT, blocked with TBS containing 5% BSA for 4 hours at 4°C with agitation, and washed three times with TBS (5 min each wash). Protoxin, trypsin-processed Vip3Aa_Wt, or truncated constructs (4 μg/mL or equimolar concentrations for truncated constructs) were incubated overnight at 4°C in TBS with 1% BSA and agitation. After washing three times with TBS, membranes were probed for 1h at RT with a primary anti-Vip3Aa antibody raised in rabbit (1/5,000 dilution in TBS-0.1% BSA), followed by three more washing steps with TBS and incubation with an anti-rabbit HRP-conjugated secondary antibody (Sigma-Aldrich; 1/20,000 dilution) for 1 h at RT. All steps were performed with agitation. After three final washes with TBS, visualization was performed using a LI-COR C-Digit chemiluminescence western blot scanner and the WESTAR ECL-Sun HRP detection kit (K1-0052, GENEFLOW LIMITED). At least two replicates were performed for each dot-blot assay.

The following lipid standards were sourced from Avanti Polar Lipids with the following references and concentrations: sphingomyelin (860062, 10 mg/mL in chloroform), lyso-sphingomyelin (860600, 10 mg/mL in chloroform), glucosylceramide (131304, 2 mg/mL in ethanol), phosphatidylcholine (131601, 10 mg/mL in chloroform), ceramide phosphoethanolamine (CPE, 860066, 10 mg/mL in chloroform), porcine brain total ganglioside extract (860053P, 2 mg/mL in chloroform:ethanol 2:1) and C20 ceramide (860520P, 10 mg/mL in ethanol). Mixed bovine gangliosides (1065, 10 mg/mL in chloroform:ethanol 2:1) was sourced from Matreya LLC.

II.5. TLC-overlay assays

TLC for overlay assays was performed by using glass-backed silica-60 HPTLC plates (Merck). Plates equilibration, sample application, running, drying and visualization of the stained plates was performed as described above. For overlay assays with protein, Vip3Aa was trypsin-activated as described above and Biotin-labelled with a Biotinylation Kit (ab201795, abcam) following the instructions provided by the manufacturer. Plates were fixed with 50 mL hexane for 2 min and 50 mL of 0.1% polyisobutyl methacrylate (PIBM) in hexane for 2 min. Plates were dried at 50°C for 10 min and blocked with 0.5% BSA in PBS containing 0.01% Tween-20 for 30 min at RT. Plates were probed with biotin-labelled trypsin-activated Vip3Aa (4 μg/mL in blocking buffer) for 2 h at RT with shaking. Then, plates were washed twice with 10 mL of blocking solution and incubated with streptavidin-linked alkaline phosphatase (ALP, AK-5000 Vectastain Kit, Vector Labs) in blocking buffer for 1 h at RT without shaking. After three 1-min washes, plates

were incubated with a solution of 5-Bromo-4-Chloro-Indolyl-Phosphatase (BCIP) and Nitro blue Tetrazolium (NBT) solution (BCIP/NBT-Blue, B3679 Sigma-Aldrich) 10–15 min until bands were visible and air-dried overnight. At least two replicates were performed for each TLC-overlay assay.

III. Results

III.1. *Spodoptera spp.* midgut lipids separation by TLC

S. exigua and *S. littoralis* lipid extracts were obtained by the Svennerholm partitioning method and separated by TLC (**Figure 5.1**). The midgut lipids profile obtained for both insect species was very similar. Both phases of the extract (upper and lower phase) showed similar patterns as well, displaying differences on the relative abundance of some lipid species which were enriched in the lower phase, resulting in an overall higher concentration for this phase.

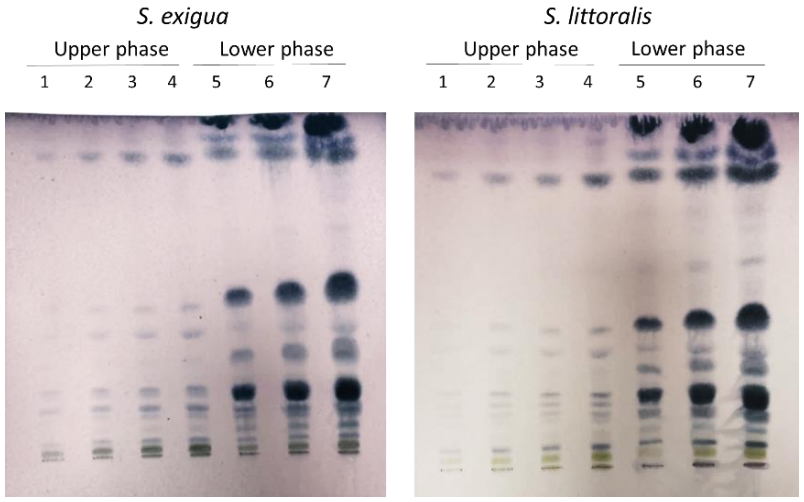

Figure 5.1. *Spodoptera spp.* lipids separation by TLC. Increasing amounts (2, 10, 20 and 30 µl) of upper phase (lanes 1-4) and increasing amounts (5, 10 and 20 µl) of lower phase (lanes 5-7) of *S. exigua* (left panel) and *S. littoralis* (right panel) lipid final extracts were run in TLC plates and stained with p-anisaldehyde.

III.2. Vip3Aa binding to *Spodoptera spp*. and standard lipids

Vip3Aa was used as protoxin and trypsin-processed to probe dot-blots loaded with *S. exigua and S. littoralis* midgut lipids and standard lipid samples. The results showed that the protein was able to bind upper and lower phases of lipid extracts of both insect species (**Figure 5.2** row A). In addition, the protein clearly bound lyso-sphingomyelin (**Figure 5.2** position B1), phosphatidylcholine (**Figure 5.2** position B3) and glucosylceramide (**Figure 5.2** position C2). A milder interaction was observed for gangliosides (**Figure 5.2** position B2 and C3), sphingomyelin (**Figure 5.2** position C1), and ceramide phosphoethanolamine (CPE, **Figure 5.2** position B4), whereas it did not interact with C20 ceramide (**Figure 5.2** position C4). Overall, no differences were observed between protoxin and trypsin-processed Vip3Aa (**Figure 5.2**).

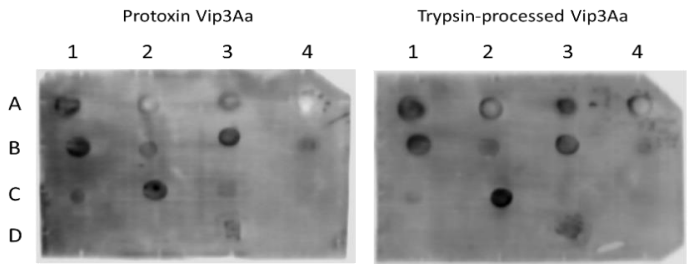

Figure 5.2. Protoxin and trypsin-processed Vip3Aa binding to lipids. *Spodoptera spp.* upper and lower phase lipids extracts (5 µl) were loaded in row A: (A1) *S. exigua* upper phase; (A2) *S. exigua* lower phase; (A3) *S. littoralis* upper phase and (A4) *S. littoralis* lower phase. Standard lipid samples (2 µl) were loaded in rows B and C: (B1) lyso-sphingomyelin; (B2) gangliosides (porcine); (B3) phosphatidylcholine; (B4) ceramide phosphoethanolamine (CPE); (C1) sphingomyelin; (C2) glucosylceramide; (C3) gangliosides (bovine); (C4) C20 ceramide. Membranes were incubated with Vip3Aa (as protoxin and trypsin-processed) and bound protein was immunodetected. Organic solvents (5 µl) were loaded as negative controls in row D: (D1) methanol; (D2) chloroform:methanol 1:1, as well as 5µg of Vip3Aa as positive control for the antibody detection (D3).

III.3. Vip3Aa truncated constructs binding to lipids

In order to evaluate the capacity of the different structural domains of the protein to bind lipid molecules, different truncated constructs containing only some domains were used in dot-blot assays along with the full-length protein (Vip3Aa_WT). Increasing concentrations of upper and lower phases of *S. exigua* midgut lipids and standard lipids were used. Overall, the truncated construct Vip3Aa_I-III showed the same binding pattern as the full-length protein, whereas the constructs containing only the C-t domains displayed slight differences with the WT pattern and membranes exhibited lower background (**Figure 5.3**). All truncated constructs could bind to the upper phase of *S. exigua* midgut lipids extract (**Figure 5.3** row A). However, the interaction observed for the construct Vip3Aa_IV-V was milder, only being detected at the highest lipid concentration used (**Figure 5.3** position A1). The constructs Vip3Aa_I-III and Vip3Aa_III-V could also bind to the lower phase of *S. exigua* midgut lipids extract, whereas no signal was detected for the Vip3Aa_IV-V construct (**Figure 5.3** row B). More concentrated lipid samples (neat samples) exhibited white dots due to the saturation of the signal (i.e., **Figure 5.3** positions A1 and B1), indicating strong interaction.

As the WT protein, the truncated construct lacking Domains IV and V (Vip3Aa_I-III) bound to lyso-sphingomyelin, sphingomyelin, phosphatidylcholine and glucosylceramide standards (**Figure 5.3** positions C1, C2, C3-C4 and D1 respectively), whereas it could not bind to C20 ceramide (**Figure 5.3** position D2). Similarly, the truncated constructs containing only the C-t domains displayed complementary

binding patters: Vip3Aa_III-V bound to lyso-sphingomyelin (**Figure 5.3** position C1) and Vip3Aa_IV-V bound to sphingomyelin (**Figure 5.3** position C2), phosphatidylcholine (**Figure 5.3** position C3-C4), and glucosylceramide (**Figure 5.3** position D1), together showing the same binding pattern as the WT protein to standard lipids.

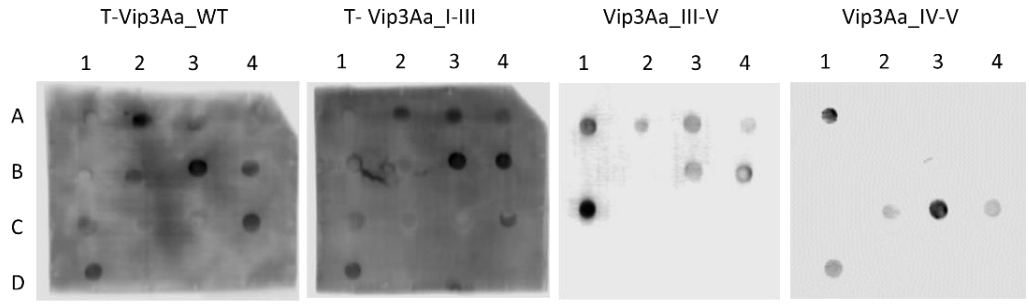

Figure 5.3. Vip3Aa truncated constructs binding to lipids. Serial dilutions of *Spodoptera exigua* upper phase lipids (5 µl) were loaded in row A: (A1) neat; (A2) 1/2 dilution; (A3) 1/5 dilution; (A4) 1/10 dilution. Serial dilutions of *S. exigua* lower phase lipids (2 µl) were loaded in row B: (B1) neat; (B2) 1/2 dilution; (B3) 1/5 dilution; (B4) 1/10 dilution. Rows C and D were loaded with standard lipids and organic solvents (2 µl): (C1) lyso-sphingomyelin; (C2) sphingomyelin; (C3) phosphatidylcholine (neat); (C4) phosphatidylcholine (1/10 dilution); (D1) glucosylceramide; (D2) C20 ceramide; (D3) methanol; (D4) chlorophorm:methanol 1:1. Membranes were incubated with trypsin-processed Vip3Aa (T-Vip3Aa) or equimolar concentrations of the truncated constructs T-Vip3Aa_I-III (trypsin-processed domains I-III), Vip3Aa_III-V (domains III-V) and Vip3Aa_IV-V (domains IV-V). Bound Vip3Aa (WT or truncated versions) was immunodetected.

III.4. TLC-overlay of *Spodoptera spp*. midgut lipids with Vip3Aa

To further characterise Vip3Aa's ability to bind *Spodoptera spp.* midgut lipids, we decided to compare the TLC profiles of *S. exigua and S. littoralis* lipid extracts in TLC-overlay assays with trypsin-activated Vip3Aa. Our results revealed very similar binding patterns for both species, with some lipid bands to which Vip3Aa was binding, present both in upper and lower phases of lipid extracts (**Figure 5.4**).

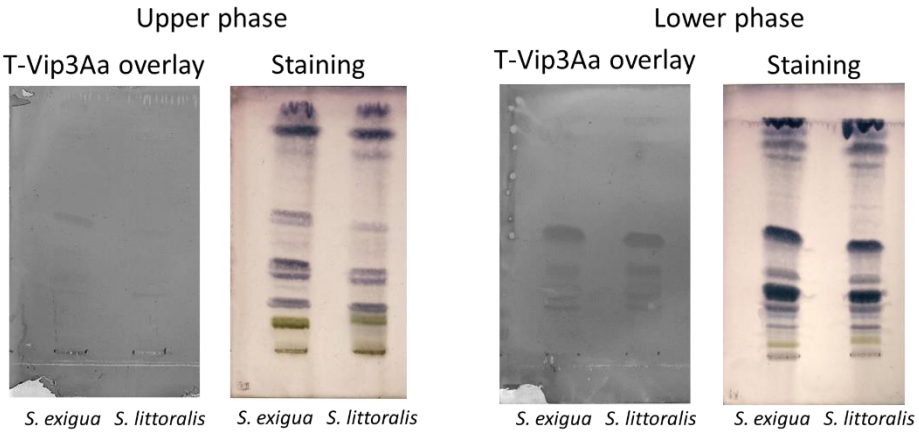

Figure 5.4. Vip3Aa TLC-overlay assays with *Spodoptera spp.* lipids. *Spodoptera exigua* and *Spodoptera littoralis* upper phase (20 µl, left panel) and lower phase (2.5 µl right panel) of lipid extracts were separated by TLC in duplicate plates. One plate was stained with p-anisaldehyde (right plates on each panel), while the other was used in overlay assays with Biotin-labelled trypsin-processed Vip3Aa (T-Vip3Aa, left plates on each panel) and bound-protein signal was developed by Streptavidin-linked ALP reaction.

III.5. Vip3Aa binding to lipids from different insect orders

Finally, to investigate the existence of a correlation between the toxicity spectrum of the Vip3Aa protein and its lipid-binding ability, lipid samples were extracted from various insect species belonging to different taxonomic orders and dot-blot assays were conducted using trypsin-processed Vip3Aa. Lipid samples from *S. exigua* and *M. sexta* were included as examples of lepidopteran insects susceptible to Vip3Aa (**Figure 5.5** row A). Lipid samples from two different mosquito species (*A. aegypti* and *C. quinquefasciatus*) and from *D. melanogaster* were used as representative samples from dipteran insects (**Figure 5.5** row B), which are not susceptible to Vip proteins. *A. obtectus, Z. morio, P. marginata* and *D. virgifera* lipids were included as examples of coleopteran species (**Figure 5.5** positions C1-4), also non-suceptible to Vip proteins. Lipids from *P. americana* were used as an example of

Blattodea insects (**Figure 5.5** position C5). The results showed that the protein is capable of binding to lipids of non-susceptible insects regardless of its lepidopteran-specific activity.

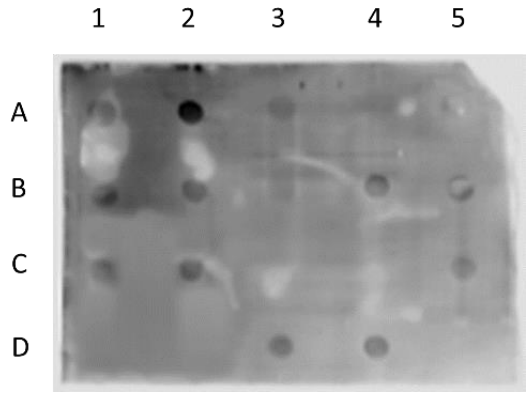

Figure 5.5. Vip3Aa binding to lipid samples from different insect orders. (A1 and D3) *Spodoptera exigua* upper phase (neat); (A2 and D4) *S. exigua* lower phase (1/5 dilution); (A3) *Manduca sexta* upper phase (neat); (A4) *M. sexta* upper phase (1/5 dilution); (A5) *M. sexta* lower phase (1/5 dilution); (B1) *Aedes aegypti* upper phase (neat); (B2) *A. aegypti* lower phase (neat); (B3) *Culex quinquefasciatus* upper phase (1/5 dilution); (B4) *C. quinquefasciatus* lower phase (neat); (B5) *Drosophila melanogaster* total lipids (1/5 dilution); (C1) *Acanthoscelides obtectus* total lipids (1/5 dilution); (C2) *Zophobas morio* total lipids (1/5 dilution); (C3) *Pachnoda marginata* total lipids (1/5 dilution); (C4) *Diabrotica virgifera* total lipids (1/5 dilution); (C5) *Periplaneta americana* total lipids (1/5 dilution); (D1) methanol; (D2) methanol:chlorophorm 1:1. Total lipids corresponds to 1:1 mixture of upper and lower phases of the extract. Membrane was incubated with trypsin-processed Vip3Aa and bound protein was immunodetected.

IV. Discussion

Several proteins have been proposed as Vip receptors, primarily based on studies with Sf9 cultured cells (An *et al.*, 2022; Estruch and Yu, 2001; Jiang *et al.*, 2018a, 2018b; Osman *et al.*, 2018, 2019; Singh *et al.*, 2010), but none have been validated *in vivo*, leaving their midgut receptors unidentified (Ferré *et al.*, 2023). *In vitro* binding assays to brush border membrane vesicles (BBMV) indicate lower binding affinity and a broad range of binding sites for Vip3A proteins compared to Cry proteins

(Chakroun and Ferré, 2014; Lázaro-Berenguer *et al.*, 2022b, 2024; Quan *et al.*, 2021a), though not all contribute to toxicity (Lázaro-Berenguer *et al.*, 2022b). Unlike Cry protein resistance, which usually involves altered midgut binding (Jurat-Fuentes *et al.*, 2021), Vip3Aa-resistant strains generally do not show binding changes (Chakroun *et al.*, 2016b; Pinos *et al.*, 2020; Quan *et al.*, 2021b), except in one *Helicoverpa zea* strain with reduced binding (Kerns *et al.*, 2023). Altogether, and given the structural homology of Vip C-t domains with glycan-binding proteins, it is reasonable to think that Vip proteins could be interacting with different types of glycoconjugates in the apical membrane of midgut cells.

In this study, we have evaluated the ability of the Vip3Aa protein to bind to *Spodoptera spp*. midgut lipids and standard lipid molecules commonly present in cellular membranes. We have used protoxin and trypsin-processed Vip3Aa, as well as different truncated constructs to infer the role of the different structural domains of the protein in the binding to lipid samples. Results from dot-blot assays revealed that Vip3Aa is able to bind to both phases of midgut lipid extracts of *Spodoptera spp.* (**Figure 5.2** row A), binding to upper phase lipids suggests binding to carbohydrate containing lipids, as this phase is enriched in glycolipids. In addition, Vip3Aa was able to bind both as protoxin and after trypsin treatment, suggesting that both structural conformations (protoxin and activated protein) are able to interact with lipid molecules, and that binding epitopes are not affected by the proteolytic activation of the protein, in agreement with previous reports on *in vitro* binding assays to BBMV and *in vivo* competition assays in *S.*

exigua (Lázaro-Berenguer *et al.*, 2024). Furthermore, *S. exigua* and *S. littoralis* lipid TLC profiles were very similar, in agreement with the observed binding to extracts of both species (**Figures 5.1 and 5.4**). Identifying the lipid molecules to which Vip3Aa binds in the TLC-overlays would provide valuable insights on putative midgut lipid receptors. Also, dot-blot assays performed with different Vip3Aa truncated constructs revealed that all C-t domains of the protein (Domains III-V) seem to participate in the binding to midgut lipids, since all constructs were able to bind to *S. exigua* upper phase lipids (**Figure 5.3** row A), and that the lack of Domain III seems to affect binding to the lower phase lipids (**Figure 5.3** row B). In addition, we have reported that this binding might not be species-specific, since we have detected the ability of Vip3Aa to bind lipid extracts from non-susceptible insects (**Figure 5.5**) regardless of its lepidopteran-specific insecticidal activity. Interestingly, it has also been described that Vip3A proteins can bind specifically to BBMV from non-susceptible insects (Gomis Cebolla *et al.*, 2017; Lee *et al.*, 2003), and therefore, as for Cry proteins, binding to the midgut epithelium was proven necessary though not sufficient for toxicity. In agreement with this observation, truncated Vip3A constructs lacking the C-t CBM Domains IV and V, are able to specifically bind to *Spodoptera spp.* BBMV *in vitro* (Quan *et al.*, 2021a; **Figure 4.1** in Chapter 4) but lack of toxicity *in vivo* (Lázaro-Berenguer *et al.*, 2022a). These data suggest that factors beyond specific binding to midgut receptors play a crucial role in the protein's toxic action.

Additionally, Vip3Aa also interacts with some standard lipids, among which sphingomyelin, lyso-sphingomyelin, glucosylceramide and phosphatidylcholine were the most evident interactors (**Figure 5.2** rows B and C and **Figure 5.3** rows C and D). Sphingomyelin and lyso-sphingomyelin are phosphosphingolipids, and glucosylceramide is a cerebroside (a type of glycosphingolipid), all of them having a ceramide backbone attached to a polar headgroup. Sphingomyelin and lyso-sphingomyelin share the phosphocholine hydrophilic headgroup, whereas glucosylceramide contains a glucose headgroup instead. Phosphatidylcholine however, is a glycerophospholipid with a glycerol backbone linking the hydrophobic tail to the phosphocholine headgroup. The structures of these molecules are summarized in **Figure 5.6**. All these lipids are integral components of cellular membranes in eukaryotic cells (van Meer *et al.*, 2008). Phosphatidylcholine is one of the most abundant phospholipids in the outer leaflet of the plasma membrane (Alberts *et al.*, 2015; Sakuragi and Nagata, 2023; van Meer *et al.*, 2008), it plays an essential role in maintaining membrane permeability barriers and serves as a substrate for generating second messenger signalling molecules (Boumann *et al.*, 2006; de Kroon *et al.*, 2007; van Meer *et al.*, 2008). Sphingomyelin, lyso-sphingomyelin and glucosylceramide are present in lipid rafts (Bieberich, 2018; Quinn, 2014), these sphingolipid-rich membrane microdomains behave as major modulators of membrane geometry, membrane trafficking and a wide number of signal transduction processes (Simons and Ikonen 1997; Brown and London 1998), including cell survival and apoptosis (Deans *et al.*, 2002; George *et al.*, 2012; Mollinedo and Gajate, 2015).

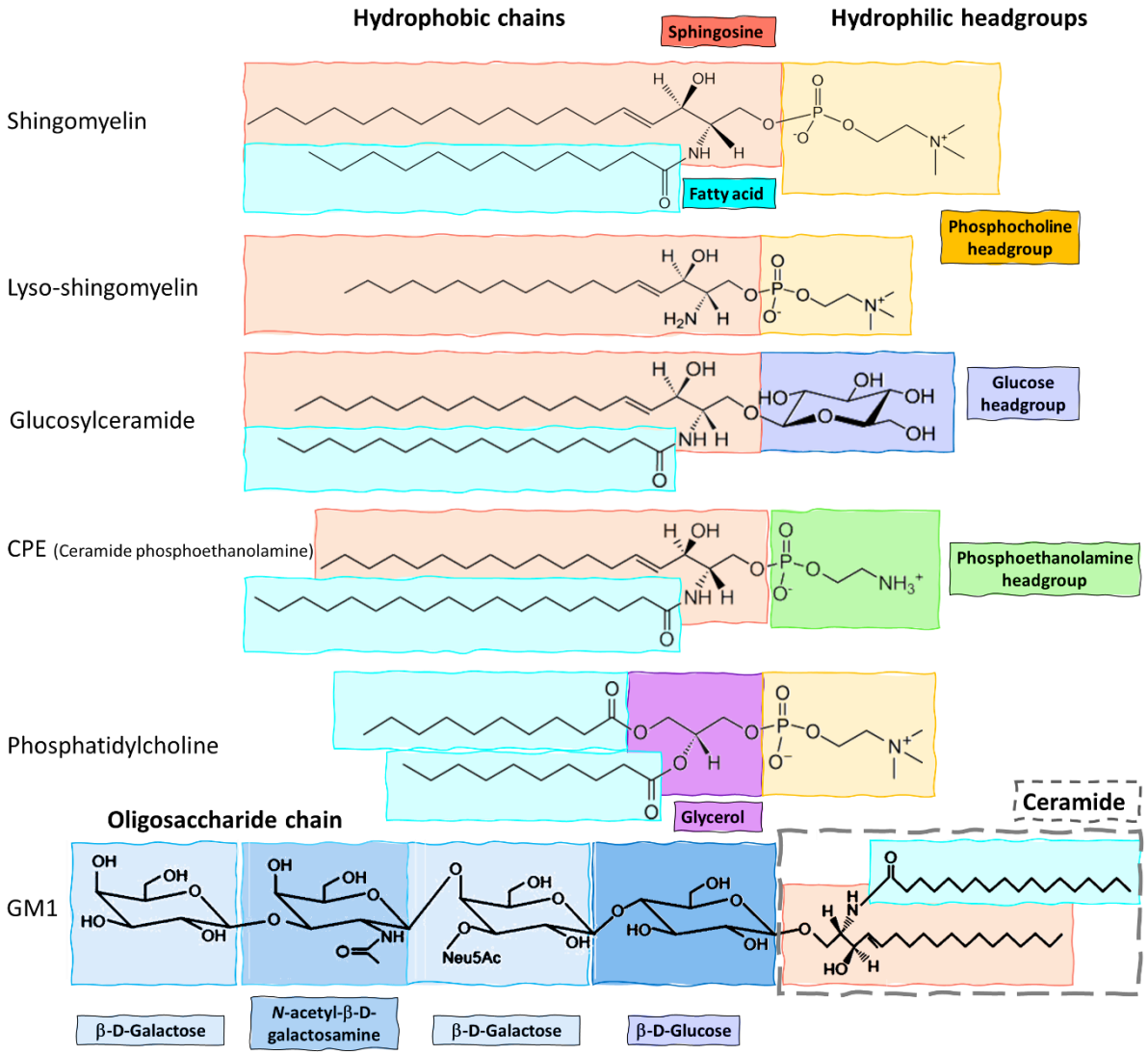

Figure 5.6. Molecular structure of cell membrane lipids. Sphingomyelin and lyso-sphingomyelin are phosphosphingolipids, containing a phosphocholine headgroup attached to a sphingosine backbone. Glucosylceramide is a cerebroside (glycosphingolipid), containing a glucose headgroup attached to a ceramide backbone (a sphingosine amid-linked to a fatty acid chain). Ceramide phosphoethanolamine CPE is also a ceramide and a phosphosphingolipid, containing a phosphoethanolamine headgroup attached to a ceramide backbone. Phosphatidylcholine is a class of phospholipid (a glycerophospholipid), containing a glycerol backbone linking two fatty acid chains to the phosphocholine hydrophilic headgroup. Gangliosides, such as GM1, are glycosphingolipids that include a ceramide backbone and an oligosaccharide chain with terminal galactose residues and one or more sialic acids attached as headgroup.

Given the amphipathic nature of lipids, only hydrophilic headgroups remain exposed to the solvent and therefore Vip3Aa would most likely interact with these lipid molecules through them. Based on the results obtained, we can establish a binding pattern where Vip3Aa preferentially binds to the glucose headgroup found in glucosylceramide, and the phosphocholine headgroup present in sphingomyelin, lyso-sphingomyelin and phosphatidylcholine (**Figure 5.6**). While phosphocholine is a headgroup mainly found in lipids (phosphospingolipids) (Nelson and Cox 2021b; Varki *et al.*, 2009), glycoproteins generally have glycans that consist of monosaccharides like glucose, mannose, galactose, fucose, and N-acetylglucosamine (GlcNAc) (Nelson and Cox, 2021b; Varki *et al.*, 2009). However, phosphocholine can be involved in specialized glycosylation processes such as the formation of glycosylphosphatidylinositol (GPI) anchors, which link proteins to the cell surface (Kinoshita, 2016; Varki *et al.*, 2009), as happens for Cry receptors ALP and APN (Bravo *et al.*, 2023). Vip proteins could be binding to the cell membrane by interacting with lipids or glycoproteins containing these motifs, which could mediate toxicity. Interestingly, a previous report showed the ability of Vip3Aa to interact with chitin and chitosan (Jiang *et al.*, 2020b), long-chain polymers composed of GlcNAc units, lacto-N tetraose (also containing GlcNAc) and several monosaccharides such as deoxy-hexoses and fucoses which also originate from glucose metabolism and are common glycan moieties found in glycoproteins (Nelson and Cox, 2021b; Varki *et al.*, 2009). Later, it was reported that the interaction of Vip3Aa with the PM (mainly composed by chitin and glycoproteins), occurred

through Domain V and had implications in the toxicity against *Spodoptera frugiperda* (Jiang *et al.*, 2023b). Also, all membrane insertion experiments involving Vip proteins have been conducted using artificial liposomes composed of DOPC:DOPE in 6:4 and 1:1 ratios (Byrne *et al.*, 2021; Kunthic *et al.*, 2017; Shao *et al.*, 2024). Based on this, we hypothesize that binding to phosphatidylcholine (or DOPC) could play a role in triggering membrane insertion. However, since phosphocholine and glucose residues are not exclusive residues found in the membrane of Lepidoptera midgut cells, other Vip3Aa receptors may exist to provide both, target species specificity and tissue specificity. Besides, based on our results with lipid standards, Vip3Aa would show diminished binding to the amino alcohol headgroup present in all ceramides, the phosphoethanolamine headgroup present in ceramide phosphoethanolamine (CPE), or the terminal galactose found in oligosaccharide chains of gangliosides (**Figure 5.6**). The preference of Vip3Aa for sphingomyelin and lyso-sphingomyelin over CPE is puzzling, as CPE is the predominant sphingolipid in arthropods and acts as specific receptor of other insecticidal proteins such as Ostreolysin A6 (Milijaš Jotić *et al.*, 2021), whereas sphingomyelin is more common in mammalian and Nematoda cells (Best *et al.*, 2023; Panevska *et al.*, 2019). Gangliosides, which are complex glycosphingolipids composed of a ceramide backbone with long oligosaccharide chains and sialic acid residues, are also abundant in mammalian cells (Best *et al.*, 2023; Yu *et al.*, 2011). However, their presence in insect membranes remains debated (Ghosh *et al.*, 2018; Marchal *et al.*, 2001), making it less likely that these glycolipids function as receptors for insecticidal toxins.

V. Conclusions

Overall, we have showed the ability of Vip3Aa to interact with *Spodoptera spp*. midgut lipids although the specificity of the binding and whether this facilitates toxicity is still to be investigated. Specially given that Vip3Aa also binds to lipid extracts of non-susceptible insects. Nevertheless, we can hypothesize that a primary binding to lipids and glycoconjugates on the midgut cell surface, even if it is in a non-selective or non-specific way, may assist the protein in approaching the membrane, thereby facilitating further interactions with specific receptors and mediating toxicity. Similar two-stage binding mechanisms have been also hypothesised for other Bt proteins (Best *et al.*, 2022; Bravo *et al.*, 2004, 2007; Jenkins *et al.*, 2000). In addition, we have identified different standard lipids which Vip3Aa is able to bind: phosphosphingolipids (sphingomyelin, lysosphingomyelin) and glycosphingolipids (glucosylceramide), as well as simpler phospholipids (phosphatidylcholine), all common molecules in cellular membranes. These results provide preliminary insights into residues which could act as putative receptor moieties for the binding to cellular membranes (phosphocholine and glucose headgroups). Furthermore, we have reported that the three C-t domains of the protein seem to be involved in these interactions.

General discussion

Bacillus thuringiensis (Bt) insecticidal proteins have been widely used in Bt-crops to control major agricultural pests since the 1990s (Estruch *et al.*, 1997; Gassmann and Reisig, 2023; James, 1997). Among these proteins, Vip proteins are particularly important for managing lepidopteran insects that have developed resistance to the conventionally used Cry proteins (Ferré *et al.*, 2023; Gupta *et al.*, 2021). To enhance insect control and delay resistance development, both Vip and Cry proteins are often combined in pyramided Bt-crops (Carrière *et al.*, 2015; Moar and Anilkumar, 2007). A deeper understanding of their toxic mechanisms and unique characteristics is crucial for optimizing their commercial application.

In this thesis, we have investigated the mode of action of the lepidopteran-specific Vip3Aa insecticidal protein by studying the behaviour of several point mutations and truncations of the protein in its structure, the stability against midgut proteases, the ability to bind to specific and functional receptors in the midgut epithelium and the toxicity against *Spodoptera spp.* pests. Overall, our results point out to several structural features which are essential for the protein's function.

Firstly, tetramer formation is essential for protein stability, binding to functional receptors and toxicity. The presence of the N-terminal (N-t) Domain I is key for tetramer formation (Jiang *et al.*, 2020a; Núñez-Ramírez *et al.*, 2020), as none of the constructs lacking of this part of the protein would be able to form tetramers and none is stable against midgut proteases (**Figure D1**).

In addition to its structural role allowing oligomerization, Domain I undergoes a dramatic structural remodelling after proteolytic activation by midgut proteases (Byrne *et al.*, 2021; Núñez-Ramírez *et al.*, 2020) which has also shown to be an essential feature for the protein's toxicity (Lazaro-Berenguer *et al.*, 2022a), since structural mutants unable to remodel into the activated conformation due to crosslinking of Domain I α-helices (Vip3Aa_S-S and Vip3Aa DIP1), show a lack of toxicity against *S. exigua* larvae (**Figure D1**). Furthermore, the presence of the C-terminal (C-t) Domains IV and V has shown to be essential for the structural remodelling of the protein into the activated conformation, as the lack of these domains (Vip3Aa_I-III construct) results in an impaired remodelling (Lázaro-Berenguer *et al.*, 2022a), which could be the cause of the lack of toxicity exhibited by this truncated protein (**Figure D1**).

The N-t helix α1 of Domain I (residues 1 to 39) has also shown to be critical for the protein's toxic action, given that its absence (Vip3Aa_$\Delta\alpha$1 mutant) results in a lack of toxicity against *S. exigua* (Lazaro-Berenguer *et al.*, 2022a; **Figure D1**). This region of the protein contains a predicted transmembrane region between residues 12 and 30 (Lázaro-Berenguer *et al.*, 2024) and several reports have shown the ability of the protein to insert into artificial liposomes through it (Byrne *et al.*, 2021; Shao *et al.*, 2024). Furthermore, a point mutation located within helix α1 (Vip3Aa_M34L) has shown enhanced toxicity against *S. exigua* (**Figure D1**), potentially due to improved membrane insertion given the higher hydrophobicity index of Leu compared to Met (Lázaro-Berenguer *et al.*, 2022a), this was also observed for Vip3Af in *S. littoralis* (Banyuls *et al.*, 2021). However, though nowadays it is widely accepted that after

insertion into the membrane Vip3A proteins produce osmotically-induced cell lysis by pore formation (Byrne *et al.*, 2021; Kunthic *et al.*, 2017; Lee *et al.*, 2003; Liu *et al.*, 2011), the details of the events that lead to toxicity are not fully understood.

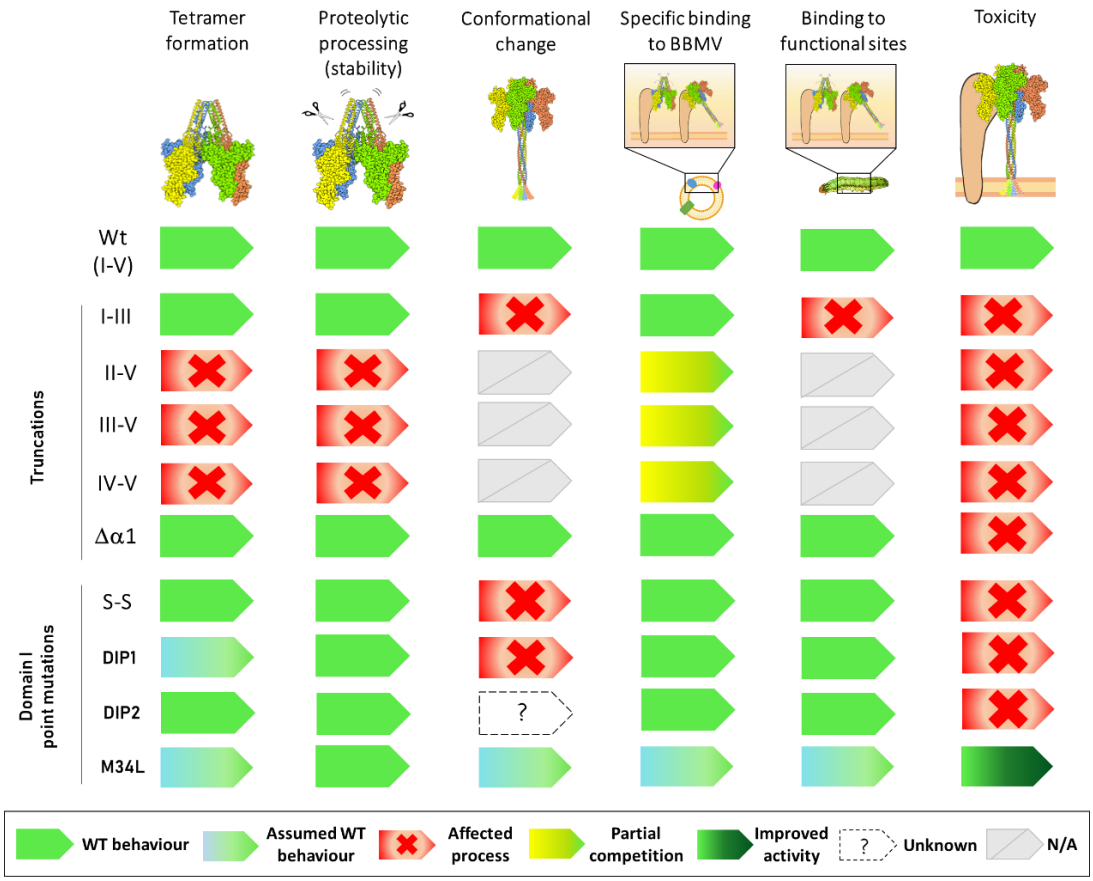

Figure D1. Role of the different domains of the Vip3Aa in the mode of action as deduced by truncations and point mutations. The upper part of the figure schematizes the most likely sequence of events based on available data (summarized in Figure I10). Wt (I-V) refers to the full length wild type protein, roman numbers refer to structural domains; Δα1 denotes deletion of N-t helix α1; S–S indicates a crosslink by two disulphide bridges between α-helices 2 and 3 of Domain I (by introduction of mutations D66C, N69C, Q96C and L100C); DIP refers to disabled insecticidal Vip3Aa variants, having DIP1 also a disulphide bridge introduced in Domain I (mutations S164C and L166C) and DIP2 a point mutation in the same domain (E168A); M34L refers to a point mutation within helix α1; N/A, not applicable.

In addition to its role in the toxic action of the protein, helix α1 also plays an important structural role in maintaining the protoxin conformation by interacting with Domain II helices (Núñez-Ramírez *et al.*, 2020). Thus, its absence results in the spontaneous remodelling into the activated conformation without the need of proteolytic processing to occur at the primary trypsin site located in the loop between Domains I and II of the Vip3Aa protein (Lázaro-Berenguer *et al.*, 2022a).

Regarding the protein's ability to bind to specific receptors in the brush border membrane of midgut cells, we have reported that protein conformation is not critical, given that both protoxin and activated toxin conformations (inferred by the use of structural mutants with locked conformations Vip3Aa_$\Delta\alpha$1 and Vip3Aa_S-S) showed specific binding to *S. exigua* BBMV in *in vitro* binding assays with radiolabelled Vip3Aa (Lázaro-Berenguer *et al.*, 2024; **Figure D1**). Domain III of the protein has shown to be the most relevant domain for the specific binding, as the construct lacking Domains IV and V (Vip3Aa_I-III) shows complete competition for the binding sites of Vip3Aa (**Figure 4.1** and **Figure D1**) and Vip3Af (Quan *et al.*, 2021a) in *Spodoptera spp.* BBMV. However, a potential contribution of the C-t domains IV and V in the specific binding of Vip3Aa cannot be ruled out, as the truncated construct containing only these domains (Vip3Aa_IV-V) partially displaced the WT's specific binding to *S. exigua* BBMV (**Figure 4.1** and **Figure D1**). Tetramer formation is neither critical for the specific binding, as truncated constructs lacking of Domain I which could not tetramerize (Vip3Aa_II-V, Vip3Aa_III-V and Vip3Aa_IV-V) can partially displace

the full-length protein's binding in *in vitro* assays with *S. exigua* BBMV (**Figure 4.1** and **Figure D1**).

To date, various receptors have been proposed for Vip proteins (An *et al.*, 2022; Estruch and Yu, 2001; Jiang *et al.*, 2018a; Jiang *et al.*, 2018b; Osman *et al.* 2018; Singh *et al.*, 2010), although none have been fully validated *in vivo*, so the identity of Vip surrogate receptors remains unknown (Ferré *et al.*, 2023). The *in vitro* binding data obtained from assays with radiolabelled Vip3A proteins and BBMV from *Spodoptera spp*. suggest a large population of binding sites with lower affinity compared to Cry proteins (Chakroun and Ferré, 2014; Lázaro-Berenguer *et al.*, 2022b; Lázaro-Berenguer *et al.*, 2024; Quan *et al.*, 2021a). Furthermore, the population of Vip3Aa binding sites revealed in *in vitro* assays does not fully reflect the receptors involved in the protein's toxicity, as some binding sites detected *in vitro* are not functional as revealed by *in vivo* competition assays (Lázaro-Berenguer *et al.*, 2022b), a technique which has proved to be very useful for the distinction of functional shared binding sites between different insecticidal proteins (Chen *et al.*, 2021; Hernández-Martínez *et al.*, 2022; Jerga *et al.*, 2019; Wang *et al.*, 2019). By performing *in vivo* competition assays among different Vip proteins in *S. littoralis*, we have reported that despite the observed partial competition of Vip3Ca for the binding sites of Vip3Aa *in vitro*, it is unable to block the toxicity of Vip3Aa and Vip3Af WT proteins *in vivo* (Lázaro-Berenguer et al., 2022b). This indicates the existence of various binding sites for Vip3A, proteins among which, the sites shared between Vip3A and Vip3C are not involved in Vip3A's toxicity (Lázaro-Berenguer *et al.*, 2022b). *In vivo* competition assays also

allow for the detection of differences in receptor binding affinity, as observed between Vip3Aa and Vip3Af in *S. littoralis*, with Vip3Aa showing a higher affinity by blocking the toxicity of Vip3Af at a lower competitor ratio (Lázaro-Berenguer *et al.*, 2022b). Additionally, through *in vivo* competition assays performed with the structural mutants Vip3Aa_Δα1 and Vip3Aa_S-S in *S. exigua*, we have observed that protein conformation is not a critical feature either for the recognition of functional receptors (**Figure D1**), as both protoxin and activated protein conformations are able to block the WT's toxicity, suggesting that the conformational change of the proteolytically-processed protein could occur either in a pre-binding or a post-binding to midgut receptors stage (Ferré *et al.*, 2023; Lázaro-Berenguer *et al.*, 2024).

Although the presence of Domains I-III is sufficient for the specific binding to BBMV *in vitro*, the presence of Domains IV and V is necessary for Vip3Aa's toxicity *in vivo* (Lázaro-Berenguer *et al.*, 2022a). Given that both conformations of the protein bind to functional receptors, we can assume that the lack of toxicity in the Vip3Aa_I-III construct is not due to the absence of conformational change or protein instability, as this construct remains stable against midgut proteases of *Spodoptera spp*. (**Figures 4.2** and **S4.3**). Therefore, we hypothesize that the lack of toxicity in this truncated protein must be related to the absence of binding to functional sites (**Figure D1**), as no inhibition of Vip3Aa's toxicity was observed in *in vivo* competition assays conducted on *S. exigua* and *S. littoralis* (**Figure 4.3**). This could be linked to the disruption of a step in the mode of action prior to the binding step, such as the interaction with the peritrophic matrix recently described through the

protein's Domain V (Jiang *et al.*, 2023), although further studies are needed to validate this hypothesis.

Given the structural homology of Vip3A C-t domains III and IV-V to β-prism fold lectins and CBM16 hydrolases, respectively (Bae *et al.*, 2008; Jiang *et al.*, 2020a; Núñez-Ramírez *et al.*, 2020; Sharma *et al.*, 2007), together with their broad population of low-affinity binding sites (Chakroun and Ferré, 2014; Lázaro-Berenguer *et al.*, 2022b; Lázaro-Berenguer *et al.*, 2024; Quan *et al.*, 2021a), and the existence of some non-functional binding sites (Lázaro-Berenguer *et al.*, 2022b), we hypothesised that Vip proteins could be binding to different types of glycosylated molecules in the apical membrane of midgut cells. To test this hypothesis, we have explored the ability of the Vip3Aa protein to bind lipid molecules, which are present in high numbers in cellular membranes and have been described as receptors for other pore forming proteins (Geny and Popoff, 2006; Griffitts *et al.*, 2003; Sepcić *et al.*, 2004; Tweten, 2005; Yamaji *et al.*, 1998). Our findings suggest that Vip3Aa could be interacting with midgut lipids of *Spodoptera spp*. both as protoxin and trypsin-processed (**Figure 5.2**), most probably by binding to their hydrophilic headgroups. However, the specificity of this binding and its potential role in facilitating toxicity remain to be determined, especially since Vip3Aa also binds to lipid extracts from non-susceptible insects (**Figure 5.5**). Nevertheless, we propose that a two-step binding mechanism could be occurring, where an initial interaction with lipids and glycoconjugates on the midgut cell surface may help the protein approach the membrane and enable further interactions with specific receptors mediating toxicity, as has been

suggested for other Bt proteins (Best *et al.*, 2022; Bravo *et al.*, 2004, 2007; Jenkins *et al.*, 2000). Furthermore, our findings suggest that the three C-t domains III-V of Vip3Aa could participate in these interactions, as all truncated constructs used in the assays were able to bind to midgut and standard lipid samples (**Figure 5.3**).

In summary, the resolution of the 3D structure of Vip proteins has significantly advanced our understanding of their mode of action. Key discoveries include the identification of two distinct structural conformations—protoxin and activated protein (Núñez-Ramírez *et al.*, 2020)— as well as the activated protein's ability to insert into lipid membranes via its N-t region, facilitating ion flow (Byrne *et al.*, 2021). Additionally, structural homology has been identified between the C-t domains and glycan-binding proteins (Byrne *et al.*, 2021; Jiang *et al.*, 2020a; Núñez-Ramírez *et al.*, 2020; Zheng *et al.*, 2020). These insights have enabled a more targeted investigation into the mode of action of Vip proteins. Our research has focused on evaluating the receptor-binding capacity of both structural conformations, exploring the critical role of the N-t region (Domain I) and its remodelling for the toxicity, and hypothesizing potential interactions with biomolecules of different biochemical natures through the C-t domains. However, many aspects of Vip proteins' mode of action remain unknown, requiring further research. Key open questions include the identity of functional receptor molecules in the midgut epithelium of target species, the *in vivo* role of Domains IV and V, the biological significance of the interaction with the peritrophic matrix, the biochemical basis of insect resistance and the

characterization of the mechanisms underlying toxicity, such as membrane disruption, pore formation, and potential alternative pathways like apoptosis. Expanding our knowledge in these areas will enhance their application as powerful biotechnological tools for agricultural pest control.

Conclusions

CONCLUSIONS

1. Vip proteins share binding sites in the brush border membrane of *Spodoptera littoralis*. Vip3Aa has multiple binding site populations, but the ones it shares with Vip3Ca do not contribute to its toxicity. In contrast, Vip3Aa and Vip3Af share functional binding sites *in vivo*, with Vip3Aa showing a higher affinity for them.

2. Several structural features of the Vip3Aa protein are essential for its toxicity against *Spodoptera exigua*: tetramer formation, the remodelling of Domain I into the activated conformation after proteolytic cleavage at the primary site (in the loop between Domains I and II) and the integrity of the N-terminal helix α1.

3. Both protoxin and activated protein structural conformations of the Vip3Aa protein bind to functional binding sites in *S. exigua*. Although binding of the protoxin is mainly non-specific whereas activated protein shows specific binding and higher binding affinity.

4. Domains IV and V are not required for tetramer formation nor protein stability against midgut proteases; however, their absence impairs the remodelling into the activated conformation. Furthermore, these domains are not essential for the binding of Vip3Aa to specific binding sites in the brush border membrane of *S. exigua in vitro*, though their presence is essential for the *in vivo* binding to functional sites and toxicity in *S. exigua* and *S. littoralis*.

5. Vip3Aa can bind to lipids extracted from *S. exigua* and *S. littoralis* midgut samples, though its binding specificity and role in toxicity remain unclear. Its ability to bind non-susceptible insect lipids suggests a potential two-stage binding mechanism, where initial non-specific interactions might help the protein reach specific receptors in the membrane. Additionally, glycan residues may serve as binding epitopes for these interactions through Vip3Aa's C-terminal Domains III-V.

CONCLUSIONES

1. Las proteínas Vip comparten sitios de unión en la membrana del borde en cepillo de *Spodoptera littoralis*. Vip3Aa tiene múltiples poblaciones de sitios de unión, pero las que comparte con Vip3Ca no contribuyen a su toxicidad. En contraste, Vip3Aa y Vip3Af comparten sitios de unión funcionales *in vivo*, siendo Vip3Aa la que muestra una mayor afinidad por ellos.

2. Varias características estructurales de la proteína Vip3Aa son esenciales para su toxicidad contra *Spodoptera exigua*: la formación de tetrámeros, el remodelado estructural del Dominio I en su conformación activada tras el procesamiento proteolítico en el sitio de corte primario (entre los Dominios I y II) y la integridad de la hélice α1 en el extremo N-terminal.

3. Tanto la conformación estructural de protoxina como la de proteína activada de Vip3Aa se unen a sitios de unión funcionales en *S. exigua.* Aunque la unión de la protoxina es principalmente no específica, la proteína activada muestra una unión específica y de mayor afinidad.

4. Los Dominios IV y V no son necesarios para la formación del tetrámero ni para la estabilidad de la proteína frente a las proteasas intestinales; sin embargo, su ausencia afecta cambio de conformación de la proteína activada. Además, estos dominios no son esenciales para la unión de Vip3Aa a sitios específicos en la membrana del borde en cepillo de *S. exigua in vitro*, aunque su presencia es crucial para la unión *in vivo* a sitios funcionales y la toxicidad en *S. exigua* y *S. littoralis*.

5. Vip3Aa puede unirse a los lípidos extraídos del tejido intestinal de larvas de *S. exigua* y *S. littoralis*, aunque la especificidad de su unión y el papel en la toxicidad siguen sin estar claros. Su capacidad para unirse a los lípidos de insectos no susceptibles sugiere un posible mecanismo de unión en dos etapas, donde interacciones iniciales no específicas podrían ayudar a la proteína a alcanzar receptores específicos en la membrana. Además, los residuos de glicanos podrían servir como epítopos de unión para estas interacciones a través de los Dominios C-terminales III-V de la proteína.

References

Abdelgaffar HM, Oppert C, Sun X, Monserrate J, Jurat-Fuentes JL. 2019. Differential heliothine susceptibility to Cry1Ac associated with gut proteolytic activity. Pestic Biochem Physiol 153, 1–8. https://doi.org/10.1016/j.pestbp.2018.10.001

Abdelkefi-Mesrati L, Boukedi H, Chakroun M, Kamoun F, Azzouz H, Tounsi S, Rouis S, Jaoua S. 2011. Investigation of the steps involved in the difference of susceptibility of *Ephestia kuehniella* and *Spodoptera littoralis* to the *Bacillus thuringiensis* Vip3Aa16 toxin. J Invertebr Pathol 107, 198–201. https://doi.org/10.1016/j.jip.2011.05.014

Abrishami V, Zaldívar-Peraza A, de la Rosa-Trevín JM, Vargas J, Otón J, Marabini R, Shkolnisky Y, Carazo JM, Sorzano CO. 2013. A pattern matching approach to the automatic selection of particles from low-contrast electron micrographs. Bioinformatics, 29, 2460–2468. https://doi.org/10.1093/bioinformatics/btt429

Adang MJ, Crickmore N, Jurat-Fuentes JL. 2014. Diversity of *Bacillus thuringiensis* Crystal Toxis and Mechanism of Action. Adv Insect Phys 47. http://dx.doi.org/10.1016/B978-0-12-800197-4.00002-6

Alberts B, Johnson A, Lewis J, Raff M, Roberts K, Walter P. 2015. Molecular Biology of the Cell (6th ed.). Garland Science. Part IV. Internal Organization of the Cell, Chapter 10. Membrane Structure.

Allen D and Department for Environment, Food & Rural Affairs (DEFRA), Army worms (*Spodoptera spp*.) Plant Pest Factsheet 2022. https://planthealthportal.defra.gov.uk/assets/factsheets/Plant-pest-Factsheet-Spodoptera-Spp.pdf [accessed 29.12.2024].

Alexandratos N, Bruinsma J. 2012. World agriculture towards 2030/2050: the 2012 revision. Land Use Policy 20, 375.

An B, Zhang Y, Li X, Hou X, Yan B, Cai J. 2022. PHB2 affects the virulence of Vip3Aa to Sf9 cells through internalization and mitochondrial stability. Virulence 13, 684–697. https://doi.org/10.1080/21505594.2022.2064596

Anilkumar KJ, Rodrigo-Simón A, Ferré J, Pusztai-Carey M, Sivasupramaniam S, Moar WJ. 2008. Production and characterization of *Bacillus thuringiensis* Cry1Ac resistant cotton bollworm *Helicoverpa zea* (Boddie). Appl Environ Microbiol 74, 462–469. https://doi.org/10.1128/AEM.01612-07

Aranda E, Sánchez J, Peferoen M, Guereca L, Bravo A. 1996. Interactions of *Bacillus thuringiensis* crystal proteins with the midgut epithelial cells of *Spodoptera frugiperda* (Lepidoptera: Noctuidae). J Invertebr Pathol 68, 203–212. https://doi.org/10.1006/jipa.1996.0087

Azidah AA, Sofian-Azirun M. 2006. Life history of *Spodoptera exigua* (Lepidoptera: Noctuidae) on various host plants. Bull Entomol Res 96, 613–618. https://doi.org/10.1017/ber2006461

Azizoglu U. 2019. *Bacillus thuringiensis* as a biofertilizer and biostimulator: a mini-review of the little-known plant growth-promoting properties of Bt. Curr Microbiol 76, 1379–1385. https://doi.org/10.1007/s00284-019-01705-9

Bachler A, Padovan A, Anderson CJ, Wei Y, Wu Y, Pearce S, Downes S, James B, Tessnow A, Sword GA, Williams M, Tek Tay W, Gordon KHJ, Walsh TK. 2024. Identification of a novel resistance gene which provides insight into 4 Vip3Aa mode of action in *Helicoverpa armigera*. bioRxiv 2024.08.11.607516. https://doi.org/10.1101/2024.08.11.607516

Bae B, Ohene-Adjei S, Kocherginskaya S, Mackie RI, Spies MA, Cann IK, Nair SK. 2008. Molecular basis for the selectivity and specificity of ligand recognition by the family 16 carbohydrate-binding modules from *Thermoanaerobacterium polysaccharolyticum* ManA. J Biol Chem 283,12415-12425. https://doi.org/10.1074/jbc.M706513200

Banu AN, Balasubramanian C, Moorthi PV. 2014. Biosynthesis of silver nanoparticles using *Bacillus thuringiensis* against dengue vector, *Aedes aegypti* (Diptera: Culicidae). Parasitol Res 113, 311–316. https://doi.org/10.1007/s00436-013-3656-0

Banyuls N, Hernández-Rodríguez CS, Van Rie J, Ferré J. 2018. Critical amino acids for the insecticidal activity of Vip3Af from *Bacillus thuringiensis*: Inference on structural aspects. Sci Rep 8, 1–14. https://doi.org/10.1038/s41598-018-25346-3

Banyuls N, Quan Y, González-Martínez RM, Hernández-Martínez P, Ferré J. 2021. Effect of substitutions of key residues on the stability and the insecticidal activity of Vip3Af from *Bacillus thuringiensis*. J Invertebr Pathol 11, 107439. https:// doi. org/ 10.1016/j. jip. 2020. 107439

Barkhade UP, Thakare AS. 2010. Protease mediated resistance mechanism to Cry1C and Vip3A in *Spodoptera litura*. Egypt Acad J Biol Sci 3, 43–50. https://doi.org/10.21608/eajbsa.2010.15188

Bel Y, Banyuls N, Chakroun M, Escriche B, Ferré J. 2017. Insights into the structure of the Vip3Aa insecticidal protein by protease digestion analysis. Toxins 9, 131. https://doi.org/10.3390/toxins9040131

Bell RA, Joachim FG. 1976. Techniques for rearing laboratory colonies of tobacco hornworms and pink bollworms. Ann Entomol Soc Am 69, 365–373. https://doi.org/10.1093/aesa/69.2.365

Belousova ME, Malovichko YV, Shikov AE, Nizhnikov AA, Antonets KS. 2021. Dissecting the Environmental Consequences of *Bacillus thuringiensis* Application for Natural Ecosystems. Toxins 13(5), 355. https://doi.org/10.3390/toxins13050355

Ben Hamadou-Charfi D, Boukedi H, Abdelkefi-Mesrati L, Tounsi S, Jaoua S. 2013. *Agrotis segetum* midgut putative receptor of *Bacillus thuringiensis* vegetative insecticidal protein Vip3Aa16 differs from that of Cry1Ac toxin. J Invertebr Pathol 114, 139–143. https://doi.org/10.1016/j.jip.2013.07.003

Bergamasco VB, Mendes DRP, Fernandes OA, Desidério JA, Lemos MVF. 2013. *Bacillus thuringiensis* Cry1Ia10 and Vip3Aa protein interactions and their toxicity in *Spodoptera* spp. (Lepidoptera). J Invertebr Pathol 112, 152–158. https://doi.org/10.1016/j.jip.2012.11.011

Berliner E. 1911. Über die Schlaffsucht der Mehlmottenraupe. Zeitschrift für das gesamte Getreidewesen, 3. Jahrg., p. 63 (original in German).

Berliner E. 1915. Über die Schlaffsucht der Mehlmottenraupe (*Ephestia Kuehniella*, Zell.) und ihren Erreger *Bacillus thuringiensis*, n. sp. Z Angew Entomol 2, 29–56 (original in German). https://doi.org/10.1111/j.1439-0418.1915.tb00334.x

Bernardi O, Bernardi D, Amado D, Sousa RS, Fatoretto J, Medeiros FC, Conville J, Burd T, Omoto C. 2015. Resistance risk assessment of *Spodoptera frugiperda* (Lepidoptera: Noctuidae) and *Diatraea saccharalis* (Lepidoptera: Crambidae) to Vip3Aa20 insecticidal protein expressed in corn. J Econ Entomol 108, 2711–2719. https://doi.org/10.1093/jee/tov219

Bernardi O, Bernardi D, Horikoshi RJ, Okuma DM, Miraldo LL, Fatoretto J, Medeiros FC, Burd T, Omoto C. 2016. Selection and characterization of resistance to the Vip3Aa20 protein from *Bacillus thuringiensis* in *Spodoptera frugiperda*. Pest Manag Sci 72, 1794–1802. https://doi.org/10.1002/ps.4223

Best HL, Williamson LJ, Heath EA, Waller-Evans H, Lloyd-Evans E, Berry C. 2023. The role of glycoconjugates as receptors for insecticidal proteins. FEMS Microbiol Rev 47, fuad026. https://doi.org/10.1093/femsre/fuad026

Best HL, Williamson LJ, Lipka-Lloyd M, Waller-Evans H, Lloyd-Evans E, Rizkallah PJ, Berry C. 2022. The Crystal Structure of *Bacillus thuringiensis* Tpp80Aa1 and Its Interaction with Galactose-Containing Glycolipids. Toxins 14, 863. https://doi.org/10.3390/toxins14120863

Bett B, Gollasch S, Moore A, James W, Armstrong J, Walsh T, Harding R, Higgins TJV. 2017. Transgenic cowpeas (*Vigna unguiculata* L. Walp) expressing *Bacillus thuringiensis* Vip3Ba protein are protected against the Maruca pod borer (*Maruca vitrata*). Plant Cell Tissue Organ Cult 131, 335–345. https://doi.org/10.1007/s11240-017-1287-3

Betz FS, Hammond BG, Fuchs RL. 2000. Safety and advantages of *Bacillus thuringiensis*-protected plants to control insect pests. Regul Toxicol Pharmacol 32, 156–173. https://doi.org/10.1006/rtph.2000.1426

Bhalla R, Dalal M, Panguluri SK, Jagadish B, Mandaokar AD, Singh AK, Kumar PA. 2005. Isolation, characterization and expression of a novel vegetative insecticidal protein gene of *Bacillus thuringiensis*. FEMS Microbiol Lett 243, 467–472. https://doi.org/10.1016/j.femsle.2005.01.011

Bieberich E. 2018. Sphingolipids and lipid rafts: Novel concepts and methods of analysis. Chem Phys Lipids 216, 114–131. https://doi.org/10.1016/j.chemphyslip.2018.08.003

Black SD, Mould DR. 1991. Development of hydrophobicity parameters to analyse proteins which bear post-or cotranslational modifications. Anal Biochem 193, 72–82. https://doi.org/10.1016/0003-2697(91)90045-u

Boonyos P, Trakulnaleamsai C, Rungrod A, Chongthammakun S, Promdonkoy B. 2021. Antagonistic effect of truncated fragments of *Bacillus thuringiensis* Vip3Aa on the larvicidal activity of its full-length protein. Protein Pept Lett 28, 131–139. https://doi.org/10.2174/0929866527666200625205846

Borastom AB, Bolam DN, Gilbert HJ, Davies GJ. 2004. Carbohydrate binding modules: fine-tuning polysaccharide recognition. Biochem J 382, 769–781. https://doi.org/10.1042/BJ20040892

Boumann HA, Gubbens J, Koorengevel MC, Oh CS, Martin CE, Heck AJ, Patton-Vogt J, Henry SA, de Kruijff B, de Kroon AI. 2006. Depletion of phosphatidylcholine in yeast induces shortening and increased saturation of the lipid acyl chains: evidence for regulation of intrinsic membrane curvature in a eukaryote. Mol Biol Cell 17, 1006–1017. https://doi.org/10.1091/mbc.e05-04-0344

Bradford MM. 1976. A rapid and sensitive method for the quantitation of microgram quantities of protein utilizing the principle of protein-dye binding. Anal Biochem J 72, 248–254. https://doi.org/10.1016/0003-2697(76)90527-3

Bravo A, Gill SS, Soberón M. 2007. Mode of action of *Bacillus thuringiensis* Cry and Cyt toxins and their potential for insect control. Toxicon 49, 423–435. https://doi.org/10.1016/j.toxicon.2006.11.022

Bravo A, Gómez I, Conde J, Muñoz-Garay C, Sánchez J, Miranda R, Zhuang M, Gill SS, Soberón M. 2004. Oligomerization triggers binding of a *Bacillus thuringiensis* Cry1Ab pore-forming toxin to aminopeptidase N receptor leading to insertion into membrane microdomains. Biochim Biophys Acta 1667, 38–46. https://doi.org/10.1016/j.bbamem.2004.08.013

Bravo A, Jansens S, Peferoen M. 1992. Immunocytochemical localization of *Bacillus thuringiensis* insecticidal crystal proteins in intoxicated insects. J Invertebr Pathol 60, 237–246. https://doi.org/10.1016/0022-2011(92)90004-N

Bravo A, Pacheco S, Gómez I, Soberón M. 2023. Mode of action of *Bacillus thuringiensis* cry pesticidal proteins. Adv Insect Physiol 65,55–92. https://doi.org/10.1016/bs.aiip.2023.09.003

Broadwell AH, Baumann P. 1987. Proteolysis in the gut of mosquito larvae results in further activation of the *Bacillus sphaericus* toxin. Appl Envion Microbiol 53, 1333–1337. https://doi.org/10.1128/aem.53.6.1333-1337.1987

Brown DA, London E. 1998. Functions of lipid rafts in biological membranes. Annu Rev Cell Dev Biol 14, 111–36. https://doi.org/10.1146/annurev.cellbio.14.1.111

Burton SL, Ellar DJ, Li J, Derbyshire DJ. 1999. N-acetylgalactosamine on the putative insect receptor aminopeptidase N is recognised by a site on the domain III lectin-like fold of a *Bacillus thuringiensis* insecticidal toxin. J Mol Biol 287, 1011–1022. https://doi.org/10.1006/jmbi.1999.2649

Byrne MJ, Iadanza MG, Perez MA, Maskell DP, George RM, Hesketh EL, Beales PA, Zack MD, Berry C, Thompson RF. 2021. Cryo-EM structures of an insecticidal Bt toxin reveal its mechanism of action on the membrane. Nat Commun 12, 2791. https://doi.org/10.1038/s41467-021-23146-4

Caccia S, Chakroun M, Vinokurov K, Ferré J. 2014. Proteolytic processing of *Bacillus thuringiensis* Vip3A proteins by two *Spodoptera* species. J Insect Physiol 67, 76–84. https://doi.org/10.1016/j.jinsphys.2014.06.008

Cady SD, Schmidt-Rohr K, Wang J, Soto CS, Degrado WF, Hong M. 2010. Structure of the amantadine binding site of influenza M2 proton channels in lipid bilayers. Nature 463, 689–692. https://doi.org/10.1038/nature08722

Campelo F, McMahon HT, Kozlov MM. 2008. The hydrophobic insertion mechanism of membrane curvature generation by proteins. Biophys J 95, 2325–2339. https://doi.org/10.1529/biophysj.108.133173

Cancino-Rodezno A, Porta H, Soberón M, Bravo A. 2009. Defense and death responses to pore forming toxins. Biotechnol Genet Eng Rev 26, 65–82. https://doi.org/10.5661/bger-26-65

Carmona D, Rodríguez-Almazán C, Muñoz-Garay C, Portugal L, Pérez C, de Maagd RA, Bakker P, Soberón M, Bravo A. 2011. Dominant negative phenotype of *Bacillus thuringiensis* Cry1Ab, Cry11Aa and Cry4Ba mutants suggest heterooligomer formation among different Cry toxins. PLoS ONE 6, e19952. https://doi.org/10.1371/journal.pone.0019952

Carrière Y, Crickmore N and Tabashnik BE. 2015. Optimizing pyramided transgenic Bt-crops for sustainable pest management. Nat Biotechnol 33:161–168. https://doi.org/10.1038/nbt.3099

Chakroun M, Banyuls N, Bel Y, Escriche B, Ferré J. 2016a. Bacterial vegetative insecticidal proteins (Vip) from entomopathogenic bacteria. Microbiol Mol Biol Rev 80, 329–350. https://doi.org/10.1128/MMBR.00060-15

Chakroun M, Banyuls N, Walsh T, Downes S, James B, Ferré J. 2016b. Characterization of the resistance to Vip3Aa in *Helicoverpa armigera* from Australia and the role of midgut processing and receptor binding. Sci Rep 6, 24311. https://doi.org/10.1038/srep24311

Chakroun M, Bel Y, Caccia S, Abdelkefi-Mesrati L, Escriche B, Ferré J. 2012. Susceptibility of *Spodoptera frugiperda* and *S. exigua* to *Bacillus thuringiensis* Vip3Aa insecticidal protein. J Invertebr Pathol 110, 334–339. https://doi.org/10.1016/j.jip.2012.03.021

Chakroun M, Ferré J. 2014. *In vivo* and *in vitro* binding of Vip3Aa to *Spodoptera frugiperda* midgut and characterization of binding sites by ^{125}I radiolabelling. Appl Environ Microbiol 80, 6258–6265. https://doi.org/10.1128/AEM.01521-14

Chen JW, Tang LX, Song SY, Yuan MJ, Pang Y. 2003. Comparison of the expression of *Bacillus thuringiensis* full-length and N-terminally truncated vip3A gene in *Escherichia coli.* J Appl Microbiol 95, 310–316. https://doi.org/10.1046/j.1365-2672.2003.01977.x

Chen D, Moar WJ, Jerga A, Gowda A, Milligan JS, Bretsynder EC, Rydel TJ, Baum JA, Semeao A, Fu X, Guzov V, Gabbert K, Head GP, Haas JA. 2021. *Bacillus thuringiensis* chimeric proteins Cry1A.2 and Cry1B.2 to control soybean lepidopteran pests: new domain combinations enhance insecticidal spectrum of activity and novel receptor contributions. PLoS ONE 16, e0249150. https://doi.org/10.1371/journal.pone.0249150

Chi B, Li H, Zhang J, Wei P, Gao J, Liu R. 2019. In silico structure-based identification and validation of key residues of Vip3Aa involving in Lepidopteran brush border receptor binding. Appl Biochem Biotechnol 187, 1448–1459. https://doi.org/10.1007/s12010-018-02929-4

Crick FHC. 1952. Is α-keratin a coiled coil? Nature 170, 882–883. https://doi.org/10.1038/170882b0

Crick FHC.1953. The packing of α-helices: simple coiled-coils. Acta Crystallogr 6, 689–697.https://doi.org/10.1107/S0365110X53001964

Crickmore N, Berry C, Panneerselvam S, Mishra R, Connor TR, Bonning BC. 2021. A structure-based nomenclature for *Bacillus thuringiensis* and other bacteria-derived pesticidal proteins. J Invertebr Pathol 107438. https://doi.org/10.1016/j.jip.2020.107438

Crickmore N, Berry C, Panneerselvam S, Mishra R, Connor TR, Bonning BC. 2024. Bacterial Pesticidal Protein Resource Center. https://www.bpprc.org [Accessed 20.11.2024].

Crickmore N, Zeigler DR, Feitelson J, Schnepf E, Van Rie J, Lereclus D, Baum J, Dean DH. 1998. Revision of the nomenclature for the *Bacillus thuringiensis* pesticidal crystal proteins. Microbiol Mol Biol Rev 6, 807–813. https://doi.org/10.1128/MMBR.62.3.807-813.1998

Dal Peraro M, van der Goot FG. 2016 Pore-forming toxins: ancient, but never really out of fashion. Nat Rev Microbiol 14,77-92. https://doi.org/10.1038/nrmicro.2015.3

de Kroon AI. 2007. Metabolism of phosphatidylcholine and its implications for lipid acyl chain composition in *Saccharomyces cerevisiae*. Biochim Biophys Acta 1771, 343–352. https://doi.org/10.1016/j.bbalip.2006.07.010

de la Rosa-Trevín JM, Quintana A, Del Cano L, Zaldívar A, Foche I, Gutiérrez J, Gómez-Blanco J, Burguet-Castell J, Cuenca-Alba J, Abrishami V, Vargas J, Otón J, Sharov G, Vilas JL, Navas J, Conesa P, Kazemi M, Marabini R, Sorzano CO, Carazo JM. 2016. Scipion: a software framework toward integration, reproducibility and validation in 3D electron microscopy. J Struct Biol 195, 93–99. https://doi.org/10.1016/j.jsb.2016.04.010

de Maagd RA, Bravo A, Crickmore N. 2001. How *Bacillus thuringiensis* has evolved specific toxins to colonize the insect world. Trends Genet 17, 193–199. https://doi.org/10.1016/S0168-9525(01)02237-5

Deans JP, Li H, Polyak MJ. 2002. CD20-mediated apoptosis: signalling through lipid rafts. Immunology 107,176-182. https://doi.org/10.1046/j.1365-2567.2002.01495.x

Denolf P, Jansens S, Peferoen M, Degheele D, Van Rie J. 1993. Two different *Bacillus thuringiensis* delta-endotoxin receptors in the midgut brush border membrane of the European corn borer, *Ostrinia nubilalis* (Hubner) (Lepidoptera: Pyralidae). Appl Environ Microbiol 59, 1828–1837. https://doi.org/10.1128/aem.59.6.1828-1837.1993

Derbyshire DJ, Ellar DJ, Li J. 2001. Crystallization of the *Bacillus thuringiensis* toxin Cry1Ac and its complex with the receptor ligand N-acetyl-D-galactosamine. Acta Cryst D Biol Cryst 57, 1938–1944. https://doi.org/10.1107/s090744490101040x

Deshayes C, Siegwart M, Pauron D, Froger JA, Lapied B, Apaire-Marchais V. 2017. Microbial pest control agents: are they a specific and safe tool for insect pest management? Curr Med Chem 24(27), 2959–2973. https://doi.org/10.2174/0929867324666170314144311

Diep DB, Nelson KL, Raja SM, Pleshak EN, Buckley JT. 1998. Glycosylphosphatidylinositol anchors of membrane glycoproteins are binding determinants for the channel-forming toxin aerolysin. J Biol Chem 273, 2355–2360. https://doi.org/10.1074/jbc.273.4.2355

Doss VA, Kumar KA, Jayakumar R, Sekar V. 2002. Cloning and expression of the vegetative insecticidal protein (*vip3V*) gene of *Bacillus thuringiensis* in *Escherichia coli*. Protein Expr Purif 26, 82–88. https://doi.org/10.1016/s1046-5928(02)00515-6

Downes S, Mahon R. 2012. Evolution, ecology and management of resistance in *Helicoverpa* spp. to Bt cotton in Australia. J Invertebr Pathol 110,281–2864. https://doi.org/10.1016/j.jip.2012.04.005

Drin G, Antonny B. 2010. Amphipathic helices and membrane curvature. FEBS Lett 584, 1840–1847. https://doi.org/10.1016/j.febslet.2009.10.022

Dubois T, Faegri K, Perchat S, Lemy C, Buisson C, Nielsen- LeRoux C, Gohar M, Ramarao N, Kolsto A, Lereclus D. 2012. Necrotrophism is a quorum-sensing-regulated lifestyle in *Bacillus thuringiensis*. PloS Pathog 4, e1002629. https://doi.org/10.1371/journal.ppat.1002629

EFSA PLH Panel (EFSA Panel on Plant Health), 2015. Scientific Opinion on the pest categorisation of *Spodoptera littoralis*. EFSA J 13, 26. https://doi.org/10.2903/j.efsa.2015.3987

Erlandson MA, Toprak U, Hegedus DD. 2019. Role of the peritrophic matrix in insect-pathogen interactions. J Insect Physiol 117, 103894. https://doi.org/10.1016/j.jinsphys.2019.103894

Estruch JJ, Carozzi NB, Desai N, Duck NB, Warren GW, Koziel MG. 1997. Transgenic plants: An emerging approach to pest control. Nat Biotechnol 15, 137–141. https://doi.org/10.1038/nbt0297-137

Estruch JJ, Yu CG. 2001. Plant pest control. US Patent 6,291,156 B1.

Estruch JJ, Warren GW, Mullins MA, Nye GJ, Craig JA, Koziel MG. 1996. Vip3A, a novel *Bacillus thuringiensis* vegetative insecticidal protein with a wide spectrum of activities against lepidopteran insects. Proc Natl Acad Sci USA 93, 5389–5394. https://doi.org/10.1073/pnas.93.11.5389

Fang J, Xu X, Wang P, Zhao JZ, Shelton AM, Cheng J, Feng MG, Shen Z. 2007. Characterization of chimeric *Bacillus thuringiensis* Vip3 toxins. Appl Environ Microbiol 73, 956–996. https://doi.org/10.1128/AEM.02079-06

FAO (FAOSTAT, Statistics Division of the Food and Agriculture Organization of the United Nations) https://www.fao.org/faostat/es/#home [Accessed 29.12.2024].

Feng D, Chen Z, Wang Z, Zhang C, He K, Guo S. 2015. Domain III of *Bacillus thuringiensis* Cry1Ie Toxin Plays an Important Role in Binding to Peritrophic Membrane of Asian Corn Borer. PLoS One 10, e0136430. https://doi.org/10.1371/journal.pone.0136430

Ferré J, Bel Y, Lázaro-Berenguer M, Hernández-Martínez P. 2023. Vip3 insecticidal proteins: structure and mode of action. Adv Insect Phys 65, 93–122. https://doi.org/10.1016/bs.aiip.2023.09.006

Fitzgerald TD, Costa JT. 1999. Collective behavior in social caterpillars. In Information Processing in Social Insects, 1st ed.; Detrain C, Deneubourg JI, Pasteels JM, Eds. Springer Basel AG: Basel, Switzerland pp. 379–400.

Fu T, Burbage C, Tagge E, Chandler J, Willingham M, Frankel A. 1996. Double-lectin site ricin B chain mutants expressed in insect cells have residual galactose binding: evidence for more than two lectin sites on the ricin toxin B chain. Bioconjug Chem 1996 7,651–658. https://doi.org/10.1021/bc960056b

Galindo CL, Fadl AA, Sha J, Gutierrez C, Popov VL, Boldogh I, Aggarwal BB, Chopra AK. 2004. *Aeromonas hydrophila* cytotoxic enterotoxin activates mitogen-activated protein kinases and induces apoptosis in murine macrophages and human intestinal epithelial cells. J Biol Chem 279, 37597–37612. https://doi.org/10.1074/jbc.M404641200

Gassmann AJ, Reisig DD. 2023. Management of Insect Pests with Bt-crops in the United States. Ann Rev Entomol 68, 31–49. https://doi.org/10.1146/annurev-ento-120220-105502

Gayen S, Hossain MA, Sen SK. 2012. Identification of the bioactive core component of the insecticidal Vip3A toxin peptide of *Bacillus thuringiensis*. J Plant Biochem Biotechnol 21, 128–135. https://doi.org/10.1007/s13562-012-0148-8

Gayen S, Samanta MK, Hossain MA, Mandal CC, Sen SK. 2015. A deletion mutant ndv200 of the *Bacillus thuringiensis* vip3BR insecticidal toxin gene is a prospective candidate for the next generation of genetically modified crop plants resistant to lepidopteran insect damage. Planta 242, 269–281. https://doi.org/10.1007/s00425-015-2309-1

Geny B, Popoff MR. 2006. Bacterial protein toxins and lipids: pore formation or toxin entry into cells. Biol Cell 2006; 98 :667–78. https://doi.org/10.1042/BC20050082

George KS, Wu S. 2012. Lipid raft: A floating island of death or survival. Toxicol Appl Pharmacol 259, 311–319. https://doi.org/10.1016/j.taap.2012.01.007

Ghosh S. 2018. Sialylation and sialyltransferase in insects. Glycoconj J 35, 433–441. https://doi.org/10.1007/s10719-018-9835-6

Gomis-Cebolla J, Ruiz de Escudero I, Vera-Velasco NM, Hernández-Martínez P, Hernández-Rodríguez CS, Ceballos T, Palma L, Escriche B, Caballero P, Ferré J. 2017. Insecticidal spectrum and mode of action of the *Bacillus thuringiensis* Vip3Ca insecticidal protein. J Invertebr Pathol 142, 60–67. https://doi.org/10.1016/j.jip.2016.10.001

Gomis-Cebolla J, Wang Y, Quan Y, He K, Walsh T, James B, Downes S, Kain W, Wang P, Leonard K, Morgan T, Oppert B, Ferré J. 2018. Analysis of cross-resistance to Vip3 proteins in eight insect colonies, from four insect species, selected for resistance to *Bacillus thuringiensis* insecticidal proteins. J Invertebr Pathol 155, 64–70. https://doi.org/10.1016/j.jip.2018.05.004

Gouffon CV, van Vliet A, Van Rie J, Jansens S, Jurat-Fuentes J.L. 2011. Binding sites for *Bacillus thuringiensis* Cry2Ae toxin on heliothine brush border membrane vesicles are not shared with Cry1A, Cry1F, or Vip3A toxin. Appl Environ Microbiol 77, 3182–3188. https://doi.org/10.1128/AEM.02791-10

Griffitts JS, Huffman DL, Whitacre JL, Barrows BD, Marroquin LD, Müller R, Brown JR, Hennet T, Esko JD, Aroian RV. 2003. Resistance to a bacterial toxin is mediated by removal of a conserved glycosylation pathway required for toxin–host interactions. J Biol Chem 278,45594–45602. https://doi.org/10.1074/jbc.M308142200

Griffitts JS, Haslam SM, Yang T, Garczynski SF, Mulloy B, Morris H, Cremer PS, Dell A, Adang MJ, Aroian RV. 2005. Glycolipids as receptors for *Bacillus thuringiensis* crystal toxin. Science 307, 922–925. https://doi.org/10.1126/science.1104444

Gupta M, Kumar H, Kaur S. 2021. Vegetative insecticidal protein (Vip): A potential contender from *Bacillus thuringiensis* for efficient management of various detrimental agricultural pests. Front Microbiol 12, 659736. https://doi.org/10.3389/fmicb.2021.659736

Hallgren J, Tsirigos KD, Pedersen MD, Almagro-Armenteros JJ, Marcatili P, Nielsen H, Krogh A, Winther O. 2022. DeepTMHMM predicts alpha and beta transmembrane proteins using deep neural networks. bioRxiv2022.04.08.487609. https://doi.org/10.1101/2022.04.08.487609

Hannun YA, Obeid LM. 2008. Principles of bioactive lipid signalling: lessons from sphingolipids. *Nature Rev Mol Cell Biol* 9, 139–150. https://doi.org/10.1038/nrm2329

Hamadou-Charfi DB, Boukedi H, Abdelkefi-Mesrati L, Tounsi S, Jaoua S. 2013. *Agrotis segetum* midgut putative receptor of *Bacillus thuringiensis* vegetative insecticidal protein Vip3Aa16 differs from that of Cry1Ac toxin. J Invertebr Pathol 114, 139–143. https://doi.org/10.1016/j.jip.2013.07.003

Hayakawa T, Shitomi Y, Miyamoto K, Hori H. 2004. GalNAc pretreatment inhibits trapping of *Bacillus thuringiensis* Cry1Ac on the peritrophic membrane of *Bombyx mori*. 576, 331–335. https://doi.org/10.1016/j.febslet.2004.09.029

Hartmann MD. 2017. Functional and structural roles of coiled-coils. Subcell Biochem 82, 63–93. https://doi.org/10.1007/978-3-319-49674-0_3

Hartmann MD, Ridderbusch O, Zeth K, Albrecht R, Testa O, Woolfson DN, Sauer G, Dunin-Horkawicz S, Lupas AN, Alvarez BH. 2009. A coiled-coil motif that sequesters ions to the hydrophobic core. Proc Natl Acad Sci USA 106, 16950–16955. https://doi.org/10.1073/pnas.0907256106

Heckel DG. 2020. How do toxins from *Bacillus thuringiensis* kill insects? An evolutionary perspective. Arch Insect Biochem Physiol 104, e21673. https://doi.org/10.1002/arch.21673

Hernández-Martínez P, Gomis-Cebolla J, Ferré J, Escriche B. 2017. Changes in gene expression and apoptotic response in *Spodoptera exigua* larvae exposed to sublethal concentrations of Vip3 insecticidal proteins. Sci Rep 7, 16245. https://doi.org/10.1038/s41598-017-16406-1

Hernández-Martínez P, Hernández-Rodríguez CS, Van Rie J, Escriche B, Ferré J. 2013. Insecticidal activity of Vip3Aa, Vip3Ad, Vip3Ae, and Vip3Af from *Bacillus thuringiensis* against lepidopteran corn pests. J Invertebr Pathol 113, 78–81. https://doi.org/10.1016/j.jip.2013.02.001

Hernández-Martínez P, Bretsnyder EC, Baum JA, Haas JA, Head GP, Jerga A, Ferré J. 2022. Comparison of *in vitro* and *in vivo* binding sites competition of *Bacillus thuringiensis* Cry1 proteins in two important maize pests. Pest Manag Sci 78, 1457–1466. https://doi.org/10.1002/ps.6763

Hildebrand PW, Preissner R, Frömmel C. 2004. Structural features of transmembrane helices. FEBS Lett 559, 145–151. https://doi.org/10.1016/S0014-5793(04)00061-4

Höfte H, Whiteley HR. 1989. Insecticidal crystal proteins of *Bacillus thuringiensis*. Microbiol Rev 53, 242–255. https://doi.org/10.1128/mr.53.2.242-255.1989

Holm L, Sander C. 1995. Dali: a network tool for protein structure comparison. Trends Biochem Sci 20, 478–480. https://doi.org/10.1016/s0968-0004(00)89105-7

Hong M, DeGrado WF. 2012. Structural basis for proton conduction and inhibition by the influenza M2 protein. Protein Sci 21, 1620–1633. https://doi.org/10.1002/pro.2158

Hou X, Han L, An B, Zhang Y, Cao Z, Zhan Y, Cai X, Yan B, Cai J. 2020. Mitochondria and lysosomes participate in Vip3Aa-induced *Spodoptera frugiperda* Sf9 cell apoptosis. Toxins 12, 116. https://doi.org/10.3390/toxins12020116

Hou X, Li M, Mao C, Jiang L, Zhang W, Li M, Geng X, Li X, Liu S, Yang G, Zhou J, Fang Y, Cai J. 2024. Domain III β4-β5 loop and β14-β15 loop of *Bacillus thuringiensis* Vip3Aa are involved in receptor binding and toxicity. Toxins 16, 23. https://doi.org/10.3390/toxins16010023

Hosny MM, Topper CP, Moawad GM, El-Saadany GB. 1986. Economic damage thresholds of *Spodoptera littoralis* (Boisd.) (Lepidoptera: Noctuidae) on cotton in Egypt. Crop Prot 5,100–104. https://doi.org/10.1016/0261-2194(86)90088-8

Huang F, Qureshi JA, Meagher RL Jr, Reisig DD, Head GP, Andow DA, Ni X, Kerns D, Buntin GD, Niu Y, Yang F, Dangal V. 2014. Cry1F resistance in fall armyworm *Spodoptera frugiperda*: single gene versus pyramided Bt maize. PLoS One 9, e112958. https://doi.org/10.1371/journal.pone.0112958

Infante O, Gómez I, Pélaez-Aguilar AE, Verduzco-Rosas LA, García-Suárez R, García-Gómez BI, Wang Z, Zhang J, Guerrero A, Bravo A, Soberón M. 2024. Insights into the structural changes that trigger receptor binding upon proteolytic activation of *Bacillus thuringiensis* Vip3Aa insecticidal protein. PLoS Pathog 20, e1012765. https://doi.org/10.1371/journal.ppat.1012765

ISAAA. ISAAA GM Approval Database. http://www.isaaa.org/gmapprovaldatabase/ [Accessed 27.12.2024].

Ishiwata S. 1901. On a kind of severe flacherie (sotto disease) (No. 1). Dainihon Sanshi Kaiho. 114, 1–5 (original in Japanese).

Ishiwata S. 1905. About “sotokin”, a Bacillus of a disease of the silk- worm, Dainihon Sanshi Kaiho. 160, 1–8 (original in Japanese).

Jackson RE, Marcus MA, Gould F, Bradley JR Jr, van Duyn JW. 2007. Crossresistance responses of Cry1Ac-selected *Heliothis virescens* (Lepidoptera: Noctuidae) to the *Bacillus thuringiensis* protein Vip3A. J Econ Entomol 100, 180–186. https://doi.org/10.1093/jee/100.1.180

Jakka SR, Ferré J, Jurat-Fuentes JL. 2015. Cry toxin binding sites and their use in strategies to delay resistance evolution. In: Soberón, M., Gao, Y., Bravo, A. (Eds.), Bt Resistance: Characterization and strategies for GM crops producing *Bacillus thuringiensis* toxins. CABI Int, Boston, pp. 138–149.

James C. 2015. Global Status of Commercialized Biotech/GM Crops: 2015. ISAAA Brief No. 51. ISAAA, Ithaca, NY.

James C. 2017. Global status of commercialization of biotech/GM crops in 2017: Biotech crop adoption surges as economic benefits accumulate in 22 years. ISAAA Brief No. 53. ISAAA, Ithaca, NY.

Jenkins JL, Lee MK, Valaitis AP, Curtiss A, Dean DH. 2000. Bivalent sequential binding model of a *Bacillus thuringiensis* toxin to gypsy moth aminopeptidase N receptor. J Biol Chem 275, 14423–14431. https://doi.org/10.1074/jbc.275.19.14423

Jerga A, Evdokimov AG, Moshiri F, Haas JA, Chen M, Clinton W, Fu X, Halls C, Jimenez-Juarez N, Kretzler CN, Panosian TD, Pleau M, Roberts JK, Rydel TJ, Salvador S, Sequeira R, Wang Y, Zheng M, Baum JA. 2019. Disabled insecticidal proteins: A novel tool to understand differences in insect receptor utilization. Insect Biochem Mol Biol 105, 79–88. https://doi.org/10.1016/j.ibmb.2018.12.006

Jiang K, Chen Z, Shi Y, Zang Y, Shang C, Huang X, Zang J, Bai Z, Jiao X, Cai J, Gao X. 2023a. A strategy to enhance the insecticidal potency of Vip3Aa by introducing additional cleavage sites to increase its proteolytic activation efficiency. Eng Microbiol 3, 100083. https://doi.org/10.1016/j.engmic.2023.100083

Jiang K, Chen Z, Zang Y, Shi Y, Shang C, Jiao X, Cai J, Gao X. 2023b. Functional characterization of Vip3Aa from *Bacillus thuringiensis* reveals the contributions of specific domains to its insecticidal activity. J Biol Chem 299, 103000. https://doi.org/10.1016/j.jbc.2023.103000

Jiang K, Hou X, Han L, Tan T, Cao Z, Cai J. 2018a. Fibroblast growth factor receptor, a novel receptor for vegetative insecticidal protein Vip3Aa. Toxins 10, 546. https://doi.org/10.3390/toxins10120546

Jiang K, Hou XY, Tan TT, Cao ZL, Mei SQ, Yan B, Chang J, Han L, Zhao D, Cai J. 2018b. Scavenger receptor-C acts as a receptor for *Bacillus thuringiensis* vegetative insecticidal protein Vip3Aa and mediates the internalization of Vip3Aa via endocytosis. PLoS Pathog 14, e1007347. https://doi.org/10.1371/journal.ppat.1007347

Jiang K, Mei SQ, Wang TT, Pan JH, Chen YH, Cai J. 2016. Vip3Aa induces apoptosis in cultured *Spodoptera frugiperda* (Sf9) cells. Toxicon 120, 49–56. https://doi.org/10.1016/j.toxicon.2016.07.019

Jiang K, Zhang Y, Chen Z, Wu D, Cai J, Gao X. 2020a. Structural and functional insights into the C-terminal fragment of insecticidal Vip3A toxin of *Bacillus thuringiensis*. Toxins 12, 438. https://doi.org/10.3390/toxins12070438

Jiang K, Zhang Y, Chen Z, Wu D, Cai J, Gao X. 2020b. Structural insights into the insecticidal Vip3A toxin of Bacillus thuringiensis. bioRxiv 2020.01.24.918433. https://doi.org/10.1101/2020.01.24.918433 Now published in Toxins doi: 10.3390/toxins12070438

Jiménez-Juárez, Muñoz-Garay C, Gómez I, Saab-Rincon G, Damian-Almazo JY, Gill SS, Soberón M, Bravo A. 2007. *Bacillus thuringiensis* Cry1Ab mutants affecting oligomer formation are non-toxic to *Manduca sexta* larvae. J Biol Chem 282, 21222–21229. https://doi.org/10.1074/jbc.M701314200

Jin M, Shan Y, Peng Y, Wang W, Zhang H, Liu K, Heckel DG, Wu K, Tabashnik BE, Xiao Y. 2023. Downregulation of a transcription factor associated with resistance to Bt toxin Vip3Aa in the invasive fall armyworm. Proc Natl Acad Sci USA, 120(44), e2306932120. https://doi.org/10.1073/pnas.2306932120

Joh NH, Wang T, Bhate MP, Acharya R, Wu Y, Grabe M, Hong M, Grigoryan G, DeGrado WF. 2014.De novo design of a transmembrane Zn^{2+}-transporting four helix bundle. Science 346, 1520–1524. https://doi.org/10.1126/science.1261172

Jouzani GS, Valijanian E, Sharafi R. 2017. *Bacillus thuringiensis*: a successful insecticide with new environmental features and tidings. Appl Microbiol Biotechnol 101, 2691–2711. https://doi.org/10.1007/s00253-017-8175-y

Jurat-Fuentes JL, Heckel DG, Ferré J. 2021. Mechanisms of resistance to insecticidal proteins from *Bacillus thuringiensis*. Annu Rev Entomol 66, 121–140. https://doi.org/10.1146/annurev-ento-052620-073348

Kabbani AM, Raghunathan K, Lencer WI, Kenworthy AK, Kelly CV. 2020. Structured clustering of the glycosphingolipid GM1 is required for membrane curvature induced by cholera toxin. Proc Natl Acad Sci USA 117, 14978–14986. https://doi.org/10.1073/pnas.2001119117 2020

Kahn TW, Chakroun M, Williams J, Walsh T, James B, Monserrate J, Ferré J. 2018. Efficacy and resistance management potential of a modified Vip3C protein for control of *Spodoptera frugiperda* in maize. Sci Rep 8, 16204. https:// doi. org/ 10. 1038/ s41598- 018- 34214-z

Kergoat GJ, Goldstein PZ, Le Ru B, Meagher RL Jr, Zilli A, Mitchell A, Clamens AL, Gimenez S, Barbut J, Nègre N, d'Alençon E, Nam K. 2021. A novel reference dated phylogeny for the genus *Spodoptera* Guenée (Lepidoptera: Noctuidae: Noctuinae): new insights into the evolution of a pest-rich genus. Mol Phylogenet Evol 161,107–161. https://doi.org/10.1016/j.ympev.2021.107161

Kerns DD, Yang F, Kerns DL, Stewart SD, Jurat-Fuentes JL. 2023. Reduced toxin binding associated with resistance to Vip3Aa in the corn earworm (*Helicoverpa zea*). Appl Environ Microbiol 89, e0164423. https://doi.org/10.1128/aem.01644-23

Kinoshita T. 2016. Glycosylphosphatidylinositol (GPI) Anchors: Biochemistry and Cell Biology: Introduction to a Thematic Review Series. J Lipid Res 57, 4–5. https://doi.org/10.1194/jlr.E065417

Koller J, Sutter L, Gonthier J, Collatz J, Norgrove L. 2023. Entomopathogens and parasitoids allied in biocontrol: A systematic review. Pathogens 12, 957. https://doi.org/10.3390/pathogens12070957

Kumar P, Kamle M, Borah R, Mahato DK, Sharma B. 2021. *Bacillus thuringiensis* as microbial biopesticide: uses and application for sustainable agriculture. Egypt J Biol Pest Control 31, 95. https://doi.org/10.1186/s41938-021-00440-3

Kunthic T, Watanabe H, Kawano R, Tanaka Y, Promdonkoy B, Yao M, Boonserm P. 2017. pH regulates pore formation of a protease activated Vip3Aa from *Bacillus thuringiensis*. Biochim Biophys Acta Biomembr 1859, 2234–2241. https://doi.org/10.1016/j.bbamem.2017.08.018

Kranz J, Schmutterer H, Koch W. 1978. Diseases, pests, and weeds in tropical crops. Soil Sci 125, 272.

Lacey LA, Grzywacz D, Shapiro-Ilan DI, Frutos R, Brownbridge M, Goettel MS. 2015. Insect pathogens as biological control agents: Back to the future. J Invertebr Pathol 132, 1–41. https://doi.org/10.1016/j.jip.2015.07.009

Lázaro-Berenguer M, Ferré J, Hernández-Martínez P. 2024. Receptor interactions of protoxin and activated Vip3Aa structural conformations in *Spodoptera exigua*. Pest Manag Sci 80, 6142–6149. https://doi.org/10.1002/ps.8341

Lázaro-Berenguer M, Paredes-Martínez F, Bel Y, Núñez-Ramírez R, Arias-Palomo E, Casino P, Ferré J. 2022a. Structural and functional role of Domain I for the insecticidal activity of the Vip3Aa protein from *Bacillus thuringiensis*. Microb Biotechnol 15, 2607–2618. https://doi.org/10.1111/1751-7915.14110

Lázaro-Berenguer M, Quan Y, Hernández-Martínez P, Ferré J. 2022b. *In vivo* competition assays between Vip3 proteins confirm the occurrence of shared binding sites in *Spodoptera littoralis*. Sci Rep 12, 4578. https://doi.org/10.1038/s41598-022-08633-y

Lee MK, Miles P, Chen JS. 2006. Brush border membrane binding properties of *Bacillus thuringiensis* Vip3A toxin to *Heliothis virescens* and *Helicoverpa zea* midguts. Biochem Biophys Res Commun. 339, 1043–1047. https://doi.org/10.1016/j.bbrc.2005.11.112

Lee MK, Walters FS, Hart H, Palekar N, Chen JS. 2003. The mode of action of the *Bacillus thuringiensis* vegetative insecticidal protein Vip3A differs from that of Cry1Ab δ-endotoxin. Appl Environ Microbiol 69, 4648–4657. https://doi.org/10.1128/AEM.69.8.4648-4657.2003

Li JD, Carroll J, Ellar DJ. 1991. Crystal structure of insecticidal deltaendotoxin from *Bacillus thuringiensis* at 2.5 Å resolution. Nature 353,815–821. https://doi.org/10.1038/353815a0

Li C, Xu N, Huang X, Wang W, Cheng J, Wu K, Shen Z. 2007. *Bacillus thuringiensis* Vip3 mutant proteins: Insecticidal activity and trypsin sensitivity. Biocontrol Sci Tech, 17, 699–708. https://doi.org/10.1080/09583150701527177

Lin S, Oyediran I, Niu Y, Brown S, Cook D, Ni X, Zhang Y, Reay-Jones FPF, Chen JS, Wen Z, Dimase M, Huang F. 2022. Resistance allele frequency to Cry1Ab and Vip3Aa20 in *Helicoverpa zea* (Boddie) (Lepidoptera: Noctuidae) in Louisiana and three other southeastern US states. Toxins 14, 270. https://doi.org/10.3390/toxins14040270

Liu Z, Liao C, Zou L, Jin M, Shan Y, Quan Y, Yao H, Zhang L, Wang P, Liu Z, Wang N, Li A, Liu K, Tabashnik BE, Heckel DG, Wu K, Xiao Y. 2024. Retrotransposon-mediated disruption of a chitin synthase gene confers insect resistance to *Bacillus thuringiensis* Vip3Aa toxin. PLoS Biol 22, e3002704. https://doi.org/10.1371/journal.pbio.3002704

Liu JG, Yang AZ, Shen XH, Hua BG, Shi GL. 2011. Specific binding of activated Vip3Aa10 to *Helicoverpa armigera* brush border membrane vesicles results in pore formation. J Invertebr Pathol 108, 92–97. https://doi.org/10.1016/j.jip.2011.07.007

Mahon RJ, Downes SJ, James B. 2012. Vip3A resistance alleles exist at high levels in Australian targets before release of cotton expressing this toxin. PLoS One 7 e39192. https://doi.org/10.1371/journal.pone.0039192

Malovichko YV, Nizhnikov AA, Antonets KS. 2019. Repertoire of the *Bacillus thuringiensis* Virulence Factors Unrelated to Major Classes of Protein Toxins and Its Role in Specificity of Host-Pathogen Interactions. Toxins 11, 347. https://doi.org/10.3390/toxins11060347

Marchal I, Jarvis DL, Cacan R, Verbert A. 2001. Glycoproteins from insect cells: sialylated or not? Biol Chem 382, 151–159. https://doi.org/10.1515/BC.2001.023

Martin PAW. 1994. An iconoclastic view of *Bacillus thuringiensis* ecology. Am Entomol 40, 85–91. https://doi.org/10.1093/ae/40.2.85

Martínez-Solís M, Pinos D, Endo H, Portugal L, Sato R, Ferré J, Herrero S, Hernández-Martínez P. 2018. Role of *Bacillus thuringiensis* Cry1A toxins domains in the binding to the ABCC2 receptor from *Spodoptera exigua*. Insect Biochem Mol Biol 101, 47–56. https://doi.org/10.1016/j.ibmb.2018.07.006

Martyna A, Bahsoun B, Badham MD, Srinivasan S, Howard MJ, Rossman JS. 2017. Membrane remodeling by the M2 amphipathic helix drives influenza virus membrane scission. Sci Rep 7, 44695. https://doi.org/10.1038/srep44695

Mehrkhou F, Talebi AA, Moharramipour S, Naveh VH. 2012. Demographic parameters of *Spodoptera exigua* (Lepidoptera: Noctuidae) on different soybean cultivars. Environ Entomol 41, 326–332. https://doi.org/10.1603/EN10255

Meusch D, Gatsogiannis C, Efremov R, Lang AE, Hofnagel O, Vetter IR, Aktories K, Raunser S. 2014. Mechanism of Tc toxin action revealed in molecular detail. Nature, 508, 61–65. https://doi.org/10.1038/nature13015

Milijaš Jotić M, Panevska A, Iacovache I, Kostanjšek R, Mravinec M, Skočaj M, Zuber B, Pavšič A, Razinger J, Modic Š, Trenti F, Guella G, Sepčić K. 2021. Dissecting out the molecular mechanism of insecticidal activity of Ostreolysin A6/Pleurotolysin B complexes on Western Corn Rootworm. Toxins 13, 455. https://doi.org/10.3390/toxins13070455

Moar WJ and Anilkumar KJ. 2007. Plant science: the power of the pyramid. Science 318:1561–1562. https://doi.org/10.1126/science.1151313

Moar WJ, Berry C, Narva KE. 2017. The structure/function of new insecticidal proteins and regulatory challenges for commercialization. J Invertebr Pathol 142, 1–4. https://doi.org/10.1016/j.jip.2017.02.001

Mollinedo F, Gajate C. 2015. Lipid rafts as major platforms for signaling regulation in cancer. Adv Biol Regul 57, 130–146. https://doi.org/10.1016/j.jbior.2014.10.003

Mueller M, Grauschopf U, Maier T, Glockshuber R, Ban N. 2009. The structure of a cytolytic α-helical toxin pore reveals its assembly mechanism. Nature, 459, 726–730. https://doi.org/10.1038/nature08026

Munson PJ, Rodbard D. 1980. Ligand: A versatile computerized approach for characterization of ligand-binding systems. Anal Biochem 107, 220–239. https://doi.org/10.1016/0003-2697(80)90515-1

Nelson DL, Cox MM. 2021a. Lehninger Principles of Biochemistry (8th ed.) W.H. Freeman. Chapter 11. Biological Membranes and Transport.

Nelson DL, Cox MM. 2021b. Lehninger Principles of Biochemistry (8th ed.) W.H. Freeman. Chapter 7. Carbohydrates and Glycobiology. Glycoconjugates: Proteoglycans, Glycoproteins, and Glycolipids

Nimsanor S, Srisaisup M, Jammor P, Promdonkoy B, Boonserm P. 2020. Intracellular localization and cytotoxicity of *Bacillus thuringiensis* Vip3Aa against *Spodoptera frugiperda* (Sf9) cells. J Invertebr Pathol 171, 107340. https://doi.org/10.1016/j.jip.2020.107340

Niu Y, Oyediran I, Yu W, Lin S, Dimase M, Brown S, Reay-Jones FPF, Cook D, Reisig D, Thrash B, Ni X, Paula-Moraes SV, Zhang Y, Chen JS, Wen Z, Huang F. 2021. Populations of *Helicoverpa zea* (Boddie) in the southeastern United States are commonly resistant to Cry1Ab, but still susceptible to Vip3Aa20 expressed in MIR 162 corn. Toxins 13, 63. https://doi.org/10.3390/toxins13010063

Núñez-Ramírez R, Huesa J, Bel Y, Ferré J, Casino P, Arias-Palomo E. 2020. Molecular architecture and activation of the insecticidal protein Vip3Aa from *Bacillus thuringiensis*. Nat Commun 11, 3974. https://doi.org/10.1038/s41467-020-17758-5

Osman GH, Altaf WJ, Saleh IAS, Soltane R, Abulreesh HH, Arif IA, Ramadan AM, Osman YA. 2018. First report of detection of the putative receptor of *Bacillus thuringiensis* toxin Vip3Aa from black cutworm (*Agrotis ipsilon*). Saudi J Biol Sci 25, 441–445. https://doi.org/10.1016/j.sjbs.2018.01.006

Osman GH, Soltane R, Saleh I, Abulreesh HH, Gazi KS, Arif IA, Ramadan AM, Alameldin HF, Osman YA, Idriss M. 2019. Isolation, characterization, cloning and bioinformatics analysis of a novel receptor from black cut worm (*Agrotis ipsilon*) of *Bacillus thuringiensis* Vip3Aa toxins. Saudi J Biol Sci 26, 1078–1083. https://doi.org/10.1016/j.sjbs.2018.06.002

Palma L, Hernández-Rodríguez CS, Maeztu M, Hernández-Martínez P, Ruiz de Escudero I, Escriche B, Muñoz D, Van Rie J, Ferré J, Caballero P. 2012. Vip3C, a novel class of vegetative insecticidal proteins from *Bacillus thuringiensis*. Appl Environ Microbiol 78, 7163–7165. https://doi.org/10.1128/AEM.01360-12

Palma L, Muñoz D, Berry C, Murillo J, Caballero P. 2014. *Bacillus thuringiensis* toxins: an overview of their biocidal activity. Toxins 6, 3296–3325. https://doi.org/10.3390/toxins6123296

Palma L, Scott DJ, Harris G, Din SU, Williams TL, Roberts OJ, Young MT, Caballero P, Berry C. 2017. The Vip3Ag4 insecticidal protoxin from *Bacillus thuringiensis* adopts a tetrameric configuration that is maintained on proteolysis. Toxins 9, 165. https://doi.org/10.3390/toxins9050165

Panevska A, Skočaj M, Križaj I, Maček P, Sepčić K. 2019. Ceramide phosphoethanolamine, an enigmatic cellular membrane sphingolipid. Biochim Biophys Acta Biomembr 1861, 1284–1292. https://doi.org/10.1016/j.bbamem.2019.05.001

Pardo-López L, Soberón M, Bravo A. 2013. *Bacillus thuringiensis* insecticidal three-domain Cry toxins: mode of action, insect resistance and consequences for crop protection, FEMS Microbiol Rev, 37(1), 3–22. https://doi.org/10.1111/j.1574-6976.2012.00341.x

Pickett BR, Gulzar A, Ferré J, Wright DJ. 2017. *Bacillus thuringiensis* Vip3Aa toxin resistance in *Heliothis virescens* (Lepidoptera: Noctuidae). Appl Environ Microbiol 83, e03506–e03516. https://doi.org/10.1128/AEM.03506-16

Pigott CR, Ellar DJ. 2007. Role of receptors in *Bacillus thuringiensis* crystal toxin activity. Microbiol Mol Biol Rev 71, 255–281. https://doi.org/10.1128/MMBR.00034-06

Pinos D, Chakroun M, Millán-Leiva A, Jurat-Fuentes JL, Wright DJ, Hernández-Martínez P, Ferré J. 2020. Reduced membrane-bound alkaline phosphatase does not affect binding of Vip3Aa in a *Heliothis virescens* resistant colony. Toxins 12, 409. https://doi.org/10.3390/toxins12060409

Pezzini D, Taylor KL, Reisig DD, Fritz ML. 2024. Cross-pollination in seed-blended refuge and selection for Vip3A resistance in a lepidopteran pest as detected by genomic monitoring. Proc Natl Acad Sci USA 121, e2319838121. https://doi.org/10.1073/pnas.2319838121

Pogue MG. 2002. A world revision of the genus *Spodoptera* Guenée:(Lepidoptera:Noctuidae). Amer Entomological Society 43, 1–202.

Qi L, Dai H, Jin Z, Shen H, Guan F, Yang Y, Tabashnik BE, Wu Y. 2021. Evaluating Cross-Resistance to Cry and Vip toxins in four strains of *Helicoverpa armigera* with different genetic mechanisms of resistance to Bt toxin Cry1Ac. Front Microbiol 12, 670402. https://doi.org/10.3389/fmicb.2021.670402

Quan Y, Ferré J. 2019. Structural domains of the *Bacillus thuringiensis* Vip3Af protein unraveled by tryptic digestion of alanine mutants. Toxins 11, 368. https://doi.org/10.3390/toxins11060368

Quan Y, Lázaro-Berenguer M, Hernández-Martínez P, Ferré J. 2021a. Critical domains in the specific binding of radiolabelled Vip3Af insecticidal protein to brush border membrane vesicles from *Spodoptera* spp. and Cultured insect cells. Appl Environ Microbiol 87, e01787–21. https://doi.org/10.1128/AEM.01787-21

Quan Y, Yang J, Wang Y, Hernández-Martínez P, Ferré J, He K. 2021b. The rapid evolution of resistance to Vip3Aa insecticidal protein in *Mythimna separata* (Walker) is not related to altered binding to midgut receptors. Toxins 13, 364. https://doi.org/10.3390/toxins13050364

Quinn PJ. 2014. Sphingolipid symmetry governs membrane lipid raft structure. Biochim Biophys Acta 1838, 1922–1930. https://doi.org/10.1016/j.bbamem.2014.02.021

Rang C, Gil P, Neisner N, Van Rie J, Frutos R. 2005. Novel Vip3-related protein from *Bacillus thuringiensis*. Appl Environ Microbiol 71, 6276–6281. https://doi.org/10.1128/AEM.71.10.6276-6281.2005

Rees JS, Jarrett P, Ellar DJ. 2009. Peritrophic membrane contribution to Bt Cry delta-endotoxin susceptibility in Lepidoptera and the effect of Calcofluor. J Invertebr Pathol 100, 139-146. https://doi.org/10.1016/j.jip.2009.01.002

Riaz S, Nasir IA, Bhatti MU, Adeyinka OS, Toufiq N, Yousaf I, Tabassum B. 2020. Resistance to *Chilo infuscatellus* (Lepidoptera: Pyraloidea) in transgenic lines of sugarcane expressing *Bacillus thuringiensis* derived Vip3A protein. Mol Biol Rep 47, 2649–2658. https://doi.org/10.1007/s11033-020-05355-0

Roberts KL, Leser GP, Ma C, Lamb RA. 2013. The amphipathic helix of influenza a virus M2 protein is required for filamentous bud formation and scission of filamentous and spherical particles. J Virol 87, 9973–9982. https://doi.org/10.1128/JVI.01363-13

Rodríguez-Almazán C, Zavala L E, Muñoz-Garay C, Jiménez-Juárez N, Pacheco S, Masson L, Soberón M, Bravo A. 2009. Dominant negative mutants of *Bacillus thuringiensis* Cry1Ab toxin function as anti-toxins: Demonstration of the role of oligomerization in toxicity. PLoS ONE 4, e5545. https://doi.org/10.1371/journal.pone.0005545

Rohou A, Grigorieff N. 2015. CTFFIND4: fast and accurate defocus estimation from electron micrographs. J Struct Biol 192, 216–221. https://doi.org/10.1016/j.jsb.2015.08.008

Ruiz de Escudero I, Banyuls N, Bel Y, Maeztu M, Escriche B, Muñoz D, Caballero P, Ferré J. 2014. A screening of five *Bacillus thuringiensis* Vip3A proteins for their activity against lepidopteran pests. J Invertebr Pathol 117, 51–55. https://doi.org/10.1016/j.jip.2014.01.006

Saeed S, Sayyed AH, Ahmad I. 2010. Effect of host plants on life-history traits of *Spodoptera exigua* (Lepidoptera: Noctuidae). J Pest Sci 83, 165–172. https://doi.org/10.1007/s10340-009-0283-8

Sakuragi T, Nagata S. 2023. Regulation of phospholipid distribution in the lipid bilayer by flippases and scramblases. Nat Rev Mol Cell Biol 24, 576–596. https://doi.org/10.1038/s41580-023-00604-z

Salama HS, Dimetry NZ, Salem SA. 1971. On the host preference and biology of the cotton leaf worm *Spodoptera littoralis*. Z Angew Entomol 67, 261–266. https://doi.org/10.1111/j.1439-0418.1971.tb02122.x

Sanchis V, 2011. From microbial sprays to insect-resistant transgenic plants: history of the biospesticide *Bacillus thuringiensis*. A review. Agron Sustain Dev 31, 217–231. https://doi.org/10.1051/agro/2010027

Sands R, Meade B, Seale Jr JL, Robinson S, Seeger R. 2023. Scenarios of global food consumption: Implications for agriculture (Report No. ERR-323). U.S. Department of Agriculture, Economic Research Service. https://doi.org/10.32747/2023.8134356.ers

Santos EN, Menezes LP, Dolabella SS, Santini A, Severino P, Capasso R, Zielinska A, Souto EB, Jain S. 2022. *Bacillus thuringiensis*: From biopesticides to anticancer agents. Biochimie 192, 83–90. https://doi.org/10.1016/j.biochi.2021.10.003

Sauka DH, Rodríguez SE, Benintende GB. 2013. New variants of lepidoptericidal toxin genes encoding *Bacillus thuringiensis* Vip3Aa proteins. J Mol Microbiol Biotechnol 22, 373–380. https://doi.org/10.1159/000345911

Scheres SH. 2012. RELION: implementation of a Bayesian approach to cryo-EM structure determination. J Struct Biol 180, 519–530. https://doi.org/10.1016/j.jsb.2012.09.006

Schnepf E, Crickmore N, Van Rie J, Lereclus D, Baum J, Feitelson J, Zeigler DR, Dean DH. 1998. *Bacillus thuringiensis* and its pesticidal crystal proteins. Microbiol Mol Biol Rev 62, 775–806. https://doi.org/10.1128/mmbr.62.3.775-806.1998

Sellami S, Jemli S, Abdelmalek N, Cherif M, Abdelkefi-Mesrati L, Tounsi S, Jamoussi K. 2018. A novel Vip3Aa16-Cry1Ac chimera toxin: enhancement of toxicity against *Ephestia kuehniella*, structural study and molecular docking. Int J Biol Macromol 117, 752–761. https://doi.org/10.1016/j.ijbiomac.2018.05.161

Selvapandiyan A, Arora N, Rajagopal R, Jalali SK, Venkatesan T, Singh SP, Bhatnagar RK. 2001. Toxicity analysis of N-and C-terminus-deleted vegetative insecticidal protein from *Bacillus thuringiensis*. Appl Environ Microbiol 67, 5855–5858. https://doi.org/10.1128/AEM.67.12.5855-5858.2001

Sena JA, Hernández-Rodríguez CS, Ferré J. 2009. Interaction of *Bacillus thuringiensis* Cry1 and Vip3A proteins with *Spodoptera frugiperda* midgut binding sites. Appl Environ Microbiol 75, 2236–2237. https://doi.org/10.1128/AEM.02342-08

Sepcić K, Berne S, Rebolj K, Batista U, Plemenitas A, Sentjurc M, Macek P. 2004. Ostreolysin, a pore-forming protein from the oyster mushroom, interacts specifically with membrane cholesterol-rich lipid domains. FEBS Lett 575, 81–85. https://doi.org/10.1016/j.febslet.2004.07.093

Shan Y, Jin M, Chakrabarty S, Yang B, Li Q, Cheng Y, Zhang L, Xiao Y. 2022. Sf-FGFR and Sf-SR-C are not the receptors for Vip3Aa to exert insecticidal toxicity in *Spodoptera frugiperda*. Insects 13, 547. https://doi.org/10.3390/insects13060547

Shao E, Huang H, Yuan J, Yan Y, Ou L, Chen X, Pan X, Guan X, Sha L. 2024. N-terminal α-helices in domain I of *Bacillus thuringiensis* Vip3Aa play crucial roles in disruption of liposomal membrane. Toxins 16,88. https://doi.org/10.3390/toxins16020088

Sharma A, Chandran D, Singh DD, Vijayan M. 2007. Multiplicity of carbohydrate-binding sites in beta-prism fold lectins: occurrence and possible evolutionary implications. J Biosci 32, 1089–1110. https://doi.org/10.1007/s12038-007-0111-3

Sharma S, Kooner R, Arora R. 2017. Insect pests and crop losses, in Breeding Insect Resistant Crops for Sustainable Agriculture, ed. by Arora R and Sandhu S. Springer Nature, Singapore, pp. 45–66.

Sharma M, Gupta GD, Kumar V. 2018. Mosquito-larvicidal BinA toxin displays affinity for glycoconjugates: Proposal for BinA mediated cytotoxicity. J Invertebr Pathol 156, 29–40. https://doi.org/10.1007/s12038-007-0111-3

Shelton AM. 2012. Genetically engineered vegetables expressing proteins from *Bacillus thuringiensis* for insect resistance. GM Crops Food 3, 175–183. https://doi.org/10.4161/gmcr.19762

Showler AT. 2001. *Spodoptera exigua* oviposition and larval feeding preferences for pigweed, *Amaranthus hybridus*, over squaring cotton, *Gossypium hirsutum*, and a comparison of free amino acids in each host plant. J Chem Ecol 27, 2013–2028. https://doi.org/10.1023/a:1012238803311

Simons K, Ikonen E. 1997. Functional rafts in cell membranes. Nature 387, 569–572. https://doi.org/10.1038/42408

Singh M, Kumar P, Patel SK, Kalia VC. 2013. Production of Polyhydroxyalkanoate Co-polymer by *Bacillus thuringiensis*. Indian J Microbiol 53, 77–83. https://doi.org/10.1007/s12088-012-0294-7

Singh G, Sachdev B, Sharma N, Seth R, Bhatnagar RK. 2010. Interaction of *Bacillus thuringiensis* vegetative insecticidal protein with ribosomal S2 protein triggers larvicidal activity in *Spodoptera frugiperda*. Appl Environ Microbiol 76, 7202–7209. https://doi.org/10.1128/AEM.01552-10

Smith DC, Sillence DJ, Falguières T, Jarvis RM, Johannes L, Lord JM, Platt FM, Roberts L M. 2006. The association of Shiga-like toxin with detergent-resistant membranes is modulated by glucosylceramide and is an essential requirement in the endoplasmic reticulum for a cytotoxic effect. Mol Biol Cell 17, 1375–87. https://doi.org/10.1091/mbc.e05-11-1035

Stein PE, Boodhoo A, Armstrong GD, Heerze LD, Cockle SA, Klein MH, Read RJ. 1994. Structure of a pertussis toxin-sugar complex as a model for receptor binding. Nat Struct Mol Biol 1, 591–596. https://doi.org/10.1038/nsb0994-591

Storer NP, Kubiszak ME, King JE, Thompson GD, Santos AC. 2012. Status of resistance to Bt maize in *Spodoptera frugiperda*: lessons from Puerto Rico. J Invertebr Pathol 110, 294–300. https://doi.org/10.1016/j.jip.2012.04.007

Sun Y, Yang P, She M, Lin C, Ye Y, Xu C, Shen Z. 2025. A Vip3Af mutant confers high resistance to broad lepidopteran insect pests. Pest Manag Sci 81, 28–35. https://doi.org/10.1002/ps.8402

Svennerholm L, Fredman P. 1980. A procedure for the quantitative isolation of brain gangliosides. Biochim Biophys Acta 617, 97–109. https://doi.org/10.1016/0005-2760(80)90227-1

Tabashnik BE, Carrière Y. 2017. Surge in insect resistance to transgenic crops and prospects for sustainability. Nat Biotechnol 35, 926–935. https://doi.org/10.1038/nbt.3974

Tabashnik BE, Carrière Y. 2019. Global patterns of resistance to Bt-crops highlighting Pink Bollworm in the United States, China and India. J Econ Entomol 112, 2513–2523. https://doi.org/10.1093/jee/toz173

Tabashnik BE, Unnithan GC, Yelich AJ, Fabrick JA, Dennehy TJ, Carrière Y. 2022. Responses to Bt toxin Vip3Aa by pink bollworm larvae resistant or susceptible to Cry toxins. Pest Manag Sci 78, 3973–3979. https://doi.org/10.1002/ps.7016

Tarbouriech N, Curran J, Ruigrok RWH, Burmeister WP. 2000. Tetrameric coiled-coil domain of Sendai virus phosphoprotein. Nat Struct Biol 7, 777–781. https://doi.org/10.1038/79013

Terra WR. 2001. The origin and functions of the insect peritrophic membrane and peritrophic gel. Arch. Insect Biochem. Physiol. 47, 47–61. https://doi.org/10.1002/arch.1036

Terra WR, Costa RH, Ferreira C. 2006. Plasma membranes from insect midgut cells. An Acad Bras Cienc 78, 255–269. https://doi.org/10.1590/s0001-37652006000200007

Trajković A, Žikić V. 2023. Stuck in the Caterpillars' Web: a half-century of biocontrol research and application on gregarious lepidopteran pests in Europe. Sustainability, 15, 2881. https://doi.org/10.3390/su15042881

Tweten RK. 2005. Cholesterol-dependent cytolysins, a family of versatile pore-forming toxins. Infect Immun 73, 6199–209. https://doi.org/10.1128/IAI.73.10.6199-6209.2005

United Nations, Department of Economic and Social Affairs, Population Division. World Population Prospects: The 2024 Revision. https://population.un.org/wpp/ [Accessed 29.12.2024]

Valaitis AP, Podgwaite JD. 2013. *Bacillus thuringiensis* Cry1A toxin-binding glycoconjugates present on the brush border membrane and in the peritrophic membrane of the Douglas-fir tussock moth are peritrophins. J Invertebr Pathol 112,1-8. https://doi.org/10.1016/j.jip.2012.10.002

Van Meer G, Voelker DR, Feigenson GW. 2008. Membrane lipids: where they are and how they behave. Nat Rev Mol Cell Biol 9, 112–124. https://doi.org/10.1038/nrm2330

Van Rie J, Jansens S, Höfte H, Degheele D, Van Mellaert H. 1989. Specificity of *Bacillus thuringiensis* delta-endotoxins: Importance of specific receptors on the brush border membrane of the midgut of target insects. *Eur J Biochem* 186, 239–247. https://doi.org/10.1111/j.1432-1033.1989.tb15201.x

Varki A, Cummings RD, Esko JD, Freeze HH, Stanley P, Bertozzi CR, Hart GW, Etzler ME. (Eds.). 2009. Essentials of Glycobiology. (2nd ed). Cold Spring Harbor Laboratory Press.

Vélez AM, Spencer TA, Alves AP, Moellenbeck D, Meagher RL, Chirakkal H, Siegfried BD. 2013. Inheritance of Cry1F resistance, cross-resistance and frequency of resistant alleles in *Spodoptera frugiperda* (Lepidoptera: Noctuidae). Bull Entomol Res 103, 700–713. https://doi.org/10.1017/S0007485313000448

Wang Z, Gan C, Wang J, Bravo A, Soberón M, Yang Q, Zhang J. 2021. Nutrient conditions determine the localization of *Bacillus thuringiensis* Vip3Aa protein in the mother cell compartment. Microb Biotechnol 14, 551–560. https://doi.org/10.1111/1751-7915.13719

Wang J, Pielak RM, McClintock MA, Chou JJ. 2009. Solution structure and functional analysis of the influenza B proton channel. Nat Struct Mol Biol 16, 1267–1271. https://doi.org/10.1038/nsmb.1707

Wang Y, Wang J, Fu X, Nageotte JR, Silverman J, Bretsnyder EC, Chen D, Rydel TJ, Bean GJ, Li KS, Kraft E, Gowda A, Nance A, Moore RG, Pleau MJ, Milligan JS, Anderson HM, Asiimwe P, Evans A, Moar WJ, Martinelli S, Head GP, Haas JA, Baum JA, Yang F, Kerns DL, Jerga A. 2019. *Bacillus thuringiensis* Cry1Da_7 and Cry1B868 protein interactions with novel receptors allow control of resistant Fall Armyworms, *Spodoptera frugiperda* (J. E. Smith). Appl Environ Microbiol 85, e00579-e619. https://doi.org/10.1128/AEM.00579-19

Wang Y, Yang J, Zhang T, Bai S, Wang Z, He K. 2022. Inheritance and fitness costs of Vip3Aa19 resistance in *Mythimna separata*. Toxins 14, 388. https://doi.org/10.3390/toxins14060388

Welch KL, Unnithan GC, Degain BA, Wei J, Zhang J, Li X, Tabashnik BE, Carrière Y. 2015. Cross-resistance to toxins used in pyramided Bt-crops and resistance to Bt sprays in *Helicoverpa zea*. J Invertebr Pathol 132, 149–156. https://doi.org/10.1016/j.jip.2015.10.003

Wen Z, Conville J, Matthews P, Hootman T, Himes J, Wong S, Huang F, Ni X, Chen JS, Bramlett M. 2023. More than 10 years after commercialization, Vip3A-expressing MIR162 remains highly efficacious in controlling major Lepidopteran maize pests: laboratory resistance selection versus field reality. Pest Biochem Phys 192, 105385. https://doi.org/https://doi.org/10.1016/j.pestbp.2023.105385

Wolfersberger MG. 1987. Preparation and partial characterization of amino acid transporting brush border membrane vesicles from the larval midgut of the cabbage butterfly (*Pieris brassicae*). Comp Biochem Physiol 86A, 301–308. https://doi.org/10.1002/arch.940240304

Wróbel M, Śliwakowski W, Kowalczyk P, Kramkowski K, Dobrzyński J. 2023. Bioremediation of Heavy Metals by the Genus *Bacillus*. Int J Environ Res Public Health, 20, 4964. https://doi.org/10.3390/ijerph20064964

Xu C, Cheng J, Lin H, Lin C, Gao J, Shen Z. 2018. Characterization of transgenic rice expressing fusion protein Cry1Ab/Vip3A for insect resistance. Sci Rep 8, 15788. https://doi.org/10.1038/s41598-018-34104-4

Yamaji A, Sekizawa Y, Emoto K, Sakuraba H, Inoue K, Kobayashi H, Umeda M. 1998. Lysenin, a novel sphingomyelin-specific binding protein. J Biol Chem 273, 5300–6. https://doi.org/10.1074/jbc.273.9.5300

Yang F, Huang F, Qureshi JA, Leonard BR, Niu Y, Zhang L, Wangila DS. 2013. Susceptibility of Louisiana and Florida populations of *Spodoptera frugiperda* (Lepidoptera: Noctuidae) to transgenic Agrisure®Viptera™ 3111 corn. Crop Prot 50, 37–39. https://doi.org/10.1016/j.cropro.2013.04.002

Yang F, Morsello S, Head GP, Sansone C, Huang F, Gilreath RT, Kerns DL. 2018. F2 screen, inheritance and cross-resistance of field-derived Vip3A resistance in *Spodoptera frugiperda* (Lepidoptera: Noctuidae) collected from Louisiana, USA. Pest Manag Sci 74, 1769–1778. https://doi.org/10.1002/ps.4805

Yang F, González JCS, Little N, Reisig D, Payne G, Dos Santos RF, Jurat-Fuentes JL, Kurtz R, Kerns DL. 2020. First documentation of major Vip3Aa resistance alleles in field populations of *Helicoverpa zea* (Boddie) (Lepidoptera: Noctuidae) in Texas, USA. Sci. Rep. 10, 5867. https://doi.org/10.1038/s41598-020-62748-8

Yang F, Kerns DL, Little NS, Santiago González JC, Tabashnik BE. 2021. Early warning of resistance to Bt toxin Vip3Aa in *Helicoverpa zea*. Toxins 13, 618. https://doi.org/10.3390/toxins13090618

Yu CG, Mullins MA, Warren GW, Koziel MG, Estruch JJ. 1997. The *Bacillus thuringiensis* vegetative insecticidal protein Vip3Aa lyses midgut epithelium cells of susceptible insects. Appl Environ Microbiol 63, 532–536. https://doi.org/10.1128/aem.63.2.532-536.1997

Yu RK, Tsai YT, Ariga T, Yanagisawa M. 2011. Structures, biosynthesis, and functions of gangliosides - an overview. J Oleo Sci. 60, 537–544. https://doi.org/10.5650/jos.60.537

Zack MD, Sopko MS, Frey ML, Wang X, Tan SY, Arruda JM, Letherer TT, Narva KE. 2017. Functional characterization of Vip3Ab1 and Vip3Bc1: two novel insecticidal proteins with differential activity against lepidopteran pests. Sci Rep 7, 11112. https://doi.org/10.1038/s41598-017-11702-2

Zavala LE, Pardo-López L, Cantón PE, Gómez I, Soberón M, Bravo A. 2011. Domains II and III of Bacillus thuringiensis Cry1Ab toxin remain exposed to the solvent after insertion of part of domain I into the membrane. J Biol Chem 286, 19109–19117. https://doi.org/10.1074/jbc.M110.202994

Zhang J, Pan ZZ, Xu L, Liu B, Chen Z, Li J, Niu LY, Zhu YJ, Chen QX. 2018. Proteolytic activation of *Bacillus thuringiensis* Vip3Aa protein by *Spodoptera exigua* midgut protease. Int J Biol Macromol 107, 1220–1226. https://doi.org/10.1016/j.ijbiomac.2017.09.101

Zhang Y, Li X, Tian H, An B, Yan B, Cai J. 2022. Vegetative Insecticidal Protein Vip3Aa is transported via membrane vesicles in *Bacillus thuringiensis* BMB171. Toxins 14, 480. https://doi.org/10.3390/toxins14070480

Zhang Z, Wang L, Pang X, Tek Tay W, Gordon KHJ, Walsh TK, Yang Y, Wu Y. 2024. Knockout of the SfVipR1 gene confers high-level resistance to *Bacillus thuringiensis* Vip3Aa toxin in *Spodoptera frugiperda*. bioRxiv2024.09.26.615236. https://doi.org/10.1101/2024.09.26.615236

Zhao M, Yuan X, Wei J, Zhang W, Wang B, Myint Khaing M, Liang G. 2017. Functional roles of cadherin, aminopeptidase-N and alkaline phosphatase from *Helicoverpa armigera* (Hübner) in the action mechanism of *Bacillus thuringiensis* Cry2Aa. Sci Rep 7, 46555. https://doi.org/10.1038/srep46555

Zheng M, Evdokimov AG, Moshiri F, Lowder C, Haas J. 2020. Crystal structure of a Vip3B family insecticidal protein reveals a new fold and a unique tetrameric assembly. Protein Sci. 29, 824–829. https://doi.org/10.1002/pro.3803

Zhukovsky MA, Filograna A, Luini A, Corda D, Valente C. 2019. Protein amphipathic helix insertion: a mechanism to induce membrane fission. Front Cell Dev Biol 7, 291. https://doi.org/10.3389/fcell.2019.00291

Zuverink M, Barbieri JT. 2018. Protein toxins that utilize gangliosides as host receptors. Prog Mol Biol Transl Sci 156, 325–54. https://doi.org/10.1016/bs.pmbts.2017.11.010

Supplementary information

Supplementary Table S1.1. List of SDM primers for Vip DIP variants generation and sequencing. Forward (F) and reverse (R) primers flaking the target sequences and carrying the mutations were designed for introducing the desired modifications. Changed bases compared to the wild type sequence are underlined. The annealing temperature used for each primer pair (Tm) is indicated in °C. Primers flanking the modified regions were also used for DNA sequencing.

Mutant		5′ → 3′ primer sequence	Tm (°C)
		SDM primers	
Vip3Aa DIP1 (S164C L166C)	F	ATT AAC TGT ACA TGT ACT GAA ATT ACA CCT GCG TAT CAA AG	56
	R	GTA ATT TCA GTA CAT GTA CAG TTA ATA AGT ACA TTT ACA TTA ATA ATA TCC	
Vip3Aa DIP2 (E168A)	F	CTT ACT GCA ATT ACA CCT GCG TAT CAA AG	56
	R	GGT GTA ATT GCA GTA AGT GTA GAG TTA ATA AGT AC	
Vip3Ca DIP (S164C L166C)	F	ATT AAT TGT ACT TGT ACT GAA ATC ACA CCT TCA TAT CAA CGT	56
	R	TGT GAT TTC AGT ACA AGT ACA ATT AAT TAA AAC ATT TAA ATT AAC ATC	
		Sequencing primers	
Vip3Aa DIPs	F	TGG ATG GGG TGA ATG GAA GCT T	58
	R	TCC GAC CTC ACT GCC ACT TGT T	60
Vip3Ca DIP	F	ACT AAA TTA AAC GCA AGG GCC TT	55
	R	AGC TGT TTT TAA AGC CGA TCG TCC	58

Supplementary Table S1.2. Binding parameters of ^{125}I-Vip3Aa *in vitro* competition binding assays. The equilibrium dissociation constant (K_d) and the concentration of binding sites (R_t) were calculated for the homologous and heterologous competitors. At least three replicates were used for the data analysis, and the mean values ± SEM are represented.

Protein	K_d ±SEM (nM)	R_t ± SEM (pmol/mg)
Vip3Aa WT	51.0 ± 8.3	170 ± 32
Vip3Aa DIP1	81 ± 25	324 ± 128
Vip3Aa DIP2	57.7 ± 11.8	190 ± 42
Vip3Af WT	130 ± 39	492 ± 202
Vip3Af DIP	180 ± 63	605 ± 317
Vip3Ca WT	6.6 ± 1.3	18.3 ± 3.4

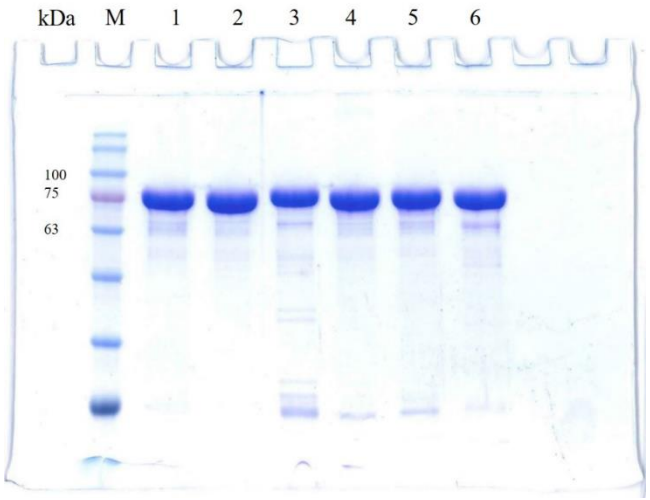

Supplementary Figure S1.1. SDS-PAGE of His-trap purified proteins used as competitors for *in vitro* binding assays. Lanes 1, Vip3Aa WT; 2, Vip3Af WT; 3, Vip3Ca WT; 4, Vip3Aa DIP1; 5, Vip3Aa DIP2, and 6, Vip3Af DIP. M, Blue Star molecular marker (NIPPON Genetics).

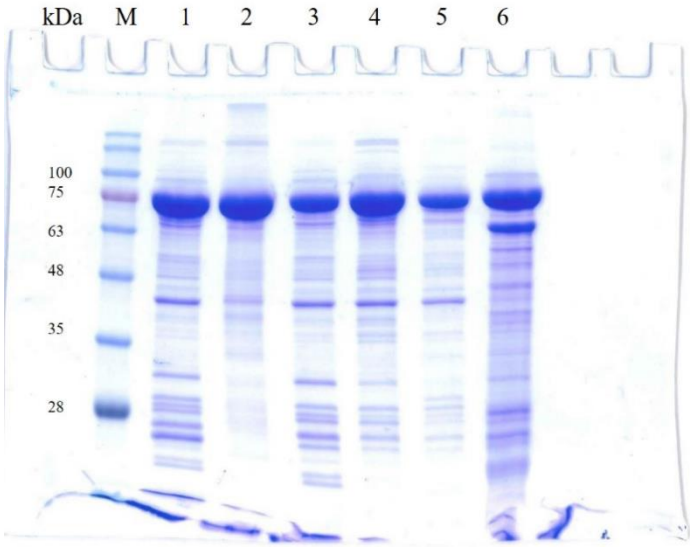

Supplementary Figure S1.2. SDS-PAGE of IPP purified proteins used for *in vivo* competitions assays. Lane 1, Vip3Aa WT; 2, Vip3Af WT; 3, Vip3Aa DIP1; 4, Vip3Aa DIP2; 5, Vip3Af DIP, and 6, Vip3Ca DIP. M, Blue Star molecular marker (NIPPON Genetics).

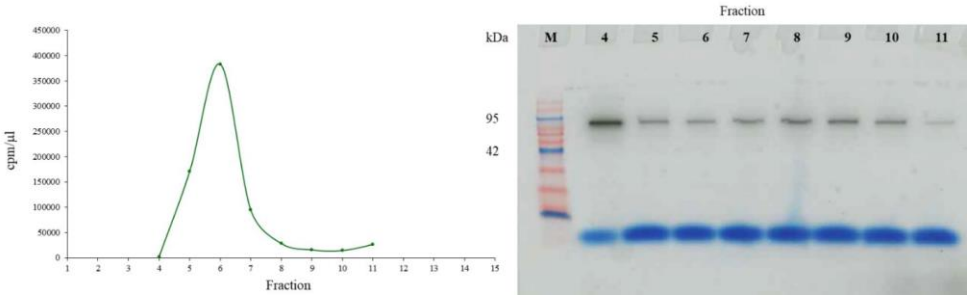

Supplementary Figure S1.3. Vip3Aa labelling with ^{125}I-Na. A) Separation of the labelled protein by gel filtration on a PD10 column; B) an equivalent number of cpm of each fraction were analysed in SDS-PAGE and autoradiography of the gel was performed. **(**M) PiNK Prestained Protein Marker (NIPPON Genetics).

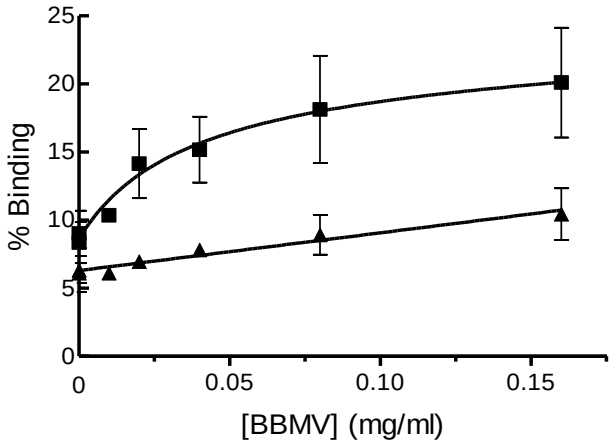

Supplementary Figure S1.4. Binding assays with ^{125}I-Vip3Aa and *S. littoralis* BBMV. *In vitro* binding assays using increasing concentrations of *S. littoralis* BBMV. Squares and triangles represent total and nonspecific binding (determined with 1000-fold unlabeled Vip3Aa), respectively. Each data point represents the mean of at least three replicates (±SEM).

Supplementary Table S2.1. Primers used for Domain I mutagenesis, C-t deletion and sequencing

Vip3Aa_mutant (residues)	5' → 3' primer sequence
	SDM primers
Δα1 (residues 40-789)	CAG GGA CCC GGT ACG GAT ACA GGT GGT GAT CTA AC
	CGA GGA GAA GCC CGG TTA CTT AAT AGA GAC ATC GTA AAA ATG TAC
S-S (residues 10-789)	
1st Double mutation	
D66C-N69C	GTG TGC GGA AGC TTA AAT GAT CTT ATC
D66C-N69C	CCC GCA CAA TTT ACC AGA AAT ATC ATT TAG
2nd Double mutation over 1st	
Q96C-L100C	AGT TTG CAA TGA TGT TAA TAA CAA ACT CG
Q96C-L100C	TGA TTG CAT TCA TTT GCA ATT TTT AAT ATT TCC
195-AVAA-198 (residues 10-789)	GCG GCG GAT GGC TCT CCT GCA GAT
	TAC CGC TGA ACT AGT TTC TGT AGC AAA AG
41-KVKK-44 (residues 10-789)	AAA AAG GAT CTA ACC CTA GAC GAA ATT TTA AAG
	TAC TTT CGT TTT AAA AAT CAT GTT CAT AAT GTC
L146M (residues 10-789)	AAG TAA ACA AAT GCA AGA GAT TTC
	AAG TAT TCT ATT TGC AGA CTT AG
L146F (residues 10-789)	AAG TAA ACA ATT CCA AGA GAT TTC TG
	AAG TAT TCT ATT TGC AGA CTT AG
ΔIV-V (residues 10-532)	CAG GGA CCC GGT ACA AGA GCC TTA CCA AGT TTT ATT G
	CGA GGA GAA GCC CGG TTA ACT TGG CGG GAC GAT CAA TTT AG
M34L (residues 1-789)	AGA CAT TTT GAA CAT GAT TTT TAA AAC GGA TAC AGG TG
	TCA TGT TCA AAA TGT CTT TGA TAC CAG TGG C
	Sequencing primers
N-terminal sequencing	CAG GGA CCC GGT ACA AGA GCC TTA CCA AGT TTT ATT G
C-terminal sequencing	TGA TCG TCC CGC CAA GTG GTT T

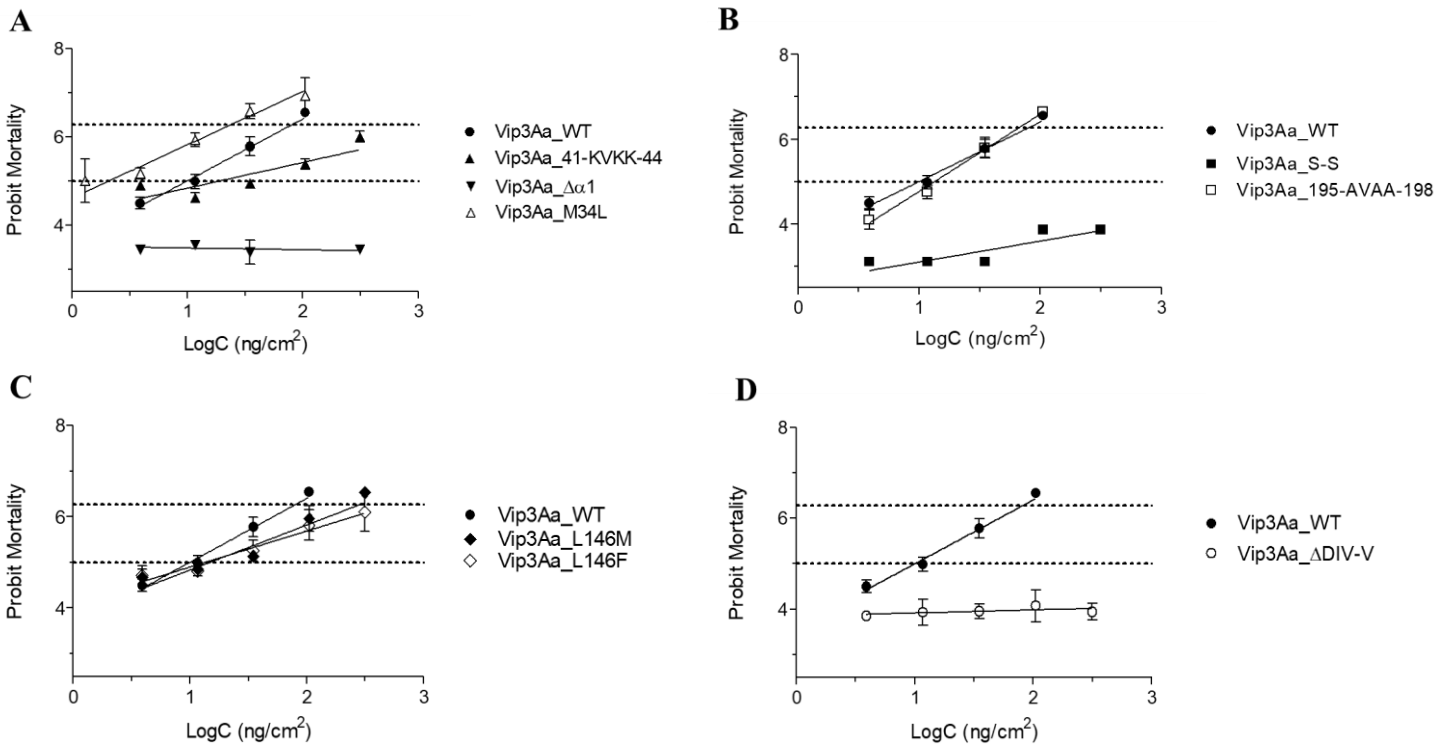

Supplementary Figure S2.1. Dose-response of the Vip3Aa WT and mutant proteins against *S. exigua* larvae. Panel A includes the mutants related to the modification of the N-t helix α1. Panel B includes the mutants related to the impairment of the trypsin processing and Domain I remodelling. Panel C includes the mutants related to the reduction of the inside diameter of the coiled-coil that Domain I forms in the activated conformation. Panel D shows the mutant lacking the C-t domains IV and V. Dashed lines indicate 50% and 90% mortality in the Probit scale.

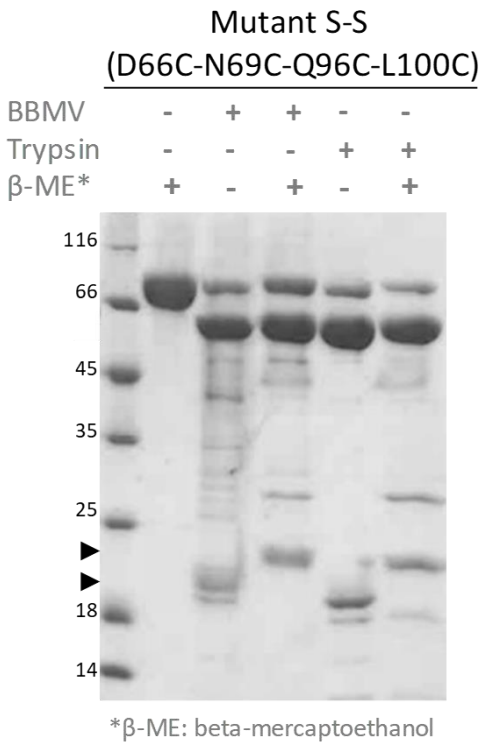

Supplementary Figure S2.2. Electrophoretic mobility of Vip3_S-S mutant in SDS-PAGE. Proteolytic processing in the presence of BBMV or trypsin together with the absence and presence of the reducing agent β-mercaptoethanol. Arrowheads indicate the bands corresponding to Domain I.

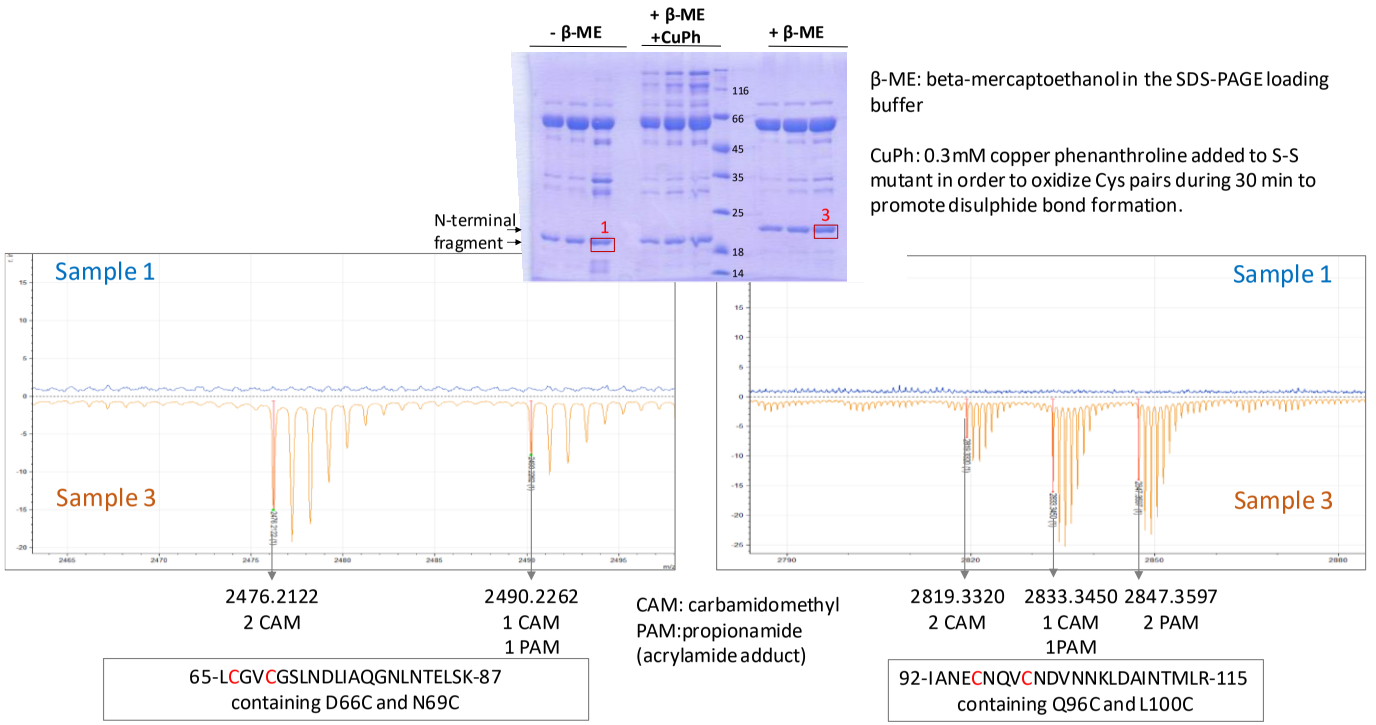

Supplementary Figure S2.3. MALDI-TOF analysis of Vip3Aa S-S N-terminal fragments. The analysis was carried out in the absence (sample 1) or the presence of the reducing agent β-ME (sample 3) obtained after trypsin digestion. Samples were excised from the gel upon usage. Peptides containing free Cys were found just in the reduced sample 3 for the peptides shown in the spectra.

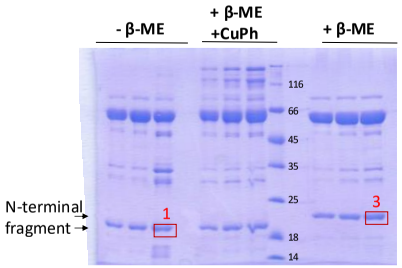

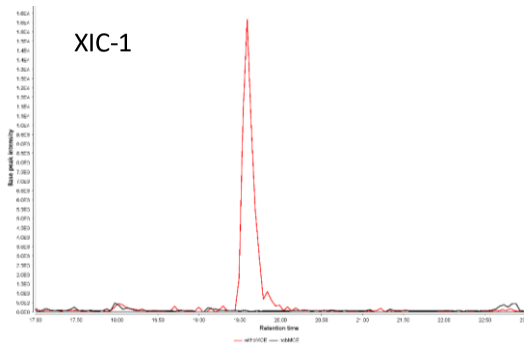

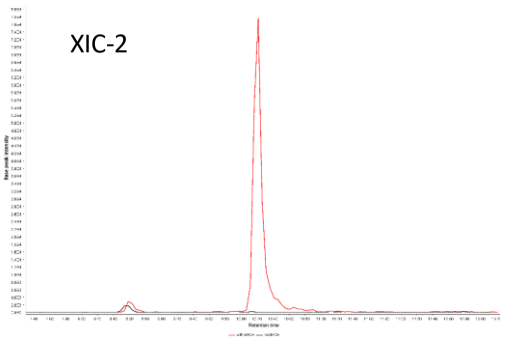

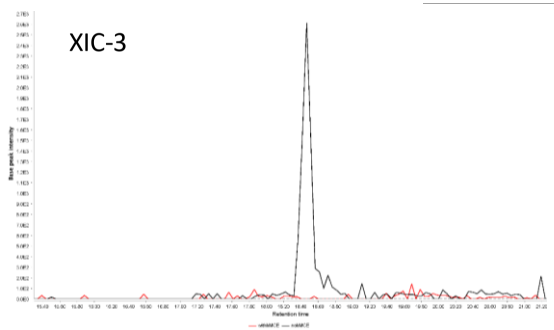

XIC	Peptide	Modification; Mass added (Da)	Monoisotopic Mass (Da)	m/z	charge
1	65-LCGVCGSLNDLIA QGNLNTELSK-87	2 CAM; (2 x 57= 114)	2475.21	619.81	4
2	92-IANECNQVC NDVNNK-106	2 CAM; (2 x 57= 114)	1790.77	597.93	3
3	Dipeptide N66C-L100C; N69C-Q96C	2 S-S bonds	4033.86	1009.47	4

65-LCGVCGSLNDLIAQGNLNTELSK-87
92-IANECNQVCNDVNNK-106

Supplementary Figure S2.4. LC-MS analysis of Vip3Aa S-S N-terminal fragments. The analysis was carried out in the absence (sample 1) or the presence of the reducing agent β-ME (sample 3) obtained after trypsin digestion. Samples were excised from the gel and processed for mass spectrometry analysis. Extracted ion chromatograms (XIC) of the peptides indicated in the table are shown. Chromatograms from sample 1 are shown in black whereas those from sample 3 are shown in red. The identity of the peptides was confirmed by tandem mass spectrometry.

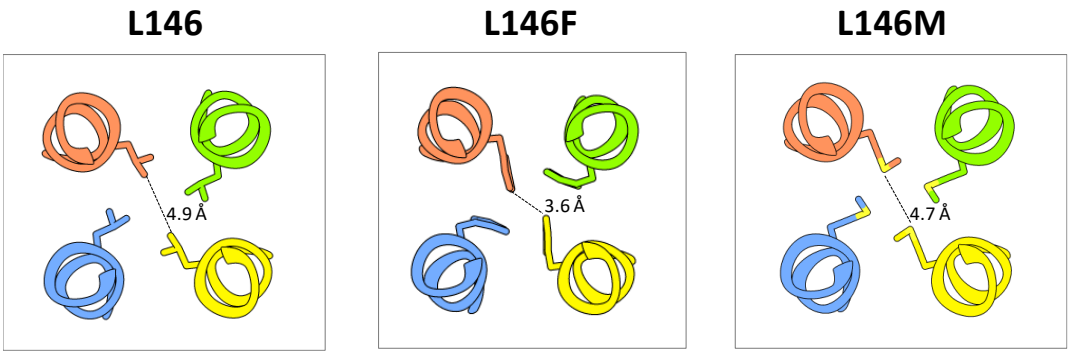

Supplementary Figure S2.5. Modelled mutations in the toxin structure of Vip3Aa (PDB: 6TFK) of L146 to Phe and Met. Minimization steps have been conducted after the mutations have been modelled using Chimera UCSF, then, distances between side chains are shown.

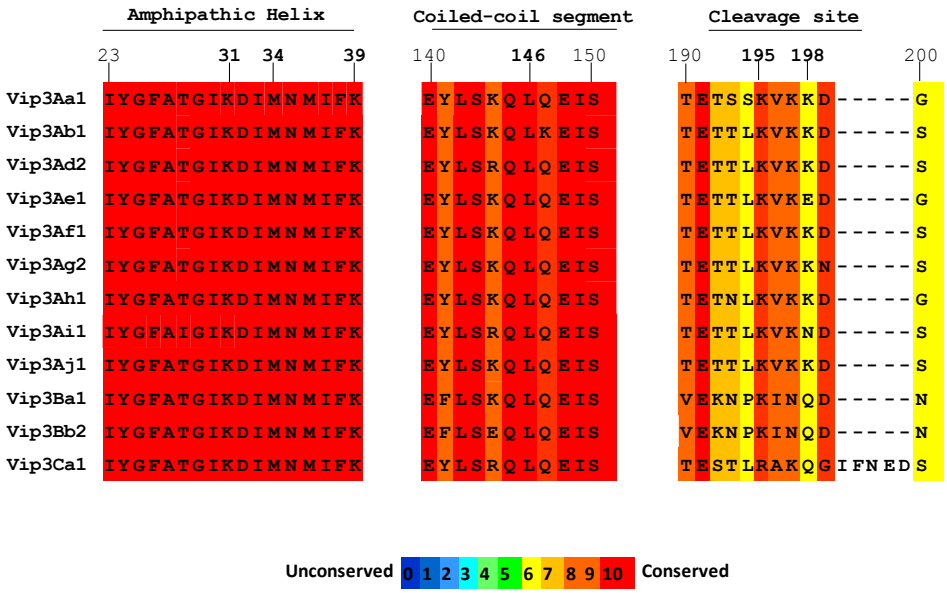

Supplementary Figure S2.6. Multiple sequence alignment of Vip family members showing conservation of residues mutated. The protein sequences used are as follows: Vip3Aa1 (GenBank accession number Vip3Aa (AAC37036), Vip3Ab1 (AAR40284), Vip3Ad2 (CAI43276), Vip3Ae1 (CAI43277), Vip3Af1 (CAI43275), Vip3Ag2 (ACL97352), Vip3Ah1 (ABH10614), Vip3Ai1 (KC156693), Vip3Aj1 (KF826717), Vip3Ba1 (AAV70653), Vip3Bb2 (ABO30520), and Vip3Ca1 (ADZ46178).

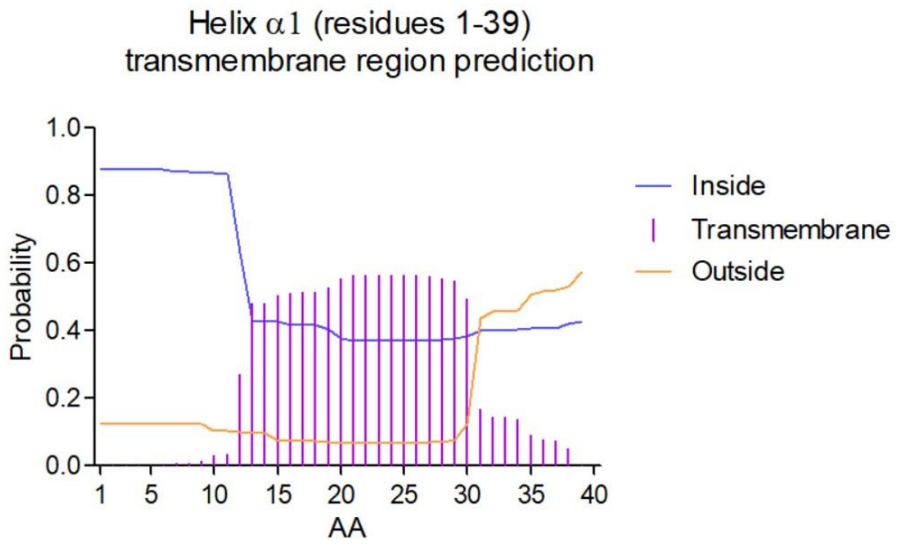

Supplementary Figure S3.1. Transmembrane region prediction on Vip3Aa helix α1 performed with Depp TMHMM prediction tool. The graph shows the probability of transmembrane region for each amino acid of the helix. The blue line indicates the probability of being inside the membrane (cytosolic region), the orange line indicates the probability of being outside the membrane and the purple lines indicate the probability of being in transmembrane position.

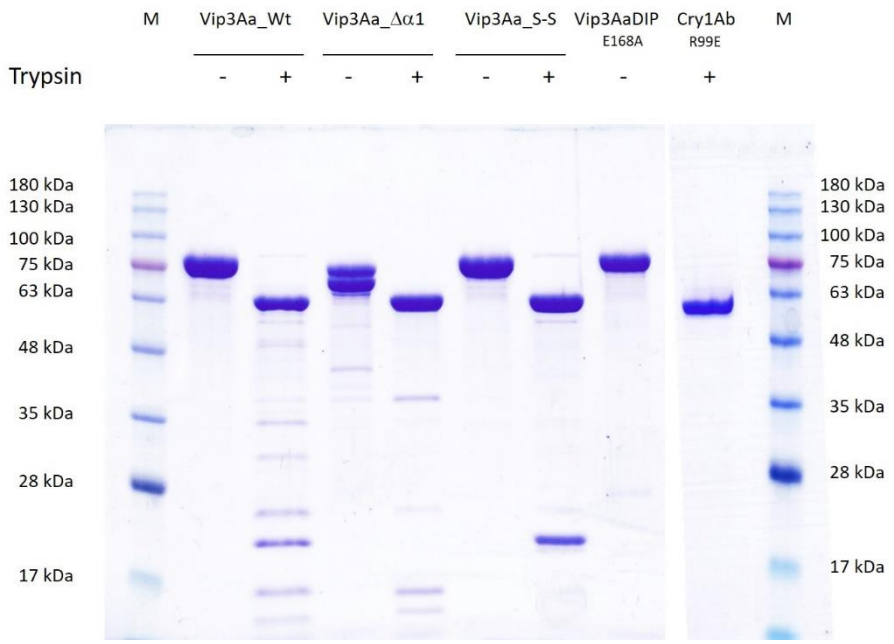

Supplementary Figure S3.2. Visualization of the different proteins used in *in vitro* and *in vivo* competition assays. 5 μg of protoxins (trypsin -) and processed proteins (tyrpsin +) incubated *in vitro* with trypsin (10% w/w) at pH 7.5 were analysed in SDS-PAGE gels. Band sizes were estimated according to the Blue Star molecular marker (M) (NIPPON Genetics).

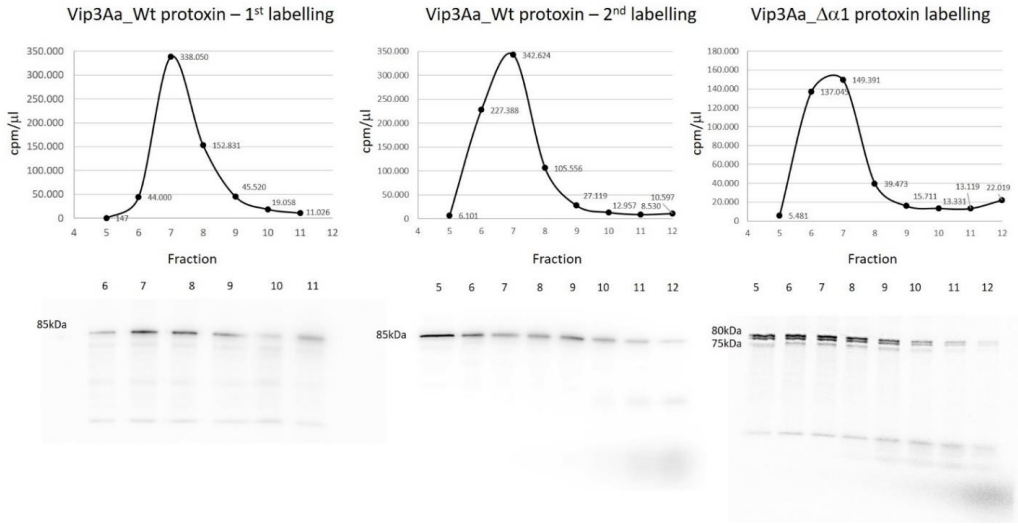

Supplementary Figure S3.3. Visualization of the radiolabelled proteins used in *in vitro* binding assays to BBMV. The upper panel shows the labelled protein fraction elution from the PD-10 desalting column after each radiolabelling reaction (Vip3Aa_Wt's first and second labelling and Vip3Aa_Δα1 labelling. The lower panel shows the corresponding SDS-PAGE (12% acrylamide) and autoradiograph of each fraction from each radiolabelling reaction, the amount of protein corresponding to 10,000 cpm was loaded on each lane.

Supplementary Table S4.1. Amplified residues and primers used for Vip3Aa truncated constructs generation. Forward (F) and reverse (R) primers flaking the target sequences were designed for amplifying the desired sequences coding for determined protein fragments, resulting in truncated proteins having only some of the structural domains of the protein.

Construct		Primer 5' → 3' sequence	aa	kDa
Vip3Aa I-III	F	CAG GGA CCC GGT ACA AGA GCC TTA CCA AGT TTT ATT G	10-532	54
	R	CGA GGA GAA GCC CGG TTA ACT TGG CGG GAC GAT CAA TTT AG		
Vip3Aa_II-V	F	CAG GGA CCC GGT GCA GAT ATT CTT GAT GAG TTA ACT G	203-789	65
Vip3Aa_III-V	F	CAG GGA CCC GGT ACA CTT TCT AAT ACT TTT TCT AAT CC	325-789	48
Vip3Aa_IV-V	F	CAG GGA CCC GGT AGT GGT TTT ATT AGC AAT ATT GTA GAG	532-789	27
All C-t constructs	R	CGA GGA GAA GCC CGG TTA CTT AAT AGA GAC ATC GTA AAA ATG TAC		

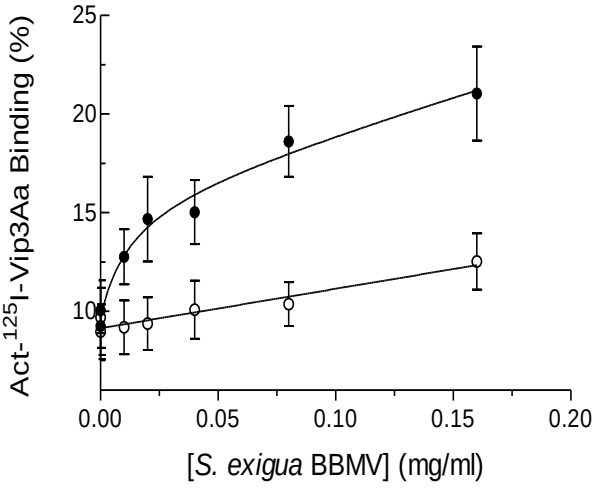

Supplementary Figure S4.1 Binding assays with ^{125}I-Vip3Aa and *S. exigua* BBMV. *In vitro* binding assays using increasing concentrations BBMV. Full circles and open circles represent total and nonspecific binding (determined with 1,000-fold unlabeled Vip3Aa), respectively. Each data point represents the mean of at least three replicates (±SEM).

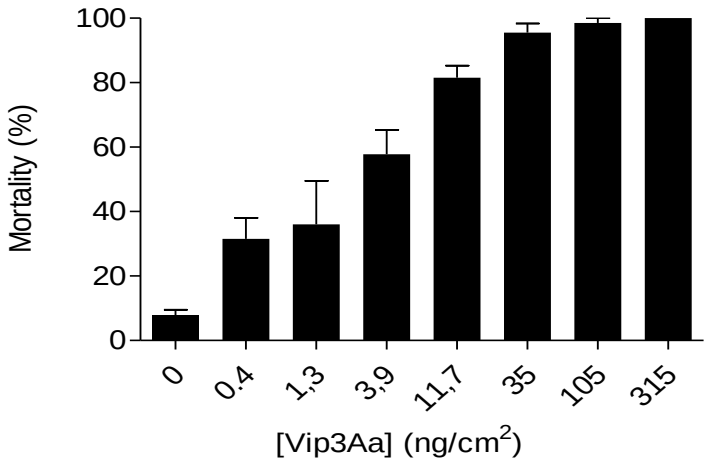

Supplementary Figure S4.2 Toxicity of Vip3Aa in *Spodoptera littoralis*. Different doses of the protein were given to neonate larvae of *S. littoralis*. Bars represent mortality recorded after 10 days. Error bars show the standard deviation (SD) among replicates. LC_{50} value and FL95% were calculated using PoloPlus software.

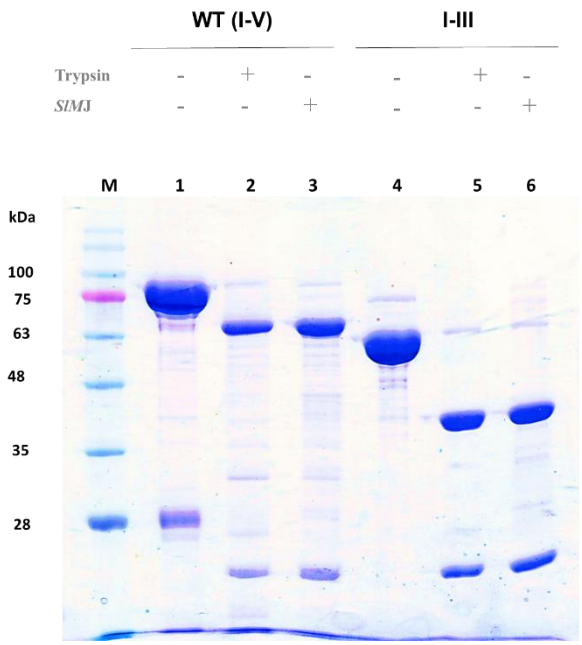

Supplementary Figure S4.3. ***In vitro*** **proteolytic processing of Vip3Aa WT and truncated constructs in** ***Spodoptera littoralis*****.** The proteins were incubated *in vitro* under different conditions and then subjected to SDS-PAGE. Lanes 1 and 4 correspond to protoxin samples; lanes 2 and 5 correspond to samples digested with trypsin (10% w/w); lanes 3 and 6 correspond to samples digested with *S. littoralis* gut juice (*Sl*MJ, 10% w/w). Band sizes were estimated according to the Blue Star molecular marker (M) (NIPPON Genetics).

Published papers

scientific reports

Check for updates

OPEN

In vivo competition assays between Vip3 proteins confirm the occurrence of shared binding sites in *Spodoptera littoralis*

María Lázaro-Berenguer, Yudong Quan, Patricia Hernández-Martínez & Juan Ferré✉

Due to their different specificity, the use of Vip3 proteins from *Bacillus thuringiensis* in combination with the conventionally used Cry proteins in crop protection is being essential to counteract the appearance of insect resistance. Therefore, understanding the mode of action of Vip3 proteins is crucial for their better application, with special interest on the binding to membrane receptors as the main step for specificity. Derived from in vitro heterologous competition binding assays using ^{125}I-Vip3A and other Vip3 proteins as competitors, it has been shown that Vip3 proteins share receptors in *Spodoptera frugiperda* and *Spodoptera exigua* brush border membrane vesicles (BBMV). In this study, using ^{125}I-Vip3Aa, we have first extended the in vitro competition binding site model of Vip3 proteins to *Spodoptera littoralis*. With the aim to understand the relevance (in terms of toxicity) of the binding to the midgut sites observed in vitro on the insecticidal activity of these proteins, we have performed in vivo competition assays with *S. littoralis* larvae, using disabled mutant (non-toxic) Vip3 proteins as competitors for blocking the toxicity of Vip3Aa and Vip3Af. The results of the in vivo competition assays confirm the occurrence of shared binding sites among Vip3 proteins and help understand the functional role of the shared binding sites as revealed in vitro.

Genetically modified crops expressing Cry insecticidal protein genes from *Bacillus thuringiensis* (Bt crops), have been used since the mid 90's to control insect pests. However, their extensive use has led to the phenomenon of field-evolved resistance to Cry proteins, for some lepidopteran and coleopteran pests[1–3]. Pyramided Bt crops (which combine different insecticidal proteins with different specificity and mode of action) have been proposed as an interesting tool to delay or avoid the appearance of insect resistance[4,5]. In this context, Vegetative Insecticidal Proteins (Vip3), known as a second generation of Bt proteins, are gaining importance in crop protection strategies. Most studies have dealt with Vip3Aa proteins, which are already expressed in commercial Bt crops, are active against lepidopteran species that have already developed resistance against the Cry proteins, and do not share binding sites with them[6–10].

Vip3 proteins have a tetrameric structure, with each monomer containing five structural domains[11–13]. The N-terminal (Nt) domains I–III are highly conserved and play a crucial role in maintaining the tetramer[12,14]. Domain I has been proposed to form, upon activation, a coiled-coil that inserts into the epithelial membrane[11,12], and domain III has recently been proposed to be responsible of binding to the midgut receptors[6,15]. The C-terminal (Ct) domains IV–V are highly variable sequence and are not essential for maintaining the tetrameric structure, though they are critical for the insecticidal activity in vivo[14,16]. These domains are carbohydrate binding modules (CBM) whose function remains still unknown[11–13].

In vitro binding assays to midgut binding sites have been used to establish binding site models which are useful to predict the appearance of cross-resistance and select the best protein combinations for pyramided Bt crops[8,10,17]. More recently, in vivo competition assays have been proposed as a novel tool to complement the in vitro binding models and obtain information about protein interactions in vivo[18–21]. Studies based on in vitro binding of ^{125}I-Vip3A to brush border membrane vesicles (BBMV) using heterologous Vip3 proteins as competitors led to propose a binding site model in which Vip3 proteins share binding sites in *Spodoptera frugiperda* and *Spodoptera exigua*[6,7]. In the present study, using ^{125}I-Vip3Aa, we have extended the in vitro binding site model of Vip3 proteins to another Spodoptera species, *Spodoptera littoralis*, with the aim to understand the relevance of binding to the midgut binding sites observed in vitro on the insecticidal activity of these proteins. For this

Institute of Biotechnology and Biomedicine (BIOTECMED), Department of Genetics, Universitat de València, 46100 Burjassot, Spain. ✉email: juan.ferre@uv.es

Received: 25 January 2022 | Accepted: 13 June 2022

DOI: 10.1111/1751-7915.14110

RESEARCH ARTICLE

microbial biotechnology

Structural and functional role of Domain I for the insecticidal activity of the Vip3Aa protein from *Bacillus thuringiensis*

Maria Lázaro-Berenguer[1,2] | **Francisco Paredes-Martínez**[2,3] | **Yolanda Bel**[1,2] | **Rafael Núñez-Ramírez**[4] | **Ernesto Arias-Palomo**[4] | **Patricia Casino**[2,3,5] | **Juan Ferré**[1,2]

[1]Department of Genetics, Universitat de València, Burjassot, Spain

[2]Institut Universitari de Biotecnologia i Biomedicina BIOTECMED, Universitat de València, Burjassot, Spain

[3]Department of Biochemistry and Molecular Biology, Universitat de València, Burjassot, Spain

[4]Centro de Investigaciones Biológicas Margarita Salas, CSIC, Madrid, Spain

[5]CIBER de Enfermedades Raras (CIBERER-ISCIII), Madrid, Spain

Correspondence
Juan Ferré, Department of Genetics, Universitat de València, Dr. Moliner 50, 46,100 Burjassot, Spain.
Email: juan.ferre@uv.es

Patricia Casino, Institut Universitari de Biotecnologia i Biomedicina BIOTECMED, Universitat de València, Dr. Moliner 5046,100 Burjassot, Spain.
Email: patricia.casino@uv.es

Funding information
This research was supported by the Spanish Ministry of Science, Innovation and Universities (Grant Ref. RTI2018-095204-B-C21 to J.F.), the Generalitat Valenciana (GVPROMETEO2020-010 to J.F.), the Spanish Ministry of Economy and Competitiveness (Grant Ref. BFU2016-78606-P to P.C.) and the Spanish Ministry of Science and Innovation (Grant Ref. PID2019-110630GB-I00 to P.C. and Grant Ref. PID2020-120275GB-I00/AEI/10.13039/501100011033 to E. A-P.). Support for M.L-B. was provided by the Generalitat Valenciana and the European Social Fund (Grant Ref. ACIF/2019/150).

Abstract

Vip3 proteins are produced by *Bacillus thuringiensis* and are toxic against lepidopterans, reason why the *vip3Aa* gene has been introduced into cotton and corn to control agricultural pests. Recently, the structure of Vip3 proteins has been determined and consists of a tetramer where each monomer is composed of five structural domains. The transition from protoxin to the trypsin-activated form involves a major conformational change of the *N*-terminal Domain I, which is remodelled into a tetrameric coiled-coil structure that is thought to insert into the apical membrane of the midgut cells. To better understand the relevance of this major change in Domain I for the insecticidal activity, we have generated several mutants aimed to alter the activity and remodelling capacity of this central region to understand its function. These mutants have been characterized by proteolytic processing, negative staining electron microscopy, and toxicity bioassays against *Spodoptera exigua*. The results show the crucial role of helix α1 for the insecticidal activity and in restraining the Domain I in the protoxin conformation, the importance of the remodelling of helices α2 and α3, the proteolytic processing that takes place between Domains I and II, and the role of the C-t Domains IV and V to sustain the conformational change necessary for toxicity.

CHAPTER THREE

Vip3 insecticidal proteins: Structure and mode of action

Juan Ferré*, Yolanda Bel, Maria Lázaro-Berenguer, and Patricia Hernández-Martínez
Institute of Biotechnology and Biomedicine (BIOTECMED), Department of Genetics, Universitat de València, Burjassot, Spain
*Corresponding author. e-mail address: Juan.ferre@uv.es

Contents

Abstract

Modern agriculture makes use of bacterial genes to protect crops from the attack of insects. Bt-crops are commercialized and express *cry* and *vip3Aa* genes from *Bacillus thuringiensis*, which confer protection against insect pests. Vip3A proteins are highly active against lepidopterans and the fact that they do not share binding sites with Cry proteins makes them perfect "partners" to be combined in insect-protected crops. The structure of Vip3Aa is composed of five well differentiated domains, and in solution the protein spontaneously forms a pyramid-shaped tetramer protoxin. The N-terminal domains of the protein (Domains I and II) are very conserved, mainly formed by α-helices, and are critical for the formation and maintenance of the tetrameric structure. The C-terminal domains (Domains III, IV and V) are highly variable, mainly consisting of β-sheets and thought of being responsible for binding to specific

Advances in Insect Physiology, Volume 65
ISSN 0065-2806, https://doi.org/10.1016/bs.aiip.2023.09.006

Research Article

Received: 9 May 2024 Revised: 12 July 2024 Published online in Wiley Online Library:

(wileyonlinelibrary.com) DOI 10.1002/ps.8341

Receptor interactions of protoxin and activated Vip3Aa structural conformations in *Spodoptera exigua*

Maria Lázaro-Berenguer, Juan Ferré and Patricia Hernández-Martínez*

Abstract

BACKGROUND: The Vip3Aa insecticidal protein, produced by *Bacillus thuringiensis*, has been effectively used in commercial Bt-crops to manage lepidopteran pests. Upon ingestion by larvae, the protoxin is processed by midgut proteases into the activated protein and binds specifically to its receptors in the midgut, leading to insect mortality. Cryo-EM resolution of the trypsin-processed Vip3Aa protein unveiled structural remodelling of the N-terminal region during the transition from protoxin to activated protein. This conformational change has been demonstrated to be crucial for toxicity against *Spodoptera exigua* larvae, a major global lepidopteran pest. In this study, we investigated the relevance of the structural remodelling for the specific binding to midgut receptors.

RESULTS: We conducted *in vitro* binding assays with radiolabelled proteins and brush border membrane vesicles (BBMV) from *S. exigua*, employing structural mutants that lock the protein in either its protoxin or its activated conformation. Our results indicate that both structural stages of the protein share binding sites in the midgut epithelium. Moreover, *in vivo* competition assays revealed that Vip3Aa is able to bind to functional receptors in *S. exigua* larvae both as protoxin and as activated protein.

CONCLUSION: Altogether, our findings point to both structural conformations contributing to receptor binding. *In vivo*, either spontaneous structural shift upon proteolytic cleavage or receptor-mediated remodelling could be occurring. However, the timing and context in which the conformational change occurs could influence membrane insertion and toxicity. Our results show the complex interplay between proteolytic processing, protein structure and receptor interactions in Vip3Aa's toxicity.

Supporting information may be found in the online version of this article.

Keywords: *Bacillus thuringiensis*; insecticidal protein; beet armyworm; biotechnological pest control; Bt-crop; biopesticide

1 INTRODUCTION

The *Spodoptera* genus, commonly known as armyworms owing to the well-known gregarious behaviour of their larvae, comprises several lepidopteran species widely recognized as major global pests.[1] These insects have become major invaders, colonizing multiple continents outside their native range.[2] Their larvae are extremely polyphagous, causing extensive damage by feeding on a wide range of crops, resulting in significant financial losses for agriculture on a global scale.[3]

Entomopathogenic bacteria can help to control these pests by providing us with a variety of insecticidal compounds. Cry proteins produced by *Bacillus thuringiensis* (Bt) are the most widely used and better studied among insecticidal proteins.[4,5] The genes coding for these proteins have been incorporated into transgenic plants (Bt-crops), offering effective pest control since the mid 90s.[6–8] However, resistance evolution to Cry proteins in some insect pests has prompted the search for alternative insecticidal proteins.[4,9–11] In this context, Vip3 proteins, also produced by Bt, have emerged as valuable candidates as a consequnce of their potency against lepidopteran insects and, most important, the fact that they do not share binding sites with Cry proteins,[12–18] and there is no reported case of cross-resistance between them.[19,20] Therefore, Vip3 proteins have become excellent partners for Cry proteins in pyramided Bt-crops, which combine different insecticidal proteins with different specificity to expand the target spectrum and prevent the appearance of insect resistance.[21–23] To date, numerous events of maize and cotton containing *vip3Aa* genes combined with *cry* genes have been approved for commercialization globally, with expectations for their adoption in many more crops in the future.[24]

Vip3 proteins are produced by Bt during its vegetative growth phase and are secreted into the media as tetrameric molecules. Each tetramer comprises four identical monomers, with each

* *Correspondence to: P Hernández-Martínez, Institute of Biotechnology and Biomedicine (BIOTECMED), Universitat de València, 46100 Burjassot, Spain, E-mail: patricia.hernandez@uv.es*

Institute of Biotechnology and Biomedicine (BIOTECMED), Universitat de València, Burjassot, Spain